Water Level Monitoring in the Karnali River, Nepal

Evaluating Satellite SAR Altimetry Techniques through Field Observations

MSc Thesis

Author: M.K. De Jong

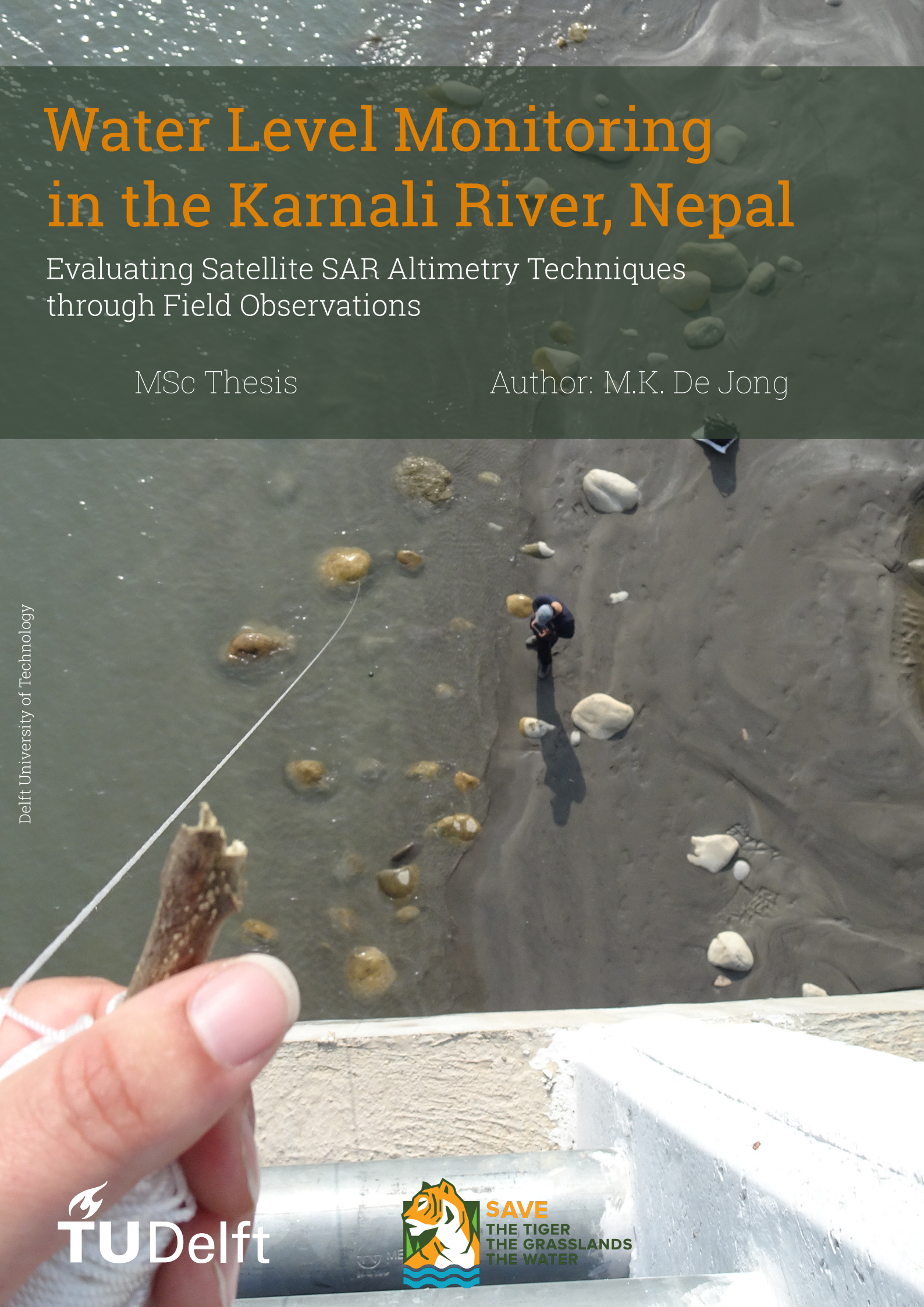

Delft University of Technology

TU Delft

SAVE
THE TIGER
THE GRASSLANDS
THE WATER

Water Level Monitoring in the Karnali River, Nepal

Evaluating Satellite SAR Altimetry Techniques through Field Observations

by

M.K. De Jong

Student Name	Student Number
Mo K. de Jong	4826140

Supervisor Water Management:	Dr. T.A. Bogaard
Supervisor Geoscience & Remote Sensing:	Dr. ir. D.C. Slobbe
Independent Supervisor:	Dr. ir. A. Blom
Project Duration:	August, 2022 - September, 2023
Faculty:	Civil Engineering & Geosciences, Delft

TU Delft

SAVE THE TIGER THE GRASSLANDS THE WATER

Preface

Throughout my entire academic career, actually already since high school, I have always had a strong ideas on what had interested me. These interests seemed all over the place however, ranging from biology to economy, from physics to ethics, and from technology to ethics. In addition, I have a great love for arts and culture, for nature and adventure.

This determination to work hard and learn a lot about the many things that can be learnt to try and understand the world a bit better can all be retraced in the choices I made in my academic career. This of course includes the choice for an individual double degree programme, combining my interest for nature and technology in the Water Management and Geoscience and Remote Sensing MSc programmes.

Although I have always been determined in projects I undertake, naturally motivated and intrigued, I have never really been sure where this might take me. Over the past years, I have slowly started to connect the dots. This thesis work is a great product of this. Combining my love for nature and technology, determined to apply my skills to contribute to nature conservation efforts. In te years to come, I hope to be able to bring my skill-set to many more corners of the world. To learn from local communities about the challenges they are facing in the light of climate change or in their nature conservation efforts, and using my skillset to help them make the world a better place.

I would have never been able to achieve what I have without the support of first and foremost my friends and family. For that I would like to thank my parents in particular, for never pushing me but always supporting and motivating me in the best way possible. I would like to thank my study friends - Emma, Sophie, Marijn en Nadine for keeping me sane during late nights and long weekends studying and keeping me motivated. I would like to thank my friends from Plankenkoorts, Jonick, Wieke, Nicole, Kees, Willem, Niels and Bart for the necessary distraction and relaxation, sometimes more needed than I was aware of. I would also like to thank Matteo and in particular Kshitiz for being a great partner and friend during the field campaign and further supporting me in my thesis work. In addition, I would like to thank Frithjof for his immense efforts in teaching me all I need to know about satellite SAR altimetry. Lastly, Youri, I cannot even start to thank you for everything you have done to support me!

Enjoy reading my thesis! Hopefully you will learn a thing of two about satellite SAR altimetry, and the challenges of hydrological data gathering in absolutely amazing but challenging landscapes.

M.K. De Jong
Delft, September 2023

Abstract

Rivers play a crucial role in shaping landscapes and supporting ecosystems. This is demonstrated by the tiger habitats in and around Bardia National Park in West-Nepal, which rely on the Karnali River. This study contributes to a larger effort aimed at sustainably managing these tiger habitats. Monitoring the rivers in this remote area is challenging, suggesting a role for remote sensing. An exploration is presented regarding the potential of satellite synthetic aperture radar altimetry (sat-SARA) for monitoring rivers situated in diverse topographic landscapes. Focusing on the Bheri, Karnali, and Geruwa Rivers, the applicability of sat-SARA techniques for water level monitoring, multiple channel identification, and channel activation detection was evaluated. For deriving water surface heights from sat-SARA data, an empirical Gaussian retracker was used. The findings are promising. While resulting water level variations align with field observations, complementary in-situ measurements are imperative for a comprehensive evaluation. Additionally, the study reveals the potential for identifying multiple channels from sat-SARA return signals, extending to channel classification and detecting channel activation. Leveraging the labour-intensive nature of sat-SARA data processing, the technique holds great promise for monitoring rivers in remote and difficult-to-access landscapes. Therewith, this study contributes to advancing the understanding of the hydrodynamics of the Lower Karnali River and opens doors for sat-SARA applications for river monitoring in challenging terrains.

Contents

Nomenclature

Abbreviations

Abbreviation	Definition
BNP	Bardia National Park
FFSAR	Fully-focused Synthetic Aperture Radar
IWH	inland water (surface) height
NFP	Nikon Forestry Pro
S3A	Sentinel-3A
S3B	Sentinel-3B
S6A	Sentinel-6A
SAR	Synthetic Aperture Radar
sat-SARA	satellite Synthetic Aperture Radar altimetry
UFSAR	Unfocused Synthetic Aperture Radar

Symbols

Symbol	Definition	Unit
a	amplitude	
B	chirp bandwidth	[Hz]
c	speed of light ($c = 2.99 \cdot 10^6\ m/s$)	
ET	solid Earth tide correction	[m]
f_c	carrier frequency	[Hz]
H	satellite altitude above reference ellipsoid	[m]
I	ionospheric-delay correction	[m]
IWH	inland water surface height	[m]
L_x	azimuth/along-track resolution	[m]
P	polar tide correction	[m]
Q	discharge	[m^3/s]
R	altimeter (retracted) range	[m]
R_{cor}	total height geophysical correction	[m]
RG_{peak}	range gate at maximum signal power	
RG_{ref}	reference range gate	
T_d	dry troposphere correction	[m]
T_w	wet troposphere correction	[m]
TD	two-way time delay pulse transmission and reference tracking point	[s]
TR	tracker range	[m]

Symbol	Definition	Unit
V	velocity of satellite	[m/ s]
V_t	two-way time-delay retracking point and reference tracking point	[s]
σ	variance	
δr	distance measured from range difference	
δRG	distance between range gates	

Definitions

Term	Definition
Water surface height	height of the water surface with respect to a reference ellipsoid
Water level	height of the water surface relative to the (direct) environment

1

Introduction

Nestled within the pristine wilderness of Nepal, Bardia National Park (BNP) serves as a vital refuge to the Bengal Tiger (Kral et al., 2017). As an endangered species, tigers worldwide face challenges caused by climate change and human interference (Goodrich et al., 2020). Nepal, as one of the signatory nations to the initiative aimed at strengthening and expanding wild tiger populations (Kral et al., 2017), has witnessed considerable success in this regard, more than doubling its tiger populations over the past decade (DNPWC and DFS, 2022). Yet, with this triumph arrive new questions on how to sustainably manage the tiger's habitat within the BNP. The crucial link between a thriving tiger population and a balanced ecosystem requires a an intricate understanding of the region's hydrodynamics (Bijlmakers et al., 2023). Insights into water level variability of the rivers in this dynamic landscape contribute to a better understanding of their hydrodynamic behaviour, supporting further research into sustainable habitat management for the Bengal Tiger. However, a significant challenge lies in the scarcity of historical hydrological data for the region, where the rivers are either poorly gauged or not gauged at all. This issue is not unique to this region, but typical of remote and hard-to-access areas worldwide.

In addition, the availability of hydrological in-situ data such as inland water level data has drastically declined in recent decades. This decline can be attributed to various factors. The reluctance of governments to share hydrological data - often considered sensitive information - has contributed to this decline (Schneider et al., 2017; Villadsen et al., 2016). Additionally, budget constraints and changing priorities push agencies responsible for data collection and maintenance to reallocate their limited resources, resulting in fewer monitoring stations, available personnel and equipment (Houghton-Carr et al., 2006). The emergence of remote sensing and satellite-based monitoring systems providing data over larger areas at reduced cost has also affected the decline in field observation data. While remote sensing technologies offer great potential, they do not entirely replace the need for in-situ data.

Satellite remote sensing technologies offer countless valuable opportunities for hydrological data collection, particularly for poorly gauged water bodies and in remote or difficult-to-access regions where the collection of in-situ measurements is more difficult and hydrological data is more scarce (Alsdorf et al., 2007; Calmant et al., 2008; O'Loughlin et al., 2016; Kim et al., 2021). Recent advancements, including the increased remote sensing product availability and constellation densification, have enhanced the utility of satellite radar altimetry, making it increasingly attractive for water level monitoring in medium to large lakes and rivers (Tarpanelli and Benveniste, 2019).

1.1. Satellite Altimetry for Inland Water Monitoring

Many satellite altimetry missions have been collecting water level data for decades. Most of the conventional and popular altimetry missions are based on radar-technologies. Laser (or LIDAR) altimetry offers an alternative to this technology. The benefit of laser altimetry over conventional radar-altimetry, is the higher spatial resolution provided by a smaller ground footprint (O'Loughlin et al., 2016). However, laser altimetry is sensitive to atmospheric conditions and clouds (Tomić and Andersen, 2023), underscoring the main limitation of the technology. Radar-altimetry, on the other hand, makes use of an active microwave sensor, allowing the signal to penetrate through clouds and sense during night-time, as illumination by the sun is not required (Murfitt and Duguay, 2021).

Radar-based satellite altimetry is well-recognised for oceanographic applications (Maillard et al., 2015). The potential of altimetry for river and lake monitoring has been demonstrated through more than 25 years of research (Berry, 2006), and was even further enhanced with the launch of Synthetic Aperture Radar (SAR) altimeters, leading to improved resolutions and accuracy (Tarpanelli and Benveniste, 2019) as compared to conventional LRM (low resolution mode). Despite none of these Satellite SAR altimetry (or sat-SARA om short) missions being designated for monitoring inland water bodies (Tarpanelli and Benveniste, 2019; Rosmorduc et al., 2018), the technology has proven a valuable resource for river and lake water level data, especially in scarcely gauged regions (Villadsen et al., 2016; Finsen et al., 2014; Schneider et al., 2017; Roohi et al., 2021; Kleinherenbrink et al., 2020; Jiang et al., 2020; Park, 2020; Schaperow et al., 2019). It offers regular and global information on water levels independent of infrastructure or local politics, greatly benefiting timely and cost-effective hydrological data collection.

Historical altimetry water level observations over large rivers and lakes from so-called 'virtual stations' are readily made available through a variety of projects such as Hydroweb (), ESA River & Lake Project (Berry et al., 2005), and the DAHITI database (Schwatke et al., 2015). Most of these virtual stations are situated at medium to large lakes or rivers, however. The Hydroweb and ESA River&Lake projects obtain(ed) their data from conventinal altimetry missions, whereas DAHITI combines data from multiple missions.

The limited along-track resolution of conventional altimetry techniques limits the application to water bodies with a diameter or river width of 300 meters at minimum (Schwatke et al., 2015), as the surrounding landscape may contaminate the altimeter signal. Maillard et al. (2015), found that the local landcover was an important factor influencing the accuracy of altimeter return signals over inland water bodies. In addition, the river shape and orientation influence the accuracy of the derived water levels (Villadsen et al., 2016). Lastly, Sulistioadi et al. (2015) and Villadsen et al. (2016) state that irregular topographies typically contaminate the return signal, making it difficult to accurately derive water surface heights in complex topographical terrains.

The application of satellite altimetry for inland waters has been tested and proven in various studies. The use of lower-resolution conventional satellite altimetry has limited the applications to large inland water bodies however (Tarpanelli and Benveniste, 2019; O'Loughlin

et al., 2016). Some studies have focused on large lakes (Berry et al., 2005; Berry, 2006; Crétaux and Birkett, 2006; **?**), or medium-sized lakes (Villadsen et al., 2016; O'Loughlin et al., 2016; Nielsen et al., 2020), whilst others focused on large rivers (O'Loughlin et al., 2016; Bonnema et al., 2016; Villadsen et al., 2016; Schneider et al., 2017; Bjerklie et al., 2018; Tourian et al., 2017; Gao et al., 2019; Michailovsky et al., 2012; Maillard et al., 2015). Few studies have investigated the potential of (FF-)SAR altimetry for small rivers (Kleinherenbrink et al., 2020; Yuan, 2019), but these are all over flat terrain. Previous studies on inland water surface height derivations from satellite altimetry have thus either been on small to medium sized rivers in flat terrains, on large rivers or on medium to large lakes.

The introduction of the Delay-Doppler principle for SAR altimetry provides an increase in accuracy and along-track resolution (Tarpanelli and Benveniste, 2019; Ranndal et al., 2020) accompanied by a naturally reduced land contamination (Rosmorduc et al., 2018), whilst the further advancement to FF-SAR processing techniques promises an even further increase quality of altimeter-derived water level data (Ehlers et al., 2023a). Sentinel-3 and Sentinel-6 also offer an increased temporal resolution with return periods of 27 and 10 days respectively (Ranndal et al., 2020; Donlon et al., 2021; ESA, 2022), as compared to the CryoSat-2 mission which has a return period of 369 daysESA (2011). This raises the question what the potential of these recent sat-SARA products is for river monitoring in poorly-gauged rivers in remote and difficult-to-access regions with complex topographies.

1.2. Study Area

In the heart of Western Nepal lies Bardia National Park (BNP), a sanctuary for diverse wildlife and essential for the conservation efforts for the endangered Bengal tigers. The BNP largely depends for its water supply on two rivers: the Babai River, meandering through the park's core, and the Karnali River. The study area covers the Lower Karnali River reaches, commencing just upstream of the confluence with the Bheri River, down to the border with India. A map of the total study area is presented in figure 1.1. The main land use types found in the study area are forests, shrubs and grasslands, water bodies and agricultural land (Dahal et al., 2020; Shrestha et al., 2022).

Originating in the Tibetan Plateau, the Karnali traverses the Himalayan mountains, flowing from the confluence with the Bheri River and through the Sivalik Range. The river departs the mountainous terrain at the town of Chisapani, after which it bifurcates into the Kauriala River on the right (West) and Geruwa River on the left (East) (Dingle et al., 2020). After departing the Sivalik Hills, the Karnali, Geruwa and Kauriala Rivers constituting a complex braided system. The Geruwa River forms the natural boundary between the BNP on its left bank and the Rajapur agricultural area on its right. Forming the natural boundary of the Bardia National Park, the Geruwa flows for a substantial portion of its length through or along the park. Approximately 6 kilometres after crossing the border with India, the Geruwa and Kauriala rivers join to become the Karnali River again and form a major tributary to the Ganges River (Bijlmakers et al., 2023).

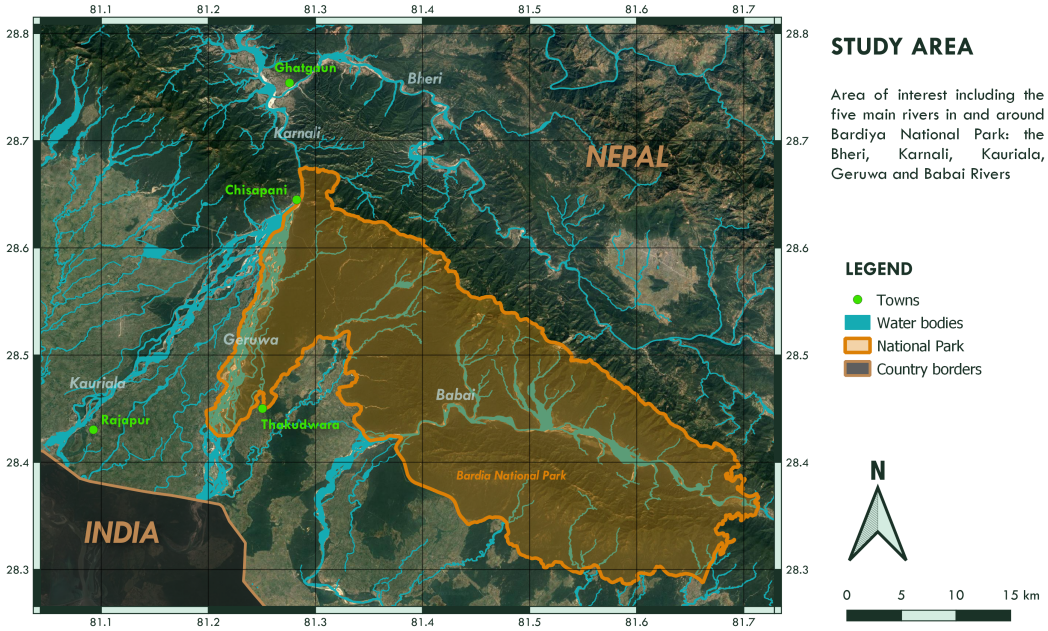

Figure 1.1: Map of study area including Bheri, Karnali, Kauriala, Geruwa and Babai Rivers in West-Nepal

The Karnali River catchment consists of a drainage area of approximately 42000 km^2 upstream of Chisapani. The discharge of the river is subject to seasonal variability. The Indian Summer Monsoon provides approximately 55-80% of the total annual precipitation. Peak flow can be observed between June and October, usually arriving in August, with peak discharges exceeding 5000m^3/s annually. The period between November to April marks the dry and low-flow season, with average discharges between 400 and 600m^3/s, but can be as low as 200m^3/s. The river discharge is dominated by these precipitation events and snow and glacier melt. These latter also contribute to the baseflow in winter (Dingle et al., 2020; Dahal et al., 2020; Duwal et al., 2023).

The Bheri River is one of the major tributaries of the Karnali River (Mishra et al., 2018; Dingle et al., 2020), and the last major tributary within the study area. The catchment comprises approximately 14000 km2. The river is approximately 264 kilometres long and the elevation varies from 7746 meters at the upstream end and 200 meters at the confluence with the Karnali(Mishra et al., 2018).

The Babai River, originates from the Sivalik hills and flows Northwestward through the BNP. Hence, the Babai is of major importance for water supply in the BNP. The river first flows parallel to the Bheri, to then turn Southward, flowing parallel to the Geruwa and Kauriala Rivers before joining the Karnali river 50 kilometers downstream of the Nepal-India border (Yadav, 2002).

1.3. Save the Tigers

The natural habitat of the Bengal Tiger is under pressure due to climate change and human interference. As a result, tigers are globally considered an endangered species (Goodrich et al., 2020). Nepal is among the countries that signed an initiative to increase their wild tiger populations ((Kral et al., 2017)). Bardia National Park in western Nepal is one of the national parks where the tiger can be found and provides an important habitat for the tiger in the Terai Arc Landscape (TAL) ((Kral et al., 2017)). So far, their efforts have been very successful as they managed to more than double the number of tigers in BNP between 2012 and 2022 (DNPWC and DFS, 2022). This raises new questions, regarding the sustainability of the tiger habitat and to which extent the current habitats have sufficient capacity to maintain and sustain the current tiger populations and potential further population growth (Aryal et al., 2015). Pressure from both tiger population growth and an increase in human activities in the area over the past decades seems to increase human-wildlife conflicts (Bhattarai et al., 2019; Shahi et al., 2022). To avoid these conflicts it is important that the habitat of the tiger is sustainably managed and the ecosystem is in balance, to prevent the tigers from roaming outside of national park boundaries and into rural villages in search for water and food. The *Save the Tigers, Save the Grasslands, Save the Waters!* project (or in short *Save the Tigers project*) aims to provide a sustainable habitat for a viable tiger population within the Terai Arc Landscape (TAL).

Tiger habitats in the TAL are subject to various environmental pressures, including human interference and changing hydrological conditions. These factors significantly influence the growth potential of grasses and the grassland dynamics (Kral et al., 2017; Bijlmakers et al., 2023). These grasslands are, in turn, essential for the deer populations which rely upon the grasses for food (Odden et al., 2005; Kral et al., 2017; Bijlmakers et al., 2023). While the intricate relationship between hydrology, hydromorphological dynamics, and grassland dynamics in the TAL remains a subject of ongoing research, it is paramount for comprehending the dynamics of tiger habitats (Bijlmakers et al., 2023). Unravelling the hydrodynamic behaviour of the rivers in the region provides valuable insights into maintaining the delicate balance of the tiger habitat and ensuring its effective long-term management.

As a contribution to the *Save the Tigers project*, this MSc thesis is dedicated to studying and addressing one of the many challenges impacting the tiger habitats in the TAL in Nepal. Collaboratively undertaken by several Dutch universities, local academic institutions in Nepal, NGOs and governmental bodies, the *Save the Tigers* project is committed to understanding and preserving a sustainable habitat for tigers in the TAL. To this extent, the intricate interplay between the natural hydrological regime, vegetation dynamics, populations of tigers and their prey are explored, while also investigating the complex influence of human activities on the habitats and the resulting human-wildlife conflicts. For comprehensive information about the overarching project, please visit their official website [1]. The current study contributes to the broader project by gaining a better hydrodynamic system understanding of the region, starting a hydrological data catalogue, as well as providing an insight into the potential use of remote sensing techniques for river monitoring in the Lower Karnali River.

[1] *Save the Tiger* official project website: https://savethetiger.nl

1.4. Problem Statement

The problems addressed in this thesis were rooted in a complex and layered issue, requiring insights from a multitude of fields of study. This thesis focused on a subset of the issues at stake in an attempt to provide insights for both hydrologists and remote sensing experts. To that extent the problem addressed in this thesis is twofold.

Firstly, there is a significant lack of information concerning this remotely situated study area, and at the time of writing, hydrological data for its rivers is very scarce. Remote Sensing solutions may provide great potential for filling some of these data gaps. This leads to the second problem addressed by this study.

Currently, no satellite SAR altimetry missions are dedicated to water level monitoring over inland water bodies. They are typically applied for ocean monitoring applications. The possibilities for satellite altimetry over inland water bodies have been studied for inland water bodies extensively. However, these applications were typically for medium to large-scale lakes and rivers in flat topographies. The current study area consists of a diverse landscape with a variety of topographical characteristics. Hence, while the application of sat-SARA had proven successful for other landscape characteristics, its applicability for the specific topographical features in the Lower Karnali River region or for resembling topographies remains unknown.

1.5. Research Objectives

Considering the two problems stated in the previous section a couple of objectives were set for this study. The overall objective of this thesis was to assess the applicability of satellite-SAR altimetry for monitoring the water level variability and identifying multiple channels in the Lower Karnali River region. To this extent, validating the satellite SAR altimetry-derived results with field observation data was required. Hence, the overarching objective implies a set of underlying aims:

- To estimate water surface heights with satellite SAR altimetry
- To identify river channels and river channel activation with satellite SAR altimetry data
- To collect in-situ hydrological data, both for building a data catalogue and for field validation of the satellite SAR altimetry results

These objectives together support the ambition to be able to monitor water levels using satellite remote sensing in remotely situated areas. Such solutions may provide multiple benefits. Firstly, it allows for continuous data collection and building of both a historic and ongoing (hydrological) database. Secondly, limited resources may be spent more effectively, as the urgent need for frequent field visits will decrease. Insights from the remotely sensed data may indicate more specifically what data is required during planned field visits. Hence, resources such as time, money and logistics may be deployed more efficiently.

To effectively validate satellite SAR altimetry, determining the required accuracy for assessing its potential in water level monitoring is essential. This accuracy requirement depends

upon specific case demands, contextual attributes of the study area, and the project's overarching objectives. The Karnali is a rather voluminous river, flowing through diverse terrain, with annual water level fluctuations anticipated to span a few up to potentially more than 10 meters. The monitoring of these variations facilitates the development of hydro- and morphodynamic models, aiding a larger-scale hydrodynamic system understanding. For these purposes, an accuracy within the order of a few decimeters should suffice. An accuracy of 1-20 centimetres would be ideal but an accuracy of 20-30 centimetres already provides some insights into the hydrodynamic system behaviour.

Secondly, to validate the results from the sat-SARA analysis, in-situ observations are imperative. As very little in-situ hydrological data was available, field observation data had to be collected. Hence, one of the main objectives was to explore the study area for suitable measurement sites, the potential for installing longer-term measurement stations and collect the first data samples to start building a field observation data catalogue. To this extent, the collection of in-situ data regarding water surface heights, flow depths, river widths and descriptions of landscape characteristics were prioritised. The field campaign itself was more elaborate, however. For more information about the full field campaign and its findings, please refer to the field report (appendix I).

1.6. Research Questions

Based on the problem statement and the objectives discussed in the previous sections this thesis aims to answer the research questions as proposed in this section.

The main research question for this thesis is:

What is the potential of satellite SAR altimetry for monitoring water level variability and river channel activation in the diverse topographical landscapes of the Lower Karnali River, Nepal?

In addressing this overarching research question, the study can be methodically divided into two essential parts. The first of which delves into the satellite SAR altimetry data analysis, exploring and testing the capacity of this technology for effectively water level monitoring and identifying channels across the diverse topographical landscapes in the study area. Complementing this is the field campaign aiming at collecting in-situ hydrological data. This data is indispensable for verifying and contextualising the findings derived from satellite SAR altimetry. By combining satellite insights with direct field observations, this approach ensures the potential uncovered by satellite SAR altimetry harmonises with on-site hydrodynamic reality. Hence, this integrated approach, bridging remote sensing and field perspectives, provides a robust foundation for answering the core research question. Below a set of sub-questions is posed for each of these two parts.

1.6.1. Sat-SARA Analysis Specific Sub-Questions

Two sets of sub-questions are posed for the analysis of satellite SAR altimetry data. The first question is aimed to support the multiple channel and channel activation analysis:

To what extent is it possible to identify multiple river channels from satellite SAR altimetry in Bheri, Karnali and Geruwa River sections?

To be able to answer this question first it should be tested whether it is possible to identify river channels from the satellite SAR altimetry return signals. These results then need to be evaluated as to whether they align with what is expected considering the landscape characteristics. In addition, if seasonal variability can be observed, this begs the question of how this manifests itself in the satellite SAR altimetry data, and whether channel activation can be detected from it. Lastly, this analysis should point out what the possibilities and limitations are for identifying multiple channels through sat-SARA.

The second question is aimed at deriving water surface heights:

To what extent is it possible to derive water surface heights at various river overpass locations in the Bheri, Karnali and Geruwa Rivers, from satellite SAR altimetry?

To be able to answer this question it is necessary to test whether water surface heights can be derived from sat-SARA data at the selected sites. To this extent, the aim is to derive water surface heights from sat-SARA data for 2021 and 2022. To achieve this, a data processing flow needs to be established, selecting suitable processing methods. The resulting data may also provide insights into seasonal variability. To assess the accuracy of the derived water surface heights, the results can then be evaluated on whether they are as anticipated and align with field observations. This workflow should help indicate challenges and limitations in case water surface height derivation for the selected sites proves challenging or impossible.

1.6.2. Field Campaign Specific Sub-Questions

Another set of questions was posed specifically in support of the collection and processing of the field observation data. This included the following questions:

What are the water surface heights, flow depths, river widths and landscape characteristics as observed in the field, at the selected sites along the Bheri, Karnali & Geruwa Rivers?

In preparation, during the field campaign and for processing and analysing the data, this entails the exploration and selection of suitable locations for field observation campaigns and for potential extended-duration measurement stations. In addition, the best suitable methods for measuring the water surface heights, flow depths and river widths in this stage of the research project have to be selected. Lastly, the accuracy with which the field observation data has to be estimated and evaluated for meeting the requirements intended for the research objectives.

2

Theoretical Background Sat-SARA

Satellite Synthetic Aperture Radar Altimetry (sat-SARA) is a satellite remote sensing technique used to measure the height over the Earth's surface and in particular over water surfaces. The launch of CryoSat-2 in 2010 marked the start of the first satellite SARA mission (Roohi et al., 2021; Villadsen et al., 2016; Ehlers et al., 2023b), after which Sentinel-3 and Sentinel-6 followed with launches in 2016 and 2020 respectively (Donlon et al., 2021; Ranndal et al., 2020). None of these missions have been specifically designed for water level monitoring over inland water bodies, but are more widely applied for water level monitoring over open oceans (Ranndal et al., 2020). For the satellite SAR altimetry data analysis, it is important to understand some of the basic principles used for this technique. This chapter provides a general theoretical background for satellite SAR altimetry.

2.1. Sat-SARA Basic Principles

Sat-SARA is, like most conventional satellite altimetry missions, based upon radar techniques and involves the active transmission and receiving of a microwave (radar) signal. The satellite transmits a signal directed to the Earth surface, which reflects the signal. The signal is scattered upon the reflection at the Earth's surface, the extent of which depends on the surface roughness. The satellite then receives (part of the original) signal moments after it has transmitted the signal (Ehlers, 2022; Villadsen et al., 2016). The time it takes for the signal to travel to the Earth's surface and back is generally known as the time delay or radar echo delay. This is used to derive the distance between the Earth's surface and the satellite (Tarpanelli and Benveniste, 2019; Ehlers, 2022). This principle is also visualised in figure 2.1.

The signal transmitted by the satellite travels toward the Earth's surface and disperses, causing a conical shape and hence a reflection at the surface over a roughly circular area (the pulse footprint). The signal hits the surface first at the location with the shortest distance to the satellite, which should for flat terrains be exactly below the satellite (nadir) (Ehlers, 2022). At the surface, the signal is reflected and may be scattered in many different directions. The more rough the surface texture, the more the signal will be scattered. Since water is a very smooth surface, a large part of the original signal will be returned to the satellite. This results in a strong signal power at the location of the water surface and makes it appear bright (Ehlers, 2022; Villadsen et al., 2016; Maillard et al., 2015). The conical shape of the pulse and the large resulting footprint area, make it near impossible, however, to derive the exact location of the bright water signal.

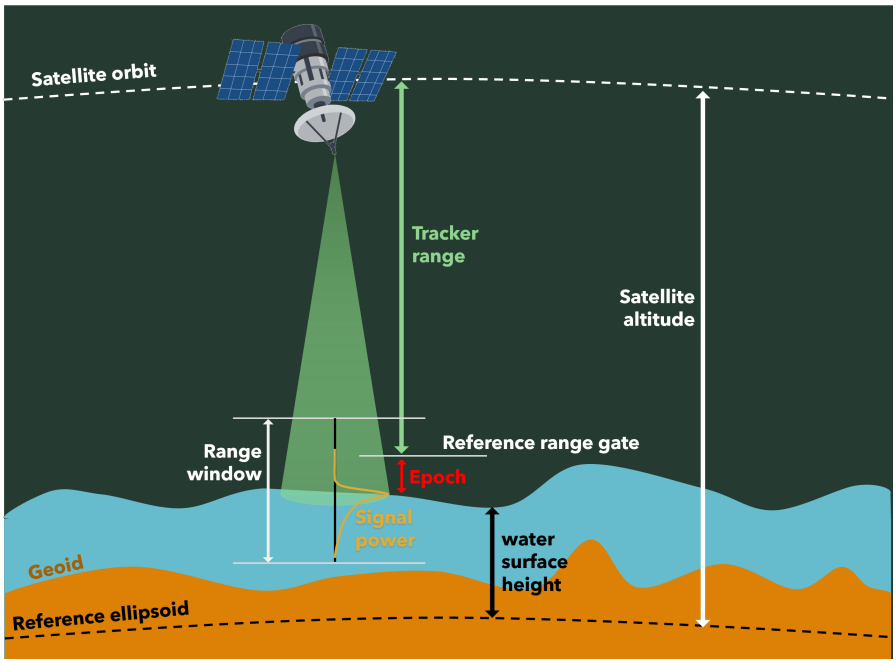

Figure 2.1: *Basic Principles of Satellite SAR Altimetry (Ehlers, 2022)*

This is where the synthetic aperture comes in, as the SAR-principle makes use of the delay-Doppler effect for processing the altimetry data (Ehlers, 2022; AVISO, 2023; Tarpanelli and Benveniste, 2019). SAR altimetry is a relatively recent technique for processing altimetry data and differs from conventional satellite altimetry in that it exploits the Doppler effect caused by the satellite's movement in the along-track direction to improve along-track spatial resolution. By combining information from multiple pulses whilst the satellite is moving along track, it can better locate the exact position of the signal, narrowing the footprint and increasing the along-track resolution (see figure 2.2)(Dinardo, 2020; Ehlers, 2022). This results in an unfocused-SAR (UF-SAR) product. Combining information from multiple UF-SAR bursts over time, the along-track resolution could be even further improved following the fully focused SAR (FF-SAR) principle (AVISO, 2023; Kleinherenbrink et al., 2020; Ehlers et al., 2023a).

The benefits of using sat-SARA lie in its enhanced resolution. To fully grasp the significance of this improvement, it's essential to understand how resolution is assigned to altimetry products across various dimensions. As mentioned before, the along-track spatial resolution is especially crucial for applications over inland water bodies and is governed by processing principles. For SAR-mode altimetry products the along-track resolution is improved as compared to conventional and low-resolution mode (LRM) products (Tarpanelli and Benveniste, 2019; Rosmorduc et al., 2018; Dinardo, 2020). The along-track resolution is determined by the length of the aperture (Ehlers et al., 2023b). In FF-SAR products, the coherent integration time dictates the number of bursts selected for focusing, affecting the along-track resolution (Ehlers et al., 2023a). For UF-SAR, the along track resolution follows from equation 2.1 (Ehlers et al., 2023a). Secondly, the range resolution is governed by the chrip bandwidth B of the pulses in the signal and depends on the instrumentation. Lastly, the temporal resolution, which is described by the return period of the satellite, may be of significant importance

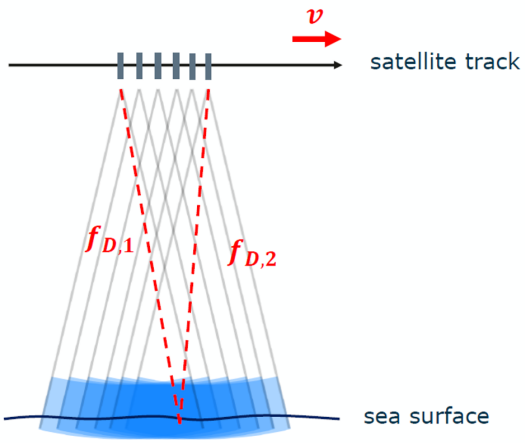

Figure 2.2: *Delay-Doppler Principle (Ehlers, 2022)*

dependint on the specific application.

$$L_x = H \cdot \frac{c}{2 f_c V_t T} \tag{2.1}$$

with:

- L_x - azimuth or along-track resolution
- T - coherent integration time (which is the burst duration for UF-SAR)
- f_c - carrier frequency
- H - satellite altitude above reference ellipsoid
- V_t - two-way time delay between retracking point and reference tracking point
- c - speed of light in a vacuum

To derive the absolute water surface height from the time delay of the signal, a bit more information is required. Firstly, the exact location of the satellite itself is required. This exact location of the satellite is often obtained from a combination of different techniques and the communication of the satellite with other satellites and ground stations. This positioning is important as the satellite may undergo drift, causing it not to perfectly follow its theoretical orbital trajectory. The drift may be in all planes: horizontally as well as vertically, and is constantly corrected for to allow the satellite to its theoretical orbit. This does mean however, that the exact height of the satellite may be variable over time, which is something that needs to be accounted for. This satellite altitude is defined as its height relative to a reference geoid.

As the distance between the satellite and the Earth's surface is very large compared to the expected water surface height deviations (close to the Earth's surface), the exact surface heights are measured within a range window. Simply put, this range window is the range in which the satellite 'expects to find the surface'. This range window is split into multiple bins or range gates. The number of range gates and the distance between each of these range gates is satellite specific. The tracker range describes the distance between the satellite and

the reference range gate. The reference range gate is a set range gate within the range window. The tracker range may vary over space and time, as the height at which the surface is expected to be found may change due to topographical variations. Ultimately, the exact height of the (water) surface could thus be derived from knowing the satellite altitude with respect to a reference ellipsoid or geoid, the tracker range, and the range gate at which the maximum power of the return signal can be found.

2.2. Data Processing

Deriving water surface heights from the return signal of the satellite is an extensive process with multiple steps. Which will briefly be discussed in this section. The work of Dinardo (2020) was used as a base for the current workflow, please refer to his work for more background. The level-1A (L1A) data is the raw and uncalibrated satellite data, level-1B the pre-processed data and level-2 data provides the geophysical output parameter; in this case water surface height (Rosmorduc et al., 2018). In the process of converting the level-1A to the level-1B data the time delay signal is translated to a return signal waveform through the application of Fourier Transforms Ehlers (2022); Rosmorduc et al. (2018). This is a computationally expensive process.

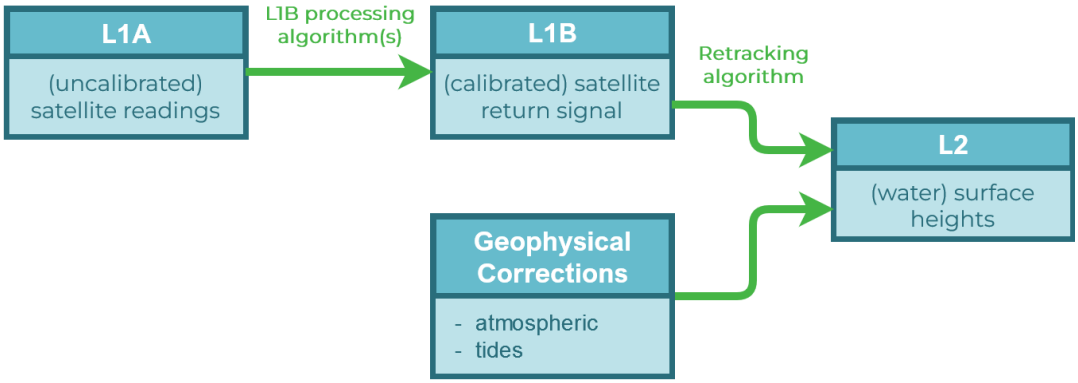

Figure 2.3: *Satellite SAR altimetry processing steps*

Obtaining the geophysical parameters required for generating the L2 data from the L1B data is called (waveform) retracking (Rosmorduc et al., 2018). A retracker is an algorithm or model used to derive the desired geophysical parameter, in this case the water surface heights, from the return signal (the waveform). Different applications over different topographies require different retracking approaches due to the differences in landscape characteristics (Villadsen et al., 2016). Hence, a range of different retracking algorithms and models exist for a variety of applications, the SAMOSA retracking models being the most famous and widely applied models for retracking water surface heights over open oceans. The retracking methods can be divided into three main categories:

- Physically-based retracking
- Statistical retracking
- Empirical retracking

Physical retrackers are based on models approximating a waveform shape based on physics (Dinardo, 2020). These types of retrackers typically have a high accuracy and precision. How-

ever, they also have a high computational cost. They are typically used for applications for which the physical conditions are predictable and can relatively easily be estimated. Physical retrackers can be built in numerous ways and be based on a variety of mathematical and physical principles. Physical models are typically applied for retracking water surface heights, significant wave heights and wind speeds over open oceans (Dinardo, 2020). Hence, these retrackers will not be further discussed in this thesis. Statistical retrackers approach the retracking problem by finding the optimal solution based on the statistical properties of a set of waveforms (Dinardo, 2020). Thus, the statistical retracker is not based on physical models. This type of retracker will not be further discussed in this thesis either.

Empirical retracking algorithms are based on pre-existing knowledge regarding the area of interest and may involve a "trial-and-error" approach to investigate what methods perform best to find the expected outcome (Dinardo, 2020). These type of retracking methods are typically applied for retracking water surface heights for inland water bodies as physical retracking can generally not be applied due to the complexity of specific landscape characteristics which cannot be theoretically approached or solved for (Dinardo, 2020). The benefits of empirical retrackers are their relative simplicity and small computational cost. However, the construction of such an empirical retracker is typically very labour intensive as it requires a lot of fine-tuning and optimisation.

2.3. Waveform Retracking for Inland Water Bodies

Deriving water surface heights from satellite SAR altimetry data is achieved in the process of waveform retracking (Dinardo, 2020; Villadsen et al., 2016; Rosmorduc et al., 2018). The typical return signal waveform differs for different terrain types. The waveform signal for inland water bodies differs fundamentally from the waveform return signal over oceans and over land. Kao et al. (2019) illustrated this nicely in their work, and figure 2.4 also presents a comparison of the different waveforms typical for the return signals over inland water bodies, ocean and land. The return signal waveform for inland water bodies typically consists of a single peak of significant signal power. This is trait especially prevalent when comparing with the waveform and the signal power of a terrestrial target. This distinctive characteristic can be used to the advantage of retracking water surface heights over inland water bodies.

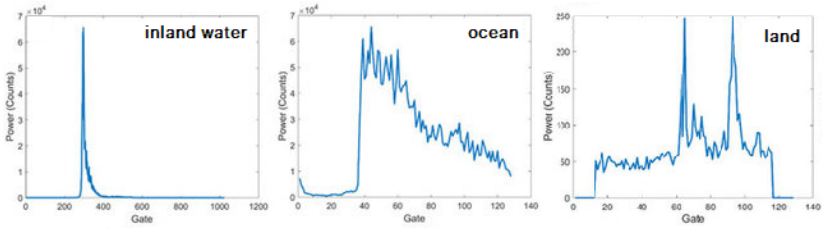

Figure 2.4: *Typical return signal waveforms over a) inland water bodies (CryoSAT-2), b) ocean (CryoSAT-2 LRM), c) land (SARAL/AltiKa) (Kao et al., 2019)*

A data point over an inland water body should provide a clear peak at the range gate corresponding to the surface height in the waveform at that location considering the signal is not contaminated by other bright scatterers or by land. Assuming the signal is symmetrical following and only showcases a single peak, the water surface height can then be derived roughly by locating the range gate at which this maximum peak is found Ehlers (2022). Lastly, these heights should then be corrected for geophysical phenomena such as atmospheric delays and tidal variations (Dinardo, 2020). It should be noted that this is an oversimplification of the basic principle, in truth it is a bit more complicated.

If it really were as simple as described before, deriving water surface heights from satellite altimetry data would have been very straightforward. As the topographical conditions of the landscape in which inland water bodies can be found vary widely, physical retrackers as used for open ocean water surface estimations can typically not be applied for inland water bodies (Villadsen et al., 2016), and has so far only been done by Kleinherenbrink et al. (2020). Often empirical retracking is required. However, several ocean retracker models such as the SAMOSA retrackers have been tested for application over large inland water bodies, such as big rivers and lakes. The best suitable retracking method is highly dependent on the characteristics of the inland water body and the surrounding landscape (Villadsen et al., 2016). Various different types of retrackers have been built and tested, such as the Multiple Waveform Persistant Peak (MWaPP) retracker by Villadsen et al. (2016), the Narrow Primary Peak Retracker (NPPR) as described by Villadsen et al. (2016) and Jain et al. (2015), the Offset Center of Gravity (OCOG) retracker (Gao et al., 2019; Rosmorduc et al., 2018), and the Threshold Retracker and Two-Step Physical-Based retracker by Gao et al. (2019). The latter of which was applied as a point target response retracker.

The theoretical derivation of inland water surface heights from sat-SARA data following equations from Dinardo (2020) entails:

$$IWH = H \cdot (TD \cdot c/2 + V_t \cdot c/2 + R_{cor}) \tag{2.2}$$

with:

IWH	-	inland water surface height
H	-	satellite altitude above reference ellipsoid
TD	-	two-way tracker time delay between pulse transmission and reference tracking point, corrected for instrumental effects
R_{cor}	-	geophysical corrections over land
c	-	speed of light in a vacuum
V_t	-	two-way time delay between retracking point and reference tracking point

Note that for this equation it is assumed that the instrumental corrections are already accounted for in the tracker delay. The geophysical corrections applied through R_{cor} will be further discussed in the next section on geophysical corrections.

2.3.1. Geophysical Corrections

The signal from which the two-way travel time is used for deriving the water surface height travels through the atmosphere twice. As the atmospheric conditions may vary over space and over time, the two-way travel time may vary despite any actual variations in the water surface height. The most straightforward example of this is humidity or rain, as water droplets in the atmosphere typically slow down a signal travelling through. These variations in time delay should be accounted for. In addition, tidal variations should also be corrected for to obtain the eventual estimated water surface height. The correction factors to be accounted for, for inland water surface height estimations are the dry troposphere, wet troposphere, ionic delay, solid earth tide and polar tide (Dinardo, 2020). All these factors are included in the R_{cor} term:

$$R_{cor} = T_{dry} + T_{wet} + I + ET + PT \tag{2.3}$$

With:

- T_{dry} - dry troposphere correction
- T_{wet} - wet troposphere correction
- I - ionospheric-delay correction
- ET - solid Earth tide correction
- PT - polar tide correction

The ionospheric delay is caused by the presence of free electrons in the ionosphere. Typically the correction for this is in the order of magnitude of $2 - 20\ cm$. The oxygen molecules in the dry troposphere are cause for the largest delay and hence requires the largest correction of approximately $2.3\ m$. However, this correction is typically relatively constant over space and time. The wet troposphere correction is dependent on water in the atmosphere such as clouds and rain. As this is dependent on weather conditions, it is highly variable through space and time. Hence it is the cause of a significant part of the spatial-temporal variability in the total geophysical correction. The magnitude of the wet troposphere correction is typically between $5 - 36\ cm$. The solid earth and polar tides are predictable periodic corrections for gravitational pull. Typically the corrections for the tidal effects require different (local) models over inland targets (Dinardo, 2020).

3

Materials & Methods

The materials and methods used for this research can roughly be divided into two separate parts as these are fundamentally different and require knowledge from two different fields of study. These two different parts comprise the handling of remote sensing data and the hydrological field observations. Hence, this chapter contains a description of materials and methods applied for obtaining sat-SARA-derived water levels, sat-SARA-derived multiple channel identification, and for the collection of field observation measurements of water surface heights, flow depths and river widths in the Bheri, Karnali and Geruwa Rivers. Finally, the methods applied for comparing the different data sets are discussed in this chapter.

3.1. Sat-SARA Data Selection

A multitude of current and historic missions provide a variety of satellite altimetry data. For this thesis, however, satellite Synthetic Aperture Radar altimeter data (sat-SARA) was used. To this date, only a handful of missions provide sat-SARA data. These are the CryoSat-2, Sentinel-3 and Sentinel-6 missions (Roohi et al., 2021; Villadsen et al., 2016; ESA, 2011, 2022; Donlon et al., 2021). For the current work, it was decided to only use data from the Sentinel-3 and Sentinel-6 missions. This section elaborates on the available data and presents the materials selected for this study, including a justification for the choice of this data.

3.1.1. Sentinel-3

The Sentinel-3 mission is a collaborative effort between ESA, the European Commission (EC) and EUMETSAT. The purpose of the mission is to monitor Earth's oceans, land surfaces and atmosphere by providing accurate, timely and continuous Earth observation data. The Sentinel-3 mission is part of the Copernicus program and consists of a two-satellite constellation. Sentinel-3A was launched on 16 February, 2016. Followed by Sentinel-3B, which was launched two years later on 25 April, 2018. Sentinel-3B was launched to ensure better temporal resolution (by ensuring better continuity, shorter revisit times and a greater global coverage). Both satellites contain a range of instruments to collect various types of data, including the OLCI, SLSTR, SRAL and MWR instruments. The relevant instrumentation for satellite altimetry is the SRAL (Synthetic Aperture Radar Altimeter) instrument. The data used for the current thesis were the 20Hz SRAL tracking measurements (Ku-band) performed in the SAR operating mode.

3.1.2. Sentinel-6

The Sentinel-6 mission includes two satellites: Sentinel-6A and Sentinel-6B. The Sentinel-6A satellite was launched on 21 November 2020 (Donlon et al., 2021). Sentinel-6B is scheduled for launch in 2025 (ESA, 2023). Hence, at the time of writing only data from Sentinel-6A is available and therefore when referring to Sentinel-6 (or S6) it can be assumed that Sentinel-6A is meant. The primary instrument for SAR altimetry measurements by the Sentinel-6 is the Poseidon-4 (POD4) altimeter (EUMETSAT, 2022; Donlon et al., 2021). Other than Sentinel-3 and its SRAL instruments, this dual-frequency (C-band and Ku-band) nadir-pointing radar altimeter has an interleaved mode allowing for greater spatial resolution and overall performance improvement (Donlon et al., 2021; Rosmorduc et al., 2018). This enables data processing in two parallel chains. The first one allowing for SAR-processing in the Ku-band for improving along-track sampling, the second providing a Low Resolution Mode (LRM) which is backward compatible with current and historic data. This allows the Sentinel-6 mission to ensure enhanced continuity from the Topex Poseidon and Jason series of satellite altimeters (Donlon et al., 2021; ESA, 2023).

The interleaved mode of Sentinel-6 refers to the open-burst transmit and receive approach, which provides twice the number of samples as compared to the Sentinel-3 SRAL instrument which operates with a closed-burst approach(Donlon et al., 2021). For the closed-burst approach, pulses are transmitted in high PRF to ensure the pulses in the transmitted and received burst are correlated. After transmitting an inter-burst interval allows for the reception of all the reflected pulses from the entire burst (Dinardo, 2020). For the open-burst approach of Sentinel-6, the transmission of pulses is arranged such that the reception occurs in between the transmitted pulses to allow for an increase in the number of measurements over a given target. This timing allows for a doubling in the number of available looks for the SAR mode and allows SAR acquisition simultaneously with the LRM data acquisition (Donlon et al., 2021). Figure 3.1 illustrates this difference in transmit & receive approach for Sentinel-3 and Sentinel-6 in their so-called chronograms.

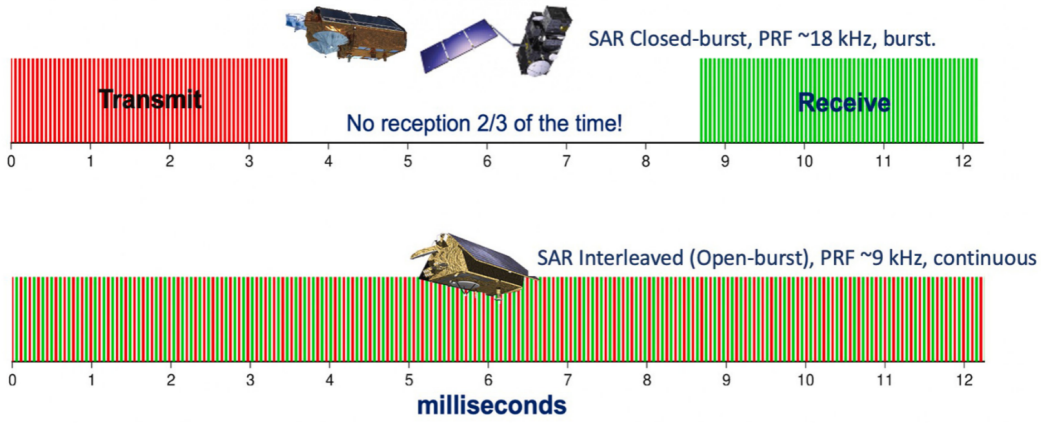

Figure 3.1: *Satellite radar altimeter chronograms showing the transmit and receive times for the open-burst approach of CryoSat-2 & Sentinel-3 and closed-burst approach of Sentinel-6 (Donlon et al., 2021)*

Whilst the Sentinel-6 data comprises 512 range bins or range gates, Donlon et al. (2021) state that after first commissioning 128 of these bins are removed from the waveform trailing edge. Hence, on-board operations may cause 'empty' data in the trailing edge of the signal in the higher range bins. These operations are put in place to save data volume, to ensure proper satellite operation and to mitigate data loss due to too much data downlink. Please refer to Donlon et al. (2021) and EUMETSAT (2022) for further details. The key takeaway is that his may cause data to be only available for the fist 300-350 range bins. As a result, despite Sentinel-6 recording return power up to range gate 512, the last range gates are empty of data, and thus the return signal waveforms for S6 data were plotted only up to range gate 300.

3.1.3. Data Selection & Justification

For both Sentinel-3 and Sentinel-6, raw level-1 data was needed for deriving the return signals. In addition, level-2 data was needed for the retrieval of geophysical corrections. The selection of the data was also dependent on (spatial) variability: for the different selected sites, data was available from different satellites. The site selection is further elaborated upon in section 3.1. An overview of mission-specific parameters is presented in table 3.1.

Parameter	**Sentinel-3**	**Sentinel-6**
Tracker range TR (km)	$\sim$ 805.78	$\sim$ 1343.54
Satellite velocity V (km/s)	$\sim$ 7.544	$\sim$ 6.97
Burst repetition frequency BRF (Hz)	$\sim$ 78.5	$\sim$ 139.26
Pulse repetition frequency PRF (kHz)	$\sim$ 18	$\sim$ 9
Chirp bandwidth B (MHz)	320	320
Carrier frequency f_c (GHz)	13.575	13.575
Chirp slope s $(10^{12}$ $Hz/s)$	7.143	10
Number of pulses in burst N_b	64	64
Burst duration T_b	N_b/PRF	N_b/PRF
Number of range gates N_{rg}	256	512

Table 3.1: Mission parameters. Values noted with "$\sim$" are rounded. *H* & *V* are example values picked from track segments, these may vary over the orbit. *PRF* and *BRF* may vary for Sentinel-6 as well

The choice of only using Sentinel-3 and Sentinel-6 data for this study was made for a couple of reasons. Firstly, the improved along-track resolution provided by the SAR-mode (approximately 0.5 meters for both Sentinel-3 and Sentinel-6) is beneficial for inland water applications (Tarpanelli and Benveniste, 2019; Rosmorduc et al., 2018; Dinardo, 2020). While the ICESat-2 mission provides a high spatial resolution (both along-track and vertically), the downside of the laser altimeter is that it is sensitive to clouds (Tomić and Andersen, 2023). Hence, no useful elevation data can be collected on cloudy days, as the signal cannot penetrate the clouds. Since the study area is very prone to clouds, especially during the wet season and the winter months, satellite SAR altimetry was deeper best suitable for the current work. This as sat-SARA allows for studying the seasonal variability of water surface heights in the area of interest, at a high spatial resolution.

As mentioned before, (open-source) data products are currently available only from three sat-SARA missions. Although CryoSat-2 provides the longest time-series data catalogue, providing data from 2010 onward, its data was not used for the current work. With a return period of 369 days (Roohi et al., 2021; ESA, 2011), the temporal resolution of CryoSat-2 was deemed insufficient . This long return period does not allow for studying seasonal variability, which is what was required for the current thesis. With a return period of 27 and 10 days for Sentinel-3 and Sentinel-6 respectively (Donlon et al., 2021; ESA, 2022), these missions do allow for studying and monitoring seasonal variability.

Of these two, Sentinel-3 has the longer time-series data catalogue with Sentinel-3A providing data from 2016 onward and Sentinel-3B from 2018 onward, whilst for Sentinel-6 data was only readily made available for 2021 and the first 4 months of 2022. Data from after April 2022 was still being (re-)processed by EUMETSAT at the time of writing. To gain insight into seasonal patterns, Sentinel-3A and -3B data was studied for the full years of 2021 and 2022. In addition, Sentinel-6 data for 2021 was studied. Although a longer data catalogue was available for Sentinel-3 data it was decided two years would suffice for gaining insight in the seasonality of the water levels in the area.

3.1.4. Data Retrieval

Sentinel-3A and Sentinel-3B Level 1 and Sentinel-6 data were retrieved from the EUMETSAT data store using their API (eumdac). A brief manual was written for Sentinel-3 data retrieval through their API in combination with the Python (Anaconda) prompt (see appendix A). Level-2 data of Sentinel-3A and Sentinel-3B was used to retrieve the values for geophysical corrections, as the information was not provided directly by the Level-1 data products. The level-2 data could not be retrieved from the EUMETSAT databases. Level-2 Sentinel-3 data is categorized into marine and land products, with EUMETSAT responsible for managing and providing access to marine data, and ESA manages the land data, made available through the Copernicus Scihub. As for this thesis water surface heights of inland water bodies were studied, the geophysical correction values had to be retrieved from the level-2 land products through the Copernicus Scihub.

It is expected that improved quality level-2 data for inland hydrology will be available in the near future, as at the time of writing ESA is reprocessing the land products into the new land hydrology product. For Sentinel-6 data the geophysical correction values also had to be derived from level-2 data. The Sentinel-6 level-2 data were also made available and downloaded through the Copernicus Scihub.

3.2. Materials for Field Observation Data Collection

In this section the measurement equipment used for field observation data collection is presented. First equipment used to collect absolute water surface heights and relative water levels is presented, followed by stage height data and the collection of flow depth measurements. **An overview of the equipment including pictures of the devices can be found in APPENDIX - refer & add**.

3.2.1. Absolute Water Surface Heights

For measuring the absolute water surface heights a custom-made differential GNSS device was used (Krietemeyer et al., 2022). This device is also referred to as the "GNSS-Rover". It was built by Hessel Winsemius and previously used in the work of van Haaren (2020). As the GNSS-Rover makes use of two separate GNSS receivers it allows for the correction of atmospheric uncertainties in the signal. With up to centimetre accuracy, this allows for much greater accuracy as compared to conventional handheld GPS systems. Conventional GPS systems typically have a horizontal accuracy in the range of a couple of meters with up to several tenths of meters in the vertical. The high accuracy of the differential GNSS device holds for both horizontal (latitudinal, and longitudinal) positioning as well as vertical positioning (altitude). (Samboko et al., 2021). The relatively low cost of the GNSS-Rover makes it a favourable choice over other (GPS) devices which can reach similar accuracy but are typically much more expensive. The drawback is that the GNSS-Rover is custom-made equipment and hence limited support is available. Unfortunately, during the field campaign, the GNSS-Rover did not work as anticipated. It was not possible to set up the device such that measured data could be read from a mobile app or downloaded to a computer.

An alternative solution was the use of handheld GPS devices. With an accuracy of a couple of meters in the horizontal and up to 10-20 meters in the vertical plane, the handheld GPS devices were not suitable for measuring the water surface heights for which an accuracy of up to a couple of decimeters was required. The handheld GPS devices were used for positioning in the field, recording the location of field observation sites.

3.2.2. Relative Water Surface Heights

During the field campaign, relative water surface heights were measured using a handheld triangulation laser rangefinder. For this the Nikon Forestry Pro ii (also referred to as NFP) was used. The NFP was originally designed to measure the height of trees but can be generally used for measuring horizontal distance, actual distance, height, angle and vertical separation with the use of two laser sensors (Nikon, 2019). This allowed the device to be used for different applications during the fieldwork, including the measurement of relative (water surface) heights and river widths.

3.2.3. Stage Height

Stage height measurements from a staff gauge at a measurement station at Chisapani were made available by the Department of Hydrology and Meteorology, Government of Nepal. This includes a time series from 1 January 1992 up to 31 December 2018 with typically 3 recordings of the observed water level per day.

3.2.4. Flow Depth

During the field campaign, multiple tools were used for measuring flow depth. Firstly, the sonar device *Fish Deeper CHIRP+* (Deeper, 2020) was used to measure flow depth continuously over full transects. Another sonar device used for the manual, discrete measurement of flow depth was the *Hawkeye* (HawkEye, 2023) handheld depth finder. Lastly, in more shallow sections of the river, flow depth was measured manually using measurement tape. For

long-term flow depth measurements, electronic water level loggers (TD-Diver) and an atmospheric pressure logger (Baro-Diver) were installed (vanEssen, 2023). It should be noted that results from the water level loggers were not yet available at the time of writing and are hence not included in nor elaborated upon further in this thesis.

3.3. Complementary Data for Contextualisation and Site Selection

For data interpretation purposes additional spatial data was used from several sources. Firstly, administrative geospatial data was collected including country borders, national park borders and Nepal's water bodies as provided by the Nepal government. The 30-meter resolution SRTM (Shuttle Radar Topography Mission) digital elevation model (DEM) was collected from NASA's Earthdata open database. This DEM was used in combination with the ESRI topographic map to generate the topography maps presented throughout the report. The theoretical satellite ground tracks for Sentinel-3 and Sentinel-6 were collected from the ESA website. These were used for site selection and applied in map visualisations. Map visualisations were created with QGIS. In addition, Google Earth Pro was used for rough distance estimations and orientation in support site selection and in support of the multiple channel identification analysis.

3.4. Sat-SARA Site Selection

Site selection for the satellite-SAR Altimetry analysis was constrained to the locations at which the Sentinel-3A (S3A), Sentinel-3B (S3B), and Sentinel-6A (S6A) satellites pass over the river reaches within the study area. Hence, for the selection of the sat-SARA analysis sites, the theoretical ground tracks of the satellites were studied (see figure 3.2).

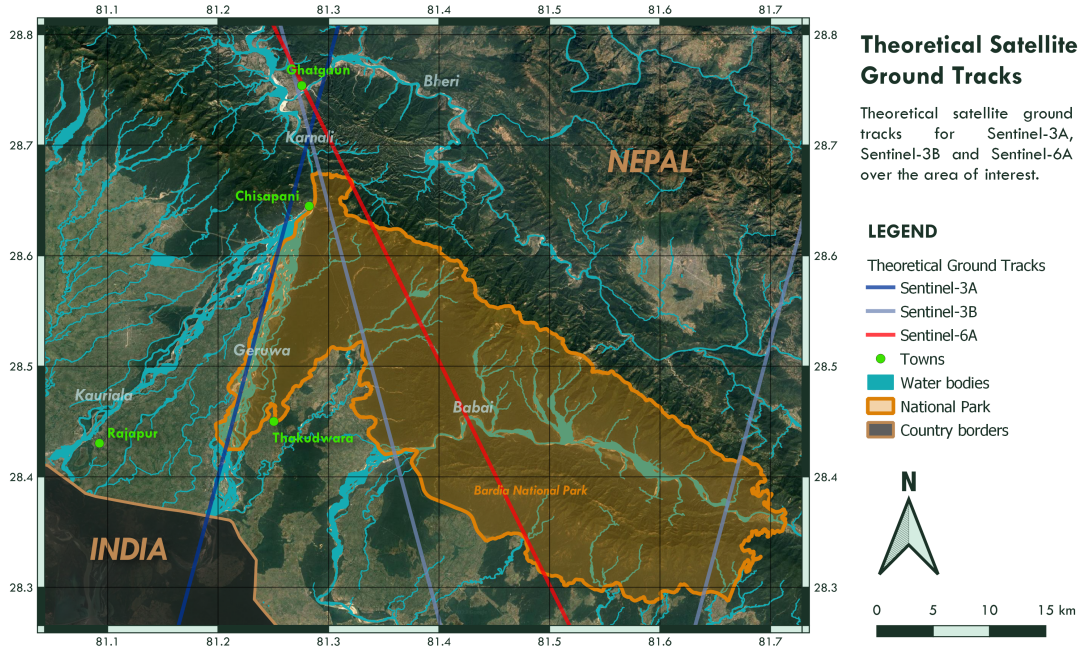

Figure 3.2: *Theoretical Satellite Ground Tracks of Sentinel-3A, Sentinel-3B, and Sentinel-6A over the study area*

For both Sentinel-6A and Sentinel-3B only one river overpass location was found within the study area. Therefore, these overpass locations were both selected: BH01 and BH02 for S6A and S3B respectively, passing over the Bheri River. As the trajectory of Sentinel-3A follows the course of the Geruwa River, and the Geruwa River consists of a braiding system containing a multitude of river channels, the satellite passes over the river at multiple locations within the study area. Therefore, for selecting the most suitable site in the Geruwa River, a few additional criteria were taken into account which will be further discussed below.

Firstly, the presence of other water bodies which could interfere with the signal, other than the Geruwa River reach itself, was considered. These water bodies included for example open irrigation canals in the Northern region of the Rajapur agricultural area. The proximity of other water bodies to the targeted river reach could complicate data interpretation as these water bodies will also appear as (signal power) peaks in the data (Ehlers, 2022; Villadsen et al., 2016). This poses challenges for identifying the targeted water body. Consequently, selecting an overpass of S3A over the Geruwa River in a single-branched river section ensured data quality and minimised the risk of signal contamination from nearby branches or water bodies. An overview of the resulting selected sites for which to apply the sat-SARA analysis is shown in figure 3.3 and an overview of selected data for these sites in appendix D.

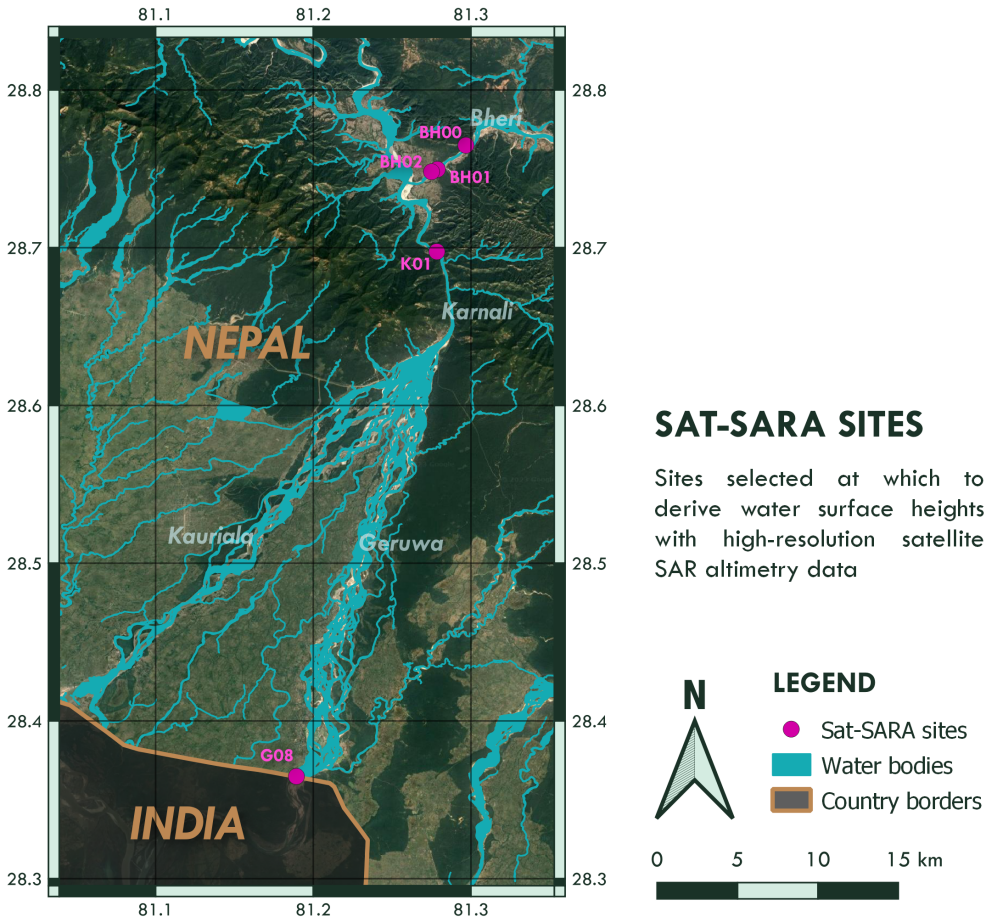

Figure 3.3: Selected Sites for Sat-SARA Analysis

The abundance of satellites carrying SARA instrumentation passing over the rivers within the study area offers great potential for studying and monitoring water levels within the region. The derivation of water surface heights from sat-SARA at different sites allows for a comparison between the sites. A multitude of available overpasses also increases the chance of finding a site where in-situ water level data can successfully be collected. Lastly, Sentinel-3A, Sentinel-3B, and Sentinel-6A all pass over the same downstream section of the Bheri River in near vicinity of each other. This allows for a comparison of data obtained from the three different satellites.

3.5. Methods for Multiple-Channel Identification with Sat-SARA

To investigate the potential of using satellite-SAR altimetry for identifying multiple channels in a river reach, the return signals were studied over part of the satellite trajectory in the area of each selected overpass site. To this extent, the level-1B SAR return signals were plotted on a logarithmic scale in a so-called echogram. The level-1B data used to this extent was the same as used in the steps for deriving inland water surface heights. For all data processing methods and specifics, please refer to section 3.6 An echogram is a graphical representation, displaying the return signal power (radar echo) as a function of range and time or along-track distance (Ehlers, 2022). In this study the the latitudinal position was depicted on the y-axis and the range bin (or range gate) on the x-axis.

The echogram illustrates the power of the return signal (larger power appears brighter), which typically appears bright for water bodies. Following the conical shape of the radar pulse this means that that multiple water bodies could appear at different range gates for the same data point or at the same latitude. A water body located closer to the satellite should appear at a low range gate, whereas a water body farther away should appear at a larger range gate (Ehlers et al., 2023b). For a satellite trajectory which follows a river stream in latitudinal direction, such as is the case for Sentinel-3A in the Geruwa River section, it should then hold that multiple channels that run approximately perpendicular to each other may appear (bright) on the echogram, at the same latitudinal location at different range gates.

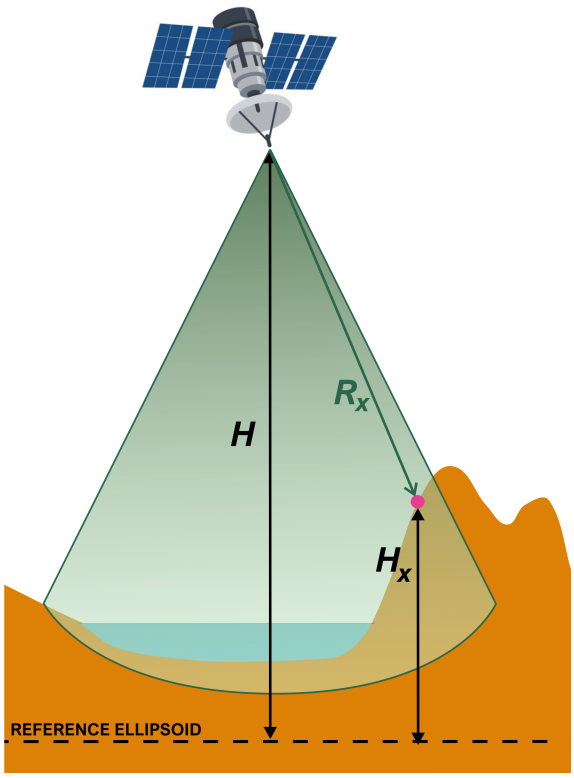

Figure 3.4: Visualisation of the effect of irregular terrain on return signals

In order to comprehensively interpret the echograms in their spatial (and temporal) context, it is vital to grasp the nuanced meanings of 'closest to the satellite.' This encompasses not

only the proximity nadir to the satellite, hence the elevation as can be observed directly below the satellite, but may also mean closer due to a stream running along a hillslope. This principle is visualised in figure 3.4, assuming the pink point X would indicate the location of a water body. Hence, to effectively interpret the echograms, a firm comprehension of the local topography surrounding the satellite's trajectory becomes imperative.

This distinction becomes particularly pertinent in areas with more irregular topographies such as the Karnali and Bheri River sections. This is where the significance of the field campaign becomes apparent, as it offers a better understanding of the landscape characteristics near the satellite overpasses. The methods for the field campaign will be further elaborated upon in section 3.7. Additionally, the local digital elevation model (DEM) were also visualised to contextualise the echograms further.

Lastly, it should be mentioned that another anomaly caused by a tracker offset may be apparent in the data. This is easily recognisable but should be taken into account to avoid misinterpretation. Over topographic surfaces, the onboard tracking system of a radar altimeter is typically unable to maintain the return signal waveform at the nominal tracking position, due to rapid range variations. As a result, the range window is shifted, resulting in an error in the telemetered range: the tracker offset (Rosmorduc et al., 2018). In an echogram of a continuous river stream, this manifests itself as a distinct shift in the range gates at which the feature appears.

The methodology utilised for the multiple channel identification analysis intended to assess whether or not it was possible to identify multiple inland water bodies from the SAR return signals. To this extent, the echograms were examined for telltale patterns typical for water bodies. For instance, a river is expected to exhibit the characteristic trait of a continuous stream in the echogram.

It should be noted that the height of these water bodies could not directly be derived from the echogram images, except for the exact locations where the satellite passes over a given river branch; in other words, for locations where the river is exactly nadir. Additionally, the exact location of the water bodies with respect to each other could not be determined directly as location can only be determined for a nadir target. Potentially, these altitudes and distances could be derived with the support of a DEM. However, this was out of the scope of the current work.

Another notice that should be taken is that the echogram is not a direct visualisation of latitude and elevation. Rather, the elevation of a river branch nadir to the satellite could be derived from a single signal return waveform using a retracker. Moreover, the exact location of the water bodies with respect to each other cannot be derived directly from the echogram either. Although river widths have been derived from SAR return signals before by Yuan (2019). This suggests that it may be possible to derive the distance between river branches from the SAR return signal and provided mission parameters in combination with a DEM. The takeaway here is that these inter-channel distances cannot be directly read from the echogram. Derivation of these distances could be an interesting follow-up topic to the

current study.

The multiple channel identification analysis was applied for all selected overpass sites. For Sentinel-3A/B only echograms for unfocused-SAR (UF-SAR) were generated and analysed for each overpass site. In theory, FF-SAR should allow for higher along-track resolution for continuous pulse data as provided by Sentinel-6A. However, this increase of along-track resolution may not be of considerable extent for burst-pulse data as provided by the Sentinel-3 mission. For Sentinel-6A at overpass BH01, both UF-SAR and FF-SAR echograms were compared, as considerable along-track resolution improvement was expected. Note that for Sentinel-6 only data for a full year was available for the year 2021. Note that for the 'dry season' and 'wet season' plots, the months were chosen with the lowest and highest estimated water surface heights respectively, as derived from the sat-SARA water surface height estimation time series.

3.6. Methods for Water Surface Height Derivation with Sat-SARA

In order to derive water surface heights from the Sentinel-3A/B SRAL and Sentinel-6A POD4 products, extensive data processing was required, following multiple steps. The steps to be followed and their (theoretical) contents for processing sat-SARA data has been discussed before in chapter 2. An overview of the steps as taken for this thesis is presented in figure 3.5. These steps will be further elaborated upon in this section.

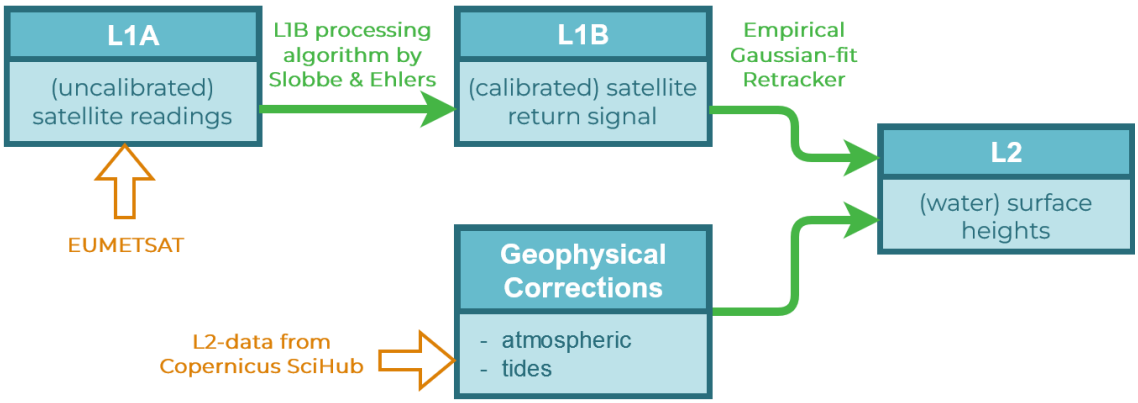

Figure 3.5: *Satellite SAR altimetry processing steps*

3.6.1. Pre-Processing (L1A to L1B)

The SAR data for Sentinel-3 and Sentinel-6 were retrieved as discussed in section 3.1.4. The level-1A products contain the raw satellite instrument reading data. Software provided by D.C. Slobbe and F. Ehlers was used to process the data from level-1A to level-1B, obtaining the UF-SAR and FF-SAR return signals, tracker range, satellite altitude and other spatial data required for positioning in space and time such as latitudinal and longitudinal coordinates. For the pre-processing of the L1A to L1B data the processing settings as presented in table 3.1 were applied.

Waveform averaging for altimetry signal processing is applied to reduce noise and improve

the signal-to-noise ration (SNR) in altimetry data. Multiple echoes (waveforms) received by the altimeter are averaged together to create a single, smoother waveform. It reduces random noise, while preserving the underlying signal. Waveform averaging is not really a concept for UF-SAR signal processing as averaging happens over the stack. For FF-SAR processing, neighbouring waveforms are averaged to reduce the very dominant speckle noise in the radargram (Ehlers et al., 2023a). Windowing in altimetry signal processing is applied to reduce or eliminate discontinuities, typically at the trailing edge of the signal to reduce leakage. For Sentinel-3 L1A to L1B processing, a Hamming window was applied. For Sentinel-6 L1A to L1B processing, windowing was turned off.

3.6.2. Waveform Retracking

Waveform retracking was applied on the UF-SAR return signals for the derivation of water surface heights. The FF-SAR data was not used for retracking, however. The L1B FF-SAR data was only used for spatial resolution comparison with the UF-SAR data and to investigate the potential for multi-channel identification.

An empirical retracker was built to derive the water surface heights from the return signal (waveform) at the selected overpass locations. In chapter 2 on the theoretical background of sat-SARA, the basic principles of retracking water surface heights has been discussed. Simply put, the water surface height can be derived from the range gate at which the maximum power for an inland water return signal waveform can be found. However, rather than finding the integer value of this range gate by simply applying a maximum peak algorithm, a Gaussian fit model was applied (like in the work of Gao et al. (2019)) to find the decimal range gate value for which the maximum peak value was found (see equation 3.1). This allowed for a larger overall accuracy. The distance between each of the range gates is approximately 23 centimetres for Sentinel-3A/B and approximately 18 centimetres for Sentinel-6. Hence, when simply applying a maximum power method, an uncertainty of 23 and 18 centimetres for Sentinel-3 and Sentinel-6 respectively is already inherent to the outcome.

$$y(x) = \frac{a}{\sigma\sqrt{2\pi}} \cdot \exp -\frac{(x-\mu)^2}{2\sigma^2} \tag{3.1}$$

with:

- x - the to be fitted curve
- a - amplitude; the maximum value found for the peak to fit to
- σ^2 - variance; with chosen value $\sigma = 2$
- μ - expected value; chosen to be the range gate at which the maximum value for the peak was found

Applying a Gaussian fit model entails the assumption that the return signal of the inland water signal is symmetrical. This is a simplification of the truth, as an inland water signal does contain a trailing edge (see 2.4). The location of the peak of the Gaussian fit is used to estimate the radar altimeter retracked range R (or range gate) for the inland water signal, which in turn is used to derive the water surface height. The retracking algorithm was based

on the theory as described in section 2.1, using the satellite altitude, satellite reference range, tracker range, the range measured at maximum signal power and the distance between the range gates. All these parameters were provided as output of the pre-processor for the L1B data. The estimated (inland) water surface height was computed following:

$$IWH = H_{sat} - (R + R_{cor}) \tag{3.2}$$

with R, the radar altimeter retracked range:

$$R = TR + \delta r \tag{3.3}$$

and:

$$\delta r = (RG_{peak} - RG_{ref}) \cdot \delta RG \tag{3.4}$$

with:

IWH	-	inland water surface height
H_{sat}	-	satellite altitude above reference ellipsoid
R_{cor}	-	geophysical corrections (see equation 2.3)
TR	-	satellite tracker range
δr	-	distance measured from range difference
RG_{peak}	-	range gate at maximum signal power
RG_{ref}	-	reference range gate
δRG	-	distance between range gates

This retracking algorithm was applied in combination with the Gaussian fit, to specific targeted locations. These targeted locations were situated in the main channel at the selected overpass sites. This is thought to increase accuracy as it reduces the (risk of) land contamination (Rosmorduc et al., 2018). Downsampling was applied to reduce computational cost, providing a data point for every approximate 9 meters along-track. The nearest neighbour data point from the targeted location was then employed for retracking. Hence, an empirical point target response retracker with a Gaussian fit model was implemented for retracking the inland water surface heights.

3.6.3. Application of Geophysical Corrections

The geophysical correction values were obtained from the level-2 data of Sentinel-3 and Sentinel-6 as made available through the Copernicus Scihub. Atmospheric corrections were applied for the dry troposphere, wet troposphere and the ionospheric delay. Tidal corrections were executed for the solid earth and polar tides. A short analysis of the significance of each of these correction values for monitoring relative water level variability was done. The objective for this analysis was to investigate whether the variability of these corrections was of sufficient magnitude to have a significant influence on the estimated water surface height

variation through space and time. From this it was assessed whether the application of the corrections was relevant for monitoring (relative) water level variability. Considering that the correction values were obtained from a different data source, omitting the correction values could simplify the data handling process.

3.7. Methods Field Observation Data collection

To assess the accuracy of the water surface heights derived from satellite SAR altimetry data field observation data is required for validation. As mentioned before, no in-situ stations measuring water surface height are currently present in the area of interest. Hence, such field observation data would have to be collected through field campaigning. To this extent, a field campaign was carried out in November 2022. This was part of the first full field campaign executed within the Save the Tiger project, during which the area of interest was explored for suitable measurement locations, collaboration with local organisations was established and the first data for various hydrological and hydrodynamic data types were collected.

Whereas in the introduction all objectives of the fieldwork were presented, this method section elaborates upon the methods for the collection of water surface height, flow depth and river width data. This is because only these data types are considered relevant for the current study. The methods for all data types are described in full in the field report (see appendix I). In this section, first, the selection of the field campaign sites is discussed, followed by the methods applied for the collection of data for the various data types.

3.7.1. Site Selection

The selection of field campaign locations was based on two factors: hydro- & morphodynamic relevance and the availability of satellite SAR data. As the overall research aims at understanding and modelling the hydrodynamic and morphodynamic behaviour of the Karnali Fluvial fan the field campaign locations should be chosen such that the measurements at these locations contribute to a representative data set. Therefore, the campaign locations along the bifurcation area, the Geruwa River, and the Kauriala River have been chosen at an interval of approximately 5 km distance along the river. This provided a set of areas of interest for reconnaissance for the eventual measurement site.

For the exact site selection, emphasis was placed upon ensuring the representativeness of the location for the hydro- and morphodynamics in that river section. To this extent, the main factors considered in the selection were the number of present river channels, flow velocity and potential obstructions of flow. Preferably a field campaign site would be situated at a location where the river reach only consisted of a minimal number of channels (preferably one or a maximum of two). Most sites proved only to be suitable for a selection of data collection methods, depending on hydrodynamic, morphodynamic, and/or landscape characteristics. Note that all visited field campaign locations are presented. However, not all of these visited locations are relevant for the current study, as the field campaign also included the collection of data for purposes outside of the scope of the current work.

Secondly, the availability of satellite SAR data was decisive for site selection. To this extent,

the theoretical orbital ground tracks of the Sentinel-3A, Sentinel-3B and Sentinel-6A were studied (see figure 3.2). From this areas of interest for exploration for suitable field campaign sites were selected (see appendix C).

During the field campaign, the visited and to be visited locations were also assessed on their accessibility. This was also decisive for timing of visitation for certain campaign locations. The accessibility of each of the campaign locations is more extensively elaborated upon in the field report (see appendix I). It should be noted however, that the field campaign locations near the Bheri and Karnali confluence are difficult to reach and expected to be inaccessible when reaching from the South during monsoon season. Generally, the criteria to assess the suitability of a site during the field campaign were:

- Accessibility of area, and the required logistics to reach it.
- Accessibility of the river bank
- Safety with regards to dangerous wildlife
- Potential for applicability of the measurement tools at hand

The sites selected and visited during the field campaign are shown on a map presented in figure 3.6. A map used prior to the field campaign with the locations selected for explorations can be found in appendix C. Note that the locations selected for the sat-SARA analysis were also all visited during the field campaign, except for sat-SARA site BH00, which is the Sentinel-3A overpass over the Bheri River.

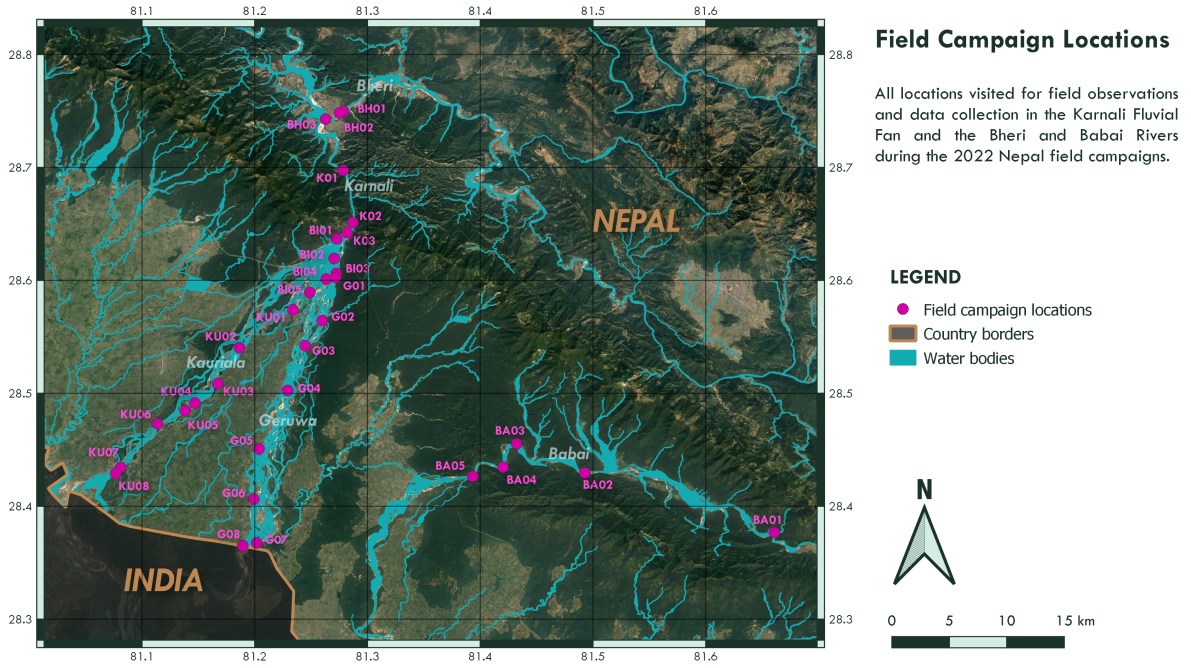

Figure 3.6: Sites selected for and visited during the 2022 field campaign, along the Bheri, Karnali, Geruwa and Kauriala Rivers, Nepal

3.7.2. Field Observation Data Collection

Unfortunately, not all data types could be collected at every field campaign site, due to accessibility, landscape or river reach characteristics or logistical limitatations. The field report contains a more extensive elaboration upon these limitations and decisions, including maps showing the locations at which each data type was collected.

Water Surface Heights

Different methods were used in an attempt to measure absolute and relative water surface heights in the Bheri, Karnali, and Geruwa Rivers. Firstly, it was desired to measure absolute the water surface heights in-situ using a differential GNSS setup as described in the methods section. Unfortunately, the GNSS-rover proved faulty during the fieldwork and hand-held GPS devices did not provide sufficient accuracy. Therefore, with the equipment at hand, it was possible to measure relative water surface heights only.

At all visited campaign locations, the exact position was also recorded using a handheld GPS-device. This was done mostly to be sure to have some sort of positioning recording for all campaign locations. It should be noted, however, that a varying set of handheld GPS devices and mobile apps was used to this extent. The accuracy of the measurements in the vertical direction was too low for determining water surface heights in the field.

In addition to the aforementioned GPS and GNSS methods for determining the exact water surface height, also relative water surface heights were determined. This was achieved using the Nikon Forestry Pro (NFP). With this device horizontal distance, height, height differences and angles could be measured. This allowed for using the NFP to estimate the vertical distance between a fixed point in the landscape and the water surface of the river (see figure 3.7). For this, it was important to choose a fixed point in the landscape for which with certainty could be said that the elevation would not change through time. In other words, a location outside of the active floodplain had to be chosen, as low and high flows, and especially floods during monsoon season could cause morphodynamic changes within the active floodplain.

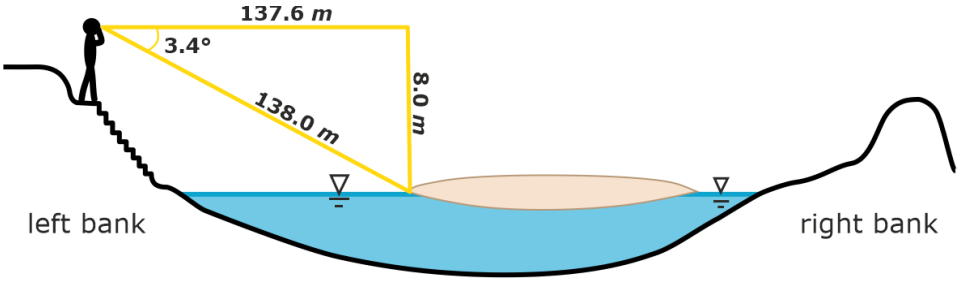

Figure 3.7: *Method for measuring relative water surface heights with the NFP*

This method allowed for the estimation of water levels relative to the landscape and hence could provide information about water surface heights relative to maximum water surface heights during full bank flow and floods. The relative vertical heights could simply be measured by pointing the NFP from the fixed point in the landscape to the river bank, just above

the water surface. The device itself would provide the vertical, horizontal and diagonal distance from the fixed point to the selected measurement point, and the angle under which was measured (following Pythagoras). As the distances were measured from eye height, only the height from the ground to eye height had to be corrected for. It is estimated that this method resulted in relative water surface heights with an accuracy of a couple of centimetres up to one or two decimeters.

If sufficiently accurate horizontal positioning is recorded and with the use of a (high resolution) DEM, the height of the fixed point and hence of the absolute water surface height could then be derived. Since no sufficiently accurate horizontal positioning and DEM's of lower resolution were available, it was decided not to derive the exact water surface heights from the collected data, and only use the relative water surface heights for further analysis. The NFP measurement device also allowed to measure the river width at most of the field campaign locations, with a range up to approximately 350 meters

Relative water surface heights were measured using this method at the campaign locations: K02, K03, BI03, G01, G03, G04, G06, G08, KU02, KU01, KU06, KU07 and KU08 (see also appendix I).

Flow Depth

The flow depth measurements used for this thesis, were measured using measurement tape or a handheld sonar device. Each of these measurements was part of a full transect measurement, measuring flow depth along a transect parallel to the river flow. At most locations, the flow depth was measured at every 2 meters along the transect. The sites for which these flow depths were collected were mostly located along the Geruwa River, as the Geruwa typically showed much lower flow depths and flow velocities, and hence allowed for crossing on foot or by raft. The locations for which the flow depths were recorded with this method include BI03, G01, G02, G04, and G06 (see appendix I).

In addition, flow depths were measured using the Fish Deeper CHIRP+ sonar device. This device was attached to a fish line and dragged along a transect across the river, approximately parallel to the flow direction. The device then performed continuous flow depth measurements along the transect, generating a cross-sectional profile of the river. For the current work, flow depth measurements from this method were only used for the locations BH01 and G08 (see appendix I for the full overview).

Stage Height

As discussed before, stage height measurements were made available by the Department of Hydrology and Meteorolgy (Government of Nepal) for Chisapani. The measurement station is located at the K03 site. These stage height measurements can be interpreted as relative water surface heights and were to that extend used to compare with other water surface height estimations and observations at K03 and other sites in the study area.

4

Sat-SARA and Field Observations

This chapter presents all the results from the satellite SAR altimetry analysis for deriving water surface heights and for multiple channel identification, as well as the field observation data regarding river widths, flow depths and (relative) water surface heights. For the presentation of the results, the region was divided into three river reaches, the Bheri River section, the Karnali River section, and the Geruwa River section. The results are presented for each of these river reaches respectively.

To contextualise the presentation of the data, a general description of the landscape characteristics is provided for each river section. A more specific description of the direct surroundings of the satellite overpass site is then given additionally. These descriptions include pictures taken during the field campaign as well as a map of the local topography in the orientation of the theoretical satellite trajectory ground track. Note that part of the area descriptions are retrieved from the field report (appendix I).

The observations are then presented, starting by showcasing the echograms that support the multiple channel identification analysis. To this extent, for Sentinel-3 the analysis was applied only to the 2022 data. The echograms for 2021 can be found in appendix F. The echograms for 2021 and 2022 are fairly similar and the data for 2022 was chosen as this enables comparison with the observations from the 2022 field campaign. For Sentinel-6, data was only available for a full year for 2021. Hence, Sentinel-6 echograms are presented for 2021.

The derivation of the water surface heights was based on the sat-SARA return signal waveforms at the overpass locations. The waveforms are presented for each of the exact overpass locations, for the dry (depicted in orange) and wet seasons (depicted in blue) of 2021 and 2022, and for the field campaign in November 2022 (depicted in green). The waveforms are plotted as signal power (on the y-axis) against the range gate (on the x-axis). Presenting only the waveforms for these moments in time allowed for easy interpretation. Note that enlarged plots can be found in appendix E for closer inspection.

A time series of the water surface heights derived with the PTR gaussian retracker from these sat-SARA return signal waveforms is presented for the years 2021 and 2022. Followed by the field observation results are presented, which include the (relative) water surface heights and flow depths.

4.1. Results for the Bheri River Section

In this section, all results for the Bheri River section are presented. The Bheri River section included overpasses for three satellites: Sentinel-3A at BH00, Sentinel-6A at BH01, and Sentinel-3B at BH02. This section presents the results from the sat-SARA analysis as well as field observation data collected for these sites. Note that for BH01 only signal return waveforms are presented for the multiple channel analysis. An overview map of the Bheri River section area is shown in figure 4.1.

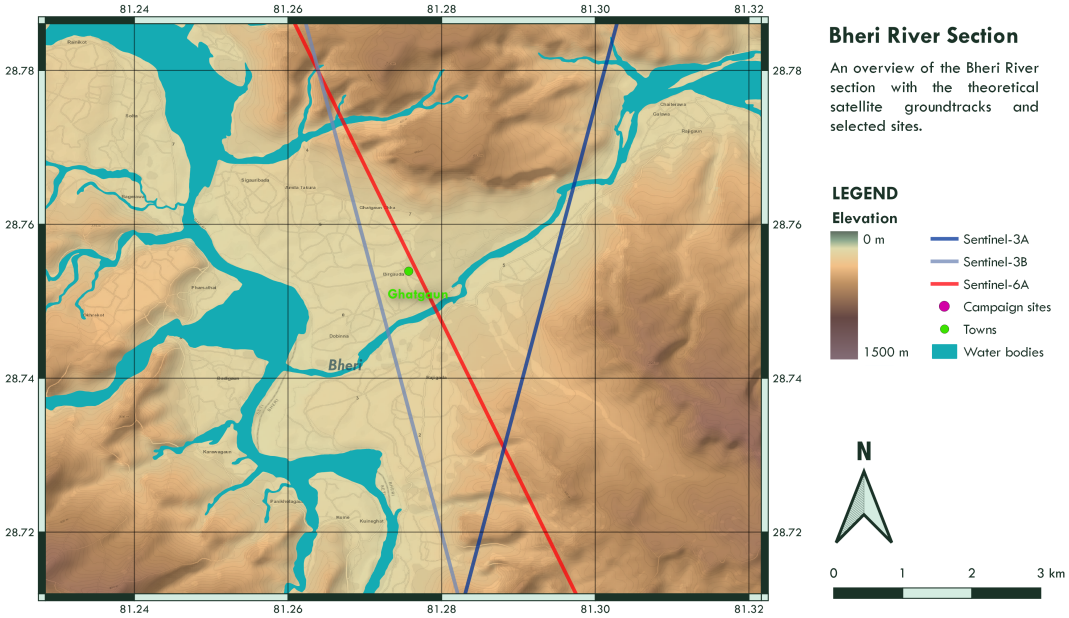

Figure 4.1: Map of Bheri River section

Figure 4.2: *Mountains at Bheri & Karnali confluence, as seen from Bheri Bridge*

The Bheri River flows through the Sivalik hills. Hence, the landscape is characterised by hillslopes on both sides of the river. This river reach was measured to be located at an elevation of approximately 200 meters above mean sea level (see appendix F.6 and I). Two bridges are located near the S6A and S3B overpasses. The area surrounding the river section from these bridges down to the confluence point is relatively flat. This region (on the left bank of the Karnali River) consists of mostly agricultural land and a few small villages. Upstream of BH01 and BH02 the landscape becomes more hilly. The hill slopes on the right and left banks from this river section peak at roughly 710 and 800 meters above mean sea level respectively. The tallest peaks can be found near the downstream end of the Bheri River, where it joins the Karnali River. Approximately 4 kilometers from the right bank of the Karnali the tallest peak of the study area can be found at 1540 meters above mean sea level. Figure 4.2 shows a picture of these moun-

tains as seen from Bheri Bridge (BH01).

Three main river channels can be identified within the area: the Bheri River flowing from East to West, the Karnali River before the Bheri confluence, and the Karnali River after the Bheri confluence. The latter two flow from North to South. From the hydrological water body data provided by the Nepal government, some other smaller tributaries to the Karnali River can be identified. During the field campaign, it became apparent that a flash flood tributary to the Bheri, flowing along a relatively steep hillslope, was located just upstream from BH01 and BH02. It was thought that this stream is only activated during high precipitation events in the wet season. Due to the proximity of this stream to the satellite overpasses, however, this tributary may appear in the echograms for all satellites.

BH00 is located farthest upstream at approximately 1.3 km distance from BH01, which is in turn located at approximately 0.4 km upstream of BH02. As the sites are located in very close proximity to one another the general landscape characteristics are the same for all locations. However, some notable differences exist between the three locations. Hence, these specific characteristics will be discussed for each location.

4.1.1. BH00

The BH00 site is located farthest upstream along the Bheri River. It was not visited during the field campaign, but the area was visible from site BH01 (see figure 4.3). In this reach, the river flows through a relatively broad valley. Moreover, the river banks upstream of BH01 were natural and not reinforced, providing space for the river to meander. Upstream some minor towns are located. From Google Earth satellite imagery it seems like bank reinforcements may be in place near these villages. Locals reported the area to be prone to flooding during the wet season.

Figure 4.3: *View from BH01, upstream toward BH00*

At BH00 Sentinel-3A passes over the Bheri River (see figure 4.4). From this map it appears that S3A passes over a small tributary of the Bheri in the North, as the Bheri approaches the satellite overpass from the East and briefly flows parallel to the satellite trajectory before S3A passes over the Bheri River at BH00. At a greater distance from the trajectory in the West, a tributary of the Karnali River is present. Progressing southward, the Bheri River converges with the Karnali, merging two distinct river streams into a unified course. From fieldwork, it is known that another tributary to the Bheri joins the river just upstream of BH01. Using the DEM for orientation and locating this tributary, it is likely that S3A passes over this tributary approximately at 28.742°N, 81.291°E.

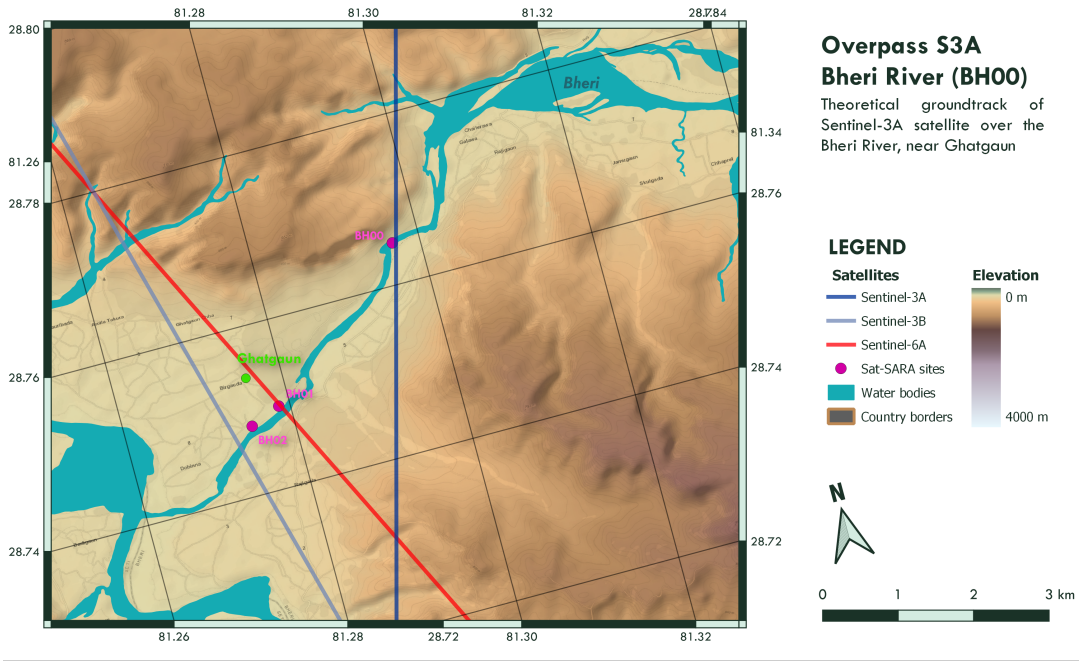

Figure 4.4: Local topography and the theoretical ground track of S3A at the BH00 overpass

Multiple Channel Identification

Figure 4.5 presents the echograms for the S3A trajectory over the Bheri River for dry season, wet season, and the field campaign of 2022. The echograms for dry season (March) and field campaign (November) appear very similar. The plot for the wet season in July differs from the other plots, mainly in that the bright features appear less distinct. This makes it more difficult to interpret the wet season echogram. The expected presence of a lot of water from the different streams in this area during the wet season in combination with a insufficient along-track spatial resolution may be the cause of the blurry echogram for the wet season. Figure 4.6 presents the UF-SAR echogram for the dry season (March 2022) together with the area map and the identification of the river sections indicated. The identification of these river sections is further elaborated upon below.

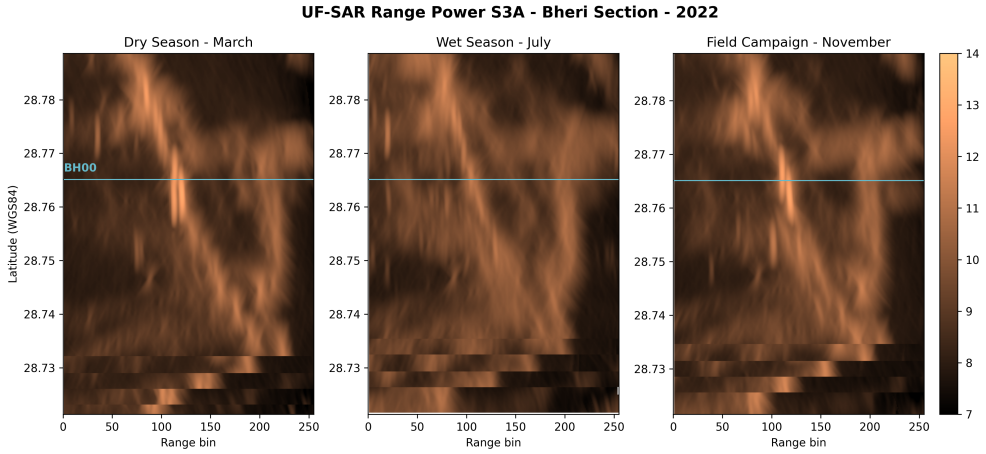

Figure 4.5: Unfocused-SAR signal power echogram for the Sentinel-3A overpass of the Bheri River

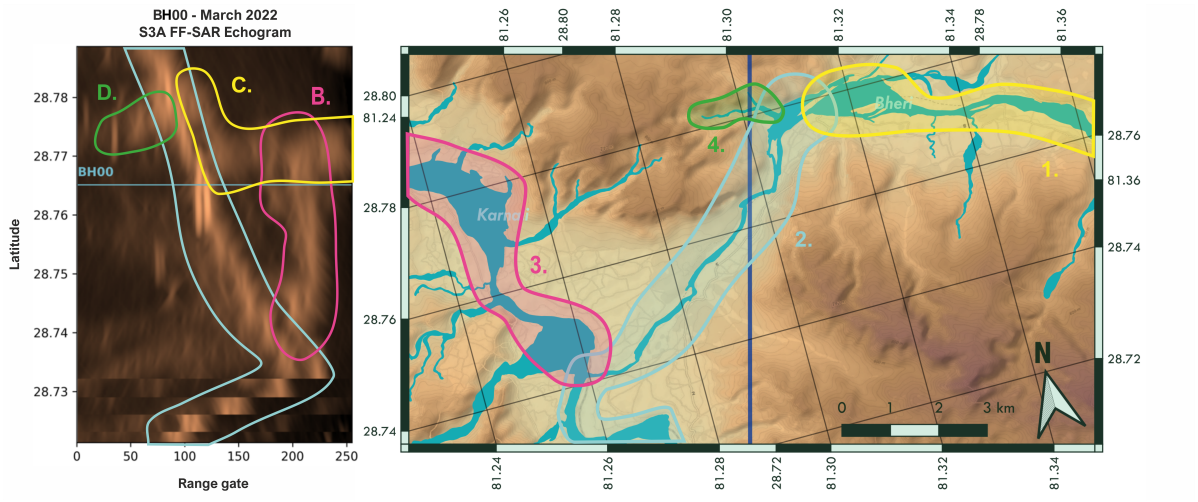

Figure 4.6: River sections identified from the stream-like features in the Sentinel-3A UF-SAR 2022 echogram over the Bheri River section area

One pattern clearly emerges in all three echograms. Three bright stream-like features are apparent, forming a triangular shape in the echogram. One of these streams (feature A) appears close to the satellite in the North, moving away from the satellite whilst progressing South. This stream appears brightest in the echogram and has a very bright feature appearing at the overpass site BH00. Another stream (feature B) appears far away from the satellite, remaining at a larger distance from the satellite whilst progressing South, seemingly joining the first stream in the South (at approximately 28.735°N).

Knowing the landscape from context, these features (A, and B) may be indicative of the Bheri and Karnali Rivers (sections 2 and 3) respectively, which join at approximately 28.4°N. The Bheri is expected to appear close to the satellite in the North as it is both situated close to the trajectory in the horizontal plane, as well as in the vertical plane because of its elevation. As the river flows down the slope before joining the Karnali, it moves further away from the satellite, both in the vertical and the horizontal plane. The Karnali River river section (section 3) in its whole is situated at a lower elevation, as well as further away from the Sentinel-3A trajectory in the horizontal plane. The Karnali is flowing down a slope as well as moving toward the trajectory in the horizontal plane, whilst progressing South. As a result it appears at higher range gates as compared to the Bheri River and remains at a relatively constant distance from the satellite and thus constant range gate whilst progressing South.

Between 28.77°N and 28.78°N, another stream-like feature (feature C) seems to appear rather close in the North, quickly moving away from the satellite whilst progressing South. This may be indicative of the Bheri River section (section 1) which quickly approaches the satellite (from the East) at this latitude, and moves parallel to the satellite trajectory for a short bit.

Lastly, two more vaguely bright-appearing features are present, which are more pronounced in the wet season echogram. One appears close to the satellite near a latitude of 28.76, moving away whilst progressing South, whereas the other appears closest to the satellite at approximately 28.73 °N, moving further away whilst progressing North. Whilst these two

features are less distinct they may be indicative of flash-flood tributaries running along the hillslopes during the wet season. This agrees with apparent depressions on the hillslopes in the DEM.

Sat-SARA Regurn Signal Waveforms

The blue line in the echograms of 4.5 marks the exact location of BH00 for which the return signal waveforms were plotted. These waveforms are presented in figures 4.7a and 4.7b.

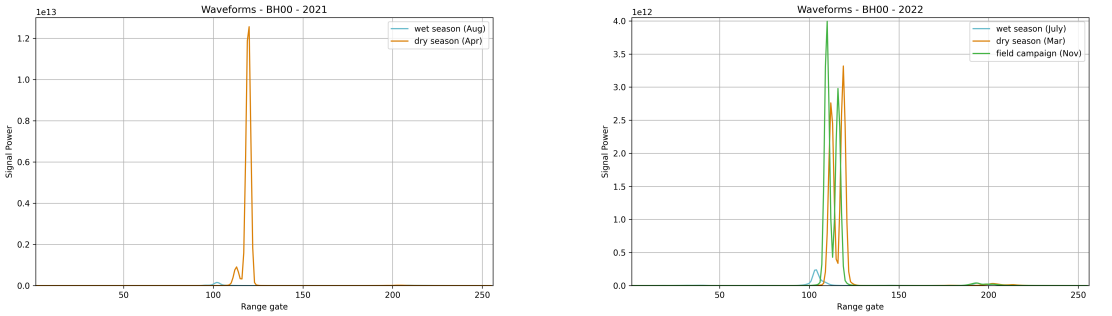

(a) *Dry & Wet Season 2021* **(b)** *Dry & Wet Season, and Field Campaign, 2022*

Figure 4.7: *Return Signal Waveforms for the Sentinel-3A Overpass of Bheri River at BH00*

A clear and strong return signal with one large peak, and a smaller peak can be observed for the dry season of 2021, indicating an inland water signal. Although, considerably less prevalent than for the dry season, a clear strong power return signal can also be observed during the wet season (see also zoomed plot in appendix E). For the 2022 season, the return signals are of significant less power and do not show a clear single peak for the dry season and field campaign period, but rather two large peaks can be observed around the same range gates (between 110-125). A single peak can be observed during the wet season, although, again at a much smaller signal power as compared to the dry season and field campaign signals. For all three waveforms another small peak can be observed around range gate 200.

Sat-SARA Derived Water Surface Heights

Time series of the absolute water surface heights throughout 2021 and 2022 as derived from the sat-SARA data for BH00 are presented in figure 4.8.

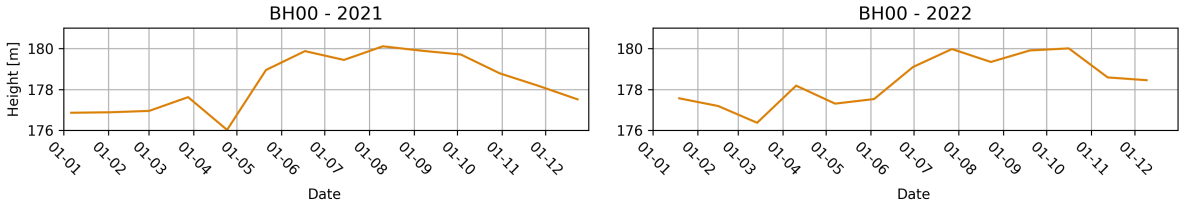

Figure 4.8: Timeseries of estimated water surface heights for the overpass locations BH00 for the years 2021 and 2021

The estimated water surface height is highest around August for both years. The months from January until the end of May show the lowest observed water surface heights for both years. The water surface height variation as derived from the sat-SARA time-series is 4.088 m in 2021 and 3.639 m in 2022.

4.1.2. BH01

The BH01 site is located at the Sentinel-6A overpass of the Bheri River, which is the exact location of the old *Ghatgaun Suspension Bridge* and newly constructed *Ghatgaun Bheri Bridge*, near Ghatgaun. A map following the trajectory of Sentinel-6A, on top of a DEM is presented in figure 4.9 for orientation. From this map it appears that the Karnali River roughly runs parallel to the S6A trajectory for this section. S6A passes over two smaller tributaries to the Karnali which run down the hillslopes North of the Bheri River. It then passes over the Bheri River at BH01, at nearly the same latitude as the confluence of the Bheri and Karnali Rivers. Assuming the flash flood tributary to the Bheri just upstream of BH01 is activated during wet season, S6A runs near parallel to this tributary, south of the Bheri overpass. The Bheri River runs nearly perpendicular to the S6A trajectory.

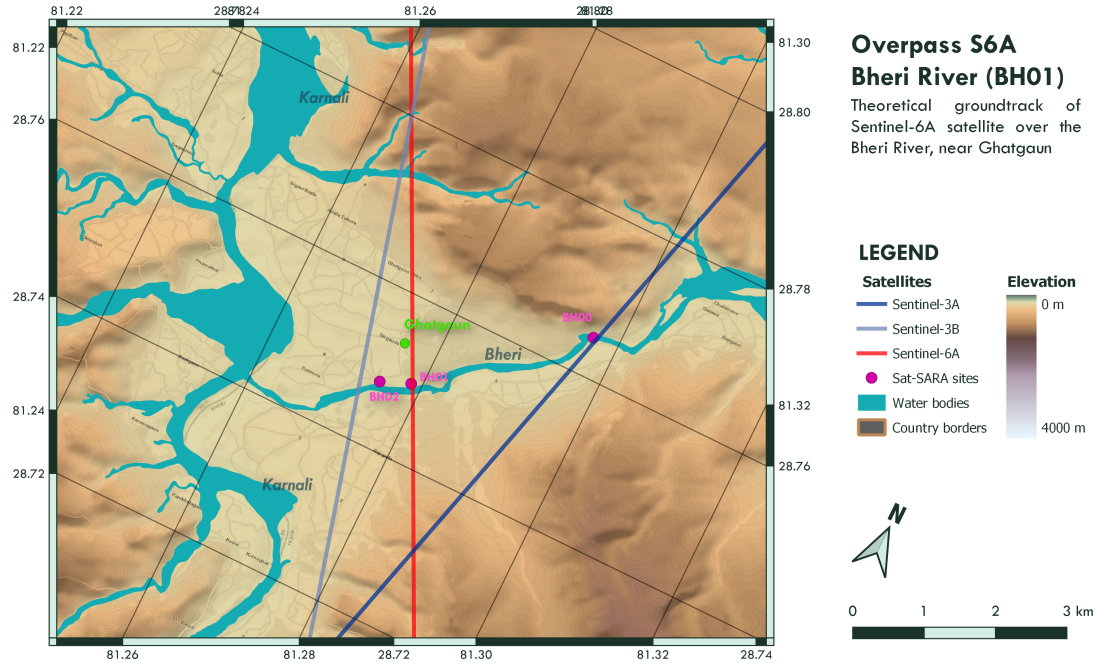

Figure 4.9: Local topography and the theoretical groundtrack of S6A at the BH01 overpass.

Although the river flows through the Sivalik hills the slopes on either side of the river are modest. The hills on the left side of the river slope more steeply than the hills on the right side. No steep mountains or hills are located in the direct vicinity of the overpass. The river width recorded at BH01 during the field campaign was approximately 82 meters (as derived from CHIRP+ coordinate readings).

Near the two bridges, the river banks are reinforced with engineered embankments. This only holds for the section in the direct vicinity of the bridges, including the river bend in which it is located. These reinforcements stretch a couple of hundred meters upstream and downstream from the bridges. The river is clearly deeper on the left side than on the right side. During the field campaign the water reached the left bank reinforcement, whereas parts of the river bed were exposed on the right side of the river. The images in figure 4.10 provide an illustration of the surroundings of BH01 during the 2022 field campaign.

(a) *Left bank Bheri River at BH01*

(b) *Bheri Bridge from left bank*

(c) *Right bank Bheri River at BH01*

Figure 4.10: *Landscape at BH01*

Multiple Channel Identification

Figure 4.11 presents the UF-SAR echograms for the S6A trajectory over the Bheri River section for dry season (April) and wet season (October). Figure 4.12 presents the FF-SAR echograms for the S6A trajectory over the Bheri River section for the dry and wet seasons respectively. A clear difference of spatial resolution can be observed, which will be further elaborated upon in the chapter 5 Discussion.

As explained in section 3.1.2, all bright-appearing features can be found at range gates lower than 300, which can be explained by the downlink mode on board of the satellite. Stream-like features appear very distinctly in all echograms and the patterns observed are highly similar for the wet and dry seasons, as well as for UF-SAR and FF-SAR. Notably, for both UF-SAR and FF-SAR, the pattern seems to be shifted, appearing at slightly lower range gates for the wet season as compared to the dry season. This means that the water surface appears closer to the satellite during the dry season plot as compared to the wet season plot. This may indicate the observation of higher water surface heights. As every range gate constitutes 18 centimetres of vertical distance, a shift in approximately 30 range gates would mean a water level rise of 5.4 meters. However, a cross-track shift of the satellite trajectory (Sentinel-6 not following exactly the same ground track) may also cause this shift in range gates, so no direct conclusions can be drawn based on solely the echogram.

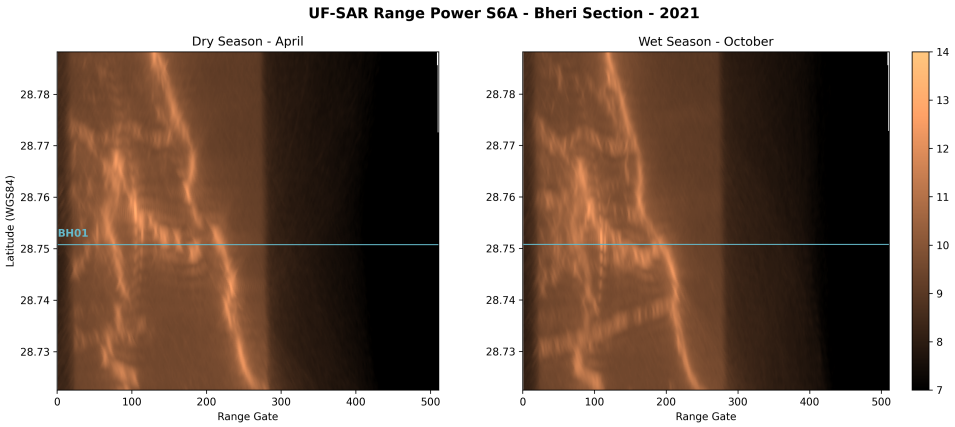

Figure 4.11: Unfocused-SAR signal power echogram for the Sentinel-6A overpass of the Bheri River

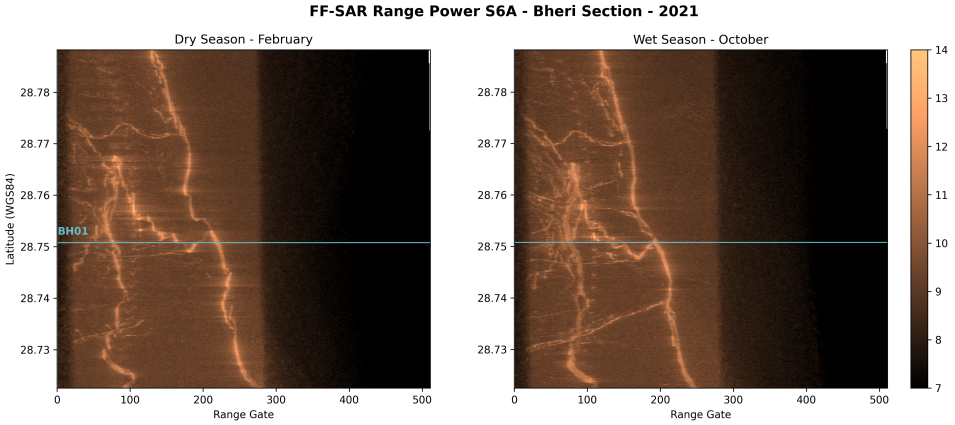

Figure 4.12: fully focused-SAR signal power echogram for the Sentinel-6A overpass of the Bheri River

Figure 4.13 shows the wet season FFSAR echogram for BH01 aligned with a map of the area to allow for easy interpretation. The image also indicates the identified river sections. The channel identification is elaborated upon in the following paragraphs.

The emerging patterns show features very characteristic of rivers. Firstly, a stream-like feature appears at the Northern end of the trajectory at approximately range gate 140, moving away from the satellite whilst progressing South (feature A). Considering the slope of the region, this is indicative of the Karnali River flowing on the West-side of the trajectory, nearly parallel to it. The Karnali River is located at a higher elevation at the North end of the trajectory, thus appearing closer to the satellite, whilst it appears farther away in the South as the valley will be situated at a lower elevation.

A second stream appears closer to the satellite at range gates between approximately 70 and 105, and remains within this range for most of the South part of the trajectory (feature C). Another stream or river section seems to connect the former two (feature B). These two streams or river sections are a little bit less intuitive to identify. Feature B appears close to the satellite at a range gate 100 at 28.768°N where it connects to the second mentioned stream,

moving away toward range gate 210 at 28.751°N where it joins the first mentioned stream.

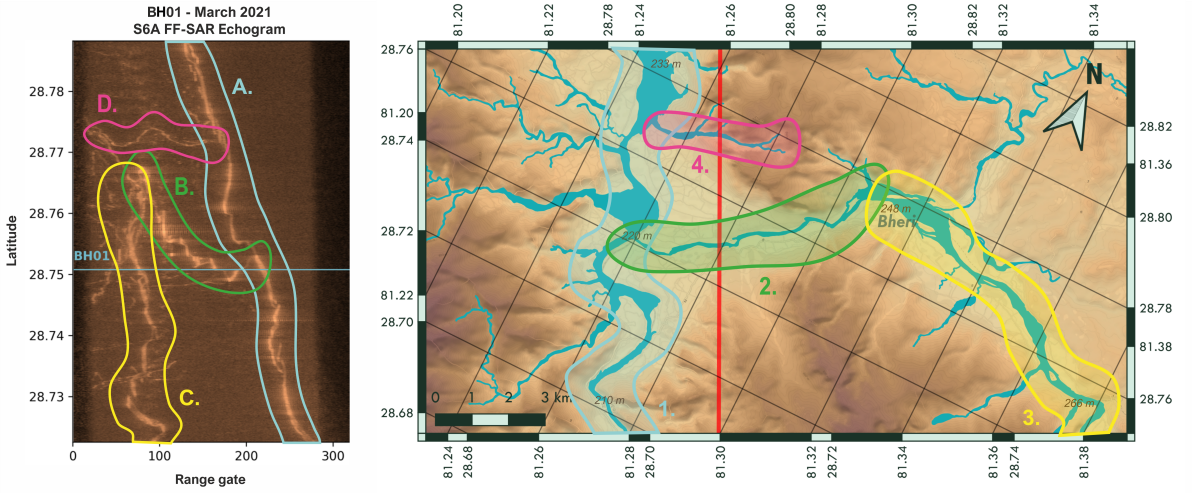

Figure 4.13: River sections identified from the stream-like features in the Sentinel-6A FF-SAR 2022 echogram over the Bheri River section area

As feature B seems to rapidly move away from the satellite, this is suggested to be representing the Bheri River (section 2). As the river flows perpendicular to the Sentinel-6A trajectory and down a relatively steep slope, the river moves away from the satellite more rapidly in the vertical plane due to elevation change than it moves toward the satellite in the horizontal plane. Throughout this section (2), the Bheri drops a rough 20 meters in elevation as it flows perpendicular to the trajectory down to the confluence with the Karnali River, over the course of approximately 6 kilometers .

Feature C seems to stay at a relative similar distance from the satellite along the trajectory. This is indicative for the Bheri River as well, but for section 3, upstream of section 2. Although here the river is slowly moving closer to the satellite in the horizontal plane, it is also flowing down a slope. This causes the stream to appear at a somewhat constant distance from the satellite. The sharp turn at a latitude of 28.755°N is clear proof of this. In the echogram the distance to the satellite suddenly increases massively as the river remains at nearly the same altitude whilst it is farther away from the satellite in the horizontal plane.

In both the dry and wet season another clear stream-like feature can be observed in the North (feature D). Whilst it remains at somewhat the same latitude, it quickly moves away from the satellite, starting at a range gate close to zero, up to approximately range gate 180 as it joins the Karnali River. This is indicative of the Karnali tributary flowing down a steep hillslope indicated in figure 4.13 as section 4.

During the wet season, even more water features are apparent. These are hard to distinguish in the UF-SAR echogram as they do not appear very distinct (figure F.2.1). They are, however, much more pronounced in the FF-SAR echograms (figure 4.11). This makes it possible to identify, for instance, a stream that appears close to the satellite at 28.73°N, moving away from the satellite quickly to apparently join one of the main river streams at 28.74°N. This is indicative of a rain-fed (flash-flood) tributary to the main branch of a river, running down a

hillslope, which is only activated during the wet season. This suggests that it is possible to observe channel activation during wet season from the Sentinel-6 SAR return signals.

Sat-SARA Return Signal Waveforms

For the Sentinel-6A overpass over the Bheri River at BH01 (depicted by the blue line in the echograms) both the unfocused-SAR and fully focused-SAR return signal waveforms were plotted for 2021 (see figures 4.14a and 4.14b.

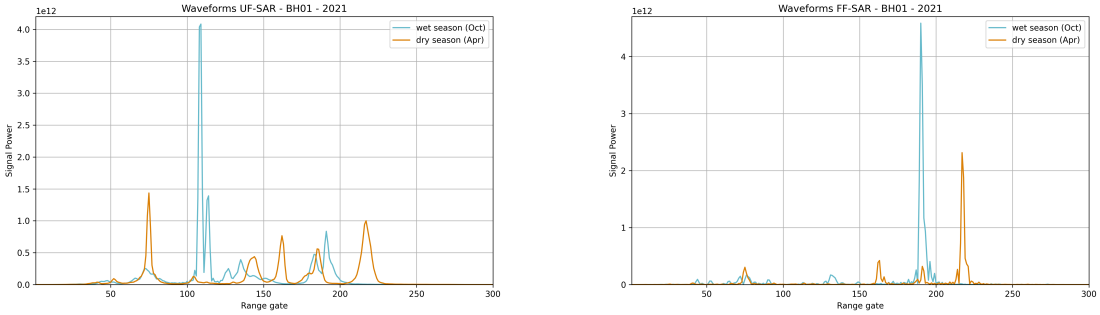

(a) *Unfocused SAR* **(b)** *Fully Focused SAR*

Figure 4.14: *Return Signal Waveforms for the Sentinel-6A Overpass of Bheri River at BH01*

The waveforms are clearly different for the UF-SAR and the FF-SAR processed return signals at the BH01 overpass site. For the UF-SAR waveforms, multiple signal power peaks can be observed. This is especially true for the dry season waveform, where the multiple peaks are also of similar magnitude. The wet season waveform has one double-peak around range gate 115 of significantly higher signal power. The FF-SAR waveforms also present multiple peaks for both the wet season and the dry season. However, for both seasons, one signal power peak is clearly of a larger magnitude.

Field Observations

The relative water surface height for BH01 was measured with respect to the top of the railing of the new *Ghatgaun Bheri Bridge*, using measurement tape. The relative water surface height was found at $16.0\ m$. The observed maximum flow depth at BH01 was $4.17\ m$.

4.1.3. BH02

The BH02 site is located at the location where Sentinel-3B passes over the Bheri River (at the exact theoretical groundtrack overpass), a few hundred meters downstream of the two bridges. Figure 4.15 shows a map of the local topography in the orientation of the S3B theoretical ground track. From this map, it appears that the Karnali River runs roughly parallel to the S3B trajectory for this section. S3B passes over two tributaries to the Karnali River, before it passes over the Bheri River at BH02, at nearly the same latitude as the confluence of the Bheri and Karnali Rivers. The Karnali River appears closest to the trajectory in the South at approximately 28.72-28.73°N. Some other small tributaries to the Karnali can be seen along the Karnali reach.

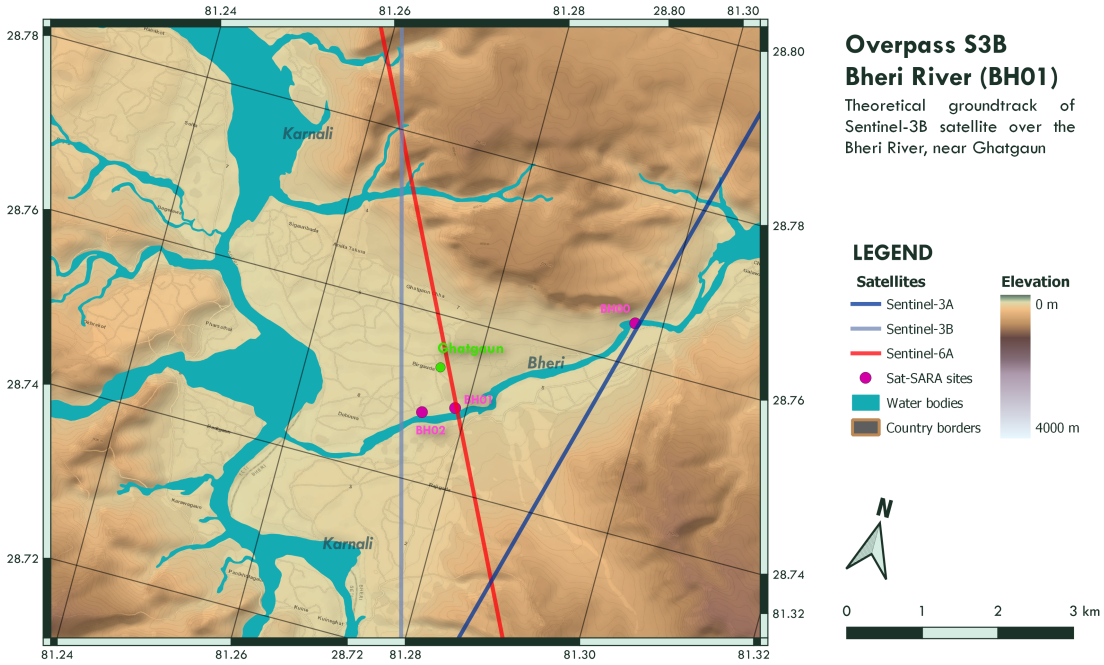

Figure 4.15: *Local topography and the theoretical ground track of S3B at the BH02 overpass*

At BH02 the river is enforced with a small dike on the right bank. On the left bank, no artificial embankment is present. During the field campaign, parts of the river bed were exposed on both sides. The pictures in figure 4.16 illustrate the landscape conditions during the 2022 field campaign. During the campaign, flow velocities were high to the extent that passing the river in a boat was deemed impossible. The surrounding area is relatively flat. Downstream of BH02, toward the confluence with the Karnali, the left bank of the river becomes very steep (also see 4.16b). The river width observed during the field campaign was 162.0 m. Note that other than river width no field observation data could be collected at this location.

(a) *Bheri Bridges as seen from BH02*

(b) *BH02 from the dike at the right bank (view in the direction of the S3B theoretical ground track)*

Figure 4.16: Landscape surrounding BH02

Multiple Channel Identification

Figure 4.17 presents the echograms for the S3B trajectory over the Bheri River section for the dry season (April), wet season (September), and field campaign (November) of 2022. Although the general pattern in the three echograms appears quite similar, some clear differences can be observed.

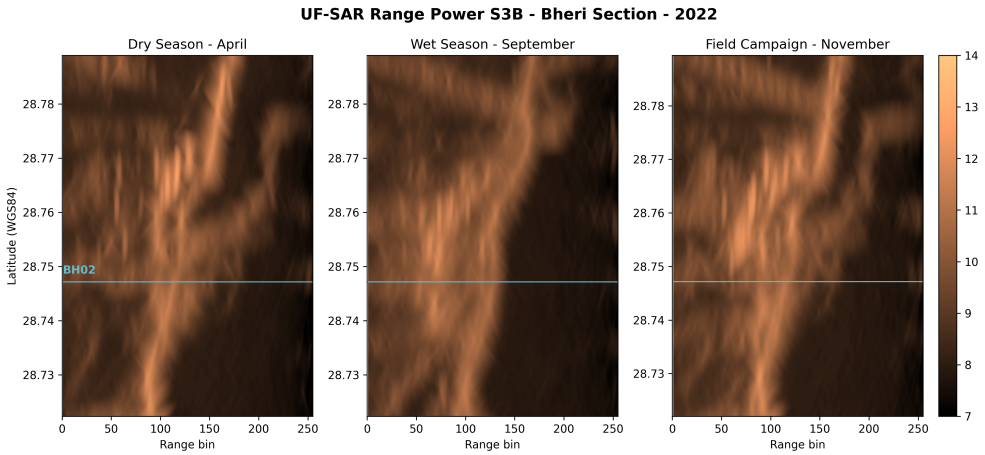

Figure 4.17: Unfocused-SAR signal power echogram for the Sentinel-3B overpass of the Bheri River

The echogram for the low flow in April presents the clearest distinction between the signal power intensities, as compared to the other two plots. One main river-like feature appears in all plots, which appears farthest away in the North, moving closer to the satellite whilst progressing Southward. Interestingly, the high flow plot of September seems to lack one of the main features showing bright targets at the higher range gates (between range gate 230 at 28.779°N and range gate 130 at 28.75°N) which the plots for April and November do depict. In all plots another bright water-body-like feature can be observed at slightly lower range gates (hence closer to the satellite) as compared to the main branch, between 28.74°N and 28.77°N. As it appears closest to the satellite near the overpass site, this may be indicative for the Bheri River. However, the features are not very distinct, therefore making it difficult to interpret the data and properly identify the river streams.

Lastly, a vague stream-like feature appears at the Northern latitudes, moving from close to the satellite (range gate 0 at 28.89°N) away from the satellite whilst progressing South.This feature is less pronounced in the dry season echogram. Hence, it is suggested to be indicative of the first Karnali tributary (running down a hillslope) the satellite passes within this trajectory. Interestingly, the larger appearing tributary to the Karnali situated between latitudes 28.79°N and 28.70 cannot distinctly be identified from the echogram.

Sat-SARA Return Signal Waveforms

The return signal waveforms for the Sentinel-3B overpass over the Bheri river at BH02 (marked by the blue line in figure 4.17) are presented in figure 4.18. For the waveform of the dry season of 2021 a clear high signal power can be observed around range gate 120, accompanied by a smaller but still considerably large signal power peak around range gate 105. For the wet season in the same year, the return signal shows considerably smaller overall signal wave power. Moreover, multiple peaks can clearly be observed between range gates 80 and 155.

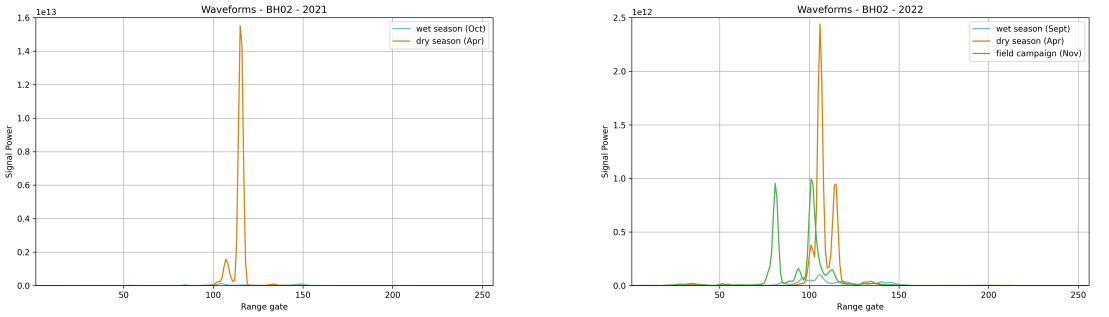

(a) *Dry & Wet Season 2021* **(b)** *Dry & Wet Season, and Field Campaign 2022*

Figure 4.18: *Return Signal Waveforms for the Sentinel-3B Overpass of Bheri River at BH02*

The observed return signal power is also smaller for all waveforms plotted for 2022, being of the same order of magnitude of the wet season wavefrom of 2021. In addition, all waveforms of 2022 show multiple signal power peaks.

Sat-SARA Derived Water Surface Heights

Time series of the absolute water surface heights throughout 2021 and 2022 as derived from the sat-SARA data for BH02 are presented in figure 4.19.

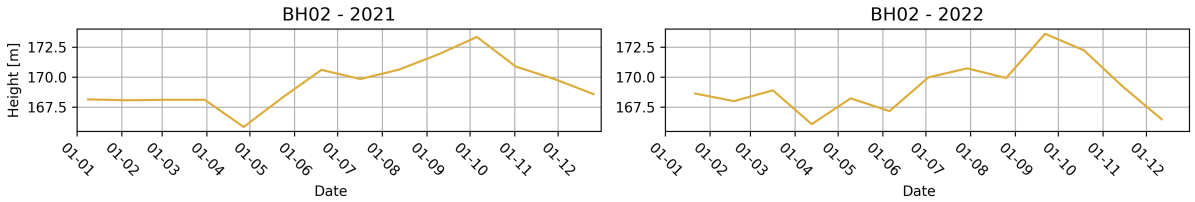

Figure 4.19: Timeseries of estimated water surface heights for the overpass locations BH02 for the years 2021 and 2021

The estimated water surface height is highest around October for both years. The months from January until the end of May or the beginning of June show the lowest observed water surface heights for both years. The water surface height variation as derived from the sat-SARA time-series is 7.48 m in 2021 and 7.51 m in 2022.

4.2. Results for the Karnali River Section

In this section, all results are presented for the section of the Karnali River where it flows through the Sivalik Hills. This section stretches from the confluence of the Bheri down to the bifurcation at Chisapani. This river section includes only a single satellite overpass from Sentinel-3A at site K01 for which the multiple channel analysis was applied and the sat-SARA derived water surface heights are presented. No field observation data could be collected at K01. Hence, field observation data is presented for sites K02 and K03 for field validation instead.

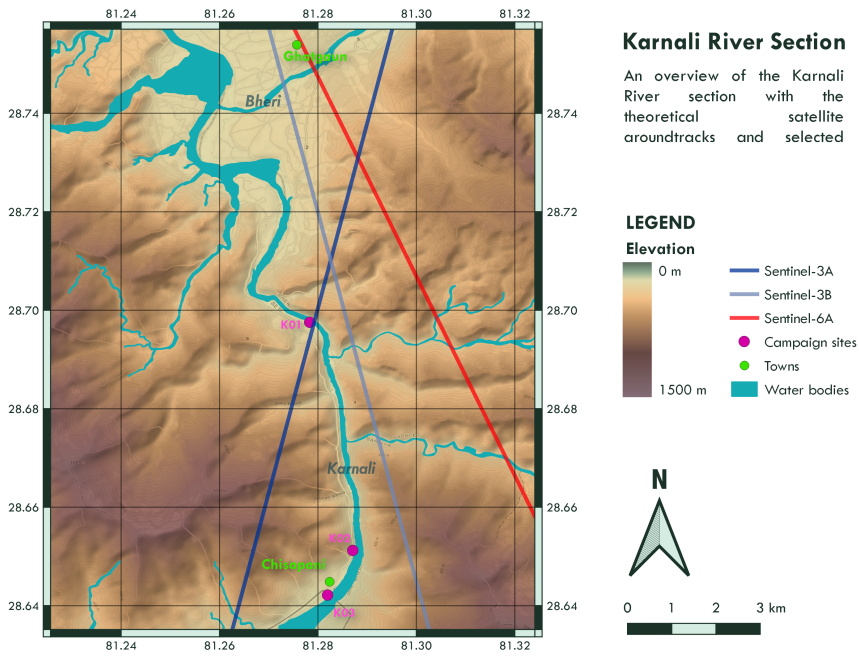

Figure 4.20: Map of Karnali River section

This section of the Karnali River cuts through the Sivalik Range. Hence, the landscape is characterised by steep hillslopes on both sides of the river. Over the course of approximately 8.5 kilometres, the river experiences an elevation drop from roughly 200 meters measured at the confluence of the Bheri River, down to roughly 180 meters above sea level as measured at Chisapani. The surrounding hills peak between roughly 700 and 1500 meters, with the tallest peak within 5 kilometres of the river, standing at 1540 meters above mean sea level. The most as well as the tallest peaks can be found on the right bank of the Karnali River.

In this area only one main river stream can be identified: the Karnali River. Multiple minor tributaries to the Karnali run down the hillslopes on both sides, most of which were actively carrying water down during the field campaign in 2022, which indicates these are not flash-flood rivers. However, this does not necessarily imply that these tributaries cannot fall dry during the drier months. As the hilltops are not covered in snow, this does imply the tributaries are rain-fed.

4.2.1. K01

The K01 site coincides with the the theoretical river overpass location of Sentinel-3A over the Karnali River. Figure 4.21 shows a map following the orientation of the trajectory of S3A over a DEM at K01. The landscape consists of steep hill slopes and a narrow valley through which the Karnali River flows. The hill slopes on the left bank are steeper than on the right bank. The photographs in figure 4.22 present the landscape as observed during the 2022 field campaign. The observed river width at K01 was 74.6 meters.

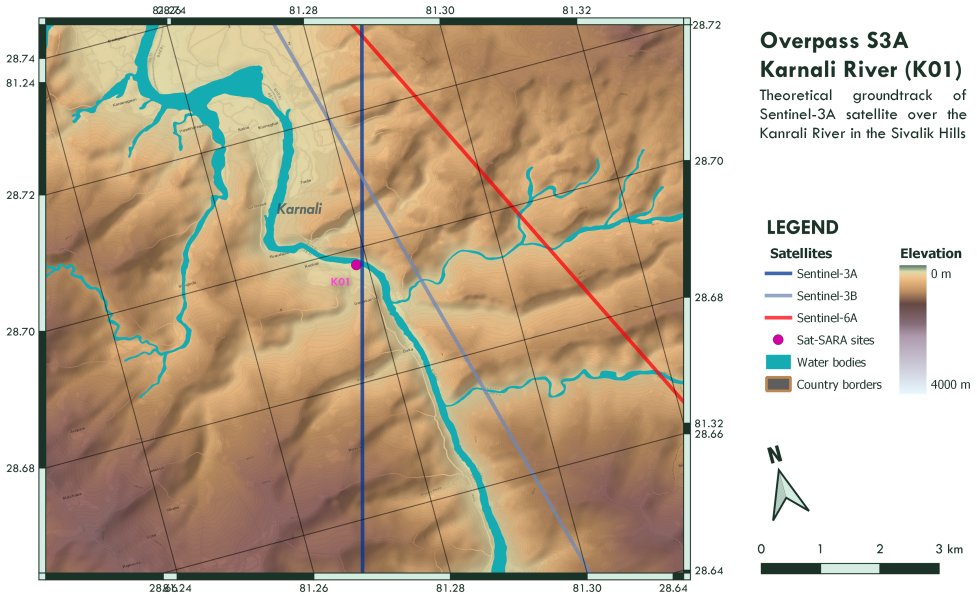

Figure 4.21: Local topography and the theoretical ground track of S3A at the K01 overpass

The only main river channel in the vicinity of the trajectory is the Karnali River. At higher latitudes it moves closer toward the trajectory in the horizontal plane, after which it flows parallel with the trajectory for a short distance, before which it makes a tight turn to run perpendicular to the satellite until right after the satellite overpass at K01. A less tight turn then causes the river to slowly move farther away from the trajectory whilst progressing Southward. A couple tributaries to the Karnali River show on the map, some of which may only be activated during the monsoon season.

(a) *K01, looking upstream* **(b)** *K01, looking downstream*

Figure 4.22: Landscape surrounding K01

Multiple Channel Identification

Figure 4.23 presents the echogram for the S3A trajectory over the Karnali River for the dry season (April), wet season (September), and field campaign (November) of 2022. A clear continuous river-like feature can be recognised in all of the plots, which would suggest the presence of a single river channel.

In the first place, it might be expected that, as the stream moves closer to the satellite before the overpass and away from the satellite after the overpass site in the horizontal plane, the feature would appear at a larger range gate in the North and South, whilst appearing at a smaller range gate at the overpass site. However, this is not what appears to be the case when studying the echograms. Here, the river feature follows a rather constant trajectory. This could be explained by the river incline. This may coincidentally cause the river to remain at a rather constant distance from the satellite, only slowly moving further away as the overall elevation of the valley drops.

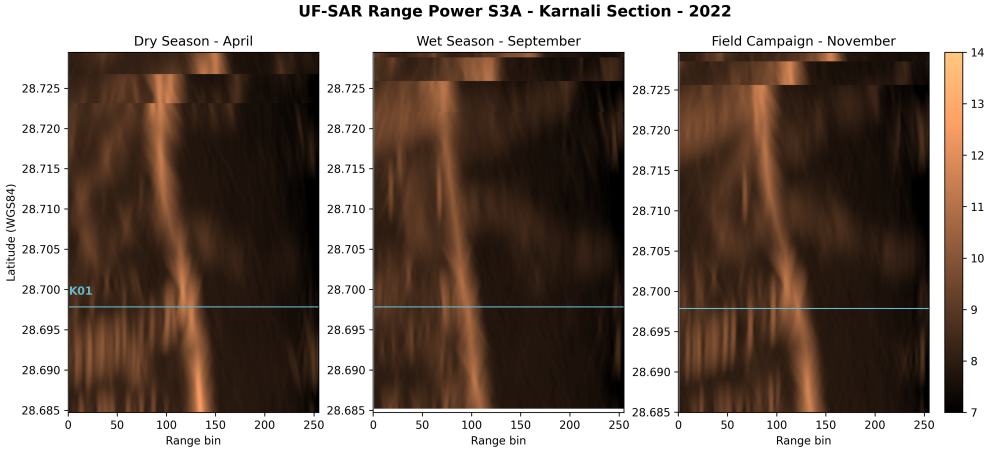

Figure 4.23: Unfocused-SAR signal power heatmap for the Sentinel-3A overpass of the Karnali River in the Silavik Hills

Figure 4.24 presents the channels as identified from the echograms shown with the November echogram together with the map of the area with DEM and in the orientation of Sentinel-3A trajectory. In the following paragraphs this identification is elaborated upon further.

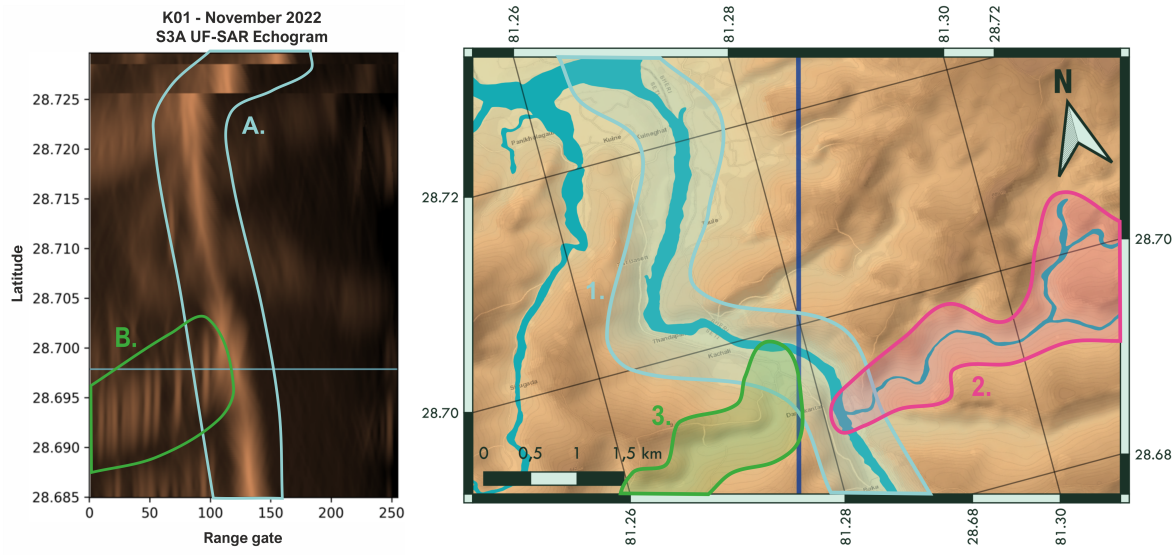

Figure 4.24: River sections identified from the stream-like features in the Sentinel-3A UF-SAR 2022 echogram over the Karnali River section area

Bright appearing targets can be observed between the 28.69°N and 28.70°N (feature B). This is most pronounced in the echograms for the dry season and the field campaign. The feature appears very close to the satellite (starting at range gate 0), moving away from the satellite up to approximately range gate 105, where it seems to meet the Karnali River. These characteristics suggest this feature is caused by a Karnali tributary running down a hillslope. Although only one tributary to the Karnali River is visualised in the water body layer on the map (section 2), from the DEM it becomes apparent there is a high chance other tributaries are also present. Considering that feature B appears closest at a lower latitude and then moves away from the satellite at the larger latitudes, this would indicate another tributary than the one presented as a water body in the map. Instead it is suggested the signal represents a tributary indicated as section 3 in figure 4.24. From the field campaign it can be confirmed a tributary was present at this location. A similar type of feature can be observed in the wet season and field campaign echograms at a higher latitude (between 28.72°N and 28.725°N), although its appearance is less pronounced.

Sat-SARA Return Signal Waveforms

The return signal waveforms for the Sentinel-3A overpass over the Karnali river at K01 are presented in figure 4.25. For the waveform of the dry season of 2021, a clear high signal power can be observed around range gate 130, accompanied by a smaller signal power peak around range gate 120. For the wet season in the same year, the return signal shows considerably smaller overall signal wave power. One large peak can be observed around range gate 95, and a smaller second peak can be observed around range gate 70. These waveforms are indicative of an inland water signal. Notably, the observed return signal power is an order of magnitude smaller for all waveforms plotted for 2022. In addition, all waveforms of 2022 show multiple signal power peaks.

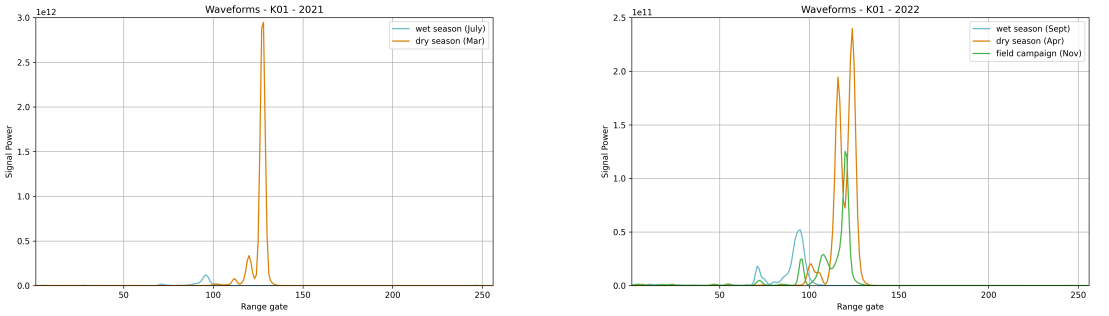

(a) *Dry & Wet Season 2021* **(b)** *Dry & Wet Season, and Field Campaign 2022*

Figure 4.25: *Return Signal Waveforms for the Sentinel-3A Overpass of Karnali River at K01*

Sat-SARA Derived Water Surface Heights

Time series of the absolute water surface heights throughout 2021 and 2022 as derived from the sat-SARA data for K01 are presented in figure 4.26.

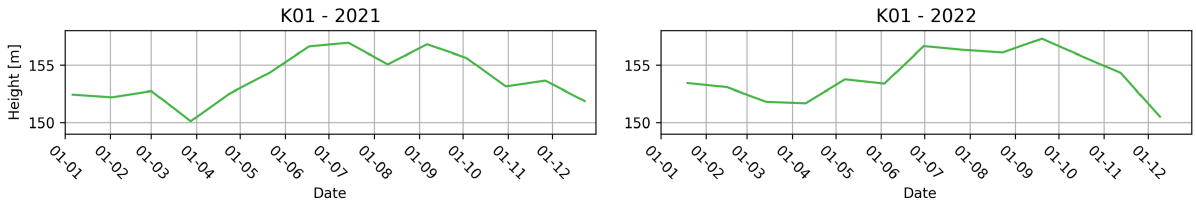

Figure 4.26: Timeseries of estimated water surface heights for the overpass locations K01 for the years 2021 and 2021

The estimated water surface height is highest between July and October for both years. In 2021 the highest water surface heights are measured somewhat earlier in the year as compared to 2022. The months from February until April show the lowest observed water surface heights for both years. The water surface height variation as derived from the sat-SARA time series was 6.82 m in 2021 and 6.78 m in 2022.

4.2.2. K02 & K03

The landscape is very similar to the landscape at K01. It consists of steep hill slopes and a narrow valley through which the Karnali River flows. The hill slopes on the left bank appear somewhat steeper than on the right bank. The photograph in figure 4.33a presents the landscape at K02, looking upstream (in the direction of K01). The photograph in figure 4.33b presents the landscape at Chisapani, at K03. Here the landscape opens up as the Sivalik Hills make place for the more flat terrain beyond. The river widths as observed during the field campaign were 160 and 283 meters for K02 and K03 respectively.

(a) *Looking upstream from K02*

(b) *K03 from fixed point*

Figure 4.27: Landscape surrounding K02 & K03

Field Validation

The relative water surface heights were measured at both K02 and K03. At K02 this was measured from the road between Chisapani and Ghatgaun at the right bank. The relative water surface height observed at K02 was $20.9\ m$. At K03 the relative water surface height was measured from the top of the stairs below the Karnali Bridge at Chisapani, leading down to the river bank. The measured relative water surface height here was measured at $10.1\ m$. No flow depths were measured at either of the two locations.

The stage height measurements at Chisapani (K03) are presented in figures 4.28 and 4.29. Figure 4.28 shows the staff gauge heights measured as a time series from 1 January 1992 up to 21 December 2018. Figure 4.29 shows the staff gauge height variation per year, presenting the staff gauge heights for each individual year, highlighting the data for 2018. In addition, it shows the average stage height per day for the entire data set.

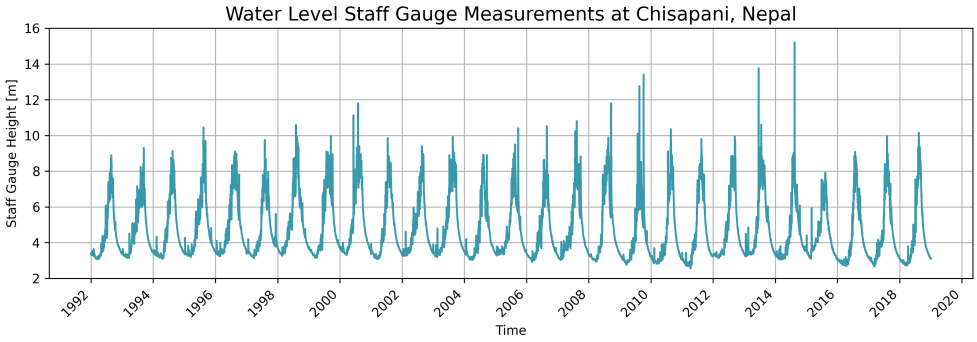

Figure 4.28: Time Series of In-Situ Stage Height Measurements at Chisapani (K03), from 1992 until 2018

The lowest stage height measured at Chisapani between 1 January 1992 and 31 December 2018 was at a height of 2.56 meters and was measured on 10 April 2011. The highest stage height measured was at a height of 15.2 meters on 15 August 2014. Assuming these are no unexpected outliers, this means a maximum water height difference of approximately 12.64 meters.

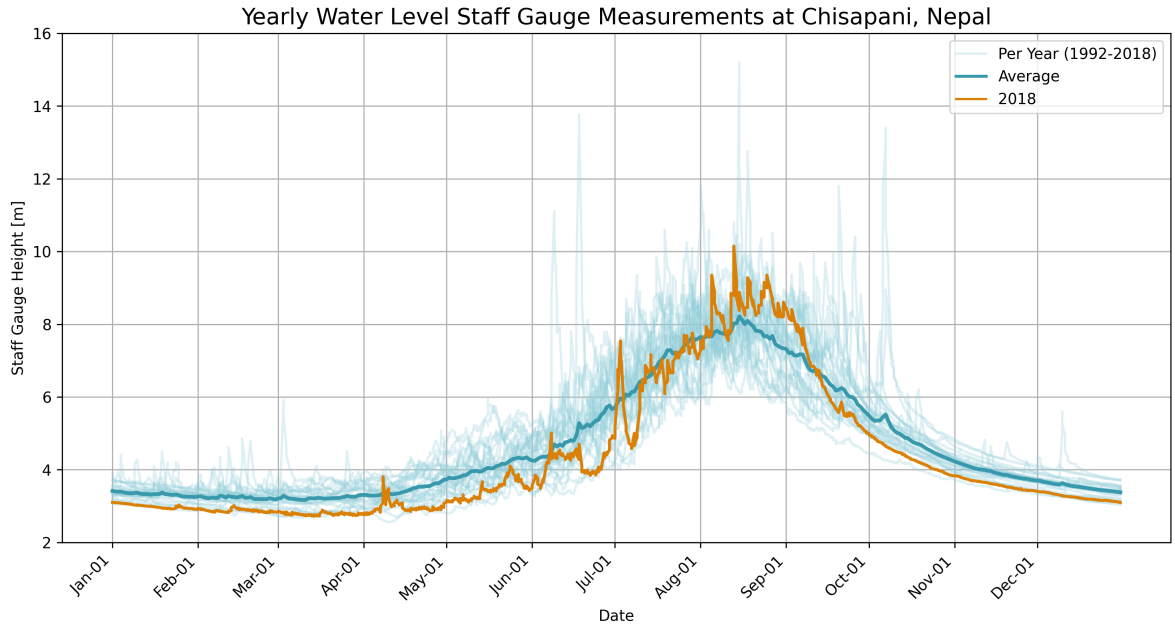

Figure 4.29: Yearly In-Situ Stage Height Measurements at Chisapani (K03), for 1992-2018

Figure 4.30 shows the maximum yearly water level variation; the maximum measured stage height minus the minimum measured stage height of each year. The largest yearly variation

of measured water stage heights was found in 2014 with a water height difference of 12.15 meters. Immediately the year after, the water level variation was lowest with a yearly water height difference of 4.89 meters. The average water level variation for this time period was 7.34 meters per year.

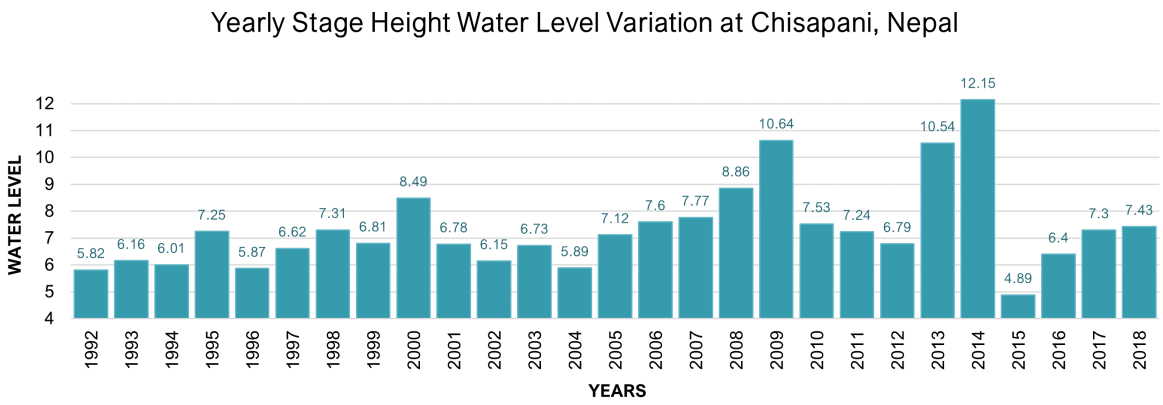

Figure 4.30: Yearly Stage Height Variation Measured at Chisapani between 1992 and 2018

4.3. Results for the Geruwa River Section

In this section, the results for the downstream end of the Geruwa River reach are presented. Whereas Sentinel-3A passes over the Geruwa River multiple times, the analysis has been conducted for the downstream overpass at G08. Figure 4.31 shows the entire Geruwa River reach.

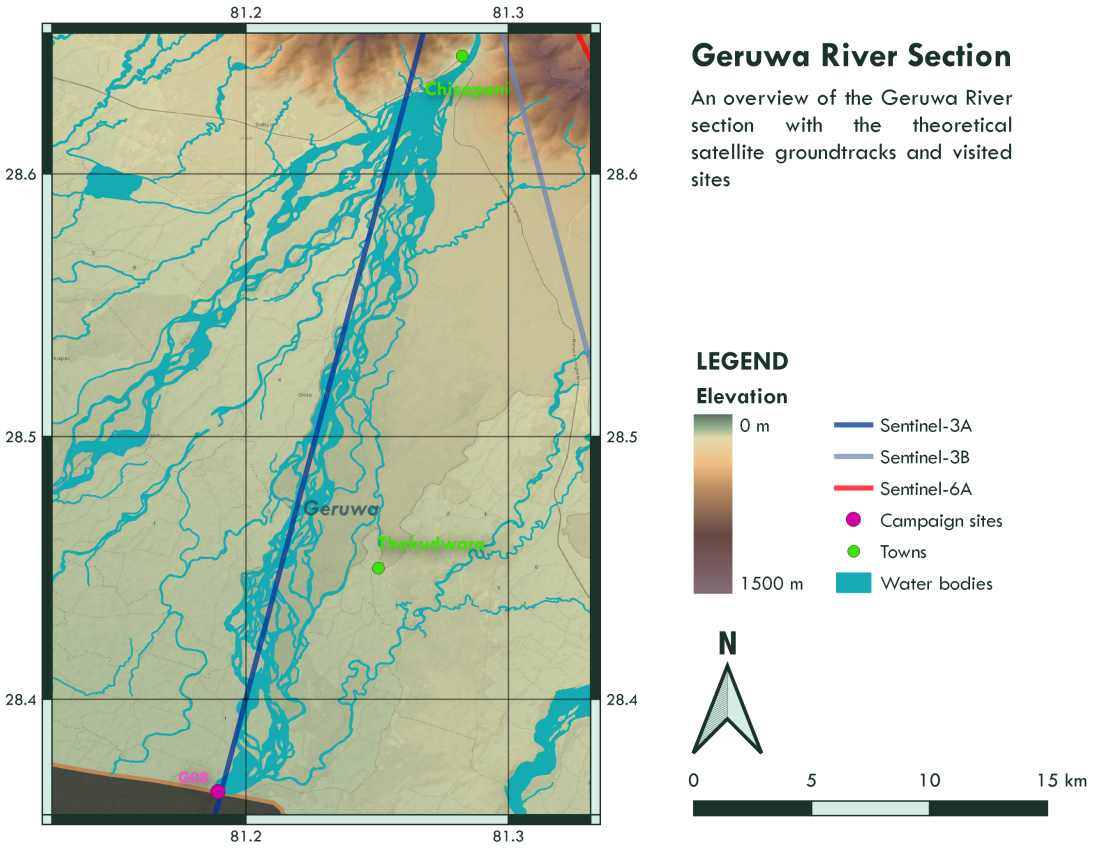

Figure 4.31: Map of Geruwa River section

The Geruwa River forms the left branch of the bifurcated Karnali River, downstream of Chisapani. It flows through flat terrain with Bardia National Park on the left bank for most of the river reach, and the Rajapur agricultural peninsula on the right bank. At the inflow, the Geruwa is situated at approximately 180 meters above sea level. The river leaves Nepal and enters India at an elevation of approximately 120 meters above sea level, as was measured during the field campaign. The Geruwa River reach is highly spatially and temporally dynamic. The river consists of multiple channels which can be activated during the wet season, whilst some may fall dry during the dry season.

4.3.1. G08

The G08 site is located where Sentinel-3A passes over the Geruwa River. Figure 4.32 shows the local topography in the orientation of the theoretical S3A ground track trajectory at the Geruwa River overpass at site G08. Note that the visualisation of the water bodies stops at the Nepal-India border. This is because the hydrological data was available for Nepal water bodies only. The rivers do continue into India and their rough outline can be observed in the map.

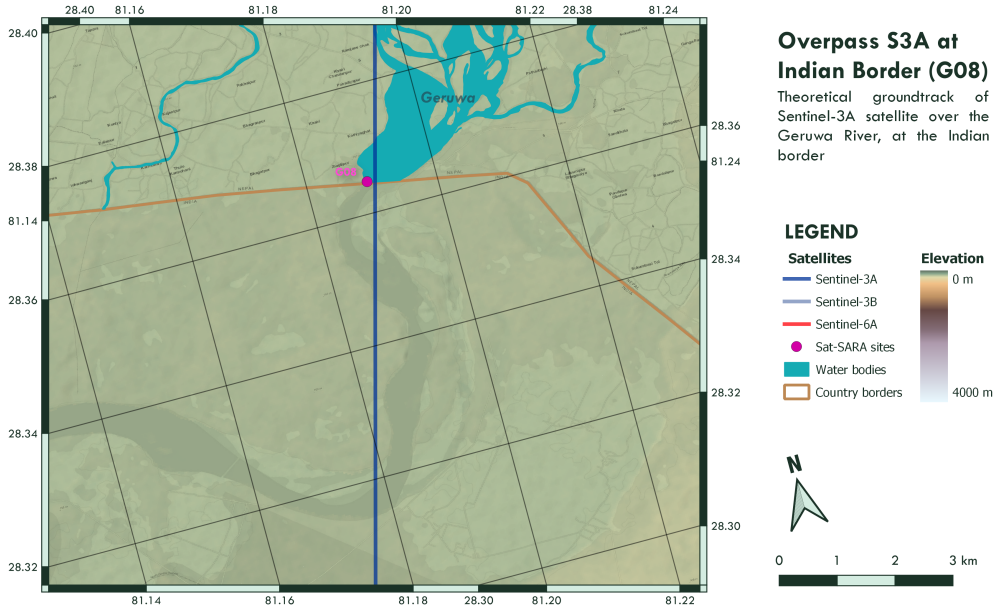

Figure 4.32: *Local topography and the theoretical ground track of S3A at the G08 overpass*

G08 is located in flat terrain. The left bank (inner bend) is scarcely vegetated with grasses. The forest is located further inland from the left bank, and almost directly on the right bank. Just upstream of G08 lays a mid-channel bar which is densely forested. The two photographs in figure 4.33 were taken during the 2022 field campaign and present the surrounding landscape of G08.

(a) *Looking upstream from G08*

(b) *Looking downstream from G08*

Figure 4.33: Landscape surrounding G08

At G08 two branches of the Geruwa converge into one, making the branch downstream of G08 the only channel of the river in this section. Whilst upstream of G08 the Geruwa still

consists of multiple branches, downstream of G08 it flows as one channel, curving towards the West before it rejoins the Kauriala River to form the Karnali River again. During the field campaign, the river was measured to be 68 meters wide at G08.

Multiple Channel Identification

Figure 4.34 presents the echogram for the S3A trajectory over the Geruwa River section at the Nepal-India border, for the dry season (January), wet season (September), and field campaign (November) of 2022. The general appearing pattern in the echograms for all seasons is very similar. In all three plots one clear river-like feature can be observed, which remains roughly at constant distance from the satellite. It moves slowly away from the satellite whilst progressing South, which can be explained by the river incline. The feature appears shifted toward a lower range gate for the wet season, indicating the river channel to be closer to the satellite. Water surface height increase during high flow may be a logical explanation for this shift.

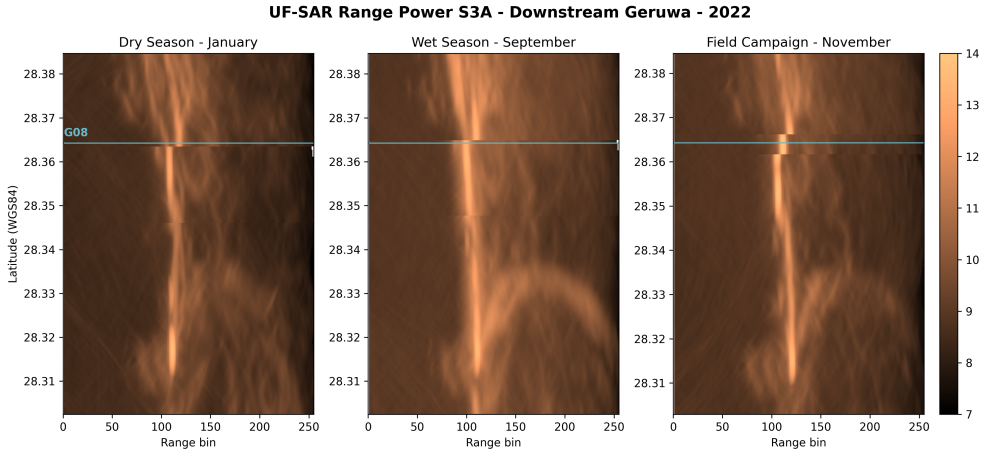

Figure 4.34: Unfocused-SAR signal power echogram for the Sentinel-3A overpass of the Geruwa River near the Indian boarder

North of G08, not one but multiple smaller bright appearing features can be observed. These multiple features are more distinct during the dry season and field campaign. However, in the wet season echogram, a wider water body also appears quite pronounced. These features are indicative of multiple channels, North of G08, which may merge into one or two major channels during high flow, or because of the wet conditions simply become less distinct in the return signal. Another distinct river-like feature can be observed in the second half of the trajectory. This stream appears far away (at large range bins) and curves as it moves closer to the satellite and approaches the suggested main river feature whilst progressing Southward.

Figure 4.35 presents the resulting identification of the river sections from the echogram features. The dry season (January) echogram is shown together with a map of the area, indicating the features and river sections. As the hydrology map for the Geruwa River did not extend across the Indian border, a open-source Google Map is presented here (instead of the SRTM and ESRI elevation map).

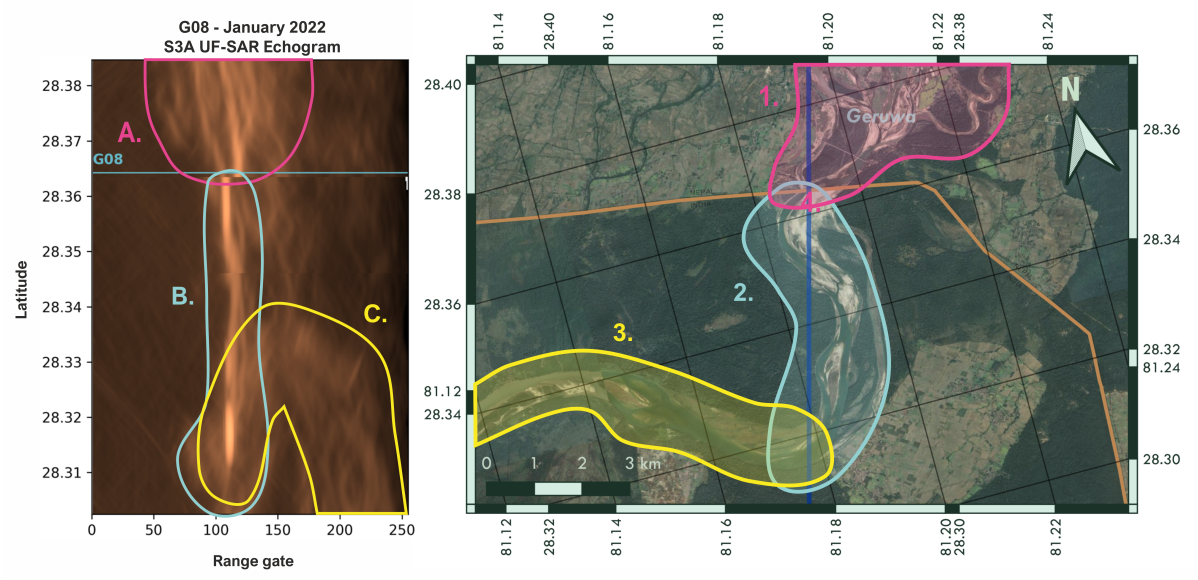

Figure 4.35: River sections identified from the stream-like features in the Sentinel-3A UF-SAR 2022 echogram over the downstream Geruwa River section area

All of the features are representing a section of the Geruwa River. With in the North the section (section 1) with multiple branches combining into one just before the overpass location, represented by the features as observed in A. The feature which remains at somewhat constant distance from the satellite (feature B) can be identified as the single Geruwa River branch which roughly follows the trajectory of the satellite (section 2). Feature C in the echogram represents the section of the Geruwa flowing towards the West (section 3), and thus away from the satellite trajectory (in both horizontal and vertical plane). This river section curves a bit to the North, which can also be observed in the echogram. Interestingly, this section appears much more pronounced in the wet season plot as compared to the field campaign and dry season echograms.

Sat-SARA Return Signal Waveforms

The return signal waveforms for the Sentinel-3A overpass over the Geruwa River at G08 are presented in figure 4.36. Although the order of magnitude of the signal power differs for the various plotted waveforms, for each of the waveforms clearly a single peak can be observed. For all presented return signals, the waveform is indicative of an inland water body, having only one clear singular peak of significant signal power. These waveforms show in fact ideal properties for retracking water surface heights.

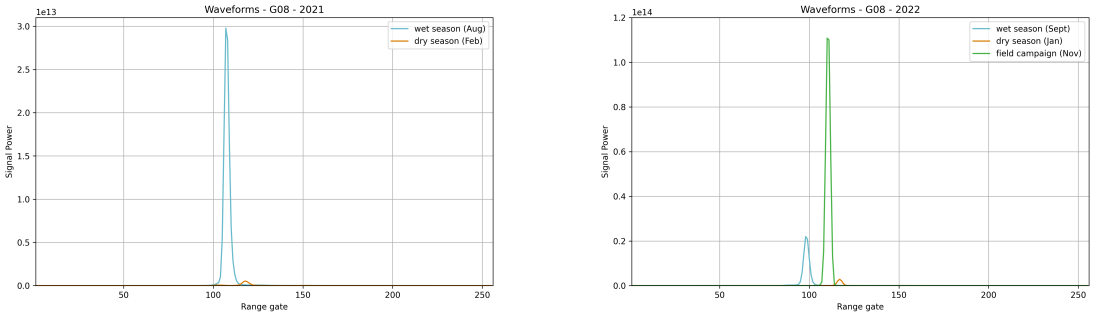

(a) *Dry & Wet Season 2021* **(b)** *Dry & Wet Season, and Field Campaign 2022*

Figure 4.36: *Return Signal Waveforms for the Sentinel-3A Overpass of Geruwa River at G08*

Sat-SARA Derived Water Surface Heights

Time series of the absolute water surface heights throughout 2021 and 2022 as derived from the sat-SARA data for G08 are presented in figure 4.37. The estimated water surface height is highest between June and September in 2021, whilst these can be found later in the year in 2022, between July and October. The months from January until late March show the lowest observed water surface heights for both years. The water surface height variation as derived from the sat-SARA time-series is $2.763\ m$ in 2021 and $2.105\ m$ in 2022.

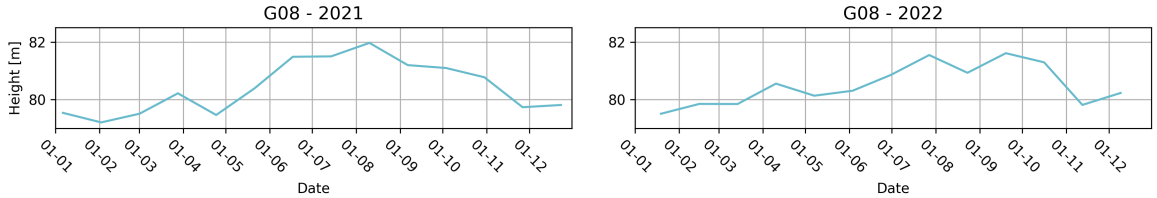

Figure 4.37: Timeseries of estimated water surface heights for the overpass locations G08 for the years 2021 and 2021

Field Observations

The relative water surface height for G08 was measured with respect to a point on the river bank assumed to be stable in time as trees were growing here. The relative water surface height was found at 4.7 m, and the observed maximum flow depth at G08 was 5.5 m (full depth readings in appendix G.

4.4. Geophysical Corrections for all River Sections

The geophysical correction values applied for determining the water surface heights from the sat-SARA data were investigated to assess uncertainties within the data and to assess whether adding the geophysical corrections is relevant for monitoring relative water level variability in the area. While spatial variability is relevant to consider for applying the geophysical corrections, temporal variability is most relevant for assessing the relevance of applying the corrections for water surface height derivations to monitor seasonal variability. The variation of each of the correction parameters and the total correction (R) over time were plotted for 2021 (see figure 4.38 and 2022 (see figure 4.39.

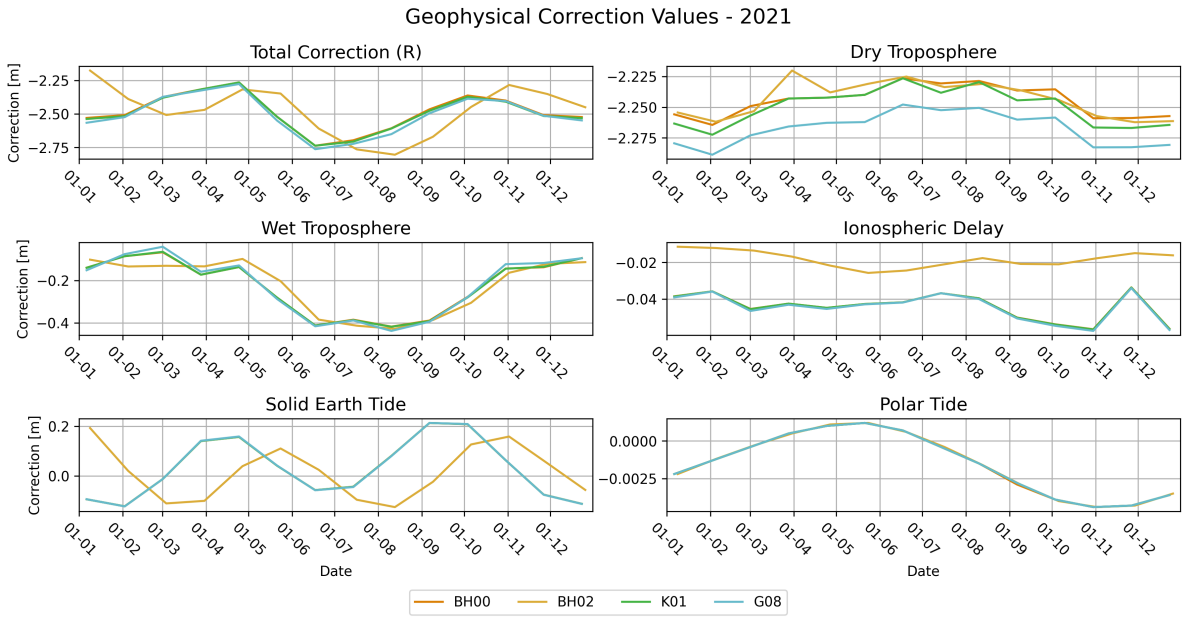

Figure 4.38: Timeseries of applied geophysical corrections for the overpass locations BH00, BH02 K01, and G08 for years 2021

Looking at the geophysical corrections for both 2021 and 2022, the correction values of BH00, K01 and G08 seem to follow the same trend for all correction factors and hence also for the total correction. They also show very similar values for all correction factors except for the dry tropospheric correction which shows an offset between the different locations of up to a few centimeters.

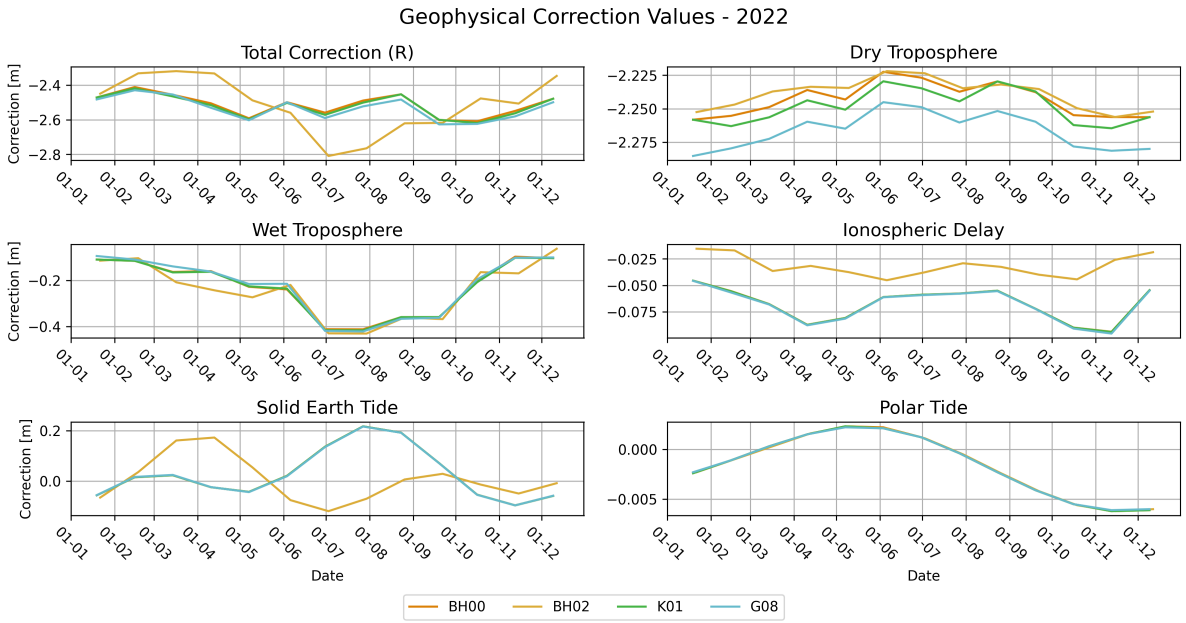

Figure 4.39: Timeseries of applied geophysical corrections for the overpass locations BH00, BH02 K01, and G08 for year2022

The polar tide correction is the same for all locations and is very small with a variation of approximately 3 millimetres throughout the year. For the ionospheric delay, the correction value for BH02 is approximately larger at any time throughout the year, compared to the other locations, with a difference of up to a few centimetres. Considering the solid earth tide, the average value for BH02 throughout a full year is very similar to the other locations, however, the temporal trend is very different. This results in a considerably different pattern of the total correction (R) over time for BH02 as compared to the other locations.

Overall, the dry tropospheric correction value accounts for the biggest part of the total correction value for all locations, with a value varying between -2.28 and -2.23 meters. With a variation of approximately 3 centimeters this does not account for the largest variability of the total correction value however. The solid earth tide and wet tropospheric correction values account for the largest temporal variability in the total correction value, with a variability of approximately 27 and 28 centimetres respectively.

5

Discussion

In this chapter the results as presented in the previous chapter are discussed. Data collected from both field observations and the satellite SAR altimetry analysis will be compared in context of the research questions posed and objectives set for this project. Thereafter, materials and methods applied to come to these results are also discussed.

Before discussing the results and methods specifically for the various approaches, it should be mentioned that the study area of the Lower Karnali River provided an exceptional opportunity for the current study, as it comprises a variety of landscapes over a relatively small spatial extent, with multiple overpasses of satellites carrying SAR altimetry instrumentation. The implementation of satellite SAR altimetry for water level monitoring remains dependent on such a satellite to pass over the river. For the Lower Karnali, this meant that the sat-SARA analyses were not possible for the Kauriala River as none of the available satellites pass over.

The Babai River on the other hand, does contain multiple overpasses of Sentinel-3 and an overpass of Sentinel-6. Hence, this river has great potential for deriving water surface heights from sat-SARA as well. The reason no analysis was executed for these overpasses was twofold. Firstly, the field campaign proved the inaccessibility of the region, making it very challenging to collect field observation data for validation, especially if consistent data collection or frequent revisiting of the sites is required. Paradoxically, this may further increase the relevance of utilising remote sensing solutions for this area. Secondly, limited time and resources for this thesis forced to be selective of the sites for which to apply the analysis, resulting in the exclusion of the Babai River for the current work.

5.1. Discussion of Multiple Channel Identification Results

The multiple channel identification was executed through the interpretation of the return signals plotted in an echogram. The Results chapter provides a presentation of both those resulting echograms, as well as an extensive interpretation of the data for each of the satellite overpass sites. When comparing the results from the different sites, a couple things become evident.

A striking observation is the difference in spatial resolutions of the echograms. In general, the features in the Sentinel-6 echograms appear much more distinct and at a higher spatial resolution as compared to the Sentinel-3 echograms. This spatial resolution improves even further for the FF-SAR echograms as compared to the UF-SAR echograms. The features

appear much more distinct in the FF-SAR echograms as compared to UF-SAR, whilst the Sentinel-6 already presents more distinct features as compared to the Sentinel-3 products. For the FF-SAR product this in turn allows to recognise more details in the features as well, such as more detailed flow direction or river incline changes.

For the sites at which it was expected to find a singular river channel or one main channel (K01 and G08), data interpretation was more straightforward as compared to the sites with a multitude of river branches (BH00, BH01, and BH02). Overall the echograms presented expected patterns: clear single stream-like features for the river sections with one main river channel, and a combination of multiple streams in sections with multiple major river channels.

It proved possible to identify multiple different channels from the echograms. Even the activation rain-fed (potential flash-flood) tributaries could be identified. The rapid change in range gates for such features was indicative of tributaries running down steep hillslopes. This proved possible for both hilly river sections of the Bheri and Karnali Rivers. At the same time multiple minor and major channels could be identified for the Geruwa River reach. However, for echograms with multiple major channels in irregular topography, the identification of which appearing feature belonged to which river stream did prove challenging. This was specifically the case for the Bheri River section.

While distances between river channels were not directly obtainable from the echograms, the relative channel orientations were deduced by combining the sat-SARA data with a DEM for data interpretation. Exact positioning of the channels couldn't be ascertained solely from the echograms; this required the supplementary aid of a DEM or other maps. For future research, exploring the feasibility of extracting precise distances among the various identified channels appearing in sat-SARA would be very interesting.

5.2. Discussion of Observed Water Surface Heights

All sat-SARA derived water surface heights have been put alongside each other in figure 5.1 for further assessment. When comparing the water surface height time series for the different sites, a few things become evident. Firstly, the general trends remain the same over all locations, with lower water levels measured during the months of January through to April and higher water levels observed between June and September. This is in accordance with what was expected based on the climate characteristics of the catchment.

Secondly, the average water heights as compared between the locations are also as expected. BH00 is located farthest upstream, at the highest elevation and also shows the highest average absolute water surface height at approximately 178 metres. BH02 being located relatively close to BH00, downstream of the Bheri River, shows an average water surface height of approximately 169 meters, only 9 meters lower than BH00. These sites show the greatest similarity in their water level variability pattern. K01 situated at lower altitude than the Bheri River section shows lower absolute water surface heights and lastly for the Geruwa the absolute water surface heights are considerably lower, as expected.

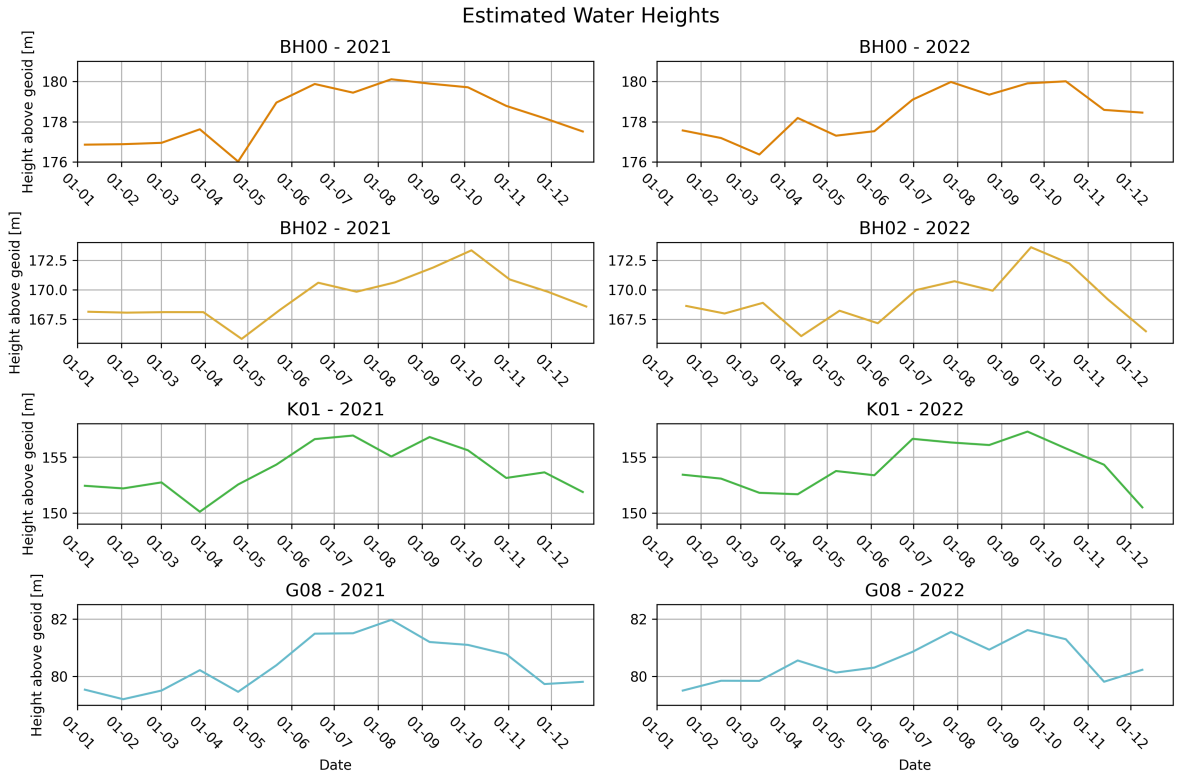

Figure 5.1: Timeseries of sat-SARA-derived water surface heights at all overpass sites

It should be noted however, that the absolute elevations at which the water surface heights were measured for each of these locations do not agree with the elevations as presented by the DEM, nor with the absolute elevations observed during the field campaign. The results suggest a systematic negative bias, which is approximately -30 metres at BH02, -23 metres at K01, and -40 metres at G08. The objective of this work is, however, not to derive the absolute water surface heights at the locations, but to derive the water surface heights with such accuracy that water level variability can be monitored for hydrological purposes. Hence, relative water surface heights for monitoring water level variability with respect to the surrounding landscape suffices.

The water level variation throughout the year as observed from the sat-SARA data was determined for each site (see table 5.1). The results seem consistent per location for the two years of 2021 and 2022. The largest water level variation can be found for location BH02, with a water level variation throughout the year of approximately 7.5 metres. The water level variation at the nearby located overpass BH00 is much smaller with 4.1 metres in 2021 and 3.6 metres in 2022. The landscape characteristics may be an explanation for this. The reinforced embankments in place for the bridges at BH01 and BH02, as well as possible backwater-curve effects from the Bheri-Karnali confluence, may cause the water level variability to be larger at BH02 as compared to BH00. No clear conclusions can be drawn here, however.

	BH00	BH02	K01	G08
2021	4.088	7.482	6.820	2.763
2022	3.639	7.509	6.779	2.105

Table 5.1: Water surface height variation (minimum - maximum water level) per year at the different overpass locations as derived from sat-SARA

The water level variation in the Karnali (at K01) for both years is approximately 6.8 metres. This is in line with in-situ observed water level variations as measured at Chisapani (K03), which range between 4.9 and 12.2 meters with an average water level variation of 7.3 meters over the years 1992 to 2018 (see section 4.2).

Relative water level observations collected during the field campaign at the selected sites are compared in 5.2 and observed flow depths at the sites were 4.2 and 5.5 meters for BH01 and G08 respectively. From this can be derived that the water level variations as observed from the sat-SARA and Chisapani stage height data align with the physical properties of the river as observed in the field. The water level variations observed remain within the boundaries of the river banks for the studied years. The field observed relative water levels may be contribute to relating sat-SARA observed water surface heights with floodplain inundation, channel activation and potential floods. Hence, this is an interesting topic for future studies, and it is recommended to complement the data catalogue during future campaigns.

	K02	K03	G07	G08
Relative IWH [m]	20.9	10.1	5.5	4.7

Table 5.2: In-situ relative water surface heights (corrected) at campaign locations along the Karnali and Geruwa River.

At the farthest downstream situated G08 in the Geruwa River, the water level variability is the smallest of this set of sites, with a variability of 2.8 metres in 2021 and 2.1 metres in 2022. This can be explained by two factors. Firstly, only a portion of the water flowing through the Karnali, flows through the Geruwa as the other portion flows through the Kauriala. Hence, a smaller volume of water flows through the Geruwa as compared to the Karnali. Secondly, at G08 the landscape provides a wide floodplain, whereas the Karnali River is restricted by steep hillslopes on both sides. With a significant increase in river discharge, a larger increase in water level is expected in the Karnali river section as compared to the Geruwa.

Putting all of this in the context of the aim to monitor water level variations from sat-SARA for hydrological purposes, the temporal resolution appears to be the biggest limitation. With the data presented, water levels can be monitored with Sentinel-3 data at 27-day time intervals. This allows for the monitoring of seasonal trends. Although not yet proven successful within the scope of this project, Sentinel-6 provides promising possibilities. With a 10-day return period and the development of FF-SAR techniques Sentinel-6 is expected to provide both higher temporal and spatial resolution. This 10-day temporal resolution would provide

sub-optimal temporal resolution. Nearly allowing hydrologists to identify flood waves down river streams following from weather events.

The orientation of the Sentinel-3A satellite trajectory with respect to the Geruwa River, following its course for the most part of the river section. This offers opportunities to derive the river incline over the course of the river section. A brief exploration was conducted but was not included in the main work presented (see appendix H). The results of this exploration suggest that it should be possible to derive river incline from combining water surface height observations at multiple overpasses along the reach. This might be an interesting topic for future research.

Lastly it should be mentioned that for the derivation of the water surface heights, the exact overpass trajectory of the satellite was not taken into account. As the satellites may undergo drift, the satellite may not always pass over the river at exactly the same location but shifted up to a few hundred metres across-track. For sites where the satellite trajectory is perpendicular to the river stream and the river experiences a steep slope, this may cause inaccuracies in the derived water surface heights. These may appear as water level variations in time-series plots. This is something which was not accounted for in the current study, but should definitely be considered for future work to increase accuracy and veracity of the data.

5.3. Discussion of Sat-SARA Data & Data Processing Methods

The collection, processing and interpretation of Sentinel-3 SRAL and Sentinel-6 POD4 data for estimating water surface heights over inland water bodies is rather complex and labour-intensive. As for the multiple-channel identification analysis, no retracking or application of geophysical corrections was required the processing flow was somewhat simplified. Nevertheless, these processing steps are not to be underestimated.

5.3.1. Sentinel-3 and Sentinel-6 Data Gaps

During the collection and processing of the Sentinel-3 and Sentinel-6 data it became apparent that substantial gaps existed within the datasets. These data gaps manifested themselves in different ways and proved especially prevalent for the Sentinel-6 data.

Firstly, Sentinel-6 data was at the time of writing still being reprocessed for 2022. Hence, Sentinel-6 data was only available for a full calendar year for 2021. However, for many of the available dates for which data was provided, the datasets was empty for the targeted coordinates. As a result, the usable Sentinel-6 dataset was much smaller than intended, comprising usable data for a mere 9 days. In comparison, with a return period of 10 days a full dataset would comprise data for approximately 36 days for a single year.

Sentinel-3 data gaps were easier to circumvent. Data for 2019 seemed corrupted whilst data for 2020 was stored elsewhere in the EUMETSAT databases. Eventually data for both years were not included for the current work, both due to these challenges as well as due to time constraints.

It should be noted that collecting the level-1 and level-2 data for Sentinel-3 and Sentinel-6 is unfortunately not straightforward. The data is collected from multiple different databases, using different retrieval methods and are provided in varying formats. This causes the process of data collection and matching of the datasets to be cumbersome.

5.3.2. Relevance of Geophysical Corrections

Contrarily to the spatial variation of the geophysical corrections, the correction factors proved highly variable over time. Hence, the application of the geophysical corrections for deriving water surface heights proved relevant to ensure accuracy in the order of magnitude of decimeters as was desired for this project. These corrections proved relevant not only for deriving absolute water surface heights but also for monitoring relative water surface height variations.

Nearest neighbour interpolation was used for applying the geophysical corrections. The accuracy of the observed water surface heights could be further improved by applying spatial linear interpolation for the correction values. With an order of magnitude of a few millimetres, the spatial variability for each of the correction factors proved to be negligibly small. This level of accuracy was not required for the current work. Hence, it was decided that nearest neighbour interpolation would suffice. If a higher accuracy is desired for another study area or application, one might consider applying a linear interpolation method to achieve an optimal correction value for the concerning location.

5.3.3. Choice of Retracker

For this study, an empirical point target response retracker making use of a Gaussian fit model was applied. Optimising the retracker algorithm is expected to increase the accuracy of the sat-SARA-derived water surface heights. Investigating the performance of the retracker itself was not deepened in the current work. Assessing the retracker performance is greatly aided by the availability of high-accuracy in-situ water surface height measurements. This would be an interesting topic for future research.

5.4. Discussion of Field Observation Data Collection Methods

Collecting valuable in-situ data proved very challenging with the limited available measurement equipment and logistical resources in the remote and difficult accessible landscape. The field campaign had an exploratory aim and confirmed more advanced measurement equipment is desired to collect data of sufficient quality. It should be noted that these challenging conditions for collecting field observation data are part of the reason that (satellite) remote sensing solutions for monitoring the hydrodynamic conditions for very remote and difficult-to-access regions would be highly valuable.

Processing of the flow depth measurements from the CHIRP+ proved challenging. No proven method was found yet to reconstruct the cross-section for an accurate representation of the river bathymetry. However, these data was deemed of sufficient quality to approximate the river cross-section and estimate the maximum flow depth with sufficient accuracy for the current work. Measuring flow depths (or cross-sections) at any river sections with either a

large river width, large river depth, high flow velocities, or any combination of these, may become possible with the use of an ADCP, where this may not have been possible during the 2022 field campaign. Since the CHIRP+ does offer a cheaper solution, another suggestion to improve the success rate for data collection is to mount it to a floating device or small boat which can be pulled across the river. This float should ensure the CHIRP+ to remain relatively stable at the water surface and keep it from jumping out of the water.

Relative water level measurements were collected with an estimated accuracy of 10-30 centimetres. Whilst field validation was made possible from the relative water level measurements and the stage height measurements at Chisapani, absolute water surface height measurements obtained from a differential GNSS device or other high-accuracy (vertical) positioning device would have been very valuable. Absolute surface water height measurements allow to directly validate the water surface heights as derived from sat-SARA data. Unfortunately, this data could not be collected during the 2022 field campaign due to equipment failure. It is recommended to collect field-observed water surface height measurements using positioning equipment with high vertical precision, such as a differential GNSS device, during the next field campaign to validate the data collected during the current study.

Singular or yearly campaign visits, while very valuable, offer only limited temporal resolution for the field observation data. These observational periods lack the capacity to capture seasonal or continuous hydrodynamic variations. Furthermore, these merely provide validation data for the sat-SARA-derived water surface heights at a single moment in time. Increasing the volume of in-situ data collection, through longer-term continuous data collection, might enhance our understanding of the proposed sat-SARA method's efficacy. However, this endeavour seems to diverge from the very premise of the study: to minimise the necessity for such intensive on-site data gathering in remote areas. Thus, the curious but commonly-known paradox for remote sensing monitoring is encountered, where the endeavour to fortify the evaluation of the method could inadvertently veer away from its central intent: to provide a less field-observation-dependent approach to monitoring.

6

Conclusion

This chapter marks the end of the exploration into the potential of satellite SAR altimetry for monitoring water level variability and river channel activation. Here, the answers to the guiding research questions are presented, drawing from insights gained from a combination of satellite remote sensing data and the outcomes from field observations. Beginning by responding to posed sub-questions, the chapter progresses to address the main research question, followed by a reflection on the achievement of set objectives is presented.

6.1. Insights from Satellite SAR Altimetry

Two sub-questions were posed for the analysis of satellite SAR altimetry data in support of answering the main research question. The first sub-question posed was: "*To what extent is it possible to identify multiple river channels from satellite SAR altimetry in Bheri, Karnali and Geruwa River sections*?" The results are promising, especially for identifying small to medium-sized tributaries in single-channel sections. As temporal variability could be observed, it was possible to detect channel activation. The Sentinel-6 FF-SAR product, providing a larger spatial resolution, excels in identifying river channels as they appear more distinctly in the data. Different typical characteristics became apparent for observed features in the echograms, enabling simple classification. Interpreting data in areas with irregular topography and with multiple major river channels remains challenging, however, especially for the Sentinel-3 UF-SAR products. Hence, channel identification is significantly aided by utilising a DEM.

The second sub-question posed was: "*To what extent is it possible to derive water surface heights at various river overpass locations in the Bheri, Karnali and Geruwa Rivers, from satellite SAR altimetry?*" For four sites, time series of water surface heights were generated for 2021 and 2022 with an interval of 27 days using Sentinel-3 SRAL data. This study proves that deriving water surface heights from sat-SARA is possible over rivers in various terrain types. Deriving water surface heights from Sentinel-6 data was not achieved with the selected retracker and processing settings. Nevertheless, the use of Sentinel-6 data holds great promise. Especially, as with a 10-day return period it provides an increased temporal resolution compared to Sentinel-3 with a 27-day return period.

From the sat-SARA-derived water surface height time series, it was possible to observe seasonal variability. These seasonal trends were consistent with prevailing climatic conditions, and the observed patterns as well as the order of magnitude of water level variations also

aligned with field observations. These field observations allowed for validation of water level variations. Unfortunately, it was not possible to quantify the exact accuracy of the absolute water levels due to the unavailability of the required field validation data. This study establishes a framework for field validation of the sat-SARA-derived water surface heights, emphasizing the importance to prioritise the collection of high-accuracy in-situ absolute water surface heights during future campaigns. All things combined, the primary purpose of monitoring water level variations with sat-SARA in the Lower Karnali River reaches remains promising.

Whilst the spatial resolution appears sufficient for water level monitoring purposes, temporal resolution currently appears to be the main limiting factor. Sentinel-6 may provide a great leap forward in this regard. In addition, data availability proved to be a major limitation for the current work, manifesting itself mostly in data gaps for Sentinel-6 data and for high-accuracy in-situ measurements of absolute water surface heights.

6.2. Insights from Field Observations

The field campaign aimed to measure and document water surface heights, flow depths, river widths, and landscape characteristics at the selected sites along the Bheri, Karnali and Geruwa Rivers. To this extent, a total of 32 sites have been visited during the field campaign, whilst six of those have been used for the current work. Some field observation data types were unattainable at certain sites due to local landscape or river characteristics. Relative water levels, river widths and flow depths were measured with an estimated accuracy of 10-30 centimetres. At all sites pictures were taken and descriptions of the landscape were documented to contextualise both remote sensing and field observations. Stage height measurements at Chisapani proved particularly helpful for validating sat-SARA-derived water levels and water level variations.

6.3. Sat-SARA for River Monitoring in Complex Topographies

Combining insights obtained through the sat-SARA analyses for multiple channel identification and water surface heights with insights from field observations, the main question posed for this research can be addressed. The main research question of this thesis was: *What is the potential of satellite SAR altimetry for monitoring water level variability and river channel activation in the diverse topographical landscapes of the Lower Karnali River, Nepal?*".

Overall, the application of Sentinel-3 and Sentinel-6 satellite SAR altimetry for water level monitoring and river channel activation for the diverse topographical landscapes of the Lower Karnali River proves promising. Sat-SARA-derived water level variations followed anticipated seasonal patterns and aligned with field observations. It appears that the temporal resolution is currently the main limiting factor in monitoring water levels for hydrological purposes. Sentinel-6 is expected to provide a great leap forward in this regard.

Sat-SARA return signals can be used to identify multiple channels in a river section. In addition, seasonal variability allows the detection of channel activation during the wet season. Typical feature characteristics for channels were recognised in the echograms, allowing for basic channel classification. Data interpretation becomes more complicated for river sections consisting of many major channels situated in an irregular topographical landscape.

7

Outlook

In light of the study's findings, several avenues for future research and further exploration emerge. These will be discussed briefly in the following sections.

7.1. Enhancing Field Observation Quality and Quantity

Three topics became apparent for recommendations for future work regarding the collection of field observation data. Firstly, the collection of higher quality and more extensive field observations would greatly contribute to advancing the accuracy and applicability assessment of satellite SAR altimetry for monitoring water surface heights in the study area. To this end, it is recommended for future field campaigns to collect in-situ water surface height measurements through advanced positioning techniques providing high accuracy in the vertical plane, such as differential GNSS. These observations will augment the validation process and enrich the overall dataset.

Secondly, continuity of field campaigns is essential for capturing long-term water surface height variations. Hence, it is recommended to sustain relative water surface height measurements as executed during the 2022 field campaign. This would provide insights into yearly patterns and again enrich the overall data catalogue. These measurements may be particularly valuable for the Geruwa River.

Lastly, the data obtained from water level loggers installed during the 2022 field campaign at the downstream ends of the Kauriala and Geruwa Rivers will become available and may be of great value for future research. Integrating this data with the satellite SAR altimetry outputs will enable the comparison and validation of water level variations in the Geruwa River from the different datasets. With the arrival of this data, water levels will then be available from sat-SARA, relative in-situ water surface height observations, flow depth measurements, and the water level loggers at the downstream end of the Geruwa.

7.2. Sat-SARA for River Incline and Discharge Estimations

While beyond the scope of this thesis, an exciting prospect lies in utilising satellite SAR altimetry to study river incline. A brief exploration as discussed in section 5.2 proved promising, and has been proven successful in the past (Tarpanelli and Benveniste, 2019). Exploring this path further could facilitate the estimation of river discharge. Incorporating this into future research would deepen the understanding of the dynamics of the Lower Karnali and further emphasise and utilise the full potential of satellite SAR altimetry for river monitoring.

7.3. Advancing Multiple Channel Identification

The intriguing results of the multiple-channel identification analysis point toward interesting directions for future studies. Exploring the development of a dedicated multiple-channel identification algorithm could enable the quantification of channel recognition and potentially even channel classification. Furthermore, investigating the feasibility of deriving distances between identified channels from the satellite SAR altimetry data remains an unexplored terrain with potential hydrological significance. Yuan (2019) has proven with her work that river widths can be derived from sat-SARA, indicating great potential for further research into the suggested topic.

References

Alsdorf, D. E., Rodríguez, E., and Lettenmaier, D. P. (2007). Measuring surface water from space. *Reviews of Geophysics*, 45(2).

Aryal, A., Lamsal, R., Ji, W., and Raubenheimer, D. (2015). Are there sufficient prey and protected area in nepal to sustain an increasing tiger population? *Ethology Ecology and Evolution*, xx:xx–xx.

AVISO (2023). Aviso+ - techniques - altimetry - principle - how altimetry works. https://www.aviso.altimetry.fr/en/techniques/altimetry/. Accessed on 9 August 2023.

Berry, P. (2006). Two decades of inland water monitoring using satellite radar altimetry. 614.

Berry, P. A., Garlick, J. D., Freeman, J. A., and Mathers, E. L. (2005). Global inland water monitoring from multi-mission altimetry. *Geophysical Research Letters*, 32:1–4.

Bhattarai, B. R., Wright, W., Morgan, D., Cook, S., and Baral, H. S. (2019). Managing human-tiger conflict: lessons from bardia and chitwan national parks, nepal.

Bijlmakers, J., Griffioen, J., and Karssenberg, D. (2023). Environmental drivers of spatio-temporal dynamics in floodplain vegetation: grasslands as habitat for megafauna in bardia national park (nepal). *Biogeosciences*, 20(6):1113–1144.

Bjerklie, D. M., Birkett, C. M., Jones, J. W., Carabajal, C., Rover, J. A., Fulton, J. W., and Garambois, P. A. (2018). Satellite remote sensing estimation of river discharge: Application to the yukon river alaska. *Journal of Hydrology*, 561:1000–1018.

Bonnema, M. G., Sikder, S., Hossain, F., Durand, M., Gleason, C. J., and Bjerklie, D. M. (2016). Benchmarking wide swath altimetry-based river discharge estimation algorithms for the ganges river system. *Water Resources Research*, 52:2439–2461.

Calmant, S., Seyler, F., and Creteaux, J. (2008). Monitoring continental surface waters by satellite altimetry. *Surveys in Geophysics*, 29.

Crétaux, J.-F. and Birkett, C. (2006). Lake studies from satellite radar altimetry. *Comptes Rendus Geoscience*, 338(14):1098–1112. La Terre observée depuis l'espace.

Dahal, P., Shrestha, M. L., Panthi, J., and Pradhananga, D. (2020). Modeling the future impacts of climate change on water availability in the karnali river basin of nepal himalaya. *Environmental Research*, 185:109430.

Deeper (2020). Fish deeper smart sonar chirp+ user manual. https://fccid.io/2AHKO-PRO/User-Manual/CHIRP-Instruction-Manual-A4-4612239. Accessed on 18 August 2023, the same manual was also provide with the equipment.

Dinardo, S. (2020). Techniques and applications for satellite sar altimetry over water, land and ice.

Dingle, E. H., Creed, M. J., Sinclair, H. D., Gautam, D., Gourmelen, N., Borthwick, A. G., and Attal, M. (2020). Dynamic flood topographies in the terai region of nepal. *Earth Surface Processes and Landforms*, 45:3092–3102.

DNPWC and DFS (2022). Status of tigers and prey in nepal 2022. department of national parks and wildlife conservation and department of forests and soil conservation. ministry of forests and environment, kathmandu, nepal.

Donlon, C. J., Cullen, R., Giulicchi, L., Vuilleumier, P., Francis, C. R., Kuschnerus, M., Simpson, W., Bouridah, A., Caleno, M., Bertoni, R., Rancaño, J., Pourier, E., Hyslop, A., Mulcahy, J., Knockaert, R., Hunter, C., Webb, A., Fornari, M., Vaze, P., Brown, S., Willis, J., Desai, S., Desjonqueres, J.-D., Scharroo, R., Martin-Puig, C., Leuliette, E., Egido, A., Smith, W. H., Bonnefond, P., Le Gac, S., Picot, N., and Tavernier, G. (2021). The copernicus sentinel-6 mission: Enhanced continuity of satellite sea level measurements from space. *Remote Sensing of Environment*, 258:112395.

Duwal, S., Liu, D., and Pradhan, P. M. (2023). Flood susceptibility modeling of the karnali river basin of nepal using different machine learning approaches. *Geomatics, Natural Hazards and Risk*, 14(1):2217321.

Ehlers, F. (2022). Coastal sar altimetry processing: An overview. Summer School TU Delft.

Ehlers, F., Schlembach, F., Kleinherenbrink, M., and Slobbe, C. (2023a). Validity assessment of samosa retracking for fully-focused sar altimeter waveforms. *Advances in Space Research*, 71(3):1377–1396.

Ehlers, F., Slobbe, C., Verlaan, M., and Kleinherenbrink, M. (2023b). A noise autocovariance model for sar altimeter measurements with implications for optimal sampling. *Advances in Space Research*, 71(10):3951–3967.

ESA (2011). Cryosat-2 product handbook. https://earth.esa.int/documents/10174/125272/CryoSat-Baseline-D-Product-Handbook.

ESA (2022). Sentinel-3 sral/mwr land user handbook. https://sentinels.copernicus.eu/documents/247904/4871083/Sentinel-3+SRAL+Land+User+Handbook+V1.1.pdf.

ESA (2023). Sentinel-6. https://www.esa.int/Applications/Observing_the_Earth/Copernicus/Sentinel-6. Accessed on 18 August 2023.

EUMETSAT (2022). Sentinel-6/jason-cs alt level 1 product generation specification (l1 alt pgs). https://www.eumetsat.int/media/48261.

Finsen, F., Milzow, C., Smith, R., Berry, P., and Bauer-Gottwein, P. (2014). Using radar altimetry to update a large-scale hydrological model of the brahmaputra river basin. *Hydrology Research*, 45:148–164.

Gao, Q., Makhoul, E., Escorihuela, M. J., Zribi, M., Quintana Seguí, P., García, P., and Roca, M. (2019). Analysis of retrackers' performances and water level retrieval over the ebro river basin using sentinel-3. *Remote Sensing*, 11(6).

Goodrich, J., Wibisono, H.and Miquelle, D., Lynam, A., Sanderson, E., Chapman, S., Gray, T., Chanchani, P., and Harihar, A. (2020). Panthera tigris. the iucn red list of threatened species 2022: e.t15955a21486201. https://www.iucnredlist.org/species/15955/214862019.

HawkEye (2023). User's guide - h22px hawkeye handheld sonar system. https://www.manualslib.com/manual/1788630/Norcross-Hawkeye-H22px.html?page=5#manual. User manual retrieved on 18-08-2023, the same manual was also provided with the equipment. URL to company website: https://hawkeyeelectronics.com/.

Houghton-Carr, H., Fry, M., and Wallingford, U. (2006). The decline of hydrological data collection for development of integrated water resource management tools in southern africa. *IAHS publication*, 308:51.

Jain, M., Andersen, O. B., Dall, J., and Stenseng, L. (2015). Sea surface height determination in the arctic using cryosat-2 sar data from primary peak empirical retrackers. *Advances in Space Research*, 55(1):40–50.

Jiang, L., Nielsen, K., Dinardo, S., Andersen, O. B., and Bauer-Gottwein, P. (2020). Evaluation of sentinel-3 sral sar altimetry over chinese rivers. *Remote Sensing of Environment*, 237:111546.

Kao, H.-C., Kuo, C., Tseng, K.-H., Shum, C., Tseng, T.-P., Jia, Y.-Y., Yang, T.-Y., Ali, T., Yi, Y., and Hussain, D. (2019). Assessment of cryosat-2 and saral/altika altimetry for measuring inland water and coastal sea level variations: A case study on tibetan plateau lake and taiwan coast. *Marine Geodesy*, 42:1–17.

Kim, D., Lee, H., Beighley, E., and Tshimanga, R. M. (2021). Estimating discharges for poorly gauged river basin using ensemble learning regression with satellite altimetry data and a hydrologic model. *Advances in Space Research*, 68(2):607–618. 25 Years of Progress in Radar Altimetry.

Kleinherenbrink, M., Naeije, M., Slobbe, C., Egido, A., and Smith, W. (2020). The performance of cryosat-2 fully-focussed sar for inland water-level estimation. *Remote Sensing of Environment*, 237:111589.

Kral, M. J. C., Lunenburg, M. V., and Alphen, J. J. M. V. (2017). The spatial distribution of ungulates and primates across the vegetation gradient in bardiya national park, west nepal. *Asian Journal of Conservation Biology*, 6:38–44.

Krietemeyer, A., Gayton, I., Winsemius, H., and Chazua, I. (2022). Positioning guidelines with the u-box zed-f9p gnss receiver. https://github.com/hcwinsemius/RTK_GNSS/blob/master/Positioning_guideline.md. Accessed on 11 November 2022.

Maillard, P., Bercher, N., and Calmant, S. (2015). New processing approaches on the retrieval of water levels in envisat and saral radar altimetry over rivers: A case study of the são francisco river, brazil. *Remote Sensing of Environment*, 156:226–241.

Michailovsky, C. I., McEnnis, S., Berry, P. A. M., Smith, R., and Bauer-Gottwein, P. (2012). River monitoring from satellite radar altimetry in the zambezi river basin. *Hydrology and Earth System Sciences*, 16(7):2181–2192.

Mishra, Y., Nakamura, T., Babel, M. S., Ninsawat, S., and Ochi, S. (2018). Impact of climate change on water resources of the bheri river basin, nepal. *Water*, 10(2).

Murfitt, J. and Duguay, C. R. (2021). 50 years of lake ice research from active microwave remote sensing: Progress and prospects. *Remote Sensing of Environment*, 264:112616.

Nielsen, K., Andersen, O. B., and Ranndal, H. (2020). Validation of sentinel-3a based lake level over us and canada. *Remote Sensing*, 12(17).

Nikon (2019). Forestry pro ii instruction manual. https://downloadcenter.nikonimglib.com/en/products/544/Forestry_Pro_II.html. Accessed online on 27-07-2023, similar manual was also provided with the equipment.

Odden, M., Wegge, P., and Storaas, T. (2005). Hog deer axis porcinus need threatened tall-grass floodplains: A study of habitat selection in lowland nepal. *Animal Conservation*, 8:99–104.

O'Loughlin, F. E., Neal, J., Yamazaki, D., and Bates, P. D. (2016). Icesat-derived inland water surface spot heights. *Water Resources Research*, 52:3276–3284.

Park, E. (2020). Characterizing channel-floodplain connectivity using satellite altimetry: Mechanism, hydrogeomorphic control, and sediment budget. *Remote Sensing of Environment*, 243.

Ranndal, H., Andersen, O. B., and Knudsen, P. (2020). Global and regional evaluation of the first year of sentinel-3: Possibilities and challenges for mss determination. pages 89–96.

Roohi, S., Sneeuw, N., Benveniste, J., Dinardo, S., Issawy, E. A., and Zhang, G. (2021). Evaluation of cryosat-2 water level derived from different retracking scenarios over selected inland water bodies. *Advances in Space Research*, 68:947–962.

Rosmorduc, V., Benveniste, J., Bronner, E., Dinardo, S., Lauret, O., Maheu, C., Milagro, M., Picot, N., Ambrozio, A., Escolà, R., Garcia-Mondejar, A., Schrama, E., Restano, M., and Terra-Hom, M. (2018). Radar altimetry tutorial - brat - broadview radar altimetry toolbox. https://altimetry.info/articles/radar-altimetry-tutorial/. Tutorial Manual provided by ESA and CNES.

Samboko, H., Schurer, S., Savenije, H., Makurira, H., Banda, K., and Winsemius, H. (2021). Evaluation of the geometry for remote river rating in hydrodynamic environments.

Schaperow, J. R., Li, D., Margulis, S. A., and Lettenmaier, D. P. (2019). A curve-fitting method for estimating bathymetry from water surface height and width. *Water Resources Research*, 55:4288–4303.

Schneider, R., Godiksen, P. N., Villadsen, H., Madsen, H., and Bauer-Gottwein, P. (2017). Application of cryosat-2 altimetry data for river analysis and modelling. *Hydrology and Earth System Sciences*, 21:751–764.

Schwatke, C., Dettmering, D., Bosch, W., and Seitz, F. (2015). Kalman filter approach for estimating water level time series over inland water using multi-mission satellite altimetry. *Hydrology and Earth System Sciences Discussions*, 12:4813–4855.

Shahi, K., Khanal, G., Jha, R. R., Joshi, A. K., Bhusal, P., and Silwal, T. (2022). Characterizing damages caused by wildlife: Learning from bardia national park, nepal. *Human Dimensions of Wildlife*, 27(2):173–182.

Shrestha, B., Zhang, L., Sharma, S., Shrestha, S., and Khadka, N. (2022). Effects on ecosystem services value due to land use and land cover change (1990–2020) in the transboundary karnali river basin, central himalayas. *SN Applied Sciences*, 4.

Sulistioadi, Y. B., Tseng, K. H., Shum, C. K., Hidayat, H., Sumaryono, M., Suhardiman, A., Setiawan, F., and Sunarso, S. (2015). Satellite radar altimetry for monitoring small rivers and lakes in indonesia. *Hydrology and Earth System Sciences*, 19:341–359.

Tarpanelli, A. and Benveniste, J. (2019). *On the potential of altimetry and optical sensors for monitoring and forecasting river discharge and extreme flood events*. Elsevier.

Tomić, M. and Andersen, O. B. (2023). Icesat-2 for coastal mss determination;evaluation in the norwegian coastal zone. *Remote Sensing*, 15(16).

Tourian, M. J., Schwatke, C., and Sneeuw, N. (2017). River discharge estimation at daily resolution from satellite altimetry over an entire river basin. *Journal of Hydrology*, 546:230–247.

van Haaren, S. (2020). Assessment of flood early warning and response in an urbanized catchment: A case study of the tub ma basin in thailand.

vanEssen (2023). Company website: https://www.vanessen.com/product-category/data-loggers/. Accessed on 05-09-2023.

Villadsen, H., Deng, X., Andersen, O. B., Stenseng, L., Nielsen, K., and Knudsen, P. (2016). Improved inland water levels from sar altimetry using novel empirical and physical retrackers. *Journal of Hydrology*, 537:234–247.

Yadav, S. K. (2002). Hydrological analysis of bheri-babai hydropower project nepal. MSc Thesis, Norwegian University of Science and Technology, Department of Hydraulic and Environmental Engineering.

Yuan, Y. (2019). Estimation of river width with fully-focused sar altimetry data.
*

A

Sat-SARA Manual

SAT-SARA MANUAL

Searching, downloading, storing & processing data from EUMETSAT using FileZilla, anaconda prompt & cluster TU Delft

1. EUMETSAT DATA STORE & API

The first section of this manual is based on a tutorial from EUMETSAT, it covers the API data access process using anaconda prompt. For more details and the application in any python interface (starts after 20 minutes) consult:
https://www.youtube.com/watch?v=xIPFG8wVL_w&t=306s

Create an account or log on to EUMETSAT Data Store:
https://eoportal.eumetsat.int/

Enter the EUMETSAT Data Store:

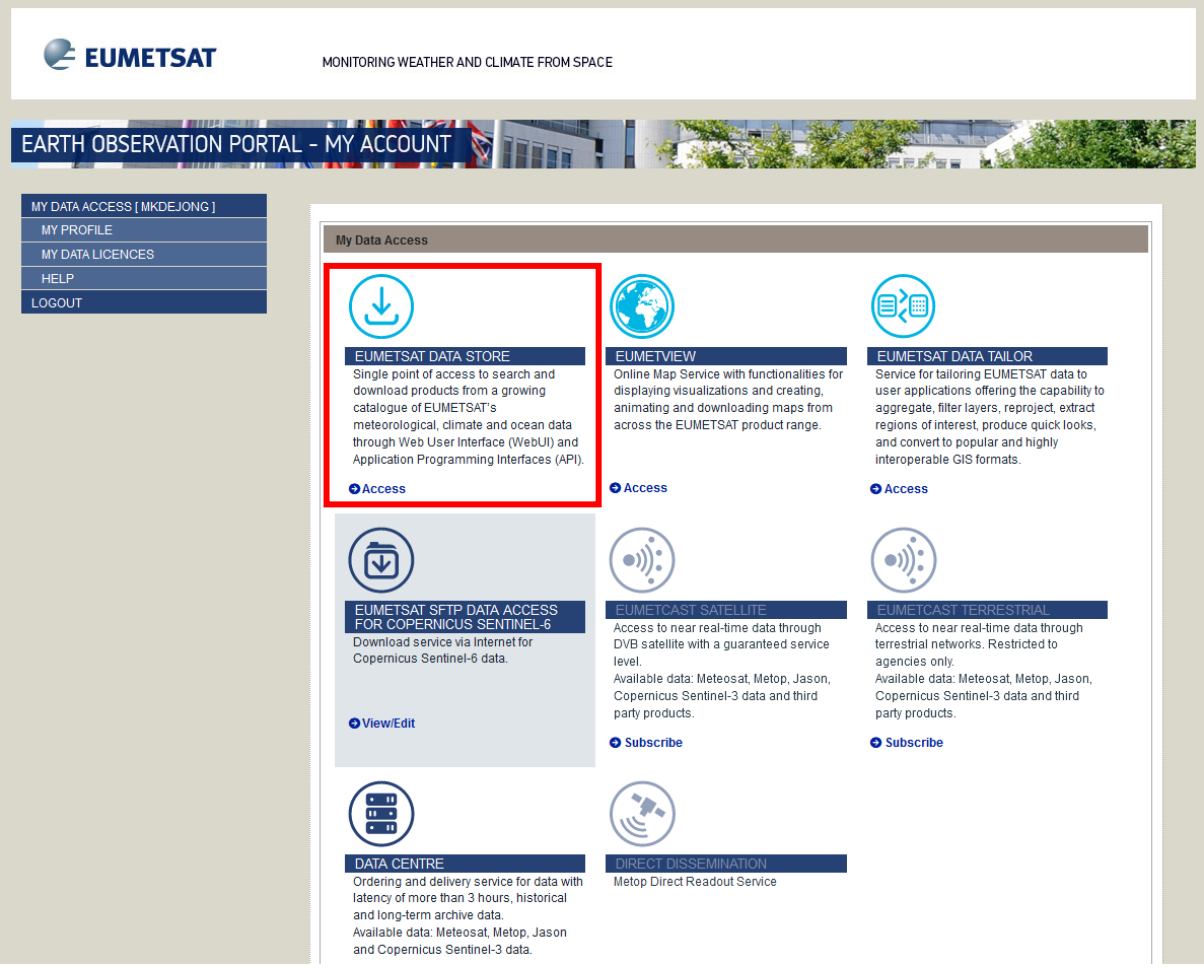

The data from EUMETSAT can be accessed through API's using the python environment. To obtain access follow these steps:

First an API key needs to be requested (a API token) to get the credentials to obtain access to the data. To do this go to the data store (see image above), and choose 'API Key' from the drop down user menu.

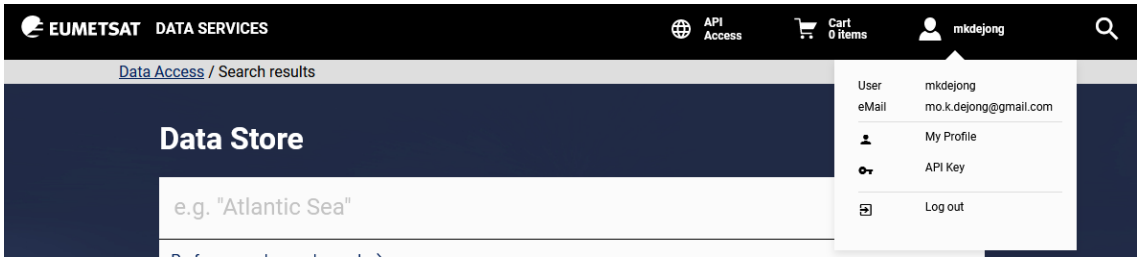

A new tab will open containing the user credentials (consumer key and consumer secret) which are required for the access via the prompt or command window. Also an API token will be created. Note that these are temporary, so you might have to request new ones over time.

Use the command window or anaconda prompt to install EUMEDAC package. In this manual this is done using the anaconda prompt.

Open Anaconda Prompt and type **`install -c eumetsat eumdac`**

Now eumdac will be installed. To obtain more information about the package you can type: **`eumdac -h`**.

To obtain access type:
`eumdac –set-credentials xx-consumer-key-xx xx-consumer-secretxx`
with the consumer key inserted in the first instance and the consumer secret inserted in the second instance.

To get an overview of all the collections you can use, type: **`eumdac describe`**
Note that the list of collections you see is dependent on your license for the Data Store.

To obtain more info about one of these collections, type:
`eumdac describe -c xx-COLLECTION-NAME-xx`

To search for products in the collection, type:
`eumdac search -c xx-COLLECTION-NAME-xx`
here no area or time is specified, by default then only the latest 10 of the entire list of products will be displayed. With **`--limit xx-integernumber-xx`** allows to set the number of latest products you want to be displayed (e.g. 1 for only latest 1 or 100 for latest 100 products).

The names of the selected files can be stored in a .txt-file using:
`eumdac search -c xx-COLLECTION-NAME-xx > filename.txt`
This will select and store only the product names that were last shown (from previous run)

If you want to download data, use `download` and then `-c` to define the collection from which to download and then specify with `-p`. When then a product name is entered, it will download this one specific product to the directory. If you want to download the products that were saved in a previously defined .txt file then add: `-p @filename.txt`. Full example:
`eumdac download – c xx-COLLECTION-NAME-xx -p @filename.txt`

How to find specific products:
`eumdac search -c xx-COLLECTION-NAME-xx`
Set additional filtering keywords:

- Set a start sending date: `-s yyyy-mm-dd`
- Set a end sending date: `-e yyyy-mm-dd`

See other filtering commands in 'Command Line User Guide' on the website of Eumetsat:
https://eumetsatspace.atlassian.net/wiki/spaces/EUMDAC/pages/1759805454/Command+Line+User+Guide

For more details on (advanced) searching, filtering and downloading:
https://eumetsatspace.atlassian.net/wiki/spaces/EUMDAC/pages/1893203985/Searching+and+downloading+products

Note that search parameters can be combined, but first search for the data, check if you obtain a desired list of data (consider using a # limit), then store these in a .txt file. Thereafter, in a new command line request to download the products as written in the .txt file.

Results can be sorted for ingestion or sensing time by:
`--sort ingestion/sensing --asc/--desc`

2. Downloading EUMETSAT Data to Cluster

First the eumdac.exe binary standalone (**for linux!**) needs to be downloaded from EUMETSAT and then uploaded to the right folder on the cluster using FileZilla. The binary standalone can be found here:

https://eumetsatspace.atlassian.net/wiki/spaces/EUMDAC/pages/1760591873/Get+EUMDAC

Note that it downloads in a compressed file (.tar). Extract this locally and then upload to the right folder on the cluster using FileZilla. In this case I'd recommend uploading to the 'Data' folder. This allows to directly use eumdac.exe in the Data folder to download EUMETSAT data using the prompt, to the Data folder on the cluster.

Log on to cluster:
`ssh -X <netid>@hpc03.tudelft.net`
choose 'yes' and enter TU Delft password.

Navigate to Data folder:
`cd ~<netid>/<projectfolder>/Data`

and check if the file is present using: `ls`

Get access to the eumdac library"
`chmod +x path/to/eumdace`

Now eumdac can be used as you would locally.

Data search history
```
eumdac search -c <eumetsat collection> --time-range <startYYYY-MM-
DD> <endYYYY-MM-DD> --bbox <minLON> <minLAT> <maxLON> <maxLAT> --
satellite <Satellite> --sort sensing --desc
```

3. PROCESSING ON THE CLUSTER

Data processing on cluster:
```
qsub-eval -nn 1 -np 2 -l <logfilename>.log "mlab -eval2
\"FFSAR_bulk_L1a_to_L1b('YYYY','MM',[minLAT, maxLAT, minLON,
maxLON])\""
```

example:
```
eumdac search -c EO:EUM:DAT:0413 --time-range 2022-01-01 2022-12-31
--bbox 81.228 28.725 81.323 28.786 --satellite Sentinel-3B --sort
sensing --desc
```

B

Satellite Theoretical Ground Tracks

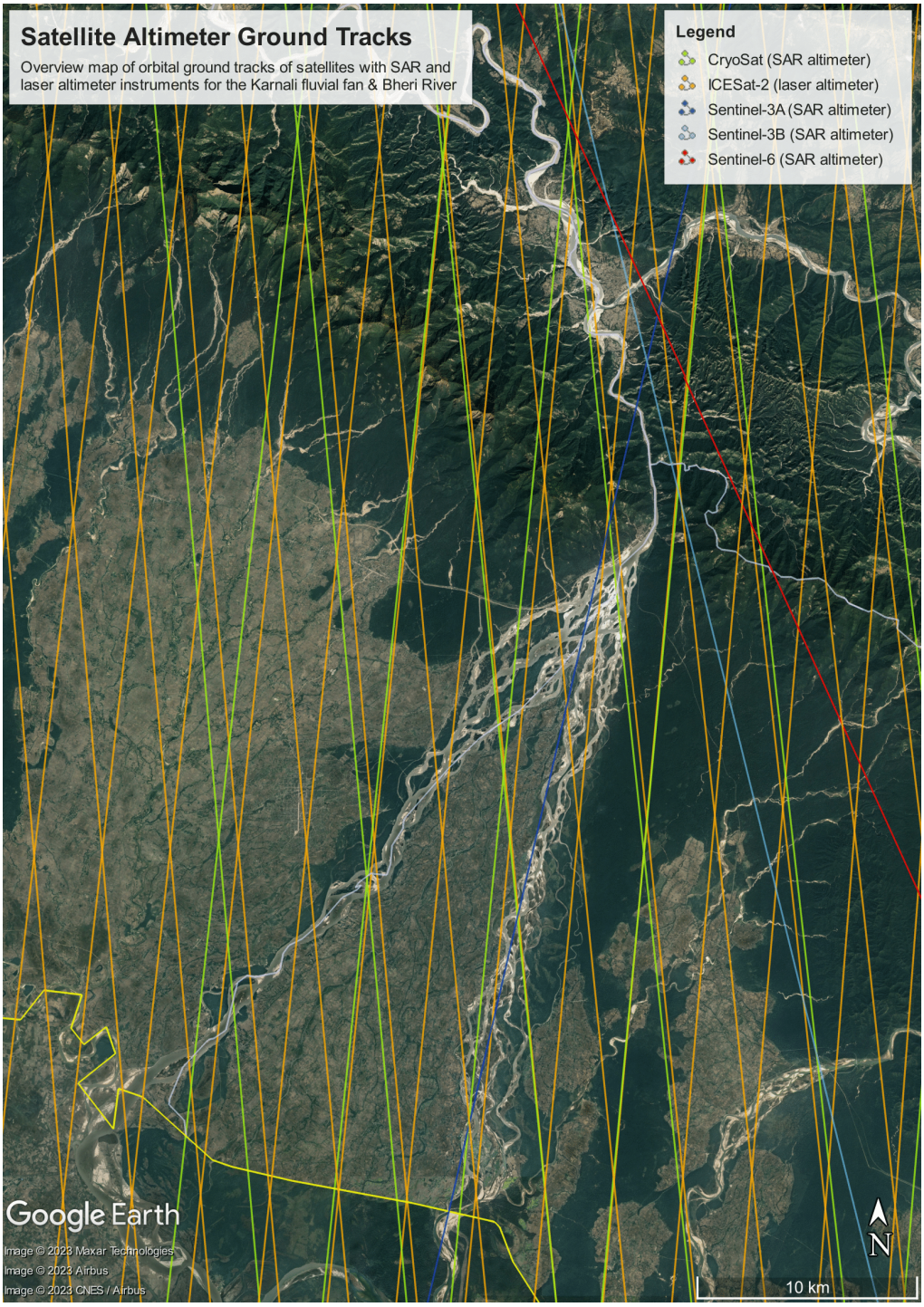

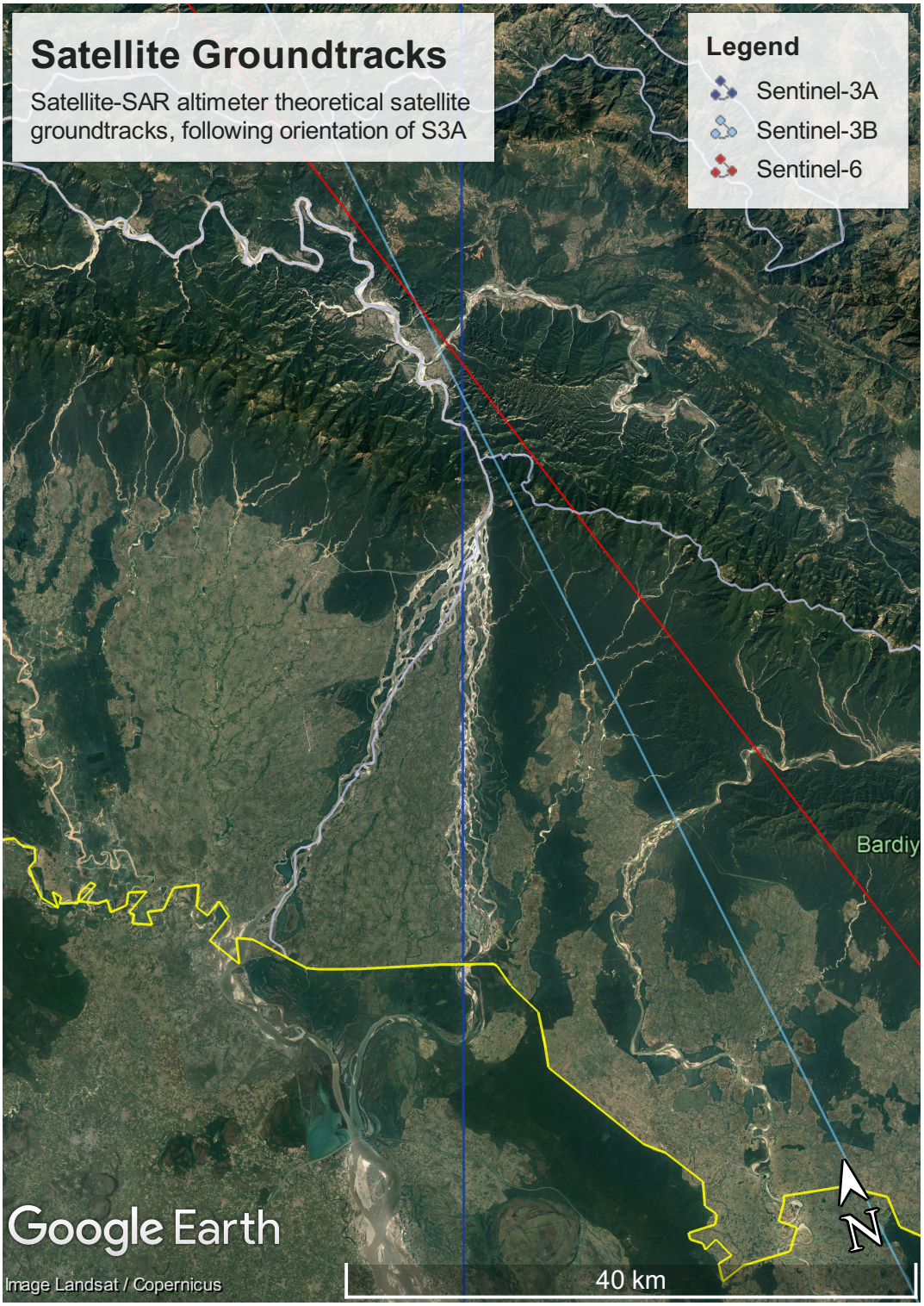
Satellite Groundtracks
Satellite-SAR altimeter theoretical satellite groundtracks, following orientation of S3A
Legend
Sentinel-3A
Sentinel-3B
Sentinel-6
Bardiy
Google Earth
Image Landsat / Copernicus
40 km
N

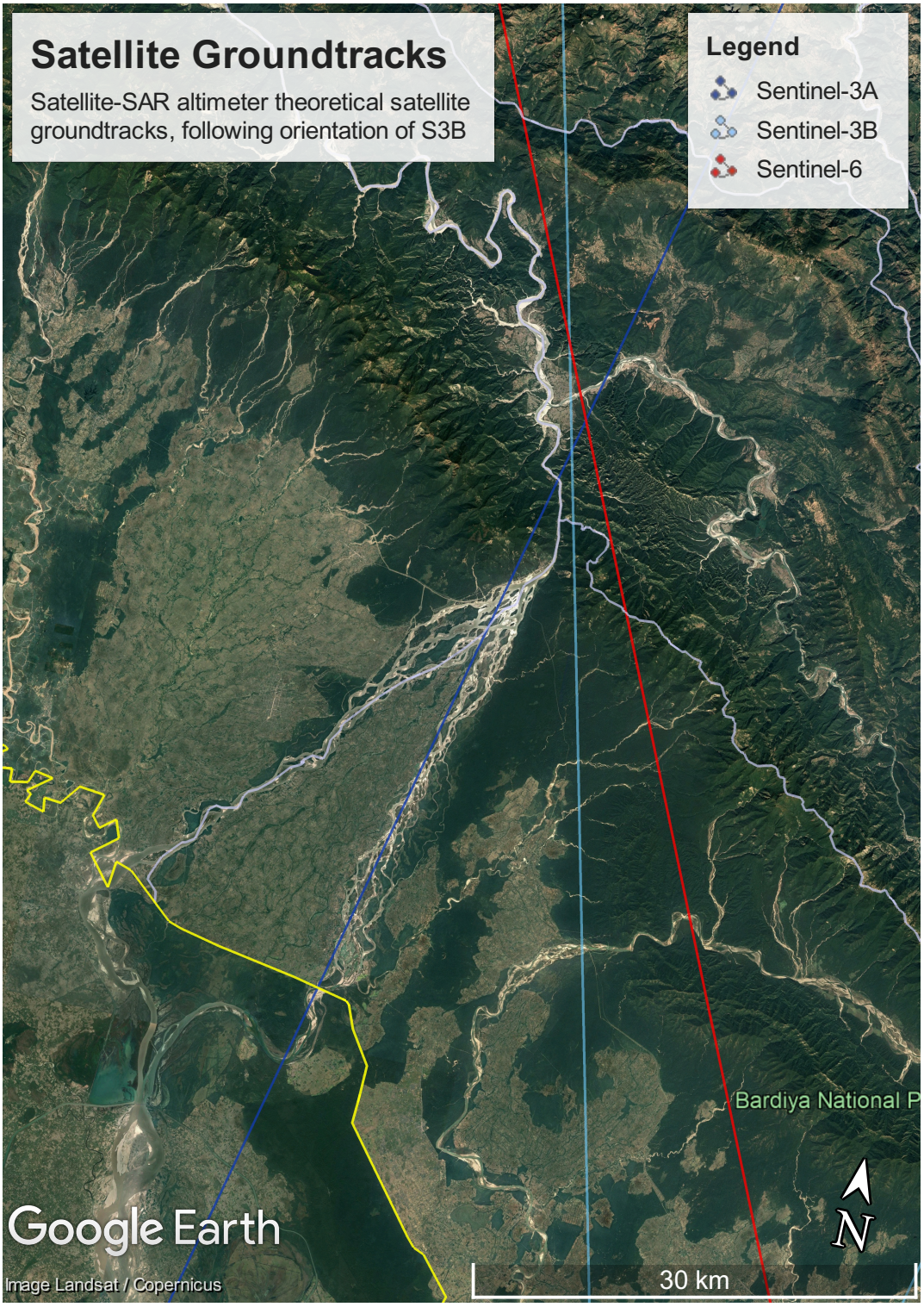
Satellite Groundtracks
Satellite-SAR altimeter theoretical satellite groundtracks, following orientation of S3B
Legend
Sentinel-3A
Sentinel-3B
Sentinel-6
Bardiya National P
Google Earth
Image Landsat / Copernicus
30 km
N

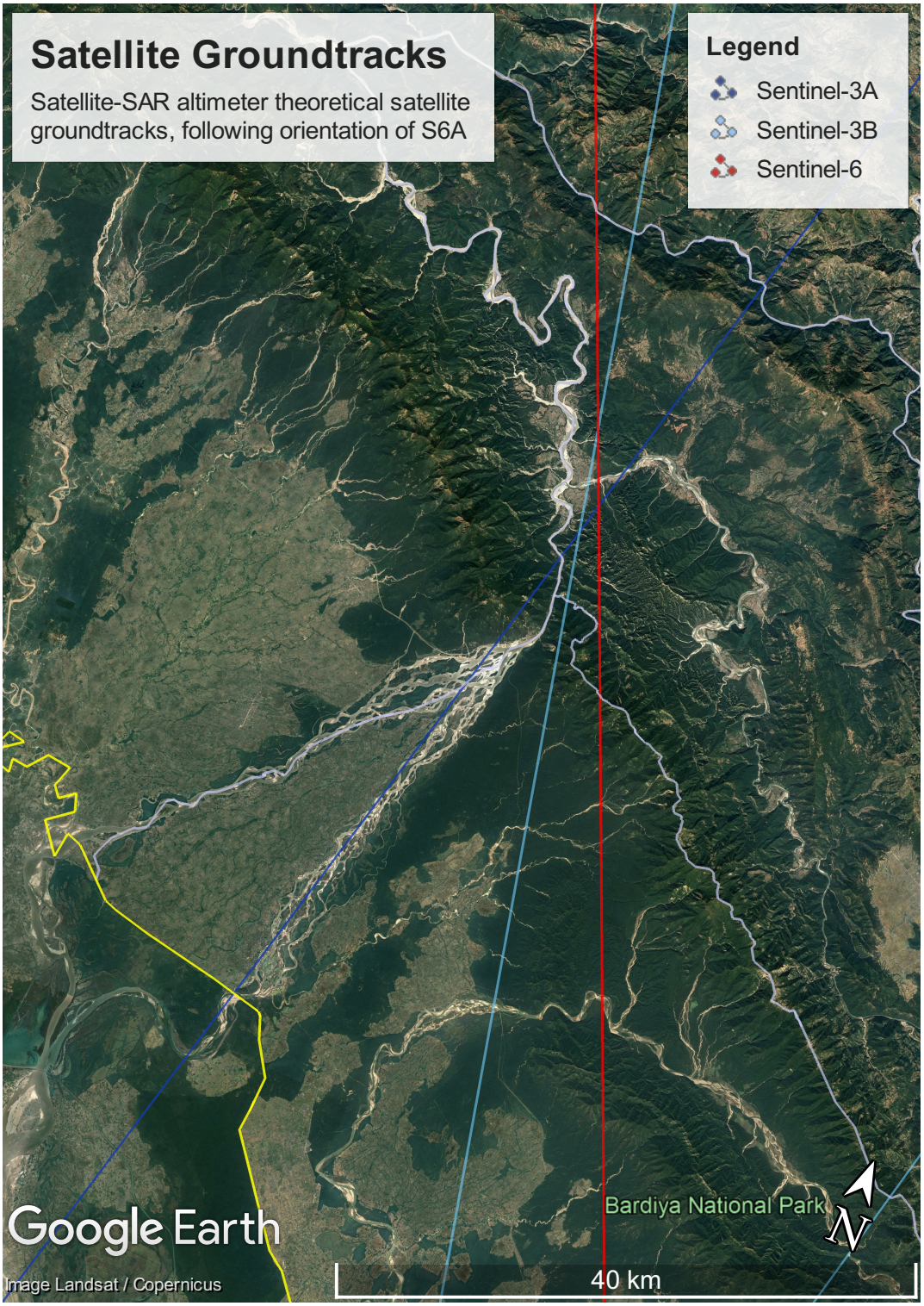
Satellite Groundtracks
Satellite-SAR altimeter theoretical satellite groundtracks, following orientation of S6A
Legend
Sentinel-3A
Sentinel-3B
Sentinel-6
Bardiya National Park
N
Google Earth
Image Landsat / Copernicus
40 km

C

Map Field Exploration Sites

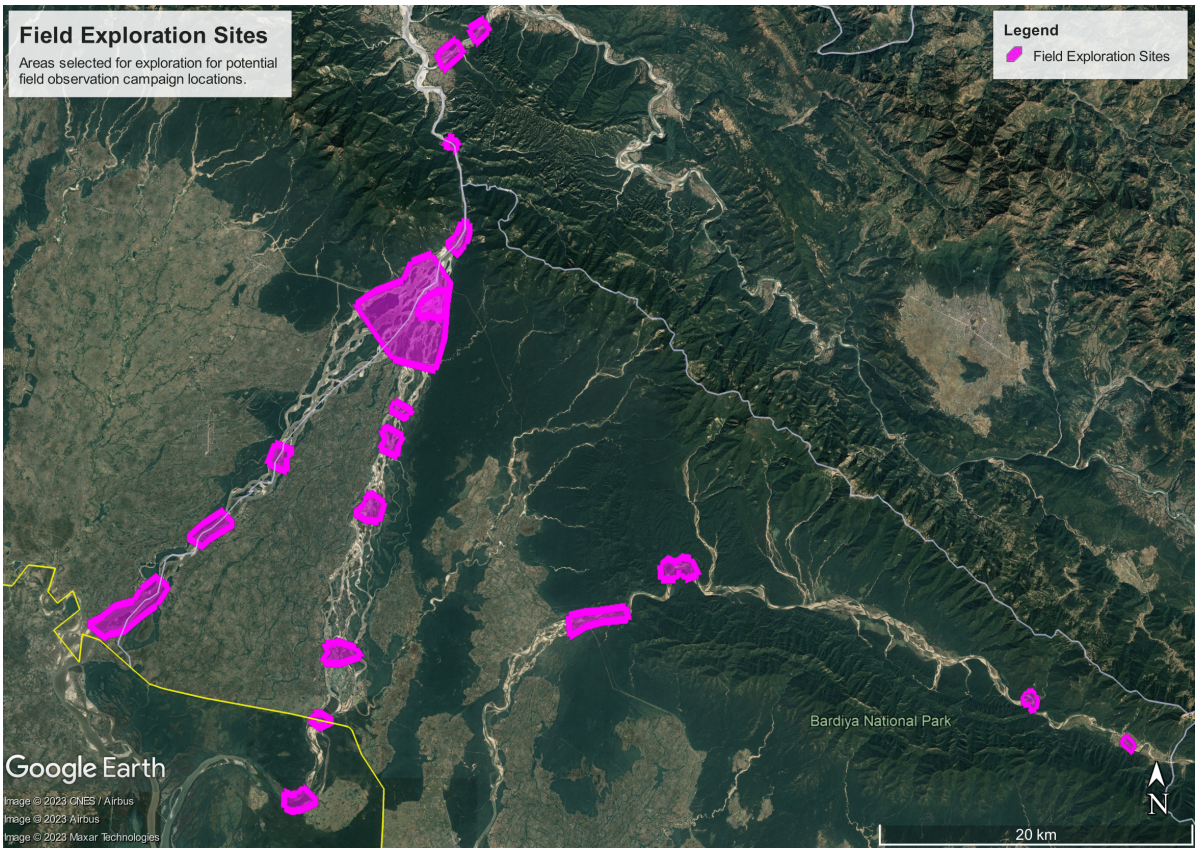

D

Overview of Collected Sat-SARA Data

SITE	SATELLITE OVERPASS	SENSOR / DATA TYPE	Relative orbit number	Bounding Box [LON - LAT]	L1A	L2
BH00	Sentinel-3A	SRAL - SAR	76	81.228 28.725 81.323 28.786	EUMETSAT data store	Copernicus SciHub
BH01	Sentinel-6A	POD4 - SAR	192	81.228 28.725 81.323 28.786	EUMETSAT data store	Copernicus SciHub
BH02	Sentinel-3B	SRAL - SAR	353	81.228 28.725 81.323 28.786	EUMETSAT data store	Copernicus SciHub
K01	Sentinel-3A	SRAL - SAR	76	81.260 28.688 81.292 28.727	EUMETSAT data store	Copernicus SciHub
G08	Sentinel-3A	SRAL - SAR	76	81.147 28.306 81.227 28.382	EUMETSAT data store	Copernicus SciHub

E

Sat-SARA Return Signal Waveforms

E.1. BH00

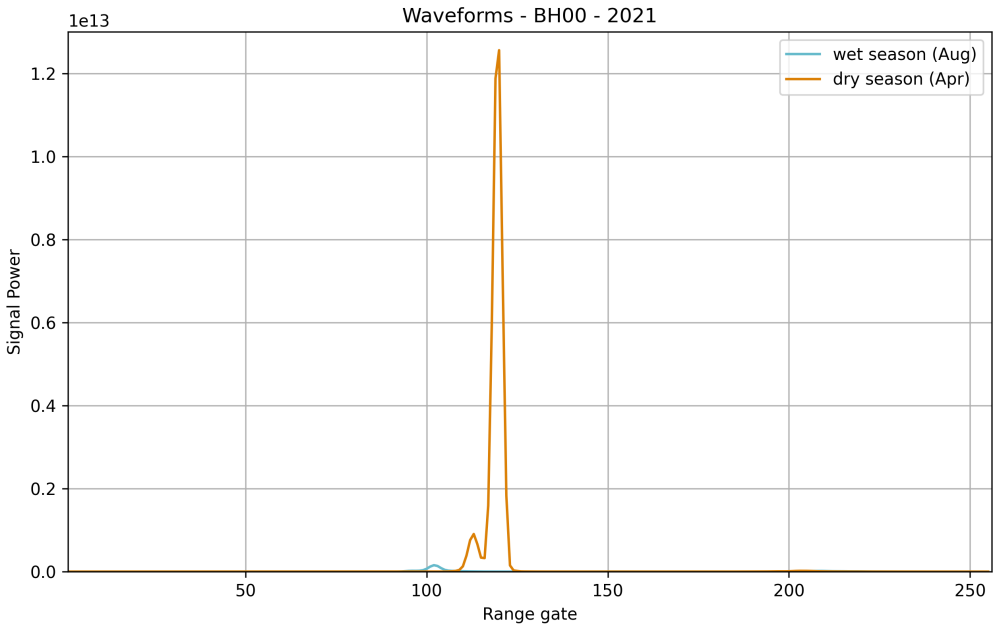

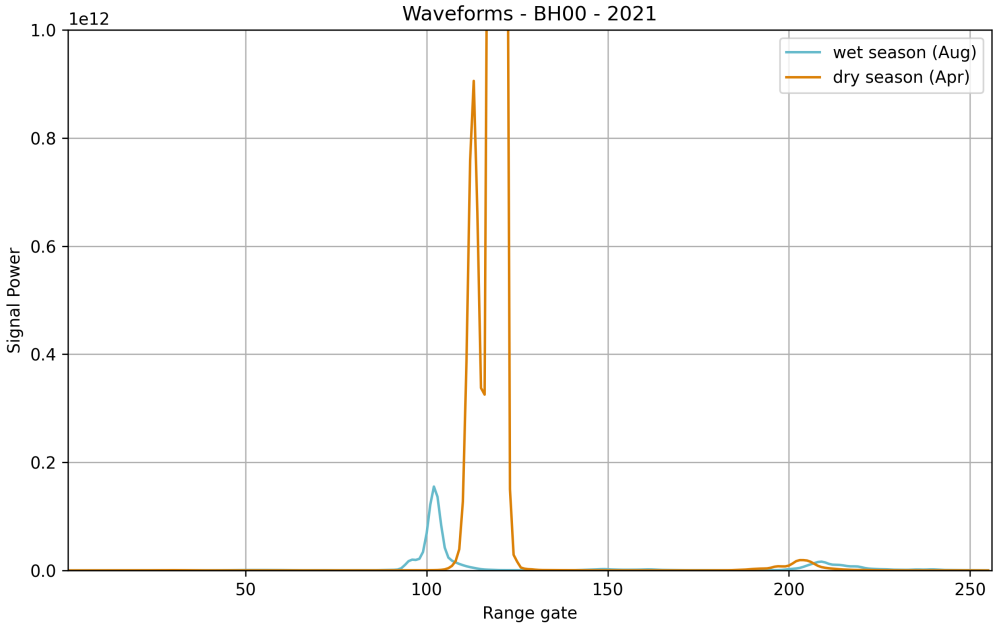
Waveforms - BH00 - 2021
1e12
1.0
0.8
0.6
0.4
0.2
0.0
Signal Power
50
100
150
200
250
Range gate
wet season (Aug)
dry season (Apr)

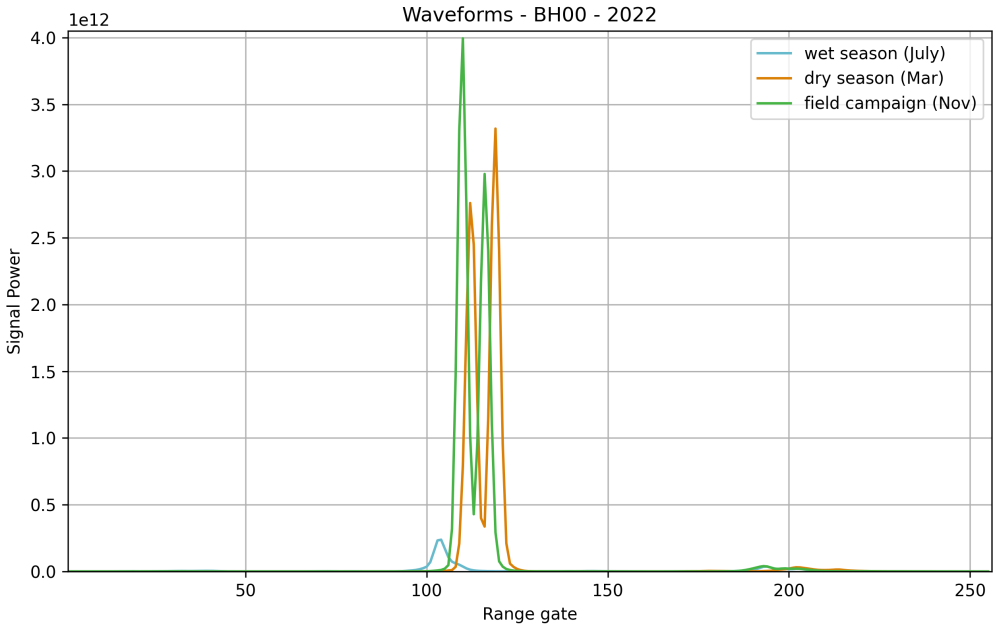
Waveforms - BH00 - 2022
1e12
4.0
3.5
3.0
2.5
2.0
1.5
1.0
0.5
0.0
Signal Power
50
100
150
200
250
Range gate
wet season (July)
dry season (Mar)
field campaign (Nov)

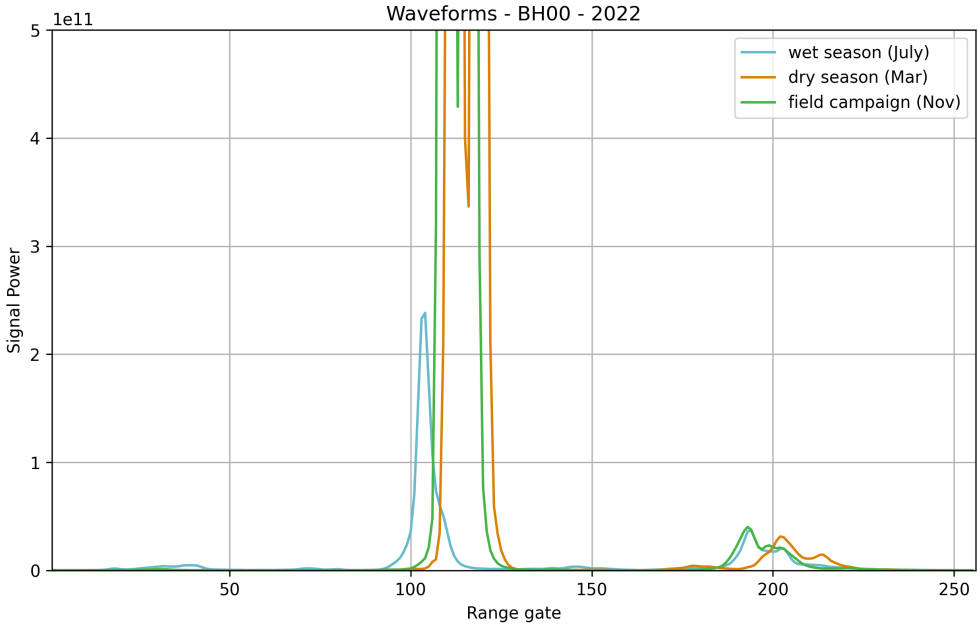
Waveforms - BH00 - 2022
1e11
wet season (July)
dry season (Mar)
field campaign (Nov)
Signal Power
Range gate
0
1
2
3
4
5
50
100
150
200
250

E.2. BH01

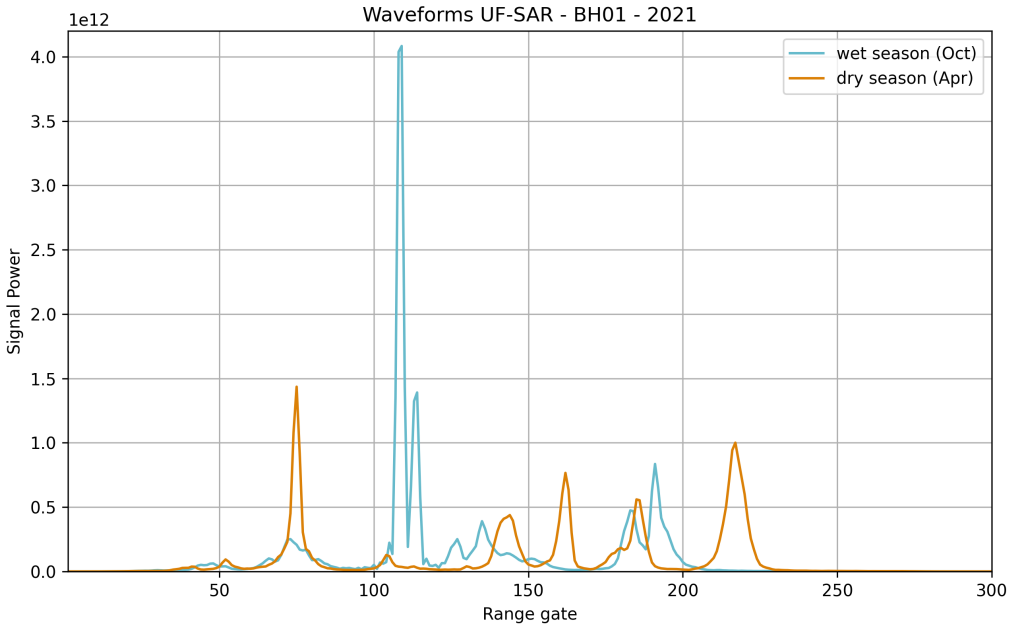
Waveforms UF-SAR - BH01 - 2021
1e12
wet season (Oct)
dry season (Apr)
Signal Power
Range gate
0.0
0.5
1.0
1.5
2.0
2.5
3.0
3.5
4.0
50
100
150
200
250
300

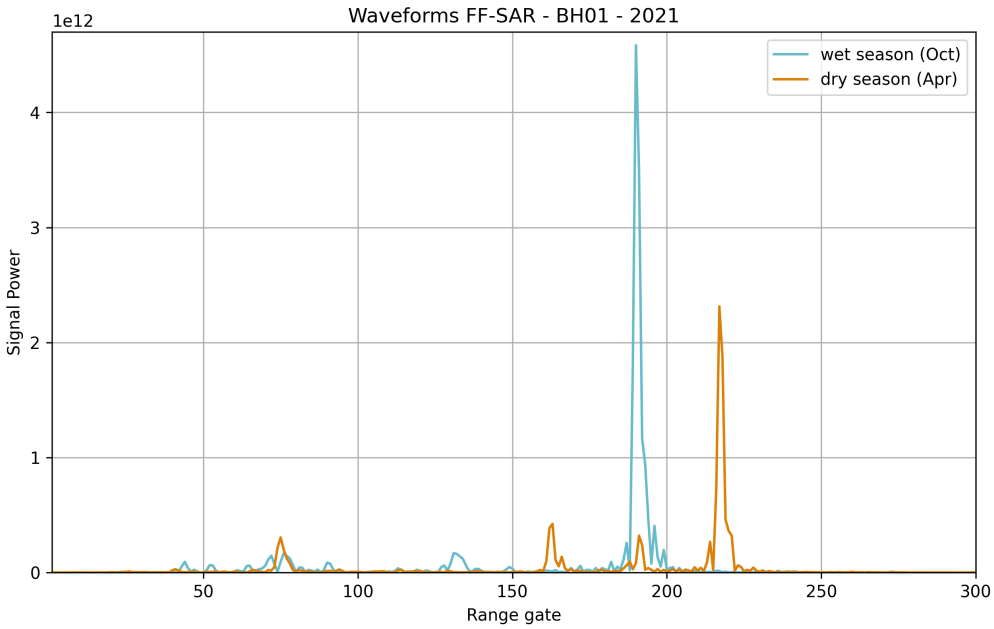
Waveforms FF-SAR - BH01 - 2021
1e12
wet season (Oct)
dry season (Apr)
Signal Power
Range gate
0
1
2
3
4
50
100
150
200
250
300

E.3. BH02

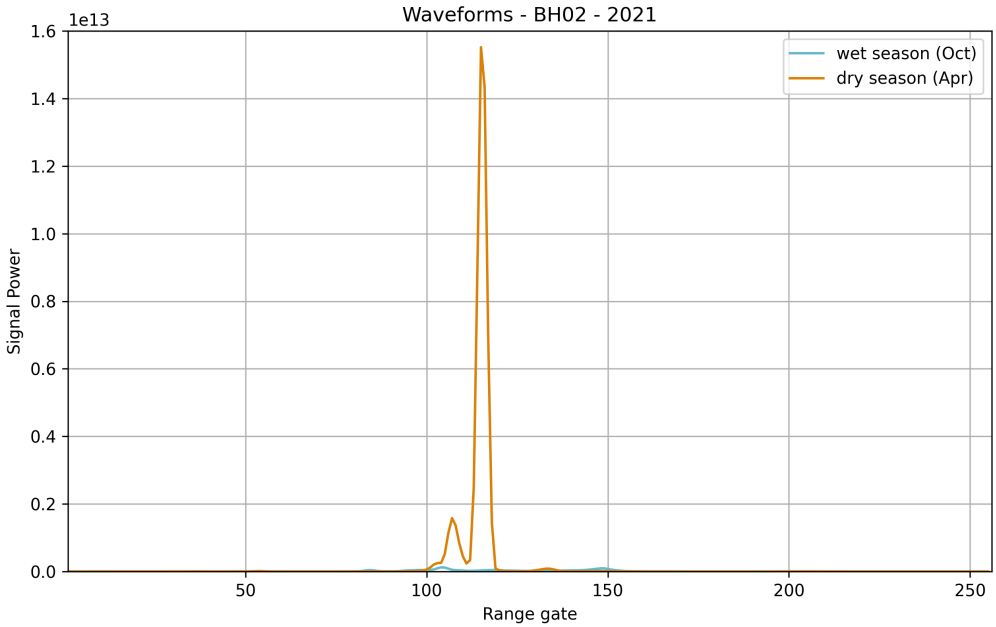
Waveforms - BH02 - 2021
1e13
wet season (Oct)
dry season (Apr)
Signal Power
Range gate
0.0
0.2
0.4
0.6
0.8
1.0
1.2
1.4
1.6
50
100
150
200
250

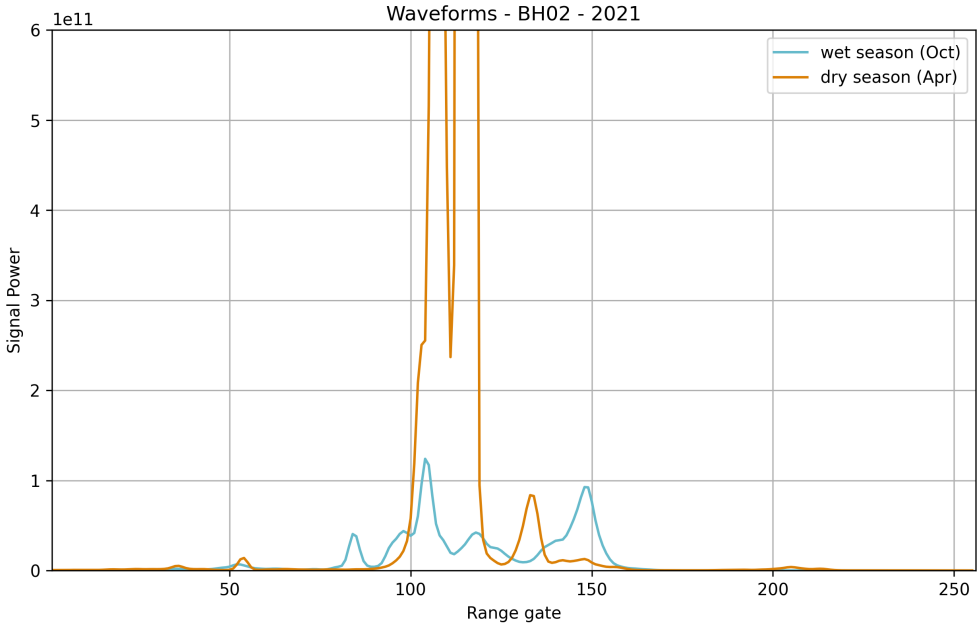
Waveforms - BH02 - 2021
1e11
6
5
4
3
2
1
0
Signal Power
50
100
150
200
250
Range gate
wet season (Oct)
dry season (Apr)

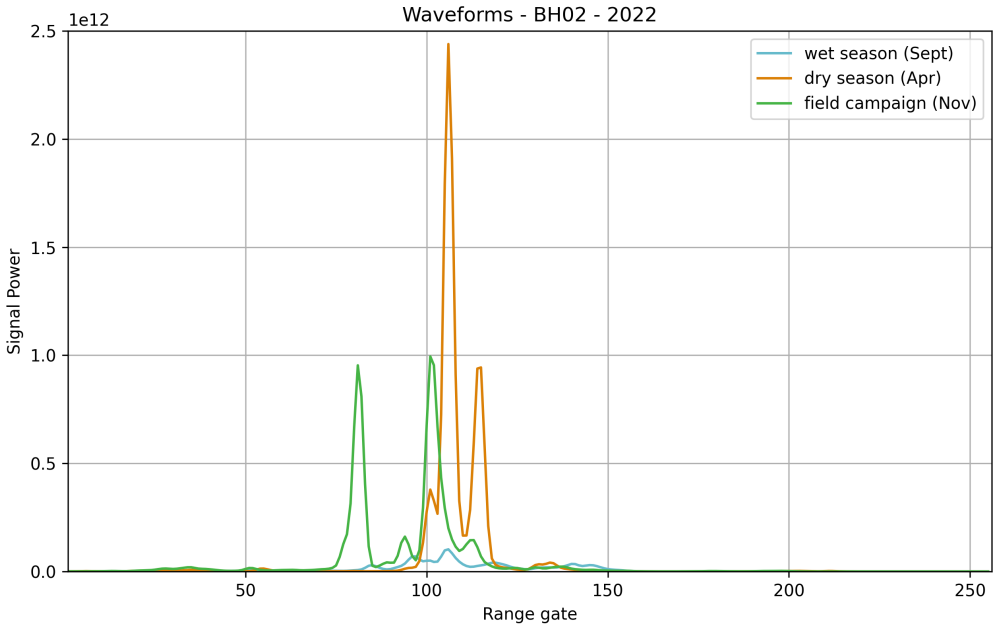
Waveforms - BH02 - 2022
1e12
2.5
2.0
1.5
1.0
0.5
0.0
Signal Power
50
100
150
200
250
Range gate
wet season (Sept)
dry season (Apr)
field campaign (Nov)

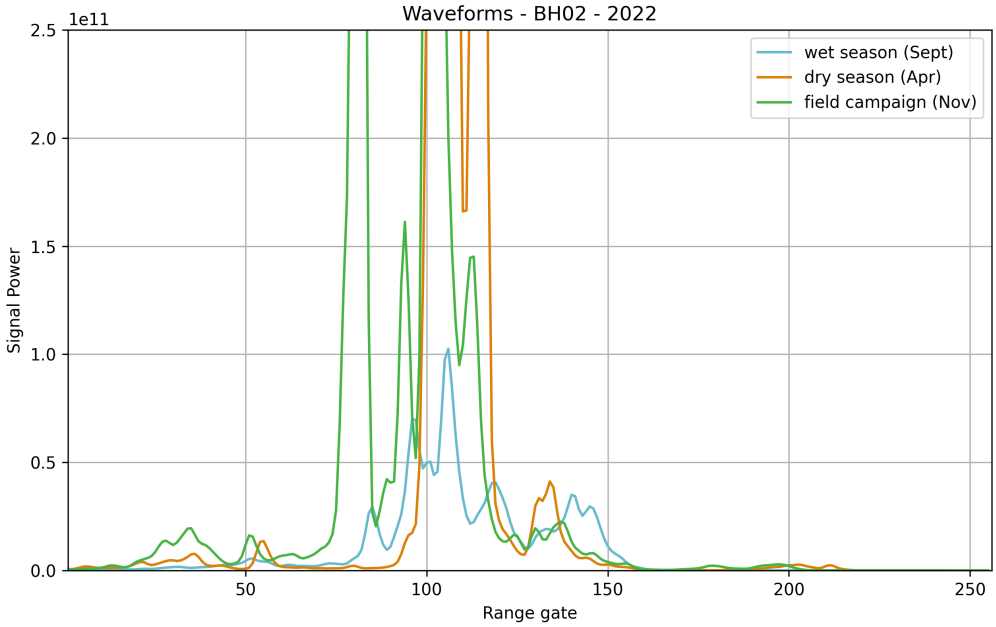
Waveforms - BH02 - 2022
1e11
2.5
2.0
1.5
1.0
0.5
0.0
Signal Power
50
100
150
200
250
Range gate
wet season (Sept)
dry season (Apr)
field campaign (Nov)

E.4. K01

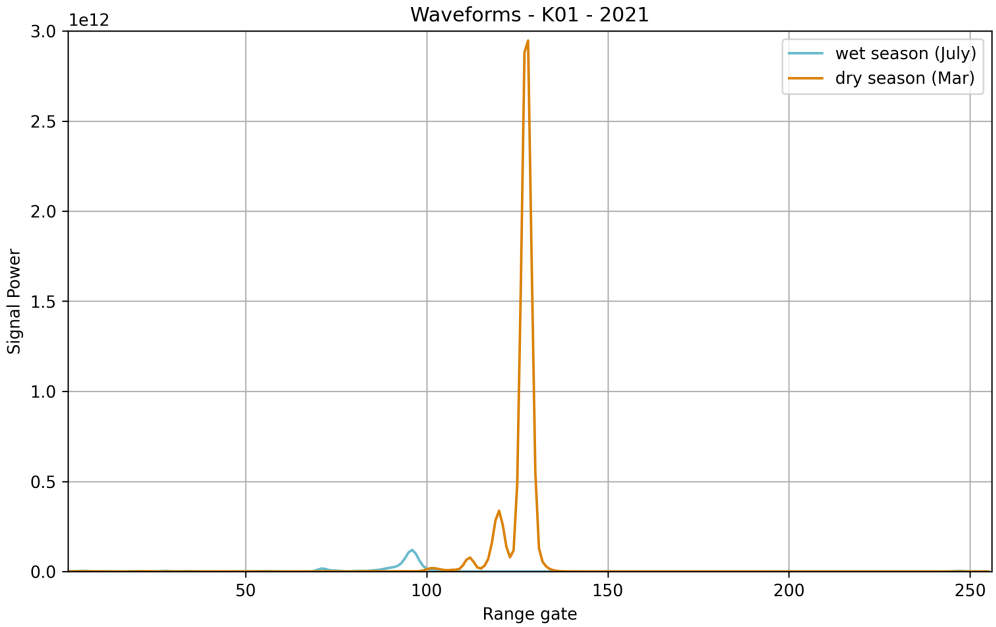
Waveforms - K01 - 2021
1e12
3.0
2.5
2.0
1.5
1.0
0.5
0.0
Signal Power
50
100
150
200
250
Range gate
wet season (July)
dry season (Mar)

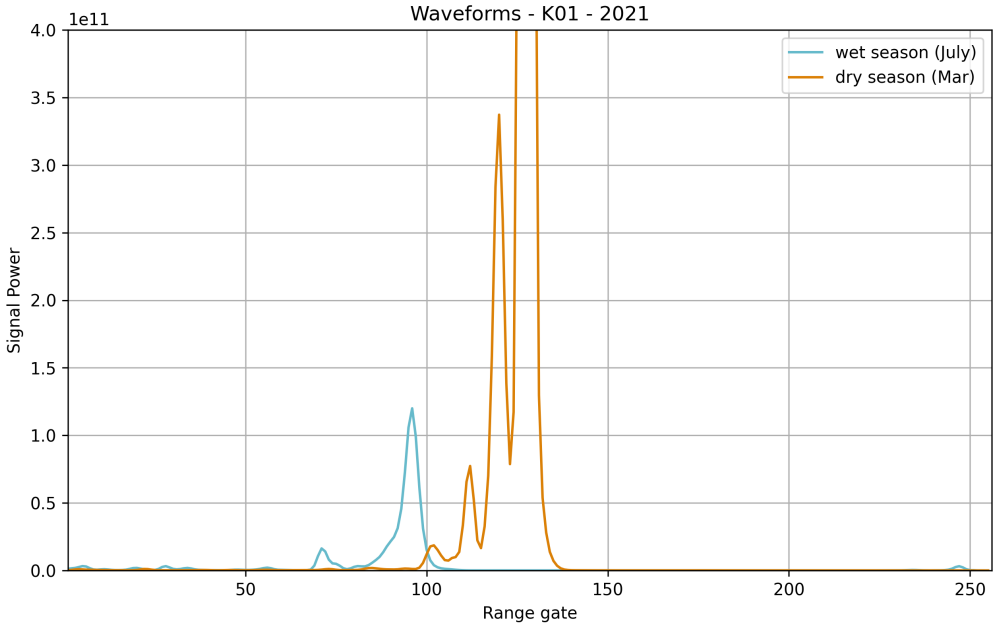
Waveforms - K01 - 2021
1e11
4.0
3.5
3.0
2.5
2.0
1.5
1.0
0.5
0.0
Signal Power
50
100
150
200
250
Range gate
wet season (July)
dry season (Mar)

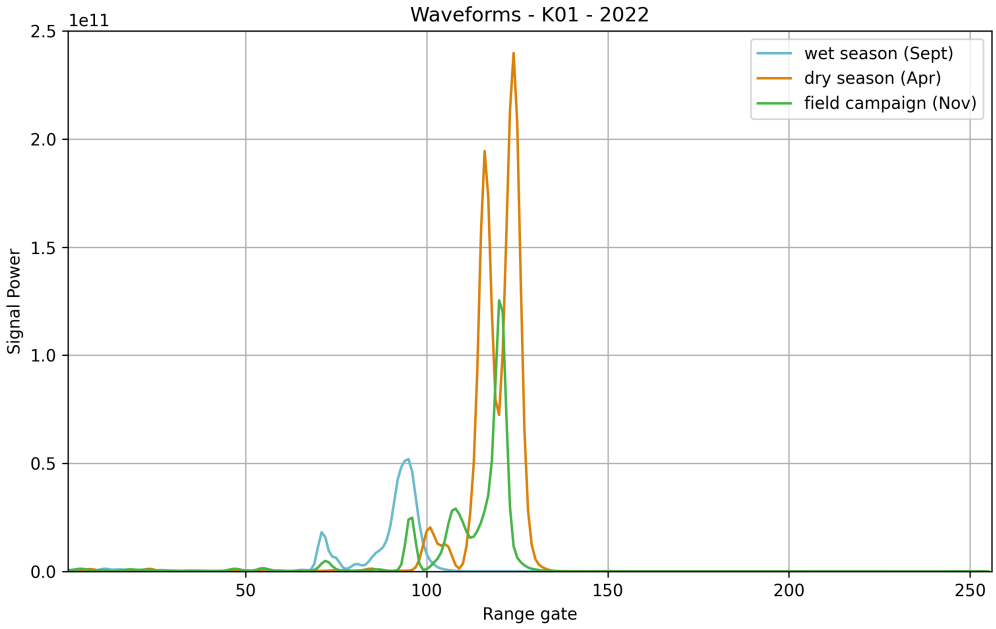
Waveforms - K01 - 2022
1e11
2.5
2.0
1.5
1.0
0.5
0.0
Signal Power
50
100
150
200
250
Range gate
wet season (Sept)
dry season (Apr)
field campaign (Nov)

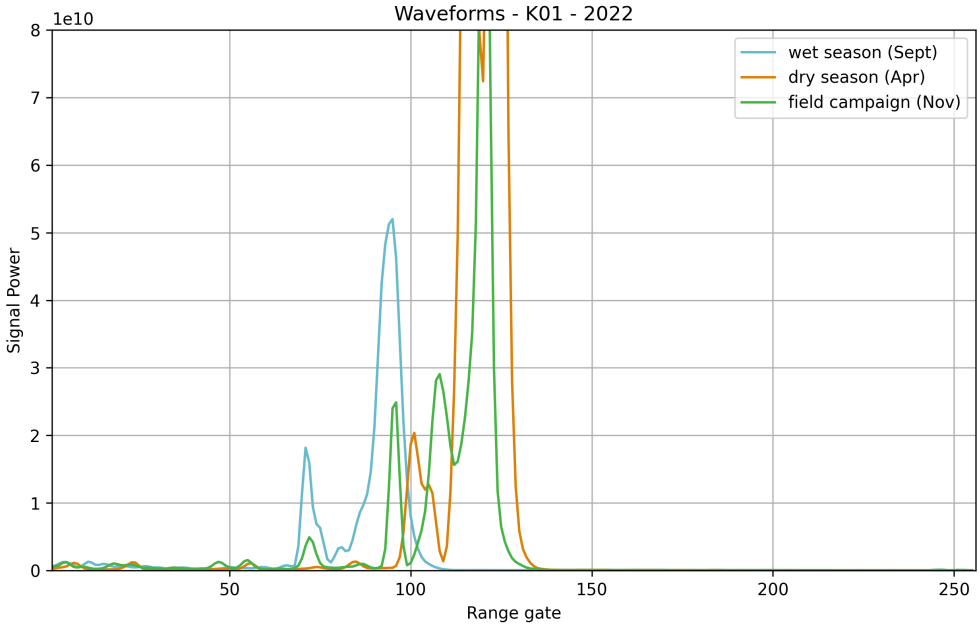
Waveforms - K01 - 2022
1e10
wet season (Sept)
dry season (Apr)
field campaign (Nov)
Signal Power
Range gate

E.5. G08

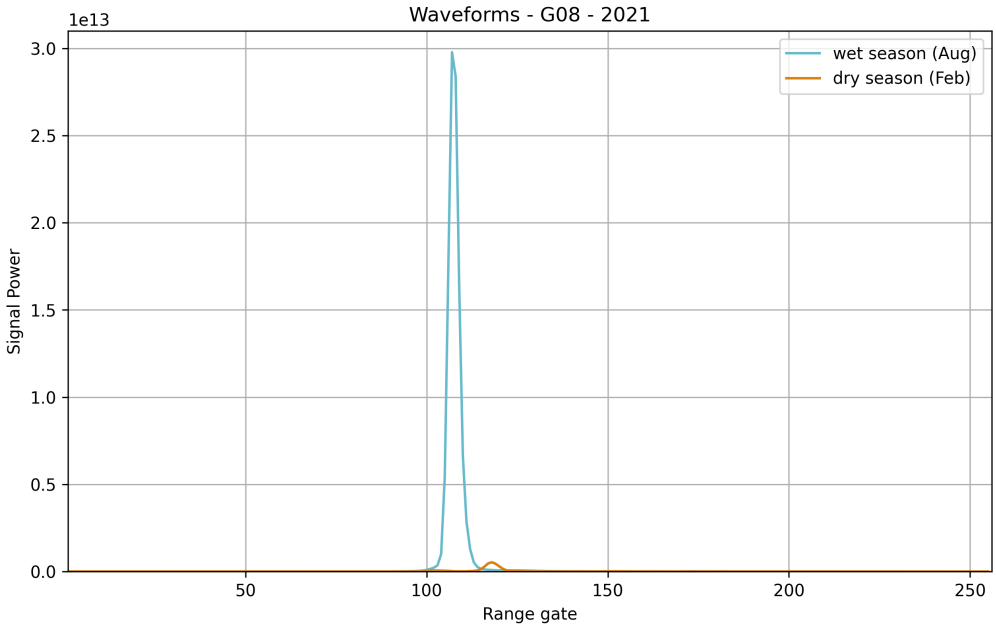
Waveforms - G08 - 2021
1e13
wet season (Aug)
dry season (Feb)
Signal Power
Range gate

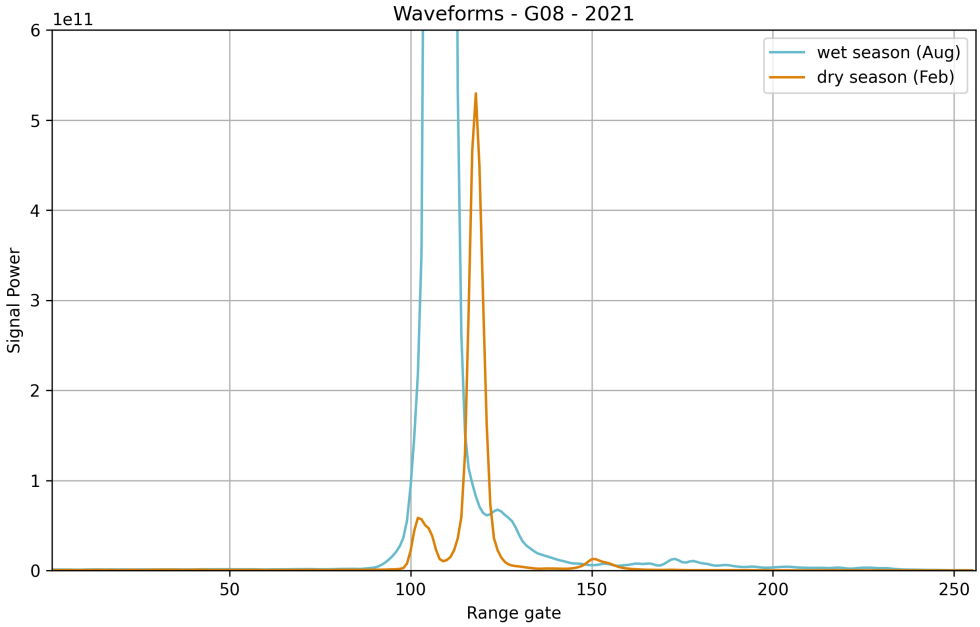
Waveforms - G08 - 2021
1e11
6
5
4
3
2
1
0
Signal Power
50
100
150
200
250
Range gate
wet season (Aug)
dry season (Feb)

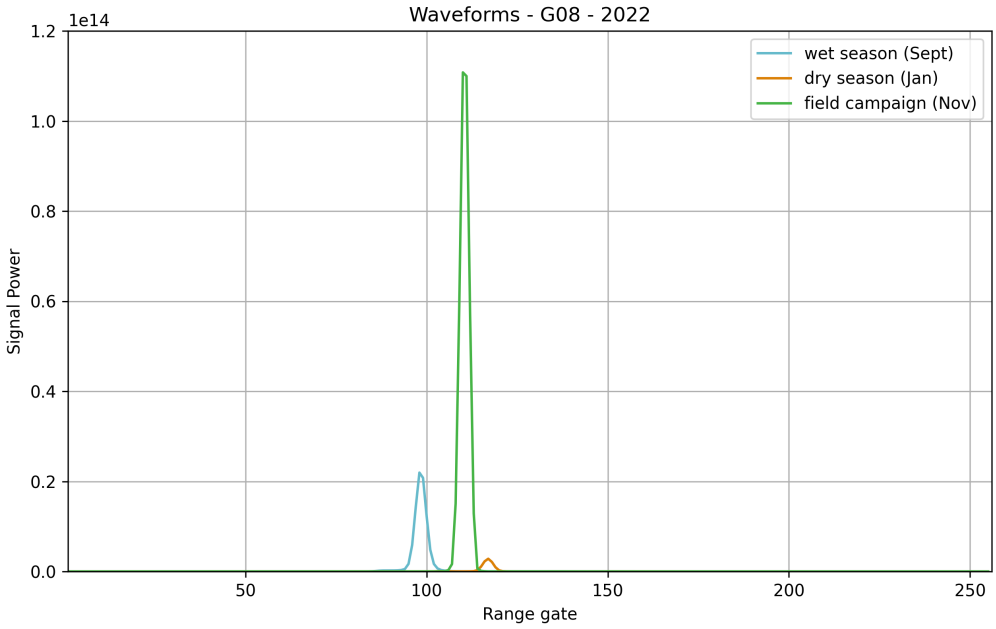
Waveforms - G08 - 2022
1e14
1.2
1.0
0.8
0.6
0.4
0.2
0.0
Signal Power
50
100
150
200
250
Range gate
wet season (Sept)
dry season (Jan)
field campaign (Nov)

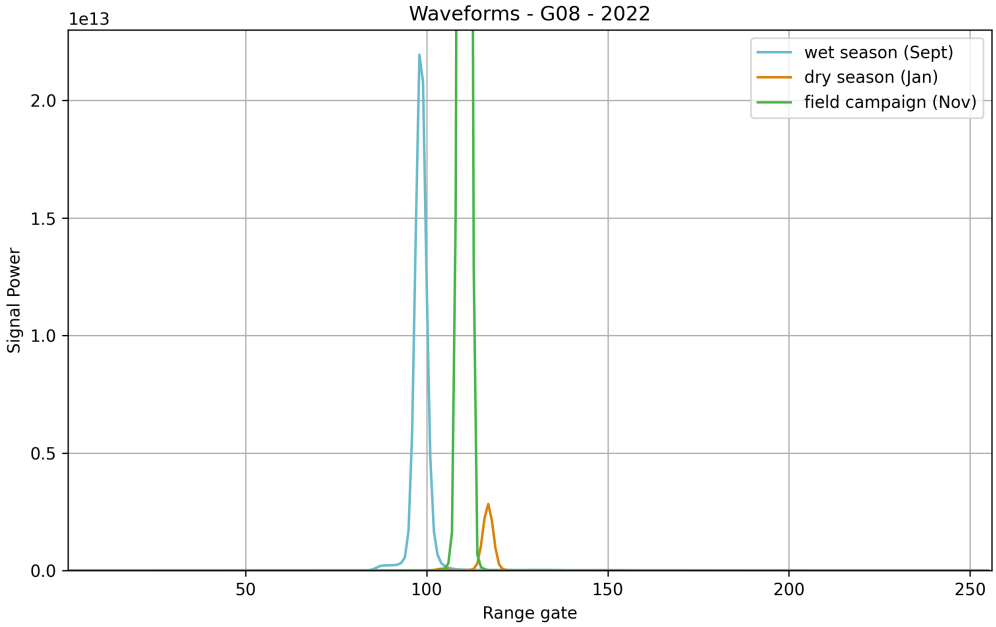
Waveforms - G08 - 2022
1e13
wet season (Sept)
dry season (Jan)
field campaign (Nov)
Signal Power
Range gate
0.0
0.5
1.0
1.5
2.0
50
100
150
200
250

F

Sentinel-3 SARA Echograms 2021

F.1. BH00

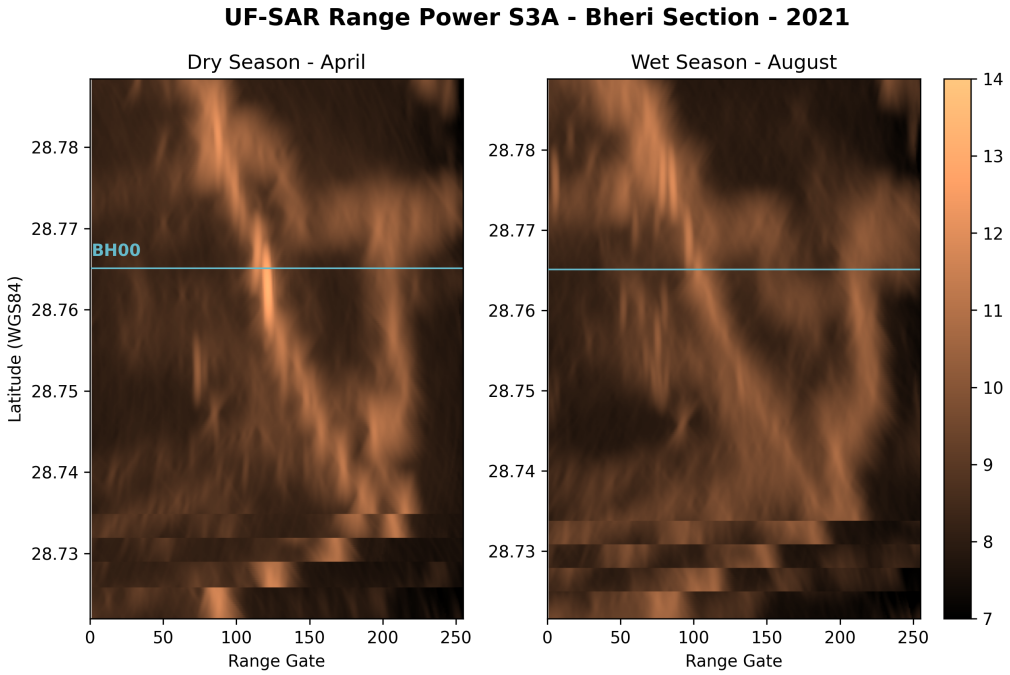

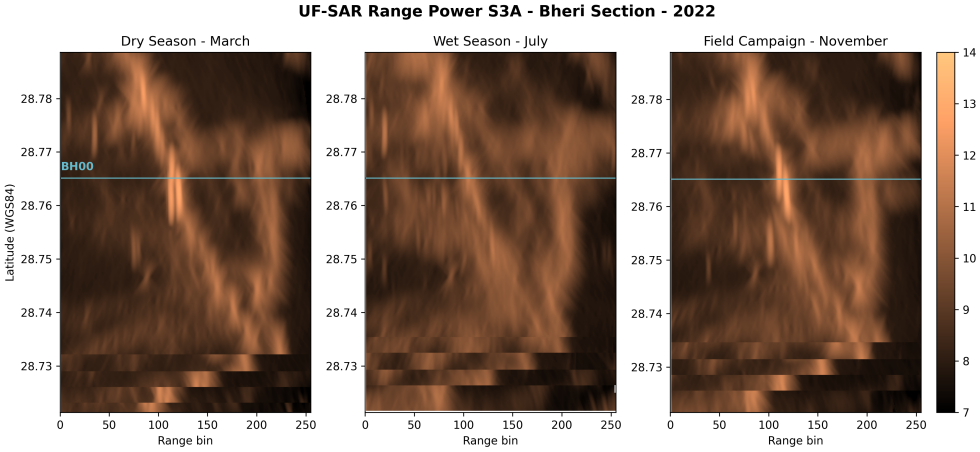

F.2. BH01

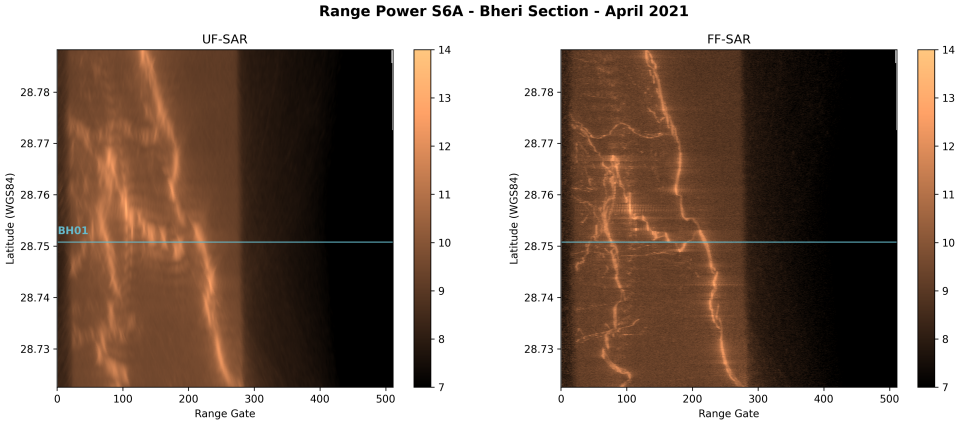

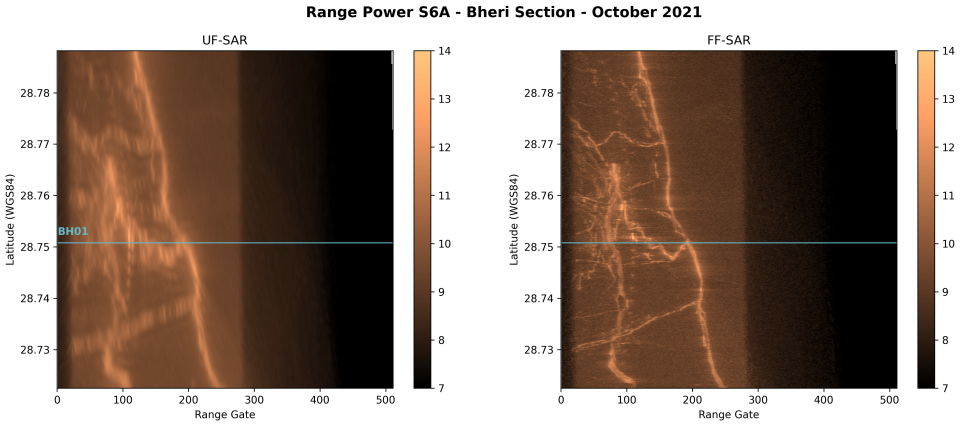

F.2.1. UF-SAR

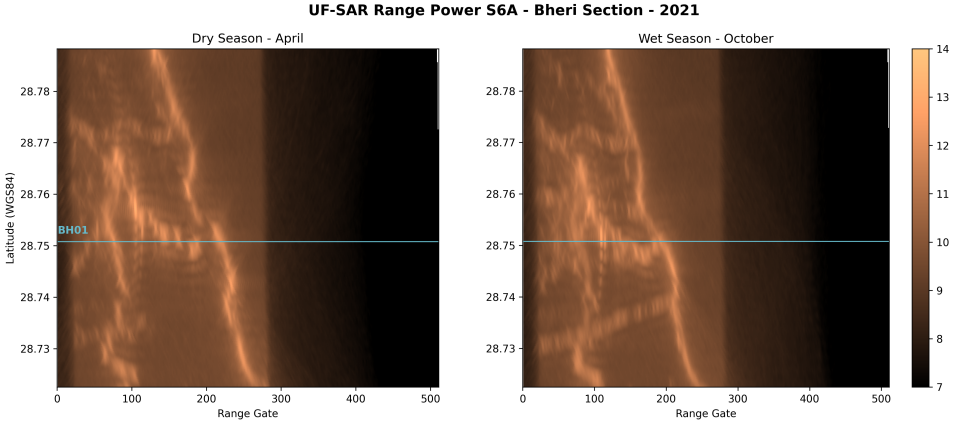

F.2.2. FF-SAR

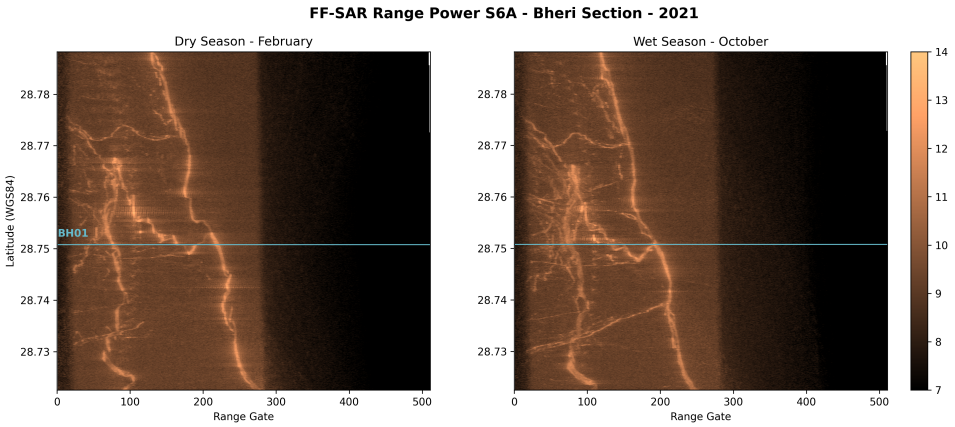

F.3. BH02

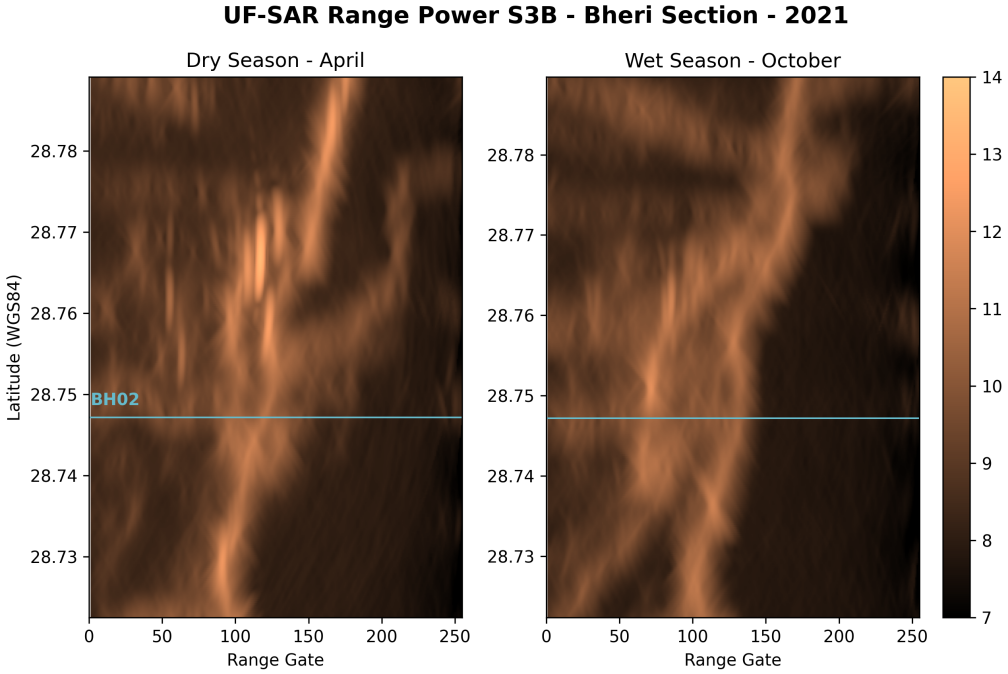

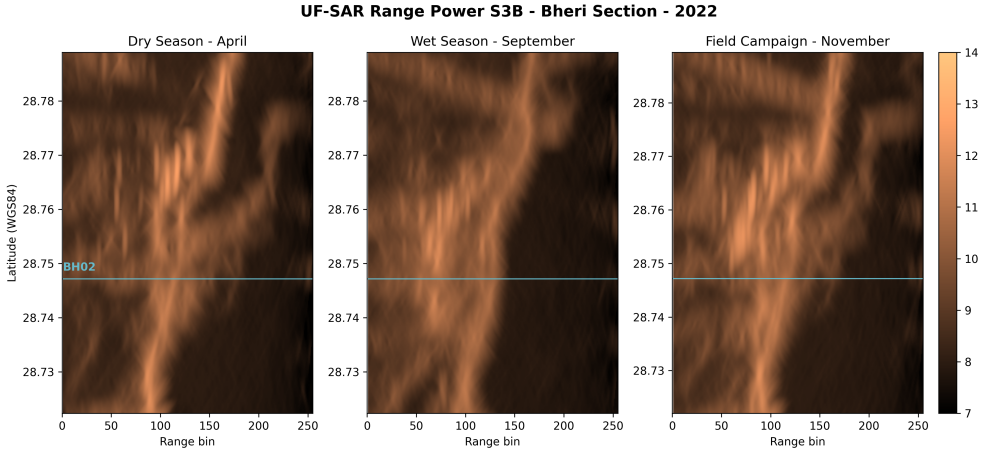
UF-SAR Range Power S3B - Bheri Section - 2022
Dry Season - April
Wet Season - September
Field Campaign - November
Latitude (WGS84)
BH02
Range bin

F.4. K01

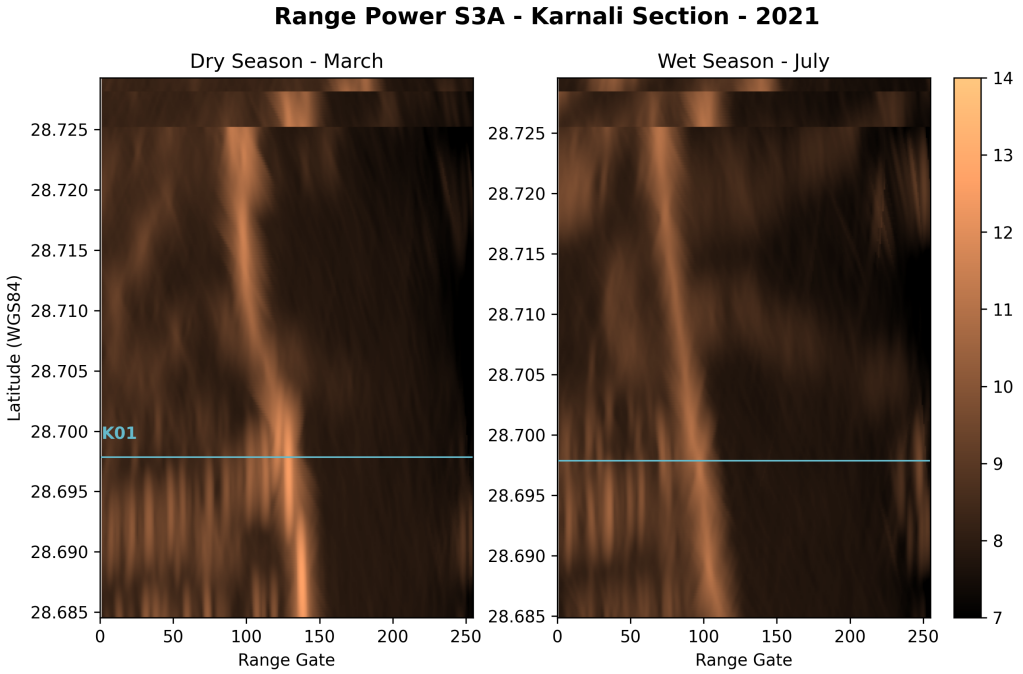
Range Power S3A - Karnali Section - 2021
Dry Season - March
Wet Season - July
Latitude (WGS84)
K01
Range Gate

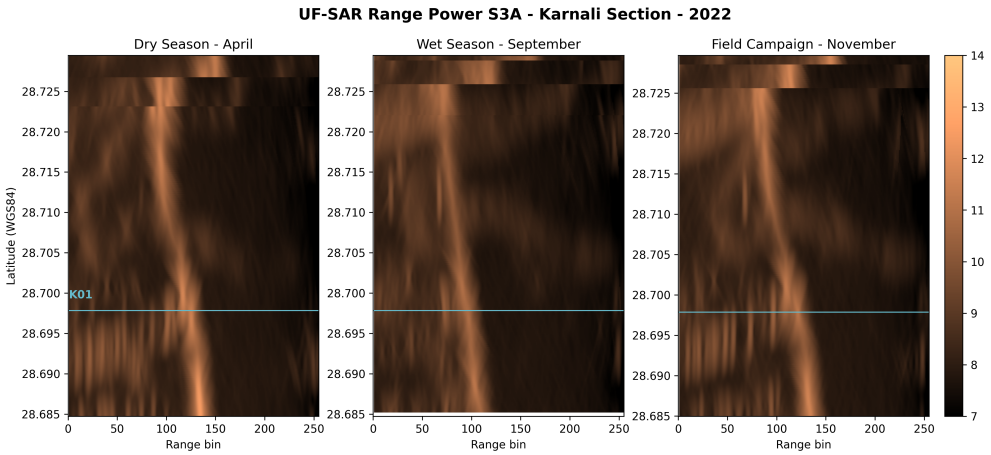
UF-SAR Range Power S3A - Karnali Section - 2022
Dry Season - April
Wet Season - September
Field Campaign - November
Latitude (WGS84)
K01
Range bin

F.5. G08

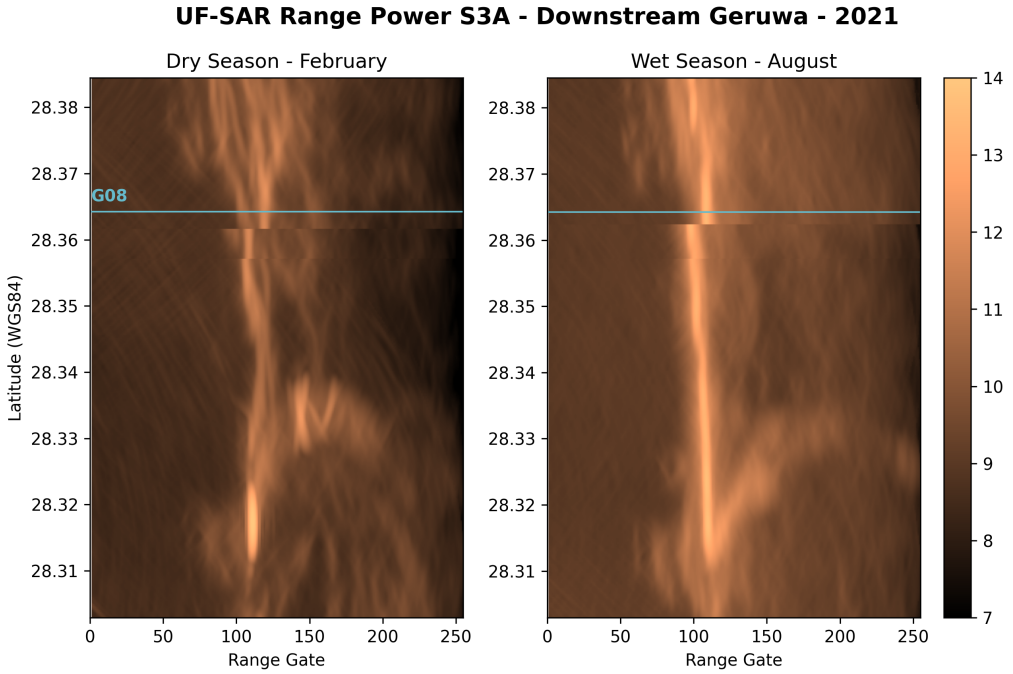
UF-SAR Range Power S3A - Downstream Geruwa - 2021
Dry Season - February
Wet Season - August
Latitude (WGS84)
G08
Range Gate

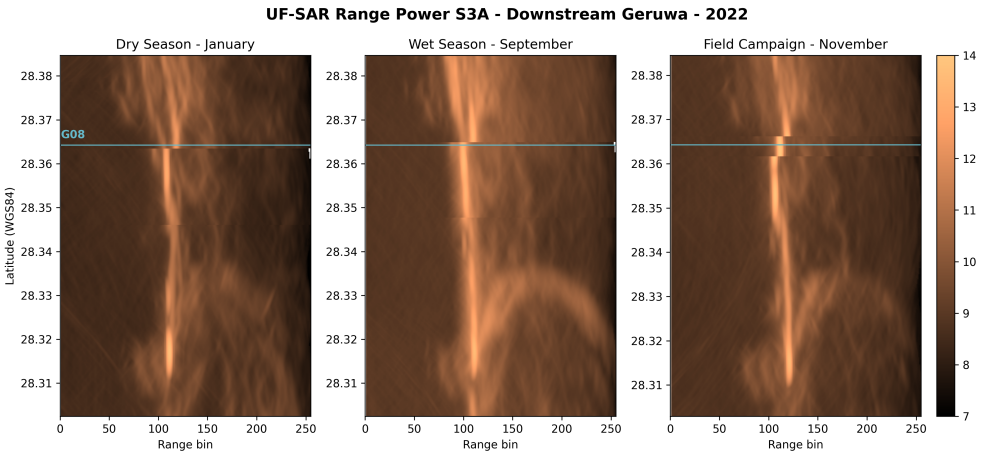
UF-SAR Range Power S3A - Downstream Geruwa - 2022
Dry Season - January
Wet Season - September
Field Campaign - November
G08
Latitude (WGS84)
28.38
28.37
28.36
28.35
28.34
28.33
28.32
28.31
0
50
100
150
200
250
Range bin
14
13
12
11
10
9
8
7

F.6. Overview of Collected Field Data

CAMPAIGN	LOCATION NAME	SEDIMENT	TRANSECT	NFP relative water level	CHIRP flow depth	RIVER WIDTH [m]	ESTIMATED water surface height [m]	SATTELITE OVERPASS
BH00	BHERI AT S3A OVERPASS	NO	NO	NO	NO	NO	NO	S3A
BH01	BHERI BRIDGE AT GHATGAUN	YES	NO	NO	YES	-	200.0	NO
BH02	BHERI AT GHATGAUN (S3B OVERPASS)	NO	NO	NO	NO	162.0	210.0	S3B
BH03	BHERI KARNALI CONFLUENCE	NO	NO	NO	NO	-		NO
K01	KARNALI AT S3A OVERPASS	NO	NO	NO	NO	74.6	178.0	S3A
K02	KARNALI UPSTREAM OF CHISAPANI	NO	NO	YES	NO	160.0	179.1	NO
K03	KARNALI BRIDGE, CHISAPANI	NO	NO	YES	NO	283.0	187.9	NO
G07	GERUWA BRIDGE: KHOTIYAGHAT	YES	NO	YES	YES	-	107.4	ICESAT
G08	GERUWA AT INDIAN BORDER	NO	NO	YES	YES	68.0	120.3	S3A

G

CHIRP+ Flow Depth Profiles

G.1. BH01

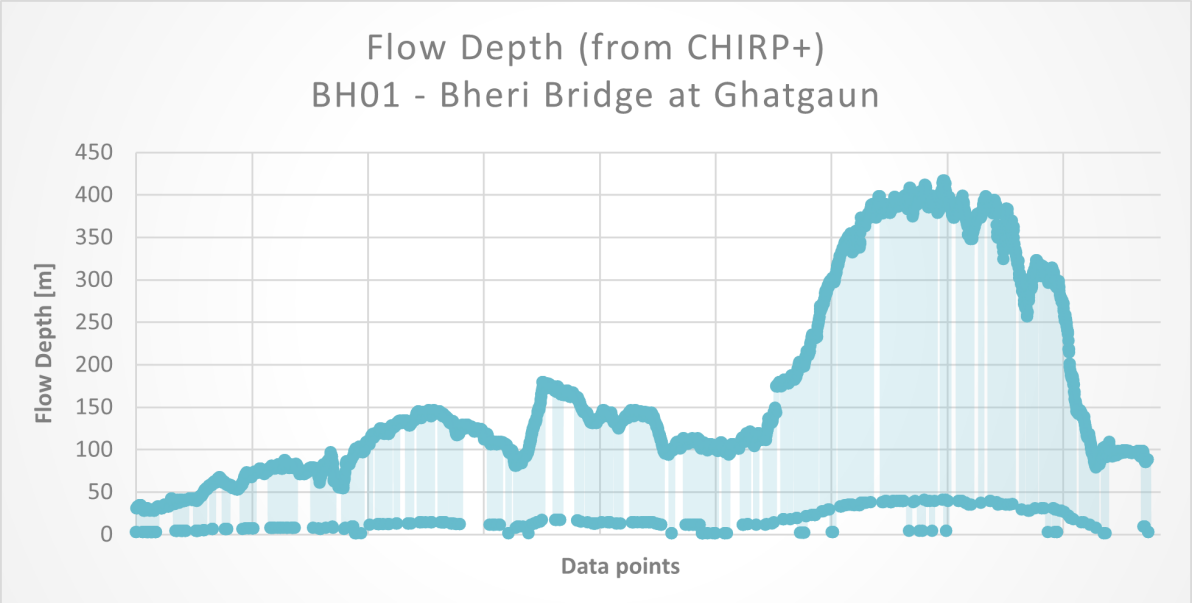

G.2. G08

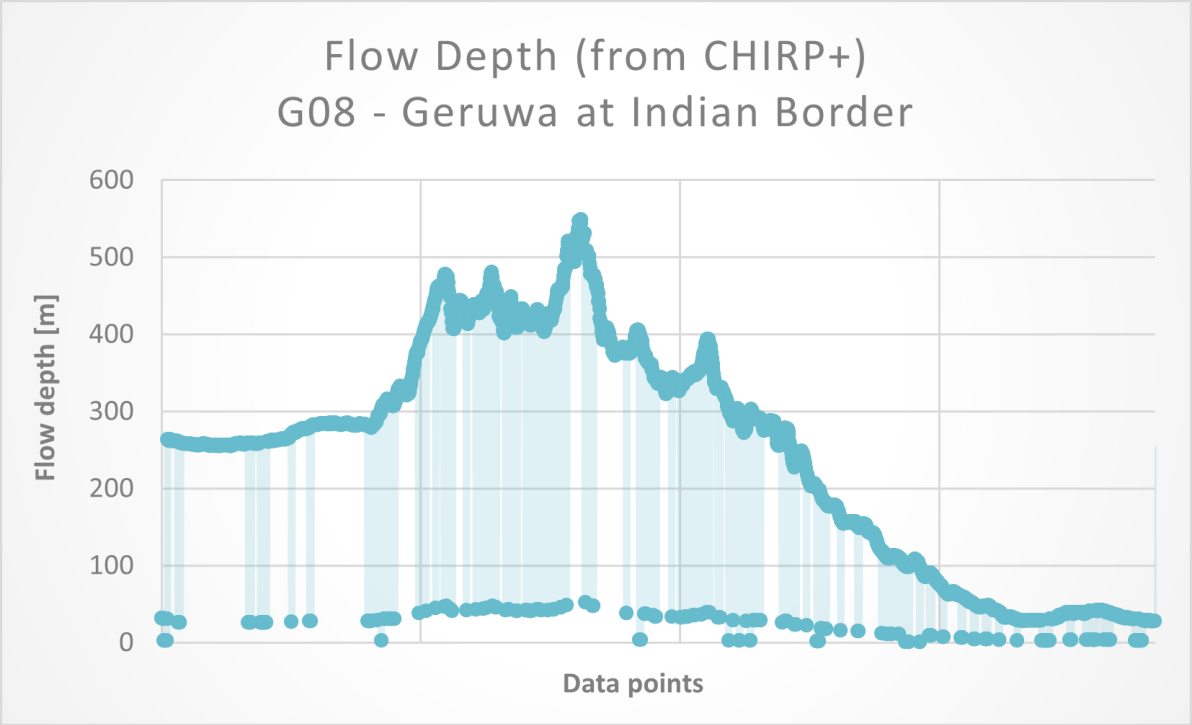
Flow Depth (from CHIRP+)
G08 - Geruwa at Indian Border
Flow depth [m]
600
500
400
300
200
100
0
Data points

H

Sentinel-3A Trajectory Height profile

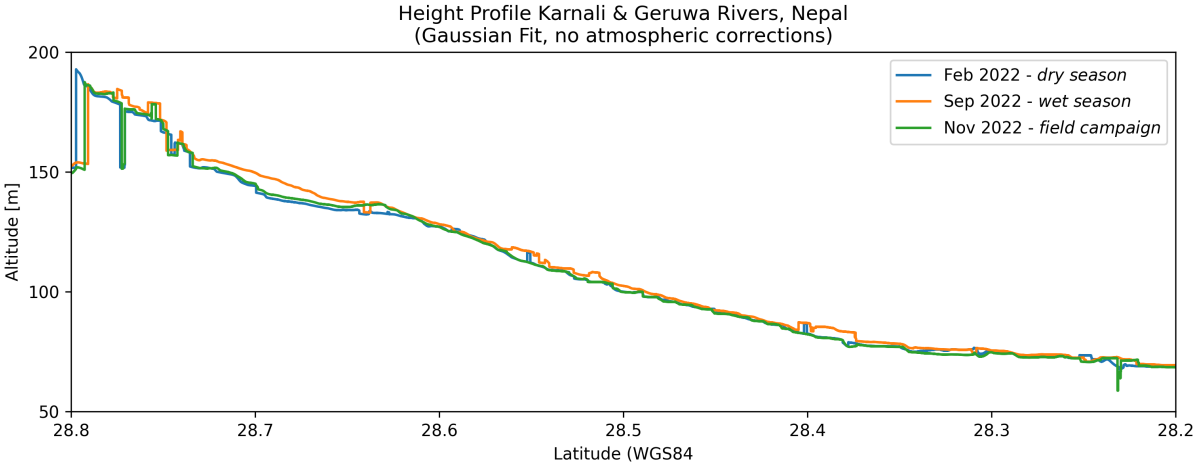

Figure H.1: Surface height profile along the S3A trajectory.

It should be noted that this figure only served an exploratory purpose. No atmospheric corrections have been applied for the derivation of these heights yet. Nevertheless, some things can be derived from this output. Firstly, for the section where the S3A follows the course of the Geruwa river, obtained water surface height estimations seem consistent. A clear pattern emerges, suggesting a concave-up river slope over the reach. Additionally, a clear water surface height difference can be observed in the upstream section where the Karnali flows through the Sivalik Hills. In the wet season the observed water surface heights are significantly larger as compared to the November field campaign and dry season observed water surface heights. Water surface heights appear larger for the wet season for most data points along the profile. Whilst this may also be caused by a satellite orbital cross-track shift, it suggests a water level increase as a result of seasonal discharge variations.

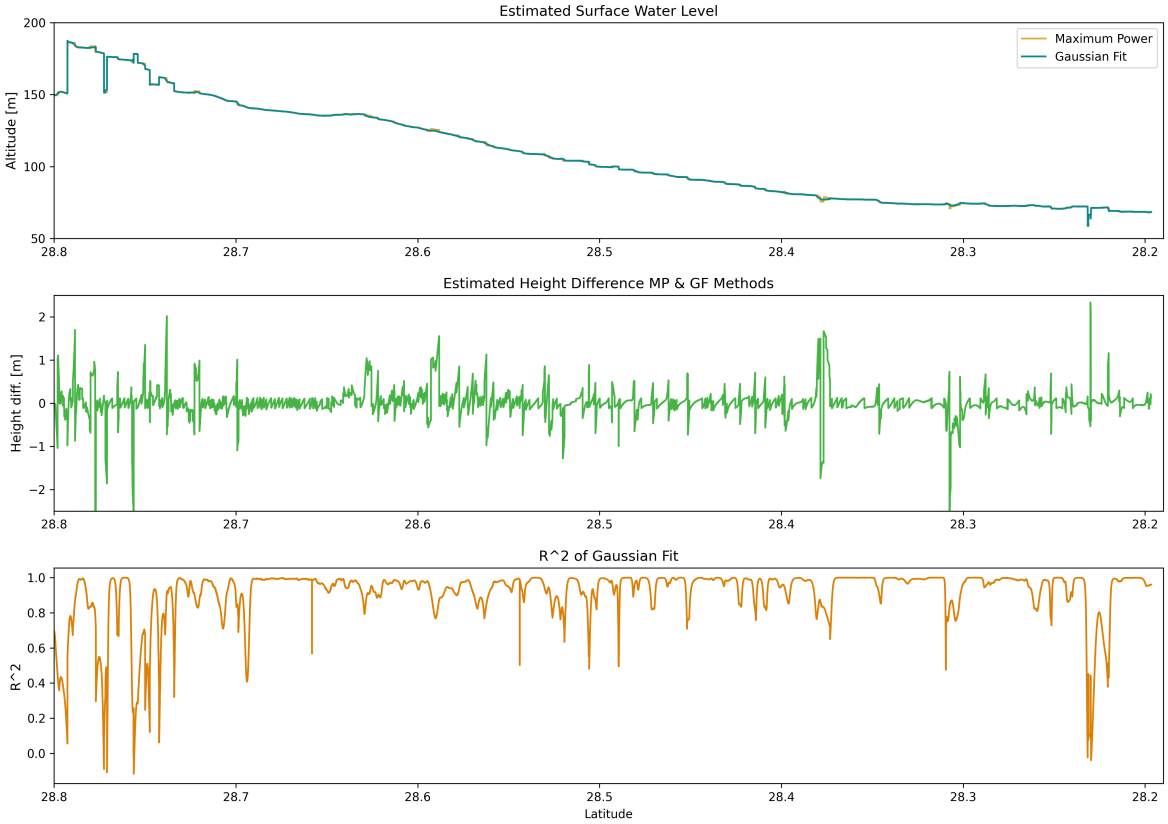

Figure H.2: Comparison of estimated water surface heights along the S3A trajectory with a maximum power retracker and a Gaussian fit retracker

From the comparison plot of the two different retracker approaches it becomes clear at what sites the return signal waveform may display multiple peaks in the signal or may be contaminated by land signal due to local topography, land use or other bright scatterers in the landscape. This may affect the derived water surface heights.

I

Field Report

2022 Karnali Field Campaign

FIELD REPORT

As part of the MSc Thesis Water Management + Geoscience & Remote Sensing:

Water level variability in the Karnali Fluvial Fan, Nepal

Authors: Mo de Jong & Kshitiz Gautam *Date: 21-02-2023*

MSc Student:

Name:	Mo de Jong
Studentnr.:	4826140
E-mail:	m.k.dejong@student.tudelft.nl
Phone:	+31 6229 85 241

Supervisors, assessment committee & contributors:

Name:	Thom Bogaard
Department:	Water Management (WM)
Role:	Thesis Supervisor WM
E-mail:	t.a.bogaard@tudelft.nl
Name:	Cornelis Slobbe
Department:	Geoscience & Remote Sensing (GRS)
Role:	Thesis Supervisor GRS
E-mail:	d.c.slobbe@tudelft.nl
Name:	Astrid Blom
Department:	River Engineering (HE)
Role:	Independent member assessment committee
E-mail:	astrid.blom@tudelft.nl
Name:	Kshitiz Gautam
Department:	Hydraulic Engineering
Role:	PhD candidate, contributor
E-mail:	k.gautam@tudelft.nl

Contents

1. Introduction

As part of the MSc thesis 'Water level variability in the Karnali Fluvial Fan, Nepal', fieldwork has been done in and around the Karnali fluvial fan. This includes measurements in the river systems in and surrounding Bardiya National Park in West Nepal, more precisely: the Karnali River, Geruwa River, Kauriala River, Babai River, and the Bheri River. The objectives of the fieldwork were to explore the area for suitable measurement campaign locations, and the potential for more permanent measurement stations. In addition, first data samples were to be collected to obtain a basic understanding and some first insights of the hydrodynamics and morphodynamics and system understanding of the Karnali Fluvial Fan. Lastly, the possibilities, challenges and limitations of data collection in the area were to be explored.

The fieldwork activities took place between 30 October and 26 November. This field report provides a summary of the activities during the field campaigns, methods used, some first results from data analysis and short descriptions of overall observations. The data collected during the fieldwork includes river widths, surface water levels, flow depth and river bathymetry, flow velocities, and sediment characteristics from collected sediment samples.

The first section will explain some of the preparatory work done for the fieldwork, including the testing of measurement instruments and the selection of areas to explore for suitable sites for collecting data (referred to as campaign locations). Thereafter, the data collection methods will be discussed, and the measurement instruments used will be presented. An overview is given of all the visited field campaign locations and what data was collected at which of these locations. For each of the visited locations a description of the river and landscape characteristics is provided, in addition to a short summary of the collected data at this campaign location. Following this section, the results of the collected data will be presented and discussed, covering water levels, river bathymetry, flow velocities, river transects including flow depth and flow velocities, and the sediment sampling. The report will conclude with a discussion of the major challenges faced during the 2022 field campaign and recommendations for future field campaigns.

2. Fieldwork preparations

2.1. Testing equipment

Measurement instruments have been tested in the WaterLab and/or in a pond on the TU Delft campus before use in the field campaigns in Nepal. These include the Nikon Forestry Pro, GeoPacks Hydrometer/current meter and the CHIRP Deeper+ instruments. Handheld GPS on the smartphones have not been tested before arrival in Nepal, other handheld GPS have been tested and used throughout the fieldwork period. A GNSS rover was taken to the field relatively last-minute. This device was expected to have high potential for measuring location coordinates in x, y and z direction with high accuracy. Unfortunately, insufficient time was available to test the equipment at TU Delft before departure. Extensive testing has been done in Nepal. Although the equipment and equipment set-up seemed to be working properly, unfortunately it was not possible to connect the device with any other device to read and download the data. Therefore, this equipment could not be used in the field. For future field campaigns it is recommended to again test the set-up and if necessary and possible fix the beforementioned issues to take the GNSS Rover and collect additional (x, y, z) location data.

2.2. Selecting sites

The selection of field campaign locations was based on two factors: hydro- & morphodynamic relevance and the availability of satellite SAR data. As the overall research aims at understanding and modeling the hydrodynamic and morphodynamic behaviour of the Karnali Fluvial fan the field campaign locations should be chosen such that the measurements at these locations contribute to a representative data set. Therefore, the campaign locations along the bifurcation area, the Geruwa River, and the Kauriala River have been chosen at an interval of approximately $5\,km$ distance along the river. This provided a set of areas of interest for reconnaissance for the eventual measurement site.

For the exact site selection the representativeness of the location regarding hydro- and morphodynamics was taken into account. To this extent the number of present river channels, flow velocity and potential obstructions were main factors to be considered in site selection. Preferably a measurement site would be situated at a location where the river reach only consisted of a minimal number of channels (preferable one or maximum two). Most sites proved to be only suitable for a selection of data collection (sediment sampling, flow velocities, river bathymetry, water level and/or river width), depending on hydrodynamic, morphodynamic, and/or landscape characteristics.

Secondly, the availability of satellite SAR data was decisive for site selection. To this extend, the orbital ground tracks of the satellites for which altimetry data is most widely available were studied. This included SAR satellites Sentinel-3 and Sentinel-6 and laser altimeter satellite ICESat-2. The availability of CryoSAT-2 data and its orbital ground tracks have also been studied. However, later it has been decided not to work with CryoSAT-2 data as the temporal resolution of the provided data was considered to be too small for the desired application. ICESat-2 will also most likely not be used as it considers satellite laser altimetry rather than satellite radar (SAR) altimetry. Both are however still incorporated in the maps and site selection process. An overview of all beforementioned ground tracks and the selected areas of interest for exploration are represented in a set of maps which can be found in Appendix A.

3. Logistics

The fieldwork included a lot of logistical planning. Based on the campaign location, the distance travelled and the conditions of roads and waterways modes of transport and accommodation were chosen. The facilities of NTNC at Thakudwara were used as a base, from where field campaigns in Bardiya National Park and near Chisapani were approached. This mainly included the left banks of the Karnali Bifurcation area, the left banks of the Geruwa River and the Babai River Expedition. Locations North of Chisapani were approached by motorbike as roads were bad due to landslides and ongoing road construction work. Chisapani was reached at multiple different instances either by motorbike, public transport, or shared jeep.

Campaign locations situated in the North section of the Geruwa River on the left bank (BI02-BI04, and G01-G03, see Figure 4) were reached by shared Jeep and/or by raft. Note that for transport with the raft NTNC personnel was required for peddling and for security reasons. For all abovementioned locations accommodation was at the NTNC BNP office. Field campaigns locations in the Southern Geruwa River reach (G04-G08) and in the Kauriala River (BI05 and KU01-KU08) were approached from Rajapur where we found accommodation, and a driver with a tuktuk was hired for a full week. At location G04 some local men were hired for security purposes. Lastly, the Babai expedition required a raft and NTNC personnel for navigation, peddling, security and expert knowledge regarding the area. The team stayed overnight at an army base in the jungle. This is the only way through which this area can be reached.

In preparation for and during the field campaigns contact and collaborations have been established with local people, local governments, institutes and other organisations. These include: NTNC, Bardiya Irrigation Project, Bardiya National Park, Rajapur Municipality, Nepal Pplice, Armed Police Force and Karnali River Management Project. A list of valuable contacts and collaborations is shown in Appendix A.

4. Data collection methods

This section gives an overview of instruments used and measurement methods applied during the field campaigns.

4.1. Instrument overview

Name & picture	Abbreviation	Used for measuring	Comments
Nikon Forestry Pro 	NFP	Horizontal distance, angle / incline, height, height differences	Uses two Leica lenses
Fish Deeper CHIRP+ 	CHIRP	Flow depth / river bathymetry, river width	Also locates fish
GeoPacks Hydrometer	Hydrometer / Current meter	Flow velocity Water depth (estimate)	Propeller type small current meter without stabilising fins
Android mobile phone	Mobile phone	GPS coordinates (x,y,z)	GPS Data App
Measurement tape	-	River width, location sediment sample, bridge height, water depth	Two different types: glass fibre tape of 100m and metal roll tape of 5 meters.
Hand scale	Scale	Sediment sample weight	Spring balance
GNSS RaspberryPi 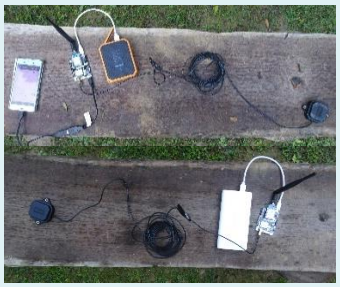	GNSS system / GNSS Rover	Accurate location with X,Y,Z coordinates	Built by Hessel Winsemius (TU Delft). Consisting of a base station + rover.
Van Essen Divers / Water Level Loggers 	Divers	Water pressure & Water levels	1x Barometer 3x Diver

Other tools used included:

- Rope to span across the river along which to collect river transect data.
- Raft for reconnaissance, accessing locations along bifurcation and Geruwa and to cross the river for collecting river transect data.
- Scoop and plastic bags to collect sediment samples

4.2. Water level

At first the water level was determined using the built-in GPS of a mobile phone in combination with a GPS data / location app. After a couple of measurements, it was discovered that the accuracy of the GPS, especially in the Z-direction, was insufficient to determine the vertical location up to the precision desired for this project. We got our hands around a handheld Garmin GPS system and tested it for its accuracy. This did not seem to be any better than the built-in GPS from the mobile phone. Since we could not get the GNSS rover system built by Hessel Winsemius working, and we did not have any other GPS or GNSS systems with us we had to find another creative way to estimate the water level.

For this we came up with the following. Since the Nikon Forestry Pro (NFP) lets us measure horizontal distance, height, height differences and angles, it was decided to use the NFP to estimate the vertical distance between a fixed point in the landscape and the water surface of the river. For this it was important to choose a fixed point in the landscape of which we were certain it would not change elevation through multiple high and low flow seasons. By knowing the longitude and latitude coordinates, the height of the fixed point could be determined using a (high-resolution) DEM. As the relative water level with respect to the landscape is known, then the exact water level could be estimated. This method also allowed to also measure the river width at most of the field campaign locations.

4.3. River width

The river width was measured using the Nikon Forestry Pro (NFP). With this device the horizontal distance between two points can directly be measured. Dependent on the environment there were two options for measuring the river width:

1. Standing at the edge of the water on the river bank the NFP was pointed to a steady point at the opposite side of the river, directly next to the edge of the water at the river bank. This steady point could for example be a pebble.
2. In case that, for any reason, edge of the water is not reachable, I chose a higher point to stand (for example a dike). Then I measured the horizontal distance from where I was standing to a steady point directly next to the edge of the water at the closest river bank. While doing so I made sure I pointed the NFP in the direction perpendicular to the longitudinal direction of the river. Then the horizontal direction to a steady point at the edge of the water at the opposite river bank was measured, directly across from the previous measured point (and hence in a straight line from where I was standing). From the difference in horizontal distances the river width could be estimated.

The latter method is expected to be slightly less accurate. However, with the NFP being highly accurate, it is estimated that the total accuracy should be within 0.5 meters maximum.

4.4. Flow depth & river bathymetry

The water flow depth and river bathymetry were measured using two different in-situ measurement methods. In addition, two temporary gauging stations were setup to measure water levels in two river sections over a longer period of time.

The bathymetry was determined using the Fish Deeper CHIRP+. This device is connected to a mobile app on which one can follow the live water depths or river bathymetry. It should be noted that with high flow velocities or when the CHIRP is dragged along the water surface too quickly, the data becomes less accurate or the device may not be able to detect or measure at all. This can be explained as when the flow velocity or dragging velocity is too large, the CHIRP may tilt. As a result it will measure the distance to the river bed under an angle, hence, the accuracy of the resulting river bathymetry will become lower and the water depth measured will be larger than the actual depth. Hence, the CHIRP should either be dragged along the transect at a very low pace, or externally held perpendicular to the water surface. This latter can either be done by hand, which is what was done during this fieldwork. Another suggested method is to attach the CHIRP to a larger float or small boat in such a way it is always sufficiently submerged at a relatively constant location with respect to the water surface (any systematic errors this may cause should be accounted for).

When either the flow velocity or dragging velocity becomes too high, or when the water is too turbulent, this may also cause the CHIRP to be pulled or jump up from the water. When the device is not partly submerged it cannot measure water depth, and hence no data can be collected. Some attempts were done to make the device more heavy in order to keep the device less under an angle and keep it partly submerged. This proved challenging, as one should do this without blocking the sensors on the bottom of the device. When testing this method it was also found to not work sufficiently to collect data. Hence, the CHIRP seems to be a good tool for measuring river bathymetry, especially in exploratory campaigns. However, it only works in calm waters with lower flow velocities and little turbulence at the water surface.

Another simple method was used to roughly estimate water depths and river bathymetry. This method was only applied for more shallow river sections when the hydrometer was used to measure flow velocities. The stick of the current meter was then used to estimate the flow depth by measuring the submerged part of the stick during the data collection.

Lastly, temporary gauging stations were installed in the downstream sections of the Geruwa and Kauriala Rivers (at G07 and KU08). It should be noted that a permanent gauging station for water level observations from which data can be obtained is also already present in the Karnali River near Chisapani. The newly installed gauging stations each included a diver installed in a pipe in or near the river bank, determining water levels from pressure signals. A barometric logger was installed in between

Figure 1: Gauging Station Setup at Geruwa Bridge (G07)

these two locations, at Rajapur, to correct for atmospheric pressure. Data can be collected from the water level and barometric loggers during the next field campaign. In addition a traditional water level gauge was installed near the Kauriala Bridge (KU08). Unfortunately, no suitable structures were present to adjust these traditional water level gauges near the Geruwa Bridge (at G07).

4.5. Flow velocities & transects

Two different methods were used to measure flow velocities. The method applied was dependent on the characteristics of the river section. The general and preferred method was by using the GeoPacks Hydrometer (current meter). However, this equipment requires the river to be shallow enough to walk through, but not too shallow as to ensure the propeller of the hydrometer to be fully submerged. In a few instances an attempt was made at measuring the flow velocities with the current meter from a raft or a boat. However, it is really important that the boat does not move (neither up- nor downstream) to ensure the motion of the boat does not affect the measurement of the flow velocity. This proved only possible in calm waters where the raft could be dragged along a line which was spun across the river. This method only succeeded in one location, being G02 in the Geruwa River at Bagh Tapu.

Where possible the collection of flow velocities with the current meter was combined with the collection of flow depths along a transect perpendicular to the river flow. Both flow velocity and flow depth would be measured at multiple points along this transect to obtain river cross-sectional data. Flow depth would be measured using the holding stick of the current meter and some measurement tape. At measurement points where flow depth was higher than the length of the hydrometer stick, the Hawkeye was used instead to measure flow depth. The river cross-sectional data that was obtained following this method will also be referred to as transect data later in this report.

At a few locations, where the river was too deep to use the current meter but flow velocities were sufficient to be reasonably measurable, a quick and dirty method was applied. For this, a local floaty prop was used. The floaty would be thrown into the water upstream and the time for it to reach a next point a determined distance downstream was measured. In some locations it was not possible to measure the flow velocity at all. These mostly included locations where flow velocities were too high, currents too strong and/or turbulence at the water surface was too large, locations where flow velocities were very low and/or river sections which were to shallow.

4.6. Sediment sampling

The study area has a variety of sediment from large boulders to fine silt and clay. Hence two different approaches were used for study of samples. First approach was to take photographs of the sediment in the floodplain with a known scale of reference. These photographs could be used to estimate and analyse the distribution of coarse sediment in the floodplain and the second approach was sediment sampling.

Surface sediment samples were taken at different locations along Karnali, Geruwa and Kauriala. One sediment sample each from Bheri and Babai were also collected. Standard surface grab collection[1,2] with scoop was performed. Collection of bed sediment from the river channels was challenging because of the high flow velocity, greater depth and logistical limitations. Hence, sediments from the active floodplain were taken as samples and at a few places from the river bed where possible. Minimum of 3 sediment samples from different points at every sampling location of Karnali, Geruwa and Kauriala were collected (except for one location where 2 were taken due to lack of accessibility). Sediment samples not less than 5kg were collected from each point using a scoop. The samples were kept in plastic bags so that no sediment would be lost from the sample. The bags were weighted on site using a spring balance and then sealed. Sample id was written on each bag with a permanent marker and the corresponding descriptions and details were recorded on the field book.

Figure 2: Photograph of coarse floodplain sediments with a scale (left), sampling using scoop (right)

Only the physical sediment studies were performed in two stages: in situ and lab environment. For the in situ investigations, following parameters were recorded in the field book:

1. Collection Date
2. Sample Id
3. Location: Latitude, longitude, Altitude
4. Sediment weight
5. Sample depth: Depth of sediment collected from the surface
6. Appearance: Dry, wet, semi-dry
7. Color
8. Texture
9. Water depth above sample
10. Location Description

Sieve analysis of the collected sample was performed in the lab of College of Engineering and Management, Nepalgunj. The sediments were sun and oven dried to the point where no

[1] Kasich, J., Taylor, M., & Nally, S. J. (2012). *Sediment Sampling Guide and Methodologies* (3rd ed.). State of Ohio Environmental Protection Agency. https://epa.ohio.gov/static/Portals/35/guidance/sedman2012.pdf

[2] Starosolszky, Ö., & Rakoczi (Eds.). (1981). Measurement of River Sediments. World Meteorological Organization. https://library.wmo.int/doc_num.php?explnum_id=1680

significant moisture or no lumps of sediment was left. 26 sieves with sizes ranging from 63mm to 0.075mm were used. Depending on the coarseness of the samples, either coarse or fine or both sieve analysis was performed. For coarse and mixed sediment analysis, the sample weight varying between 2500 gm to 3500 gm and for fine sediment analysis sample weight varying between 600 gm to 700gm was taken. For coarse analysis, the sample was passed through 10 sieves ranging from 63 mm to 4.75 mm and for fine through 17 sieves ranging from 4.75mm to 0.075mm. The weight of the retained sediments was measured to an accuracy of 0.1 gm (given the availability of instruments). Meanwhile other protocols were followed as per Indian Standard (IS) for sieve analysis which includes 10 minutes of sieving for each sample. The particle size distribution curves were obtained for each sample which are presented in the preliminary results section of this report.

Figure 3: Sieve analysis setup in the lab

5. Observation Locations

During the fieldwork campaign in November 2022, a total of 32 different locations were visited. An overview of these locations can be found in the map in *Figure 4.* An overview of the types of data collected at these campaign locations can be found in Appendix A.

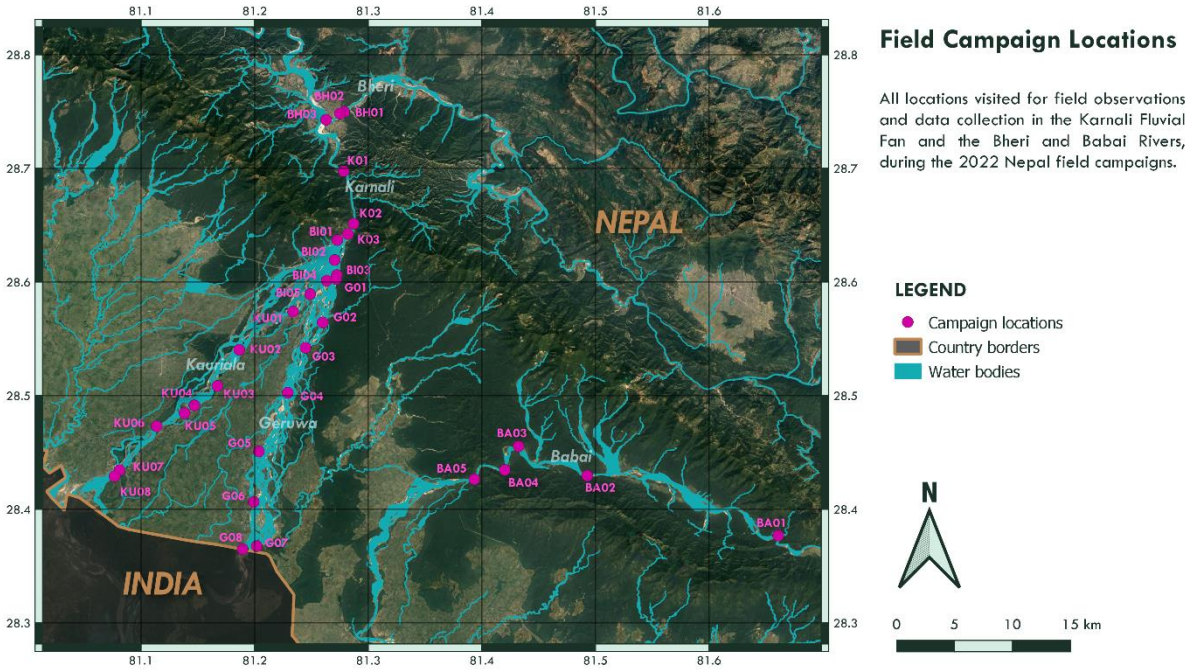

Figure 4: Overview map of all visited field campaign locations

5.1. Babai Campaigns

5.1.1. BA01 – Babai River, Upstream

Overview

Sediment samples	Transect	NFP heights	CHIRP	Width	Flow velocities
0	No	No	Yes	No	No

Environment

Hilly area, inner bend more flat with some vegetation (pioneer grasses as well as forest).

Left bank as seen from right bank

5.1.2. BA02 – Babai River at IceSAT Overpass (Upstream)

Overview

Sediment samples	Transect	NFP heights	CHIRP	Width	Flow velocities
0	No	No	Yes	74.4	No

Environment

Relatively flat topography, river bed exposed in the inner bend (right bank), mostly forest directly on the river bank on the left side. Also forested on the right side on top of a small step.

Left bank, from right bank

From right bank, looking downstream

5.1.3. BA03 – Babai River at S6 Overpass

Overview

Sediment samples	Transect	NFP heights	CHIRP	Width	Flow velocities
0	No	No	Yes	66.0	No

Environment

Located in a big river bend. Inner bend contains (dynamic) midchannel bars. During high flow a major channel also flows on the left side finding a shorter route downstream. During low flow the outer bend is the major channel (as this was the route taken with the raft during the campaign). Sediments consisted mainly of rocks too large to take sediment samples. Unfortunately, no pictures of the environment were taken at this location.

5.1.4. BA04 – Babai River at IceSAT Overpass (Downstream)

Overview

Sediment samples	Transect	NFP heights	CHIRP	Width	Flow velocities
1: 1BAB1	No	No	No	No	No

Environment

Steep vegetated rock wall on the left bank, more flat floodplains with a mix of sand and pebble sediments on the right side (hills in the distance). As no sediments could be taken from location BA03, a sample was taken from this location.

From right bank, looking upstream

From right bank, looking downstream

5.1.5. BA05 – Babai Downstream

Overview

Sediment samples	Transect	NFP heights	CHIRP	Width	Flow velocities
0	No	No	Yes	96.4	No

Environment

Hilly area with relatively flat terrain directly surrounding the river. Large rock formation on the right bank. Left bank more (densely) vegetated. Sandy river banks with a steep step on the right bank. Downstream the Babai bridge is located. This structure includes weirs as well as an irrigation inlet as part of the Babai Irrigation Project.

From raft, looking downstream at Babai Bridge

Right bank from left bank

From the Babai Bridge looking upstream

From the Babai Bridge looking downstream

5.2. Bheri & Karnali Campaigns

It should be noted that at the time of the current field campaign, the campaign locations were very difficult to reach. The road leading from Chisapani, upstream the Karnali, toward the confluence was under construction (both planned as well as resulted from landslides). This meant the roads were very bad and occasionally blocked for construction. It took approximately 3 hours by motorbike to reach from Chisapani to Ghatgaun and another 2 hours to get back. These travel times may differ depending on the chosen mode of transport (public bus or private jeep). It is advised to check road conditions before planning a field campaign to this location, and account for staying overnight in Ghatgaun if necessary.

5.2.1. BH01 – Bheri Bridge at Ghatgaun

Overview

Sediment samples	Transect	NFP heights	CHIRP	Width	Flow velocities
1: 1BHE1	No	No	Yes	120	Floaty prop

Environment

Near the bridges the river banks are enforced engineered embankments. This only holds for the section in direct vicinity of the bridges, including the river bend in which it is located. The river is clearly deeper on the left side than on the right side. This can be seen from the images below, as the river bed is partly exposed, mostly on the right side. The topography of the surroundings, especially downstream of the bridge, is relatively flat. Upstream of the bridge the area becomes more hilly. The area West of the Karnali river and downstream of the bifurcation is hilly as well. The flat area surrounding the bifurcation and Bheri Bridge, consists of mostly agricultural land and a few small villages.

From left bank

From bridge, looking downstream

From bridge, looking upstream

Left river bank

Right river bank

General notes

The presence of the two bridges (the newly constructed bridge & the old expansion bridge) allow for doing flow velocity measurements with a floaty at multiple different locations across the river. The new bridge is ideal to drag along the CHIRP for flow depth measurements.

5.2.2. BH02 – Bheri River at Ghatgaun (S3B Overpass)

Overview

Sediment samples	Transect	NFP heights	CHIRP	Width	Flow velocities
0	No	No	No	162.0	No

Environment

This location was selected as the sentinel-3B satellite ground track is located only a few hundred meters downstream of the Bheri bridges. This location is the exact location where the satellite passes over the Bheri River. The river is fast flowing in this section. The surrounding topography is relatively flat.

From right bank

Looking upstream, from right bank

General notes

Reconnaissance of this area included finding a boat to cross the river width to measure a transect with the CHIRP. Eventually, fishermen were found to have a simple traditional canoe. However, the river could not be crossed with this boat at this specific location as currents were too strong. Crossing the river a bit further downstream would have been possible. It was decided that this data would not add much to the data already collected at the bridges (BH01), compared to the required added cost and effort .

5.2.3. BH03 – Confluence Bheri and Karnali

Overview

Sediment samples	Transect	NFP heights	CHIRP	Width	Flow velocities
0	No	No	No	No	No

No data was collected at the confluence of Karnali and Bheri Rivers, other than GPS coordinates of the (high flow) location and pictures of the environment.

Environment

Confluence, looking downstream from temple

Bheri, looking upstream from right bank Bheri

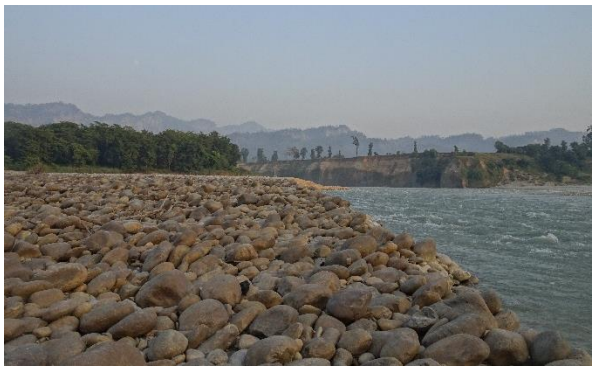

Bheri, looking upstream from confluence point.

General notes

High flow level near the temple was measured at 222 m altitude. Note that this was measured with handheld GPS, and therefore with questionable accuracy.

Locals told that during high flow the Karnali may carry much greater volumes than the Bheri, blocking the flow from the Bheri into the Karnali at the confluence point. This, together with strong rain induced flash flood, may cause major flooding in the area just upstream of the bifurcation point. The occurrence and severity of this varies per year.

5.2.4. K01 – Karnali River at S3A Overpass

Overview

Sediment samples	Transect	NFP heights	CHIRP	Width	Flow velocities
0	No	No	Partially	74.6	No

Environment

The landscape consists of steep hill slopes and a narrow valley through which the Karnali flows. The hill slopes on the left bank are steeper than on the right bank.

From right bank, looking upstream

From right bank, looking downstream

From left bank

High flow velocity & turbulence

River width measurement

General notes

Due to high surface flow velocities and turbulence it was not possible to measure flow velocities with the current meter nor with a floaty prop (as this would immediately submerge). This section would only be accessible from upstream with a boat, and even then it would be questionable whether one would be able to cross the river for measuring flow velocities & water depth along a transect (with CHIRP, current meter or ADCP) due to the high flow velocities and limiting accessibility on the left bank.

The river is relatively narrow here at approximately 75 meters width. In addition, the surrounding landscape consists of steep hillslopes. These landscape characteristics suggest that finding a signal of sufficient quality to retrieve water levels from satellite SAR altimetry would be highly challenging. Seninel-3A passes over the Karnali River at this location.

It was attempted to measure flow depths using the CHIRP. Although not a full cross-section could be made, flow depths of over 5 meters were measured. This location would be suitable for sediment collection. Due to logistical limitations, no sediment samples were taken from this location during this campaign.

5.2.5. K02 – Karnali Upstream of Chisapani

Overview

Sediment samples	Transect	NFP heights	CHIRP	Width	Flow velocities
0	No	Yes	No	160.0	No

Environment

Narrow valley with relatively steep hill slopes on both sides of the river.

Few hundred meters upstream of measurement location, on the right bank, looking upstream

NFP measurement from right bank

5.2.6. K03 – Karnali Bridge, Chisapani

Overview

Sediment samples	Transect	NFP heights	CHIRP	Width	Flow velocities
0	No	Yes	No	283	No

Environment

Just downstream of the Karnali Bridge at Chisapani a concrete staircase leads to a small beach where typically rafts are put into and taken out of the water.

From atop the concrete staircase on right bank

5.3. Karnali Bifurcation Campaigns

5.3.1. BI01 – Bifurcation S3A Overpass

Overview

Sediment samples	Transect	NFP heights	CHIRP	Width	Flow velocities
0	No	No	No	No	No

Environment

Construction works on the right bank of the bifurcation, just downstream of Chisapani.

General notes

This location is not suitable for field observations. Currently construction works are being executed, limiting the accessibility and making it subject to major changes in the landscape in the coming few years.

5.3.2. BI02 – Bifurcation Main Channel

Overview

Sediment samples	Transect	NFP heights	CHIRP	Width	Flow velocities
6: 1B1 – 1B6	No	No	Partially	No	No

Environment

Downstream end midchannel bar, looking downstream

From midchannel bar, looking upstream

Dilu (NTNC) on opposite side of the channel (right bank)

General notes

This location proved very challenging for collecting cross-sectional data of the channel. When trying to cross the river with a rope, the currents appeared too strong and the raft could not reach the opposite side of the river. After multiple tries, it was decided to only collect sediment samples here. It is advised to use a motorboat at this location for future field campaigns.

5.3.3. BI03 – Lalmati, Japanese Camp

Overview

Sediment samples	Transect	NFP heights	CHIRP	Width	Flow velocities
3: 2B1 – 2B3	Yes	Yes	Yes	164.4	Current meter

Environment

Lalmati, also called 'Japanese Camp' or 'Dolphin Viewpoint' is located right where the most eastern inlet channels of the Geruwa River are located. The left bank has a very high step with a steep cliff wall atop which saal forest vegetation can be found. This region is located considerably higher than the rest of the bifurcation area, which is generally fairly flat. The bifurcation channel located most to the right (as in sight) diverts water to any other potential inlet channels of the Geruwa and towards the Kauriala.

Overview from (Dolphin) viewpoint atop the steep wall on the left bank.

Steep cliff walls on left bank, looking upstream

From Geruwa inlets looking upstream at bifurcation

5.3.4. BI04 – Main Inlet Geruwa River

Overview

Sediment samples	Transect	NFP heights	CHIRP	Width	Flow velocities
0	No	No	No	No	No

Environment

From inside channel, looking upstream

From inside channel, looking downstream

From centre river bed, looking downstream

General notes

This channel was (previously) considered to be the main inlet to the Geruwa River. However, during reconnaissance of the area it was discovered to be almost completely dry. Only some water was still seeping through the river bed into the Geruwa. During high flow this channel is most likely still activated. As we were told by NTNC staff that the channel should still exist, the area was explored by foot up until BI05, but no other channels were discovered in between BI04 and BI05. Note for future field campaigns: this section is very high risk tiger area!

5.3.5. BI05 – Rajapur Irrigation Intake

Overview

Sediment samples	Transect	NFP heights	CHIRP	Width	Flow velocities
0	No	No	No	No	No

Environment

The pictures below were taken on 2 November, before major cleaning and restoration work on the irrigation intake was started.

Irrigation intake from Intake Park, looking upstream

Dam breach at irrigation intake, looking upstream

Sediment deposition at dam breach, looking upstream

Sediment deposition behind dam breach, (downstream)

Irrigation intake blocked by debris, looking downstream

Irrigation intake blocked by debris

General notes

Before the irrigation intake structure a dam was built to guide the water from the Kauriala into the agricultural area surrounding Rajapur. We have been told this dam was built when the majority of the water was still diverted into the Geruwa rather than the Kauriala. During the most recent high flow the dam must have collapsed, causing sediment and debris deposition in and in front of the intake structure, blocking further water intake into the irrigation channels and diverting the water into the Kauriala. When the location was revisited on 16 November, cleaning and restoration work on the intake structures had just stared.

5.4. Geruwa River Campaigns

Before describing each location measured along the Geruwa River in this section, it is important to note for future field campaigns that the entire Geruwa River Reach is a high risk tiger area zone (especially G02-G06) and one should always enter with caution, proper training, logistics, equipment and personnel.

Locations G01-G03 were accessed via raft starting at Lalmati (BI03). Locations G04-G08 were accessed by road with a tuktuk from the Rajapur area.

5.4.1. G01 – Geruwa River Left Inlets

Overview

Sediment samples	Transect	NFP heights	CHIRP	Width	Flow velocities
0 → similar to #2B3	Yes	Yes	Yes	46.2	Current meter

Environment

See also images and description of BI03 (Lalmati).

General notes

Where conventional maps show only one channel on the most left side of the Geruwa, actually two separate channels were present during the field campaign. The right channel of the two keeps a mostly rectangular cross-sectional shape at the inlet. The left channel is clearly larger and conveys more water into the Geruwa than the right channel. The left and the right channel have a width of $19{,}6\ m$ and $26{,}0\ m$ respectively, adding up to a total width of $46.2\ m$. It should be noted that the left channel stays wide whereas the right channel is very wide at the bifurcation and narrows quickly whilst also being considerably more shallow.

5.4.2. G02 – Geruwa River at Bagh Tapu

Overview

Sediment samples	Transect	NFP heights	CHIRP	Width	Flow velocities
4: 1G1 – 1G4	Yes	No	Yes	61.0	Current meter

Environment

From left bank, looking upstream

From left bank, looking downstream

General notes

The circumstances at this location were ideal for doing a full river cross-section transect.

5.4.3. G03 – Geruwa River at Gaida Machan

Overview

Sediment samples	Transect	NFP heights	CHIRP	Width	Flow velocities
0	No	Yes	Yes	27.8	Floaty

Environment

Relatively flat topography. Tall grasses growing on both river banks, directly on the water edge, left bank also forested, some sections right bank also (less densely) forested.

Upstream of Gaida Machan, inlet of channel

From left bank, looking upstream

From watchtower on left bank, main channel Geruwa visible in the distance.

General notes

The left channel as seen on the first picture above had to be chosen as turning right would lead the raft into a poorly accessible and high tiger risk zone. A watch tower and army base are located at this campaign location, making it accessible by 4x4.

5.4.4. G04 – Geruwa River at Gola

Overview

Sediment samples	Transect	NFP heights	CHIRP	Width	Flow velocities
7: 2G1 – 2G7	Yes	Yes	Yes	44.0	Current meter

Environment

Vast active floodplain area where clearly multiple (side) channels are activated during high flow. During the field campaign only one major channel flows through. As a result the active floodplain contains multiple – sometimes steep – steps at different altitudes, ranging a couple of meters. As far as the eye reaches, the surrounding area is very flat.

Right bank, looking upstream

Right bank, looking downstream

General notes

Flood marks indicating high flow levels were found at the bottom of the highest step/dike. This is a popular location for locals to let their cattle graze and to collect grasses.

5.4.5. G05 – Geruwa River at Manpur

Overview

Sediment samples	Transect	NFP heights	CHIRP	Width	Flow velocities
3: 3G1 – 3G3	No	No	No	No	No

Environment

Flat topography. The right bank of this river section is enforced with a high dike with groynes. The left bank exists of lower grasslands and is part of the buffer zone. Directly behind the dike agricultural land and a village can be found. On top of the dike a watch tower is located, providing a nice overview of the area. The dike is fenced along the entire length, during daytime the fence is opened, giving way for locals to enter the area for collecting grasses or grazing their cattle. Multiple very small and shallow channels flow through, all of which can be crossed on foot.

From watch tower on dike, looking downstream

View on river from dike on right bank.

From left channel, looking upstream

From right bank of left channel, looking downstream

Left channel from mid-channel bar

5.4.6. G06 – Geruwa River at Lalpur

Overview

Sediment samples	Transect	NFP heights	CHIRP	Width	Flow velocities
2: 4G1 – 4G2	Yes	Yes	Yes	64.0	Current meter

Environment

Flat topography, with dike on the right bank. The left bank is less steep with grasslands containing tall grasses located directly behind. This location was chosen as the river can directly be crossed by foot. Further downstream the river becomes deeper.

Left bank, from right bank

General notes

This section consists of one medium sized channel. As the river is crossable by foot during low flow, flow velocities are low, and a dike is located nearby, it seems ideal for collecting cross-sectional data. The location is not directly accessible by car, tuktuk or raft and should be approached on foot. Caution should be taken when measuring at this location, as a close encounter with a tiger was experienced here.

5.4.7. G07 – Geruwa Bridge: Khotiyaghat

Overview

Sediment samples	Transect	NFP heights	CHIRP	Width	Flow velocities
3: 5G1 – 5G3	No	Yes	Yes	No	No

Environment

Flat topography. Seemingly relatively dynamic active floodplain upstream of the bridge with more permanent, forested island/midchannel bar in between the left and right branch of Geruwa River. Downstream of the bridge the channel makes a turn to the right before meeting the right branch and flowing into India.

Geruwa Bridge from left bank

From left bank, looking upstream

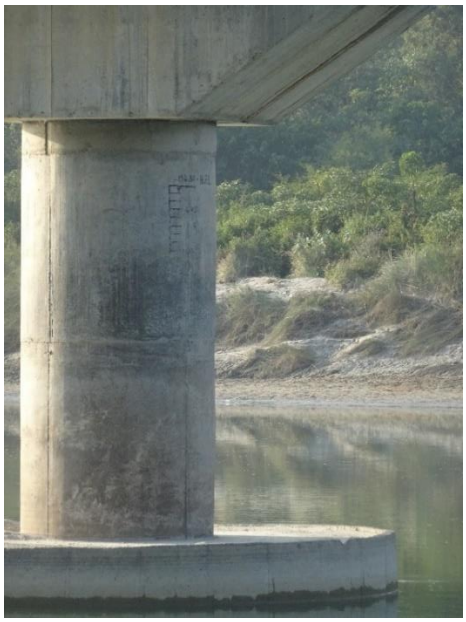

High flow level marked on bridge support

General notes

At the downstream end of the Geruwa River, before crossing the border to India a long bridge crosses the two channels of the river. During the field campaign, the majority of the water was flowing through the left channel, which is where the current observation location is located. Locals informed us that during high flow, the right channel carries more water as compared to the left channel.

The presence of the bridge and the quiet flow conditions allow for ideal circumstances to measure using CHIRP. Potentially, measurements could also be done using a raft, which we deemed not necessary at this point. This would also be an ideal location to measure with an ADCP. A gauging station with a diver was installed at this location. Unfortunately, there was no suitable location to install a water level gauge.

5.4.8. G08 – Geruwa River at Indian Border

Overview

Sediment samples	Transect	NFP heights	CHIRP	Width	Flow velocities
0	No	Yes	Partially	68.0	No

Environment

Relatively flat terrain. Left bank (inner bend) scarcely vegetated with grasses. Forest located further inland from left bank. When looking downstream, the right bank almost directly forested, located on a step, a couple of meters above current water levels. The midchannel bar which can be seen just upstream of this location is densely forested.

From right bank, looking downstream

From right bank, looking upstream

General notes

At this location the two branches of the Geruwa River converge into one, just before crossing the border to India. Seninel-3A passes over the river at this location.

5.5. Kauriala River Campaigns

5.5.1. KU01 – Kauriala River at Patabhar

Overview

Sediment samples	Transect	NFP heights	CHIRP	Width	Flow velocities
3: 4K1 – 4K3	No	No	No	No	No

Environment

Flat topography, hills in the background are the Silawik Hills, North of Chisapani. Seemingly very (morpho)dynamic area, with multiple channels and midchannel bars.

Sediment collection, left bank, looking upstream

General notes

Relative water level measurements not possible due to lack of suitable fixed point in the landscape in the vicinity of the river channels.

5.5.2. KU02 – Kauriala River at Banghusra

Overview

Sediment samples	Transect	NFP heights	CHIRP	Width	Flow velocities
0	No	Yes	No	182.6	No

Environment

Flat topography. Dike on left bank. The Kauriala seems to consist of only one channel at this location. However, satellite imagery suggests the presence of another channel located to the right. The forest located behind the sandy right of this channel would then be located on a major, stable midchannel bar. A more dynamic section with multiple smaller unvegetated midchannel bars and channels is located just upstream of this location.

Right bank / midchannel bar, from the dike on left bank

General notes

River difficult to access from the steep dike. Hence, this location proved only suitable for measurements with the NFP during this campaign.

5.5.3. KU03 – Kauriala River at Shantibazar

Overview

Sediment samples	Transect	NFP heights	CHIRP	Width	Flow velocities
3: 2K1 t/m 2K3	No	No	No	No	No

Environment

This section of the river has dikes on both sides and groynes on the left bank. Multiple midchannel bars are present in the active floodplain which consist of a mix of sand and stones. One major mid-channel bar is covered in trees and one other large mid-channel bar has some grass growing on its highest located sections. The mid-channel bars cause rapids to be present at some places in several channels.

Sediment samples, from left bank, looking upstream

From dike on left bank, looking upstream

General notes

Due to high flow velocities and relatively large flow depth the mid-channel bars could not be reached from the left riverbank. Solely sand deposition between the groynes (no stones). Small ferries operate on the most left and most right channels, between the river bank and a major mid-channel bar. No river widths or river cross sections were taken in this section of the river, as it consists of many smaller channels, some also too deep and fast flowing to cross. Location is easily accessible.

5.5.4. KU04 – Kauriala River at Marghua (Upstream)

Overview

Sediment samples	Transect	NFP heights	CHIRP	Width	Flow velocities
0	No	Yes	No	342	No

Environment

At first glance, it seems as if the river consists of only one channel in this section. However, satellite imagery suggests that there should be another channel flowing on the right of the channel seen on the image. Thus, this section probably consist of two major channels. The dike is located on the left bank and in the inner bend, explaining the sand deposition below. The right bank is vegetated with tall grasses and lower-canopy forest farther away from the bank.

From the dike on the left bank.

General notes

This short section of the river seems slightly less dynamic and the vegetated midchannel bar somewhat more stable. Location is easily accessible.

5.5.5. KU05 – Kauriala River at Marghua (Downstream)

Overview

Sediment samples	Transect	NFP heights	CHIRP	Width	Flow velocities
3: 2K1 -2K3	No	No	No	No	

Environment

Vast active floodplain area with a major midchannel bar and a few smaller midchannel bars. Dike with groynes on both banks, with a forest located right behind the dike on the right bank and agricultural land located behind the left bank.

From midchannel bar, looking downstream

Main channel as seen from (right side) midchannel bar

General notes

Due to the presence of multiple channels and midchannel bars, the river width could not be measured at this location. The same holds for collecting cross-sectional data. Hence, only sediment samples and relative water level data was collected here. Location is easily accessible.

5.5.6. KU06 – Kauriala at Daulatpur (Steamer Point)

Overview

Sediment samples	Transect	NFP heights	CHIRP	Width	Flow velocities
5: 1K1 t/m 1K5	No	Yes	Yes	310.0	Floaty prop

Environment

This section of the river has embankments including dikes and groynes on both sides. At this location a traditional steamer boat operates as a ferry between the two river banks. Note that steamers only cross the river if the flow conditions allow for it.

Right bank, from the dike, looking upstream

Right bank, from the dike

Sediment collection on left bank, looking upstream

General notes

The river is too deep and currents are too strong to cross the river by foot or with a raft. Flow velocity measurements were therefore taken using a floaty. The river was crossed (twice) with the local steamer boat. During the river crossing a cross-section was taken with the CHIRP.

5.5.7. KU07 – North of Kauriala Bridge

Overview

Sediment samples	Transect	NFP heights	CHIRP	Width	Flow velocities
4: 5K1 t/m 5K4	No	Yes	No	124.5	No

Environment

The active floodplain is fairly wide. Both the left and right riverbank are enforced with dikes and groynes. A large midchannel bar is present, with one very small channel on the right and a major channel on the left. The lack of vegetation suggests this bar has recently been flooded.

Small pond in midchannel bar

Elevation step on midchannel bar

Looking downstream from midchannel bar

Looking downstream from dike, left bank.

General notes

The river width measured at this location only comprises the width of the channel located on the most left side. This channel is considerably larger (both in width and depth) than the smaller channel on the right side of the large mid-channel bar.

5.5.8. KU08 – Kauriala Bridge: Sattighat

Overview

Sediment samples	Transect	NFP heights	CHIRP	Width	Flow velocities
0	No	Yes	No	No	No

Environment

Kauriala Bridge, from left bank (at diver station)

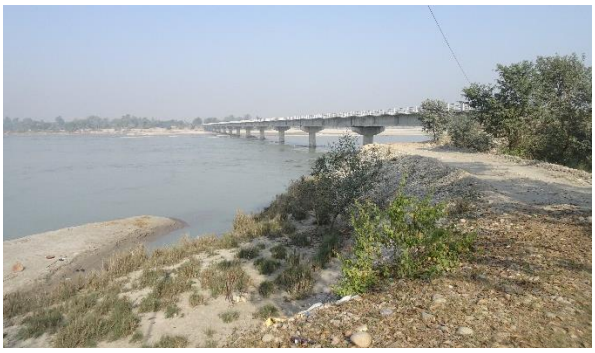

Kauriala Bridge, from left bank

General notes

The river is too wide at this location to be able to measure river width using the NFP. Currents are too strong, and turbulence at the water surface too large to measure with the CHIRP from the bridge. Currents are also too strong to cross the river with a raft. However, steamers are not located at this location either. During reconnaissance only a water scooter was found. For future campaigns a motorboat may be available from the army, and may be a suitable solution for collecting cross-sectional data. A gauging station including a diver and water level gauge was installed at this location.

6. Data

6.1. Water Levels

Relative water levels have been measured using the NFP by measuring the height difference between the water surface and a fixed point in the landscape. These measurements were executed at 16 different campaign locations as can be seen from Figure 5.

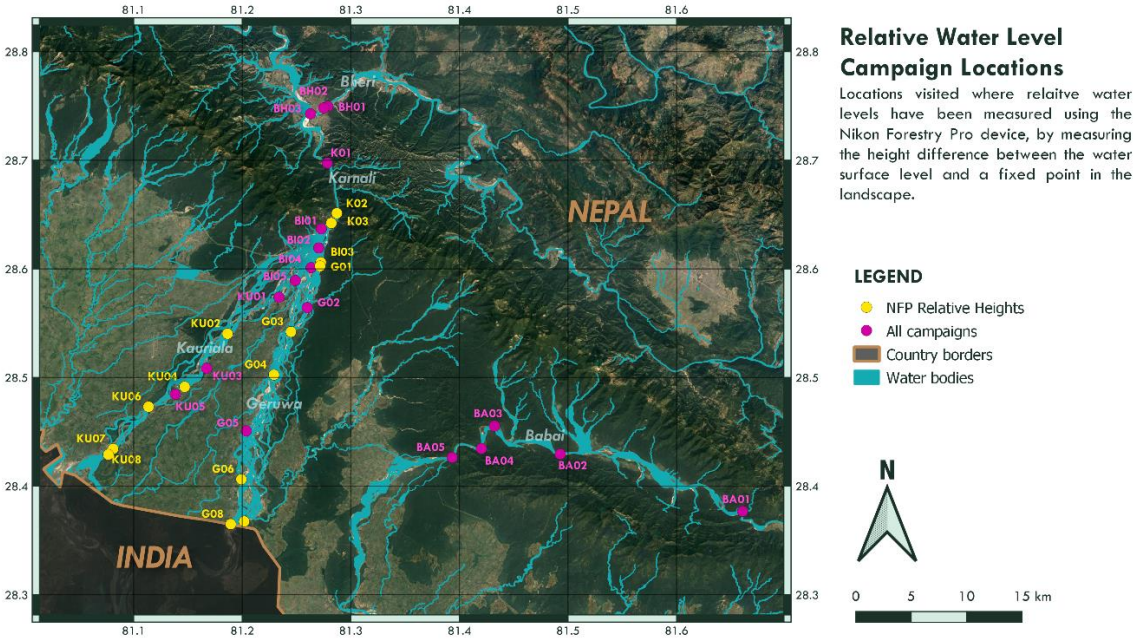

Figure 5: Relative Water Level Campaign Locations

For each of the locations for which the relative water levels were determined, a sketch was made including a schematic representation of the cross-section at that location including the measured triangulation(s) for the relative height measurement(s) and some landscape characteristics. Note that these sketches are indicative of the surroundings of the measurement locations and are not at all to scale. An example sketch is shown in Figure 6. All of the sketches and relative water level measurements can be found in Appendix D.1, and an overview of the observation data can be found in Appendix D.2.

A summary of the observation data is shown in Table 1. Note that the relative height represents the measured height difference between the water level and a fixed point in the landscape for which the height was expected to stay constant over time. All measurements with the NFP have been executed by Mo de Jong and were measured from eye-height; at $1.53\ m$ above the ground. This manual measurement method may have caused an inaccuracy estimated to be on the scale of $1-2\ cm$. The relative height as depicted in Table 1 is corrected for eye-height.

Note that no sketches were made for campaign location G04, whilst the relative water level was measured here (using the NFP). The landscape at this location is vast with many elevation changes, making it highly challenging to make an accurate estimated cross-sectional sketch of the area.

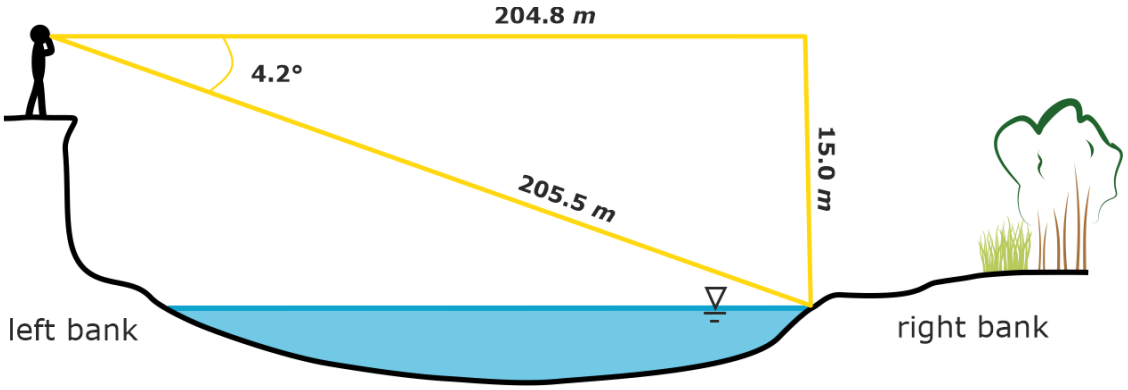

Figure 6: Example of schematic overview of a river cross-section for which relative water levels were measured, at field campaign location Lalmati

During the field campaigns it was experienced that the Nikon Forestry Pro has a very high accuracy for measuring horizontal distances. This was done by comparing distances measured with the NFP with distances measured by hand with measurement tape. It is expected that the NFP is more accurate in measuring distances, especially over greater distance and across rivers (of great width), than manually with measurement tape. For future use it would be recommended to work with objects which can be placed at both ends of the to be measured distance, to make aiming at the exact location for the measurement easier and therewith less sensitive to errors.

Campaign SN	nr.	relative height [m]	diagonal [m]	distance [m]	river width [m]	angle [deg.]
BI03	1	11.1	16.0	9.8	154.2	52.0
BI03	2	11.1	164.5	164.0	154.2	4.4
BI03	3	13.5	205.5	204.8	164.4	4.2
G01	1	13.5	38.5	35.2	19.6	23.2
G01	2	13.3	57.0	54.8	19.6	15.2
G01	3	13.5	69.0	67.2	164.2	12.6
G01	4	14.5	232.0	231.4	164.2	4.0
G03	1	1.3	28.0	27.8	27.8	5.8
G06	1	6.1	85.0	84.6	64.0	5.2
G07	1	5.5	26.5	25.4		7.0
G08	1	4.7	143.5	143.2	68.0	2.5
K02	1	20.9	55.0	50.0	160.0	24.2
K03	1	10.1	22.0	18.6	283.0	32.2
KU02	1	6.7	17.5	15.4	182.6	28.1
KU04	1	5.9	22.5	21.2	342.0	9.2
KU06	1	5.9	20.5	19.0	310.0	21.2
KU07	1	6.5	16.0	13.6	124.5	30.8
KU07	2	6.5	138.0	137.6	124.0	3.4
KU07	3	7.3	19.5	17.2	124.0	27.2
KU08	1	6.1	56.5	55.8		7.8
KU08	2	5.9	49.0	48.4		8.7

Table 1: Summary of Collected Relative Height Observation Data

Note that at many field campaign locations the river consisted of multiple channels. Hence, the total river width may be larger than the one presented in Table 1, considering the total width to be the total width of the multiple channel. Moreover, the water level in the channel may be dependent on the presence of other channels. Visual observation of the landscape shows indications that soils in the region have a high permeability. Hence, it can be expected that surface water levels will be similar across the various channels in multi-channel sections of the river.

6.2. River Width

River width has been measured at 18 locations as shown in Figure 7. At most locations the river width was measured using the Nikon Forestry Pro. At some locations the river width was (also) measured using measurement tape. Theoretically river width could also be derived from collected GPS coordinates or CHIRP data. However, these values are expected to be subject to large uncertainties and will be less accurate. These derivations have not been done for this field report and hence only river widths as measured with the NFP or measurement tape are included in the report. The river widths are shown in table Table 2.

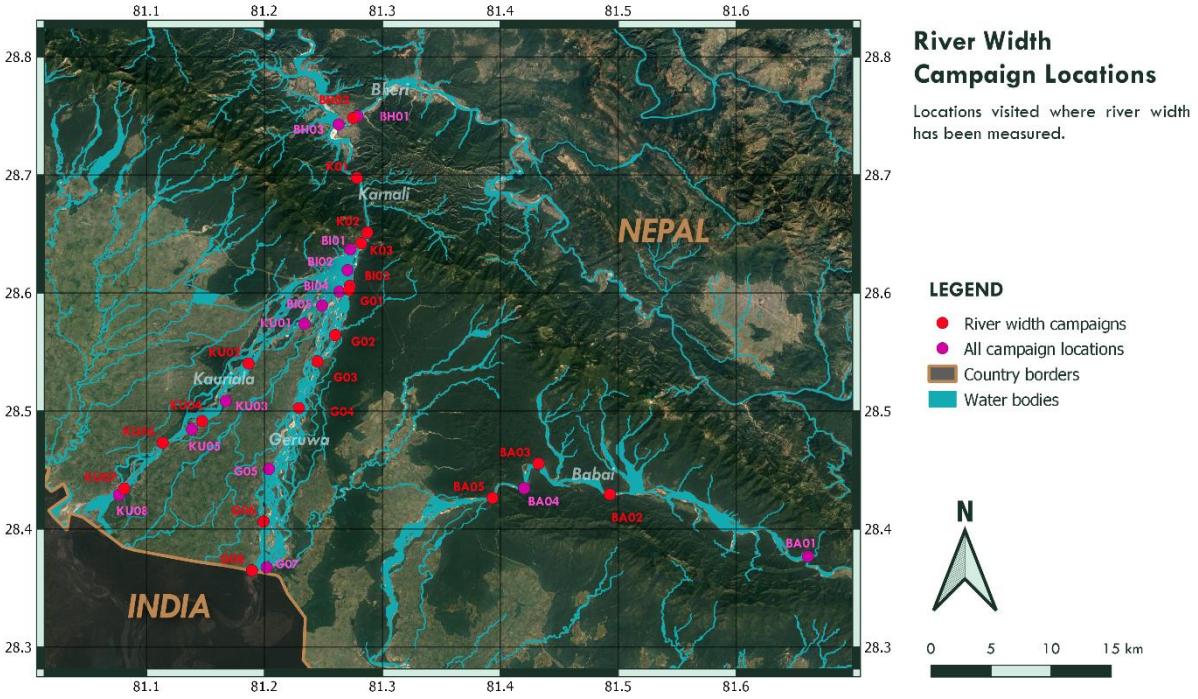

Figure 7: River Width Campaign Locations

It was estimated that the accuracy of measuring river width with the NFP is in the order approximately $5 - 20\ cm$. It should also be noted that the NFP and the measurement tape were not able to measure large river widths (typically over 350-400 meters).

CAMPAIGN	LOCATION NAME	RIVER WIDTH [m]
BA02	BABAI ICESAT OVERPASS UPSTREAM	74.4
BA03	BABAI S6 OVERPASS	66.0
BA05	BABAI DOWNSTREAM	96.4
BH02	BHERI AT GHATGAUN (S3B OVERPASS)	162.0
BI03	LALMATI, JAPANESE CAMP	164.4
G01	GERUWA LEFT INLETS	183.8
G02	GERUWA AT BAGH TAPU	61.0
G03	GERUWA AT GAIDA MACHAN	27.8
G04	GERUWA AT GOLA	44.0
G06	GERUWA AT LALPUR	64.0
G08	GERUWA AT INDIAN BORDER	68.0
K01	KARNALI AT S3A OVERPASS	74.6
K02	KARNALI UPSTREAM OF CHISAPANI	160.0
K03	KARNALI BRIDGE, CHISAPANI	283.0
KU02	KAURIALA AT BANGHUSRA	182.6
KU04	KAURIALA AT MARGHUA (UPSTREAM)	342.0
KU06	KAURIALA DAULATPUR (STEAMER)	310.0
KU07	NORTH OF KAURIALA BRIDGE	124.5

Table 2: Measured River Widths

6.3. River Bathymetry

River bathymetry data acquired using the Fish Deeper CHIRP+ has been collected at 15 different field campaign locations. These locations are shown in the map in Figure 8. It should be noted that for some locations the bathymetry data was collected only for a part of the cross-sectional transect. This holds for locations K01, BI02, G08, and KU08. Only the data at the campaign locations for which the cross-sectional data was considered to be sufficiently representative or of sufficient added value are presented in the field report (only for BI02).

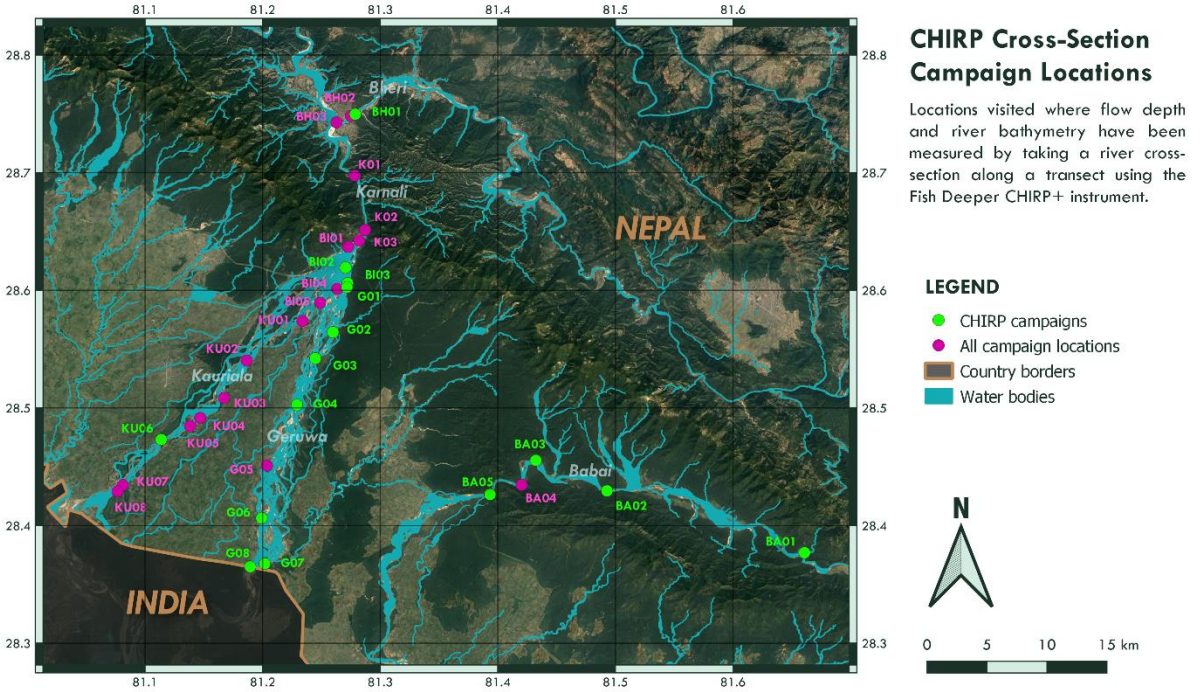

Figure 8: CHIRP River Cross-Sectional Campaign Locations

The river bathymetry using the CHIRP+ in the Gerua river is mostly for one channel. Given the condition that Gerua flows through the BNP in multiple channels and the accessibility of all channels are limited due to security reasons, the bathymetry of the accessible major channels are only taken. The data obtained from the CHIRP+ provides the depth of water relative to the water surface and not the bed surface elevation relative to mean sea level. Plotting the data from chirp is still a challenge by the time this report is being prepared. However, the data can be visualized in the Fish Deeper app and also point depths can be extracted where the GPS signals for the CHIRP+ are available (Figure 9).

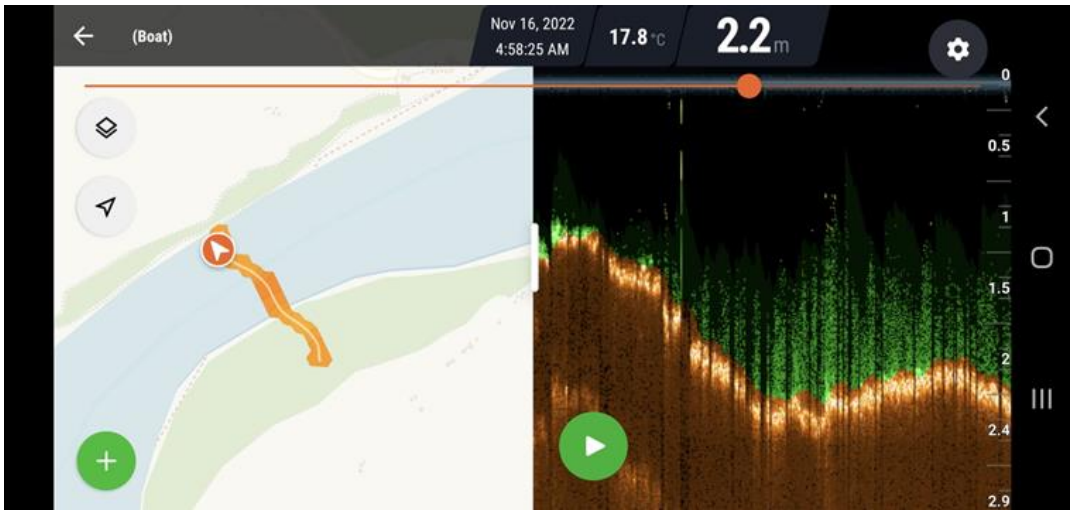

Figure 9: Visualization of bathymetry obtained at Daulatpur (KU06) from Fish Deeper app

These data may be useful for 1D hydraulic modelling purpose. In the future, if any methodology can be developed to identify the elevation of water surface at the time of measurement, this bathymetry data will have higher relevance and use.

6.4. Flow Velocities with a Floaty

The flow velocities using method of float was estimated at 2 locations given the extreme flow velocities. One being the Bheri bridge (BH01) and the other Daulatpur in Kauriala river (KU06). At least 3 measurements have been taken at each location. These velocities are a very rough estimate which may be used to estimate the discharge through those river sections.

Location	Flow Velocity [m/s]				Distance Travelled By Prop [m]	River Width [m]
	LEFT	CENTRE	RIGHT	AVERAGE		
Bheri (BH01)	2.18	2.22	2.03	2.14	120	unknown
Daulatpur (KU06)	1.23	-	1.77	1.50	Left: 57.5 Right: 36.0	310

Table 3: Flow velocity measurements obtained using floats

Such measured velocities are to be used for estimating the discharge through respective river cross sections when obtained from the processed CHIRP+ data.

6.5. River Transects with Flow Depth & Flow Velocities

At a few locations river cross-sectional data was manually collected along a transect along a river cross-section. During these campaigns flow depth (or river bathymetry), as well as flow velocities have been measured at different points along the transect. This data is referred to as transect data. Figure 10 shows at which locations transect data was collected. In the following sections the transects at each location are shown and briefly discussed.

Note that a wide range of limiting factors were present across the different locations, which did not allow for collecting transect data at those locations. These factors included: too high flow velocities, too great flow depths in combination with not having access to a raft or boat, and too shallow flow conditions.

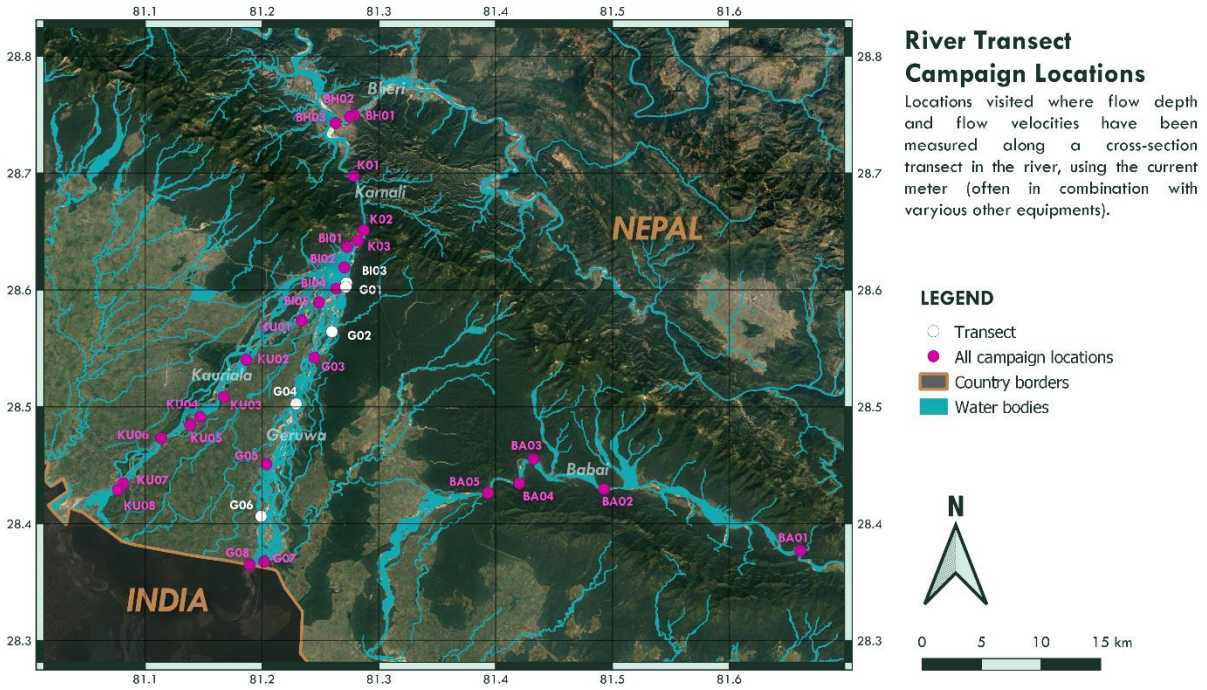

Figure 10: Transect Campaign Locations for Flow Depth & Flow Velocities

The figures in the following sections visualise the transect data collected during the field campaign. This includes river width, and flow velocities and flow depth measured at several points along the transect. The blue boxes represent the depth at which the flow velocities were measured. The visualisation also indicates left and right banks. The width is represented as the total distance from the left bank to the measured point. At the bottom the estimated discharge is computed over the column as visualised above as:

$$Q = v \cdot A = v \cdot \text{river width} \cdot \text{flow depth}$$

The total discharge is computed as the sum of the computed discharge of all columns.

For the first flow velocity and discharge estimates it was assumed that the measured flow velocity is constant over the full depth. It is commonly known however, that in general the flow velocity varies over depth, being near zero close to the river bed and highest near the water surface. As the flow velocities were mostly measured at $15\ cm$ above the river bed for shallow rivers, or at a depth of approximately $90\ cm$ for deeper rivers it can be expected that the total discharge for shallow river sections with an average depth of around $30\ cm$ may be closer to the truth, whereas the total discharge for deeper river sections may be more sensitive to

underestimation for sections with an average depth between $30 - 180cm$, and overestimation for river sections with an average depth greater than $180\ cm$. Lastly, at some campaign locations, often near the river bank, flow depths were too small to measure flow velocities (noted as *too shallow*). For these measurement points the discharge over the water column was assumed to be zero.

In Appendix F the full transect data and visualisation are presented. Also, some additional information and data is given in tables. A summary of the transect data and visualisation is presented in the sections below.

6.5.1. Results

6.5.1.1. BI03 – Lalmati, Japanese Camp

BI03	Lalmati			10/11/2022		13:15		
width [cm]	150	2500	4000	(estimated) 6755	9550	11550	13550	15050	15500
depth [cm]	depth unkonwn	450	600	450	depth unknown	190	65	40	10
flow velocity [m/s]	0.4	0.85	1.2	1.2	1.1	0.5	0.16	0.08	0.1
Q= [m3/s]	0.18	89.8875	108	148.77	184.47	19	2.08	0.48	0.045

Table 4: Flow depth, flow velocities and discharge at BI03 - Lalmati, Japanese Camp

The total estimated discharge resulting from these measurements is: $Q_{tot} = 552.91\ m^3/s$

As flow depths were too large to cross the river, these transect measurements have been executed from a raft. The current meter was held at $15\ cm$ above the river bed, or at a depth of approximately $90\ cm$ for flow depths greater than $105\ cm$. Generally, it is considered that flow velocities are greater near the surface than near the surface, and this transect considers a relatively deep river section. As a result, at depths greater than $210\ cm$, it is expected that flow velocities are overestimated. At depths between $30\ cm$ amd $210\ cm$ it is expected that flow velocities are underestimated. Approximately half of the transect has depths between $30 - 210\ cm$ (underestimating flow velocity & discharge) and half of the transect has depths greater than $210\ cm$. Therefore, no clear conclusion can be made considering the under- or overestimation of the total discharge.

Measuring flow velocities from a raft is challenging as the measurements may be affected by the velocity of the raft. During the measurements the raft was kept in place as much as possible. Nevertheless, the results are highly sensitive to measurement errors.

Note that the distances between the points measured along the transect are large, hence causing the resulting transect to be less precise. Moreover, since the estimated transect is dependent on less measurement point, it becomes more dependent on the accuracy of those few measured depths and flow velocities. Lastly,

6.5.1.2. G01 – Geruwa River Left Inlet Channels

Transect measurements were made for the two inlet channels visibly conveying water at the surface into the Geruwa River. Respectively the left and right inlet channel transects are shown below.

G01L	Geruwa left inlet	10/11/2022	15:30

width [cm]	200	1700	2700	3700	4700	4900
depth [cm]	90	150	120	65	45	
flow velocity [m/s]	0.3	0.6	0.55	0.5	0.3	
Q= [m3/s]	0.54	13.5	6.6	3.25	1.35	

Table 5: Flow depth, flow velocities and discharge at G01L - Geruwa left inlet

The total estimated discharge resulting from these measurements is: $Q_{tot} = 25.24\ m^3/s$

The left inlet channel has a total width of $49\ m$. As the measured depths over the entire transect lay between $30 - 210\ cm$ it is expected that the flow velocities are underestimated over the full transect, causing an underestimation of the total discharge through the left inlet channel.

G01R	Geruwa right inlet	10/11/2022	16:00

width [cm]	250	450	650	*775*	*900*
depth [cm]	40	65	65	*40*	
flow velocity [m/s]	0.25	0.5	0.46	0.25	
Q= [m3/s]	0.25	0.65	0.598	0.25	

Table 6: Flow depth, flow velocities and discharge at G01R - Geruwa right inlet

The total estimated discharge resulting from these measurements is: $Q_{tot} = 1.748\ m^3/s$

The right inlet channel has a total width of $9\ m$. As the measured depths over the entire transect lay between $30 - 210\ cm$ it is expected that the flow velocities are underestimated over the entire transection, causing an underestimation of the total discharge through the right inlet channel. It should be noted that it was observed that the right inlet channel had a near rectangular cross-sectional shape, and that the values closest to the right bank were assumed based on this knowledge. Note that the data given in red in Table 5 are estimated values, not measured values.

6.5.1.3. G02 – Geruwa River at Bagh Tapu

G02	Bagh Tapu				11/11/2022			12:15 - 13:10	
width [cm]	100	300	500	700	900	1100	1300	1500	1700
depth [cm]	65	80	85	90	80	65	70	65	65
flow velocity [m/s]	0	0.14	0.18	0.2	0.41	0.4	0.35	0.45	0.3
Q = [m3/s]	0	0.224	0.306	0.36	0.656	0.52	0.49	0.585	0.39
width [cm]	2000	2200	2400	2600	2900	3200	3500	3800	4100
depth [cm]	80	80	70	80	80	85	95	95	100
flow velocity [m/s]	0.4	0.4	0.7	0.55	0.6	0.6	0.7	0.6	0.7
Q = [m3/s]	0.96	0.64	0.98	0.88	1.44	1.53	1.995	1.71	2.1
width [cm]	4400	4700	5000	5300	5500	5700	5900	6100	
depth [cm]	100	70	65	50	too shallow	too shallow	too shallow	too shallow	
flow velocity [m/s]	0.7	0.6	0.5	0.3	0	0	0	0	
Q = [m3/s]	2.1	1.26	0.975	0.45	0	0	0	0	

Table 7: Flow depth, flow velocities and discharge at G02 - Geruwa River at Bagh Tapu

The total estimated discharge resulting from these measurements is: $Q_{tot} = 20.55\ m^3/s$

This channel of the Geruwa was considered the main channel and has a total width of approximately $61\ m$. As the measured depths over the entire transect lay between $30 - 210\ cm$ it is expected that the flow velocities are underestimated over the entire transect – not including the section where it was too shallow to measure – causing an underestimation of the total discharge.

6.5.1.4. G04 – Geruwa River at Gola

G04	Gola				14/11/2022			12:45	
width [cm]	300	500	700	900	1050	1300	1550	1850	2100
depth [cm]	too shallow	too shallow	too shallow	25	30	40	45	58	60
flow velocity [m/s]	0	0	0	0.15	0.2	0.15	0.25	0.25	0.33
Q = [m3/s]	0	0	0	0.075	0.09	0.15	0.28125	0.435	0.495
width [cm]	2400	2700	2950	3200	3500	3700	3900	4100	4400
depth [cm]	70	70	70	65	65	60	25	10	too shallow
flow velocity [m/s]	0.35	0.4	0.45	0.4	0.35	0.25	0.2	0.1	0
Q = [m3/s]	0.735	0.84	0.7875	0.65	0.6825	0.3	0.1	0.02	0

Table 8: Flow depth, flow velocities and discharge at G04 - Geruwa River at Gola

The total estimated discharge resulting from these measurements is: $Q_{tot} = 5.641\ m^3/s$

This channel of the Geruwa was considered the main channel at this point and has a total width of approximately $44\ m$. As the measured depths over the entire transect lay mostly between $30 - 210\ cm$ it is expected that the flow velocities are slightly underestimated over the entire transection, causing a slight underestimation of the total discharge through the left inlet channel.

6.5.1.5. G06 – Geruwa River at Lalpur

G06	Lalpur	15/11/2022								
width [cm]	300	500	700	900	1100	1300	1500	1700	1900	2100	2300
depth [cm]	20	30	30	40	50	50	50	50	50	45	40
flow velocity	0.2	0.4	0.5	0.55	0.6	0.55	0.5	0.55	0.55	0.6	0.65
Q = [m3/s]	0.12	0.24	0.3	0.44	0.6	0.55	0.5	0.55	0.55	0.54	0.52
width [cm]	2500	2700	2900	3100	3300	3500	3700	3900	4100	4300	
depth [cm]	45	40	40	40	40	30	30	25	10	too shallow	
flow velocity	0.55	0.65	0.65	0.65	0.65	0.5	0.35	0.25	0.07	0	
Q = [m3/s]	0.495	0.52	0.52	0.52	0.52	0.3	0.21	0.125	0.014	0	
width [cm]	4500	4700	4900	5100	5300	5500	5700	5900	6100	6300	
depth [cm]	too shallow	too shallow	too shallow	too shallow	too shallow	too shallow	too shallow	too shallow	too shallow	too shallow	
flow velocity	0	0	0	0	0	0	0	0	0	0	
Q = [m3/s]	0	0	0	0	0	0	0	0	0	0	

Table 9: Flow depth, flow velocities and discharge iat G06 - Geruwa River at Lalpur

The total estimated discharge resulting from these measurements is: $Q_{tot} = 8.134\ m^3/s$

This channel of the Geruwa had a total width of approximately $63\ m$. This section of the river seemed to have a near rectangular shape, with the right bank being very shallow over a great width. At points where flow depths were great enough to measure both depth and flow velocities, the flow depths laid mostly between $30 - 50\ cm$. Hence, it is expected that the flow velocities are slightly underestimated at these locations. However, no flow was assumed through the shallow parts. Hence, no clear conclusions can be made about over- or underestimation of the total discharge.

6.5.2. Discussion of the Results

Limiting factors for measuring flow depths and flow velocities along a transect perpendicular to the flow of the river included: flow depth (too deep and too shallow), flow velocities (too large and too small), and accessibility of the selected campaign location. In addition, more accurate, precise and elaborate data may be collected in the future, using more advanced measurement equipment such as an ADCP. With the availability of a motorboat more locations become accessible, especially within the Kauriala River. This, together with the availability of an ADCP may provide great potential for collecting transect data in the Kauriala River as well. Note that the Geruwa River is expected to not be accessible with a motorboat during dry season or low flow.

These measurements count as a very rough estimation of river bathymetry, flow velocities and river discharge. Measurement instruments and conditions were limiting for making more accurate estimates. Therefore, the results presented above should not be taken too strictly. The collection of data at these locations helps giving insight into what locations may be of interest for future field campaigns with more elaborate equipment. In the meantime, the current result may give a rough idea of discharge volumes flowing into and through the Geruwa River.

6.6. Sediment Samples

A total of 46 sediment samples have been collected across 14 different field campaign locations. Figure 11 provides an overview of the locations at which sediment samples have been collected. The summary of rapid assessment of the results from sieve analysis of sediment samples are presented in **Error! Reference source not found.**.

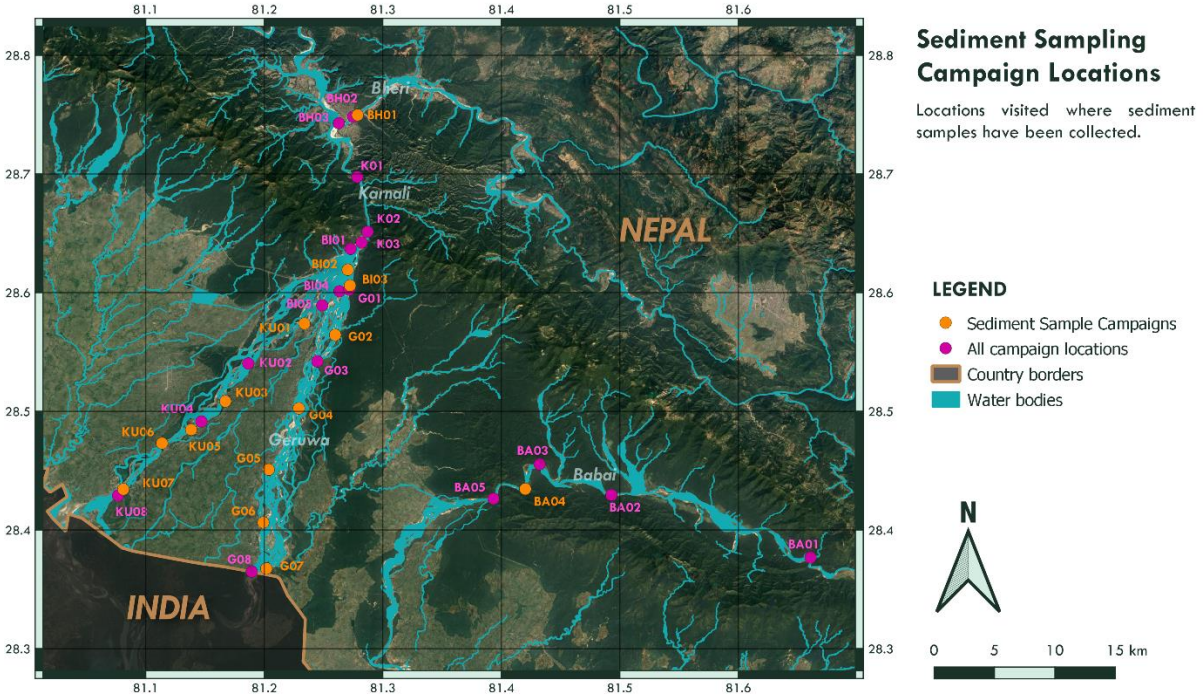

Figure 11: Campaign locations at which sediment samples have been collected

Campaign	Sediment Id	No. of samples	Type of sediment
BA04	1BAB1	1	Fine sediment
BH01	1BHE1	1	Fine sediment
BI02	1B1 t/m 1B6	6	Fine sediment
BI03	2B1 t/m 2B3	3	Fine sediment
G02	1G1 t/m 1G4	4	1 mixed (1G1), 3 fine sediment
G04	2G1 t/m 2G7	7	3 mixed (2G3,2G4,2G6), 4 fine sediment
G05	3G1 t/m 3G3	3	Fine sediment
G06	4G1 & 4G2	2	1 mixed (4G1), 1 fine sediment
G07	5G1 t/m 5G3	3	Fine sediment
KU01	4K1 t/m 4K3	3	1 coarse (4K1), 1 mixed (4K2), 1 fine (4K3) sediment
KU03	3K1 t/m 3K3	3	2 mixed (3K1, 3K3), 1 fine sediment
KU05	2K1 t/m 2K3	3	1 coarse (2K1), 2 fine sediment
KU06	1K1 t/m 1K5	5	Fine sediment
KU07	5K1 t/m 5K4	4	2 mixed (5K1, 5K3), 2 fine sediments

Table 10: Summary of rapid assessment from sieve analysis of sediment samples

Most of the sediment samples taken fall under category of fine sediment with 10 under mixed and 2 are coarse. However, it should be kept in consideration that the samples taken are taken using scoop and mostly from floodplains. The floodplains may contain layer of fine sediment which may have been deposited during the recession of the flood. Nonetheless, these samples show the sediment transport happening during the floods. Another issue to be considered is that the sampling of coarse sediment in the floodplain was not possible due to logistics and limitation of equipment. Hence, several photographs of the floodplain with the scale are taken at various sites. PSD of these coarse sediments may be determined by image analysis and may be used in combination with lab analysis to understand the sediment distributions in the floodplains of respective locations.

7. Conclusion and recommendations

This fieldwork has been very useful in gathering information about the study area as a system. The visual inspection of the area has provided an insight on the morphodynamic, hydrologic, ecological and socio-economic features of the Karnali alluvial fan. These first insights and understanding of the system was one of the main objectives of this field work and we can say that it has been successfully fulfilled.

A second major objective was to explore the area of interest for suitable locations for data collection. We succeeded to cover the entire area of interest for exploration and over 32 locations were visited along the Bheri, Karnali, Geruwa, Kauriala and Babai Rivers. At 28 of these locations data was collected using at least one of the methods as described in Chapter 4. In addition to area exploration, collaboration with various different parties were explored and initiated, which may prove very useful for future work. Hence, it is advised to keep good maintenance of these contacts and collaborations.

Another major objective was to collect the data and information to the maximum extent possible within the given time frame with the available equipment. With the collected data on bathymetry, river channel width, water level, velocities, discharge, sediment samples and geographical features, this objective is fulfilled to an extent. There have been some difficulties with the logistics and challenges regarding data collection due to limitations of the measurement instruments, but a good amount of data has been collected during this first campaign. Analysis of the gathered data will help identifying any data gaps and will help suggest methodologies for future work.

Another important objective of this campaign was to install water level monitoring stations in the two branches of the Karnali river: Gerua and Kauriala. This objective was also successfully achieved as we installed two Divers in each branch at Kothiyaghat and Sattighat to log the water level every 15 minutes in Gerua and Kauriala respectively.

7.1. Preliminary results

The preliminary results show a promising amount of information that we can deduce about the Karnali alluvial fan. To summarize, we have following results:

1. The Karnali fan is very dynamic in nature with larger number of channels in Gerua but higher channelization in Kauriala
2. The amount of water flowing into Gerua from the bifurcation point is significantly low compared to the Kauriala.
3. The floodplains of Gerua have less human interventions compared to Kauriala
4. The sediments are dynamically distributed over the floodplains. Extremely coarse (large boulders and stones) to fine sediment can be observed in the bifurcation area whereas the sediment size gradually decreases as the river flows more south and is mostly left with sand, silt and pebbles in the Sattighat and Kothiaghat area.

7.2. Major challenges

7.2.1. Data quality & accuracy

As this campaign was mostly about reconnaissance and understanding the system, we had with us quite simple equipment and methodology. Nonetheless, we gave our best efforts to gather as much and as accurate data as we could, given the circumstances. Even though the quality of data collected may not be extremely accurate to use it in high precision studies, the data are able to represent the system and useful in screening, assessment and preliminary studies. Moreover, these data are very useful in identifying the data gaps, developing further research and data collection methodologies and prepare a schematization of the system.

One of the major challenges that remains however is to connect the obtained elevation, bathymetry and water level data to the known point of reference. Since the GNSS system we had failed to work during the field campaign, we were unable to obtain the real time reference elevation above mean sea level. This poses challenge specially in relating the collected water level and bathymetry data with the satellite observed data. We will be working on a way out to solve this issue.

Additionally, the current meter we had may not be very reliable in high flows and deep river section. Observers judgement had to be used at multiple occasions when the readings in the current meter were fluctuation continuously. Also, the velocities using floats were a very rough estimate as the river is too wide and deep. These may limit the accuracy of the flow velocity measured.

The processing of the CHIRP+ data is still a challenge for us. With minimum of 1000 data points and up to 10000 data points for water depth in a section, and a very few, about 5 GPS coordinate points across the river width, the reconstruction of the cross sections may not yield very accurate results. Moreover, the drifting of the device along the flow due to high flow velocities have resulted in non-perpendicular cross sections at multiple occasions. However, the data still ca be considered relatively accurate given the mobile bed conditions of the river.

The sediment samples collected were mostly fine sediments. This analysis represents fair analysis for the distribution of fine sediments on the floodplain. However, this analysis does not represent the coarse sediment in the system. There are photographs of the floodplain taken to scale which on further image analysis may be helpful in redefining the sediment distribution in the Karnali floodplains.

7.2.2. Logistics

- Permits
- Tigers
- Accessibility of locations
- Travel distances & time
- Crossing the river & boats
- Jeep at NTNC vs. tuktuks etc.

7.2.3. Measurement methods & instruments

7.3. Recommendations for future work

This field campaign has been a perfect opportunity to learn and understand the necessity, requirements, challenges and benefits of the field work. Based on the experiences we had, we could definitely recommend for the future works.

1. Collect elevation data with high(er) accuracy measurement equipment
2. Establish benchmarks at intervals that can be used as reference for future field visits
3. Use more sophisticated equipment for flow and bathymetry measurement, especially in the Kauriala River where flow velocities and flow depths are high,
4. Collect data from the water level loggers and evaluate potential need for additional gauging stations.
5. Use field sampling and analysis methods for sediment analysis especially for coarse sediments
6. Make a plan when to visit what locations and what transport and logistics are required for which campaigns. This should also include security personnel required for high-risk tiger zones.

APPENDIX

A. Collaboration Partners

Personnel	Designation	Organization	Purpose of collaboration
Dr. Rabin Kadariya	Chief Conservation Officer	National Trust for Nature Conservation, Thakurdwara, Bardiya	Official logistics in and around BNP
Umesh Poudel	Conservation Officer	National Trust for Nature Conservation, Thakurdwara, Bardiya	Official logistics in and around BNP
Mukesh Kumar Thakur		Bardiya Irrigation Project, Gulariya, Bardiya	Ground water irrigation and other irrigation and river training projects
Makunda Sanjel	Assistant Conservation Officer	Bardiya National Park (BNP)	Official logistics in and around BNP
Dilu Chaudhary	Gamescout	Bardiya National Park (BNP)	Raft and guuide in BNP
Jagnarayan Chaudhary	Gamescout	Bardiya National Park (BNP)	Raft and guuide in BNP
Lekhraj Rai	Gamescout	BNP, Okhariya Intake	
Shankar Prasad Bhattarai	Engineer	Rajapur Municipality, Bardiya	Sediment extraction data
Raj Kumar Chudhary	Engineer	Rajapur Municipality, Bardiya	Sediment extraction data
Jora Singh Adhikari	SI	Nepal Police, Kothiyaghat, Bardiya	Security of gauging station at Kothiyaghat
Rajesh Tharu			Auto driver and manpower in Rajapur
Lakhan Lal			Contractor for borehole drill for gauging station
Bandhu Prasad Bastola	Chief District Officer	District Admininstration Office, Gulariya, Bardiya	Information about the project, recommendation for security and boats
Jahar Singh Budha	Suprintendent of Police	Armed Police Force, District Headquarters, Gulariya, Bardiya	Security personnels and technical personnels for raft and motorboat
Sushil Chandra Devkota	Project Director	Karnali River Management Project, Rajapur, Bardiya	Data sharing and installation of gauging station
Nabin Shrestha	Senior Divisional Engineer	Karnali River Management Project, Rajapur, Bardiya	Data sharing and installation of gauging station
Tika Regmi	Engineer	Karnali River Management Project, Rajapur, Bardiya	Data sharing and installation of gauging station
Mohammad Ali Raza	Sub Engineer	Karnali River Management Project, Rajapur, Bardiya	Data sharing and installation of gauging station

B. Field Campaign Location Selection

B.1. Radar Altimeter Satellite Ground Tracks

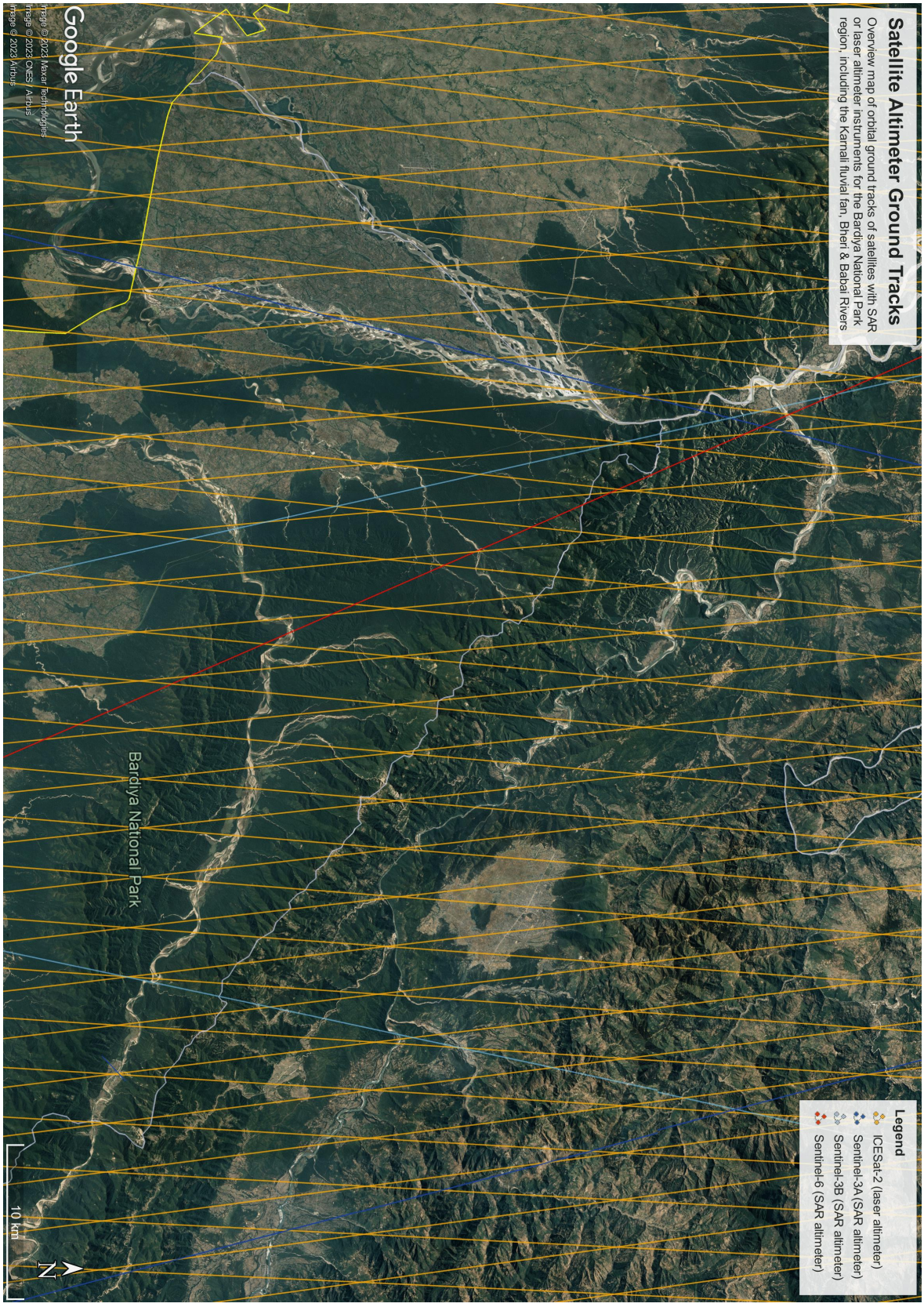

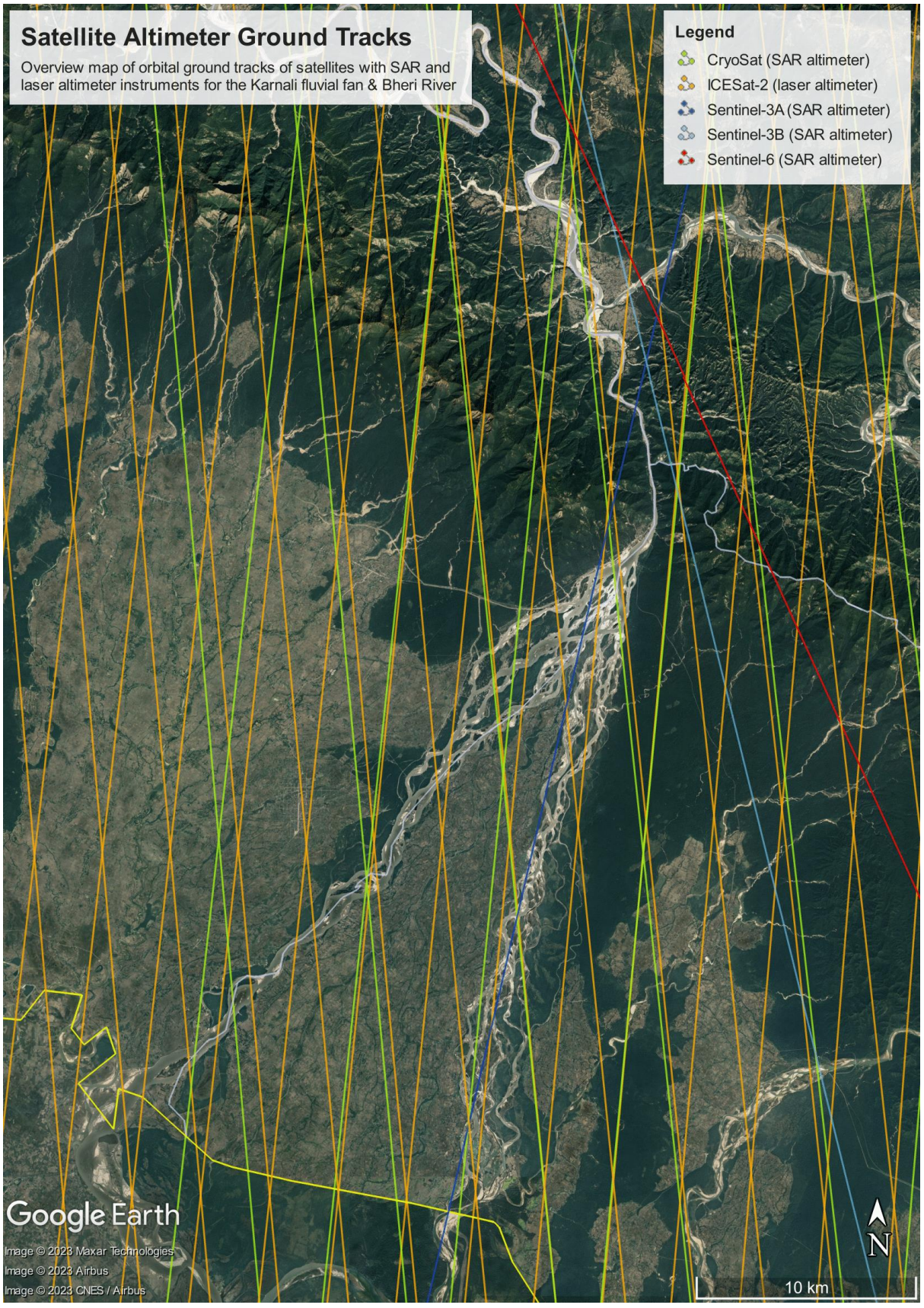
Satellite Altimeter Ground Tracks
Overview map of orbital ground tracks of satellites with SAR and laser altimeter instruments for the Karnali fluvial fan & Bheri River
Legend
CryoSat (SAR altimeter)
ICESat-2 (laser altimeter)
Sentinel-3A (SAR altimeter)
Sentinel-3B (SAR altimeter)
Sentinel-6 (SAR altimeter)
Google Earth
Image © 2023 Maxar Technologies
Image © 2023 Airbus
Image © 2023 CNES / Airbus
N
10 km

Babai Groundtracks Overview
Overview map with satellite groundtracks along Babai
Legend
ICE-SAT2
Sentinel-3A
Sentinel-3B
Sentinel-6
Bardiya National Park
10 km
N
Google Earth
Image © 2022 Maxar Technologies
Image © 2022 CNES / Airbus

B.2. Selected Areas of Interest

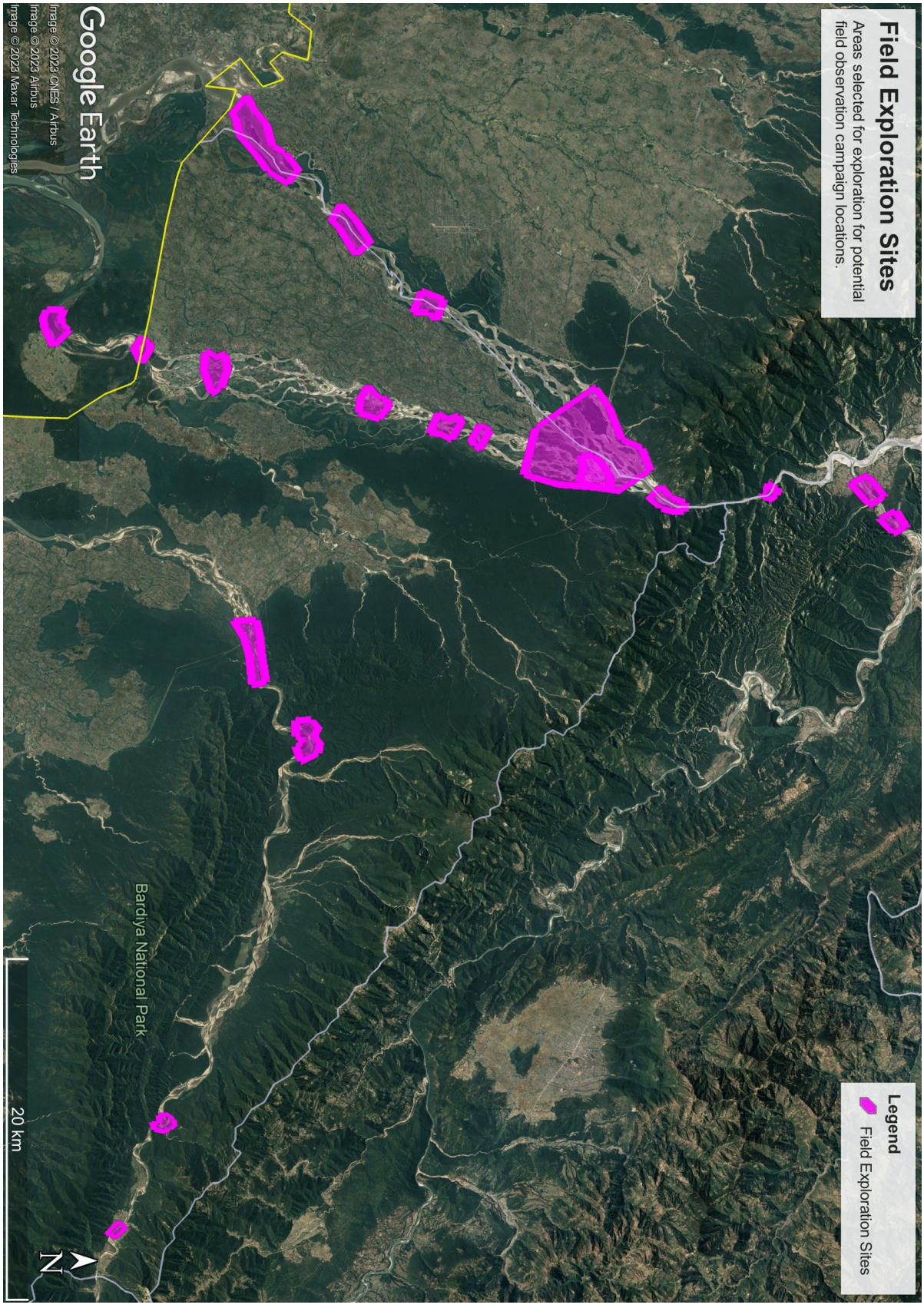

C. Field Observation Campaign Locations

C.1. Table of Field Campaign Locations & Collected Data

ID	CAMPAIGN	LOCATION NAME	SEDIMENT	SEDIMENT ID	TRANSECT	NFP WSL	CHIRP	RIVER WIDTH	RIVER WIDTH [m]	ESTIMATED WSL [m]
1	BA01	BABAI UPSTREAM	NO		NO	NO	YES	NO		269.0
2	BA02	BABAI ICESAT OVERPASS UPSTREAM	NO		NO	NO	YES	YES	74.4	208.0
3	BA03	BABAI S6 OVERPASS	NO		NO	NO	YES	YES	66.0	202.0
4	BA04	BABAI ICESAT OVERPASS DOWNSTREAM	YES	1BAB1	NO	NO	NO	NO		156.0
5	BA05	BABAI DOWNSTREAM	NO		NO	NO	YES	YES	96.4	179.0
6	BH01	BHERI BRIDGE AT GHATGAUN	YES	1BHE1	NO	NO	YES	NO		200.0
7	BH02	BHERI AT GHATGAUN (S3B OVERPASS)	NO		NO	NO	NO	YES	162.0	210.0
8	BH03	BHERI KARNALI CONFLUENCE	NO		NO	NO	NO	NO		
9	BI01	BIFURCATION S3A OVERPASS	NO		NO	NO	NO	NO		
10	BI02	BIFURCATION MAIN CHANNEL	YES	1B1 - 1B6	NO	NO	YES	NO		173.0
11	BI03	LALMATI, JAPANESE CAMP	YES	2B1 - 2B3	YES	YES	YES	YES	164.4	180.5
12	BI04	MAIN INLET GERUWA	NO		NO	NO	NO	NO		182.9
13	BI05	RAJAPUR IRRIGATION INLET	NO		NO	NO	NO	NO		
14	G01	GERUWA LEFT INLETS	NO		YES	YES	YES	YES	183.8	
15	G02	GERUWA AT BAGH TAPU	YES	1G1 - 1G4	YES	NO	YES	YES	61.0	178.0
16	G03	GERUWA AT GAIDA MACHAN	NO		NO	YES	YES	YES	27.8	149.0
17	G04	GERUWA AT GOLA	YES	2G1 - 2G7	YES	YES	YES	YES	44.0	161.0
18	G05	GERUWA MANPUR	YES	3G1 - 3G3	NO	NO	NO	NO		136.0
19	G06	GERUWA AT LALPUR	YES	4G1 & 4G2	YES	YES	YES	YES	64.0	126.7
20	G07	GERUWA BRIDGE: KHOTIYAGHAT	YES	5G1 - 5G3	NO	YES	YES	NO		107.4
21	G08	GERUWA AT INDIAN BORDER	NO		NO	YES	YES	YES	68.0	120.3
22	K01	KARNALI AT S3A OVERPASS	NO		NO	NO	NO	YES	74.6	178.0
23	K02	KARNALI UPSTREAM OF CHISAPANI	NO		NO	YES	NO	YES	160.0	179.1
24	K03	KARNALI BRIDGE, CHISAPANI	NO		NO	YES	NO	YES	283.0	187.9
25	KU01	KAURIALA AT PATABHAR	YES	4K1 - 4K3	NO	NO	NO	NO		147.7
26	KU02	KAURIALA AT BANGHUSRA	NO		NO	YES	NO	YES	182.6	161.3
27	KU03	KAURIALA AT SHANTIBAZAR	YES	3K1 - 3K3	NO	NO	NO	NO		130.0
28	KU04	KAURIALA AT MARGHUA (UPSTREAM)	NO		NO	YES	NO	YES	342.0	132.1
29	KU05	KAURIALA AT MARGHUA (DOWNSTREAM)	YES	2K1 - 2K3	NO	NO	NO	NO		
30	KU06	KAURIALA DAULATPUR (STEAMER)	YES	1K1 - 1K5	NO	YES	YES	YES	310.0	130.1
31	KU07	NORTH OF KAURIALA BRIDGE	YES	5K1 - 5K4	NO	YES	NO	YES	124.5	106.5
32	KU08	KAURIALA BRIDGE: SATTIGHAT	NO		NO	YES	NO	NO		114.9

C.2. Map Of All Field Campaign Locations

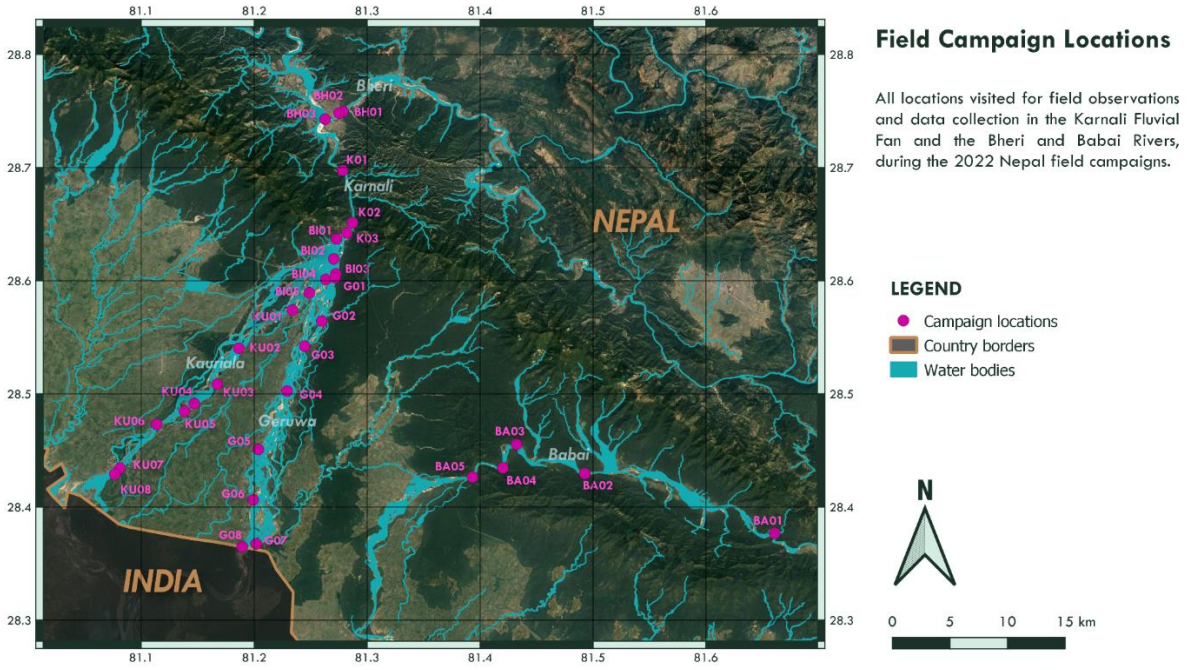

D. Water Level Data

D.1. Relative Water Level Schematic Representation River Cross-Sections

D.1.i. BI03 – Lalmati, Japanese Camp

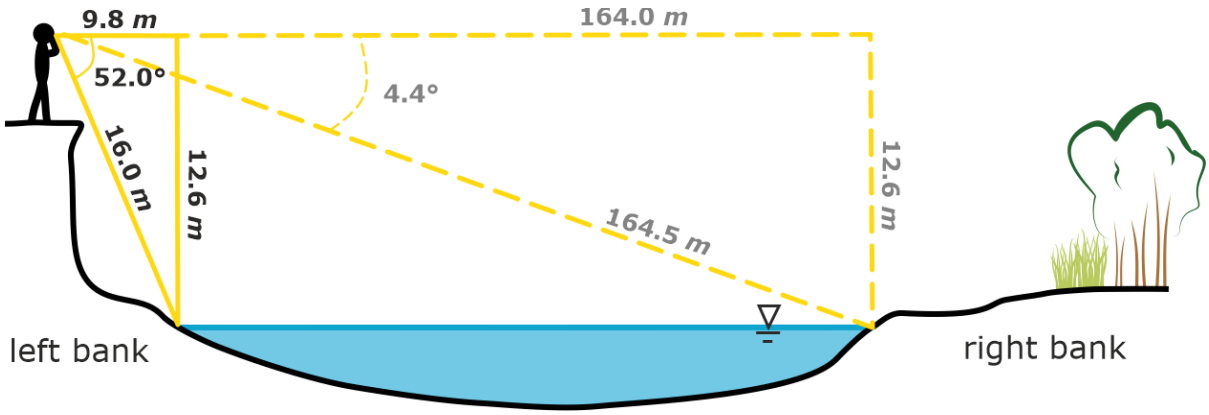

Sketch 1: Relative Water level, Bifurcation Main Channel, at Lalmati, Upstream Measurements

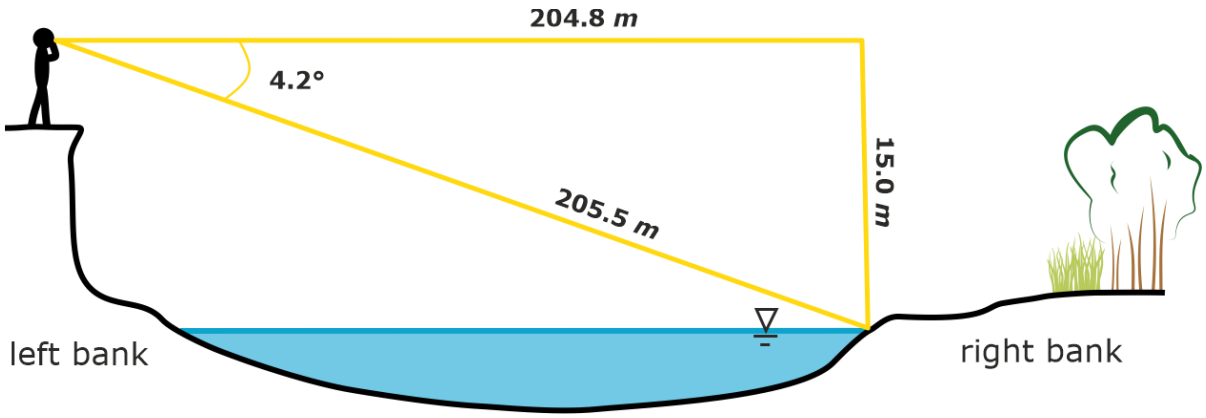

Sketch 2: Relative Water Level Bifurcation Main Channel, at Lalmati, Downstream Measurement

D.1.ii. G01 – Geruwa Left Inlets

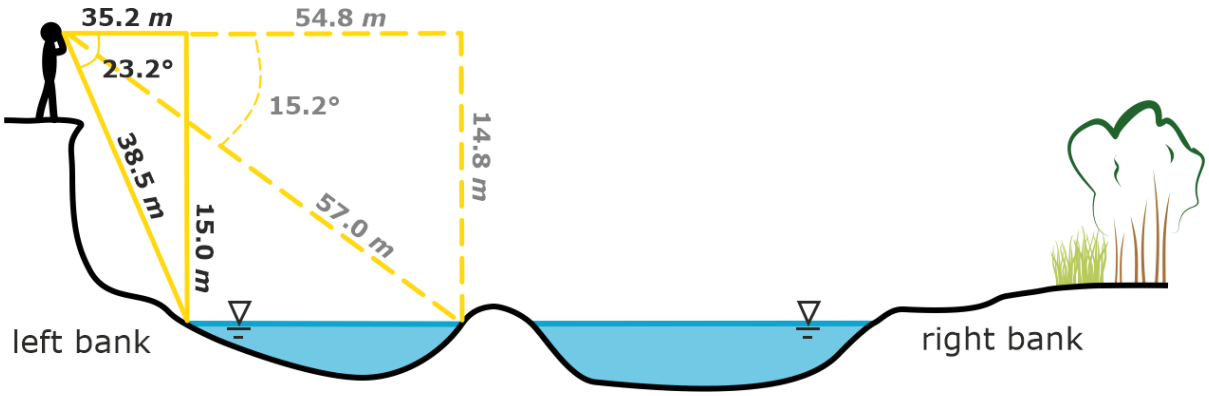

Sketch 3: Relative Water levels at Lalmati / Geruwa Inlets; Left Inlet Measurements

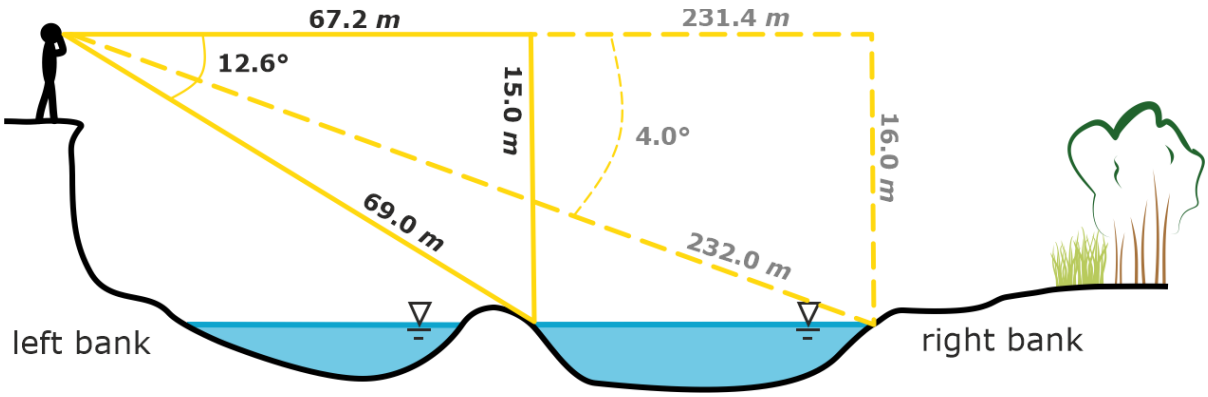

Sketch 4: Relative Water Level at Lalmati / Geruwa Inlets; Right Inlet Measurements

D.1.iii. G03 – Geruwa at Gaida Machan

Sketch 5: Relative Water Level, Side Channel Geruwa River at Gaida Machan

D.1.iv. G06 – Geruwa at Lalpur

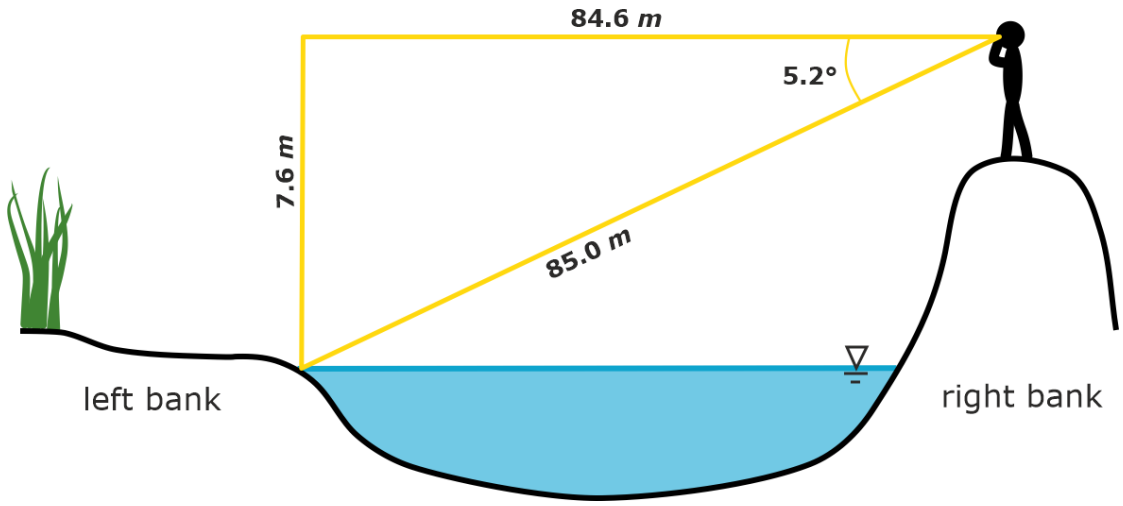

Sketch 6: Relative Water Level Geruwa River at Lalpur

D.1.v. G07 – Geruwa Bridge: Khotiyaghat

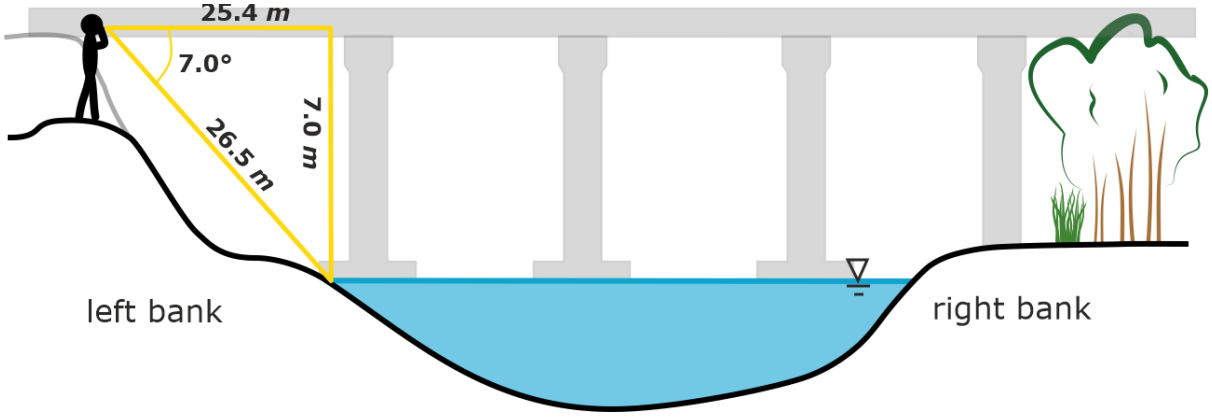

Sketch 7: Relative Water Level Geruwa River at Geruwa Bridge

D.1.vi. G08 – Geruwa at Indian Border

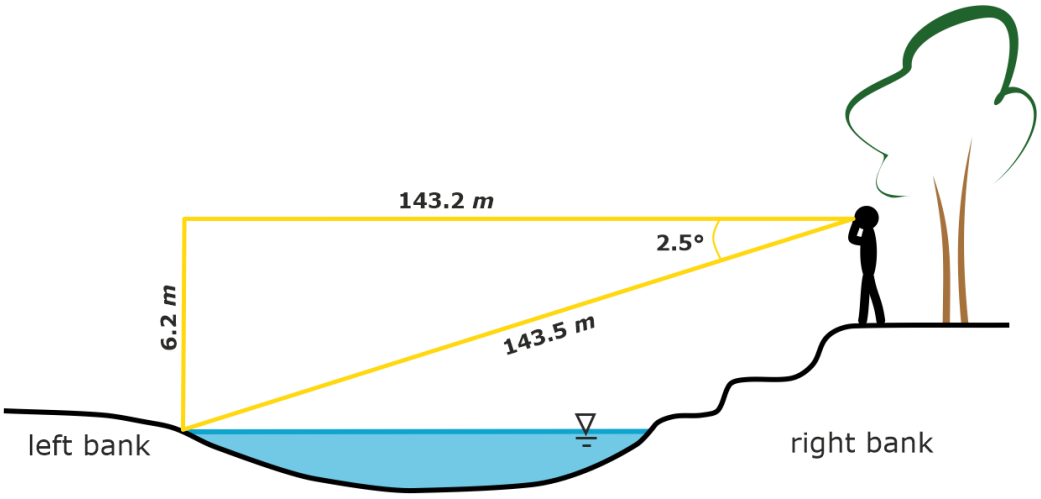

Sketch 8: Relative Water Level Geruwa River at Indian Border

D.1.vii. K02 – Karnali, Upstream Chisapani

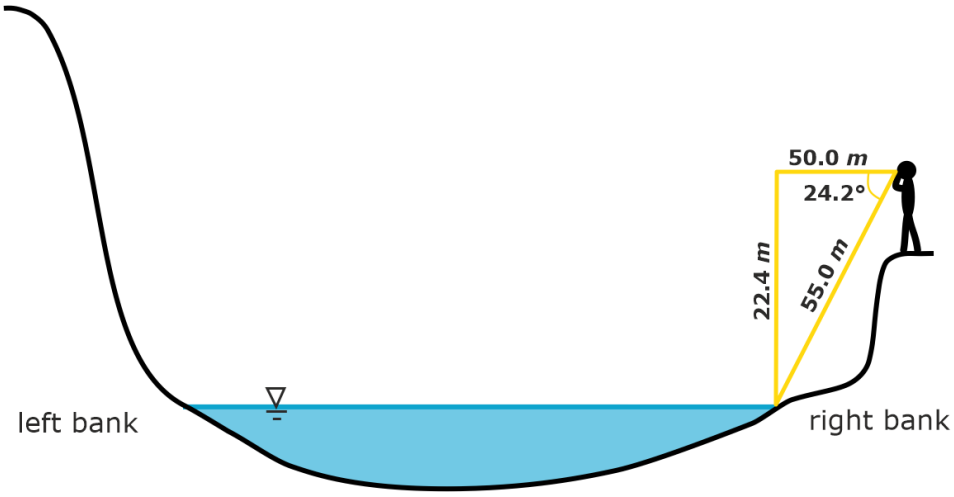

Sketch 9: Relative Water Level Karnali River, Upstream of Chisapani

D.1.viii. K03 – Karnali Bridge, Chisapani

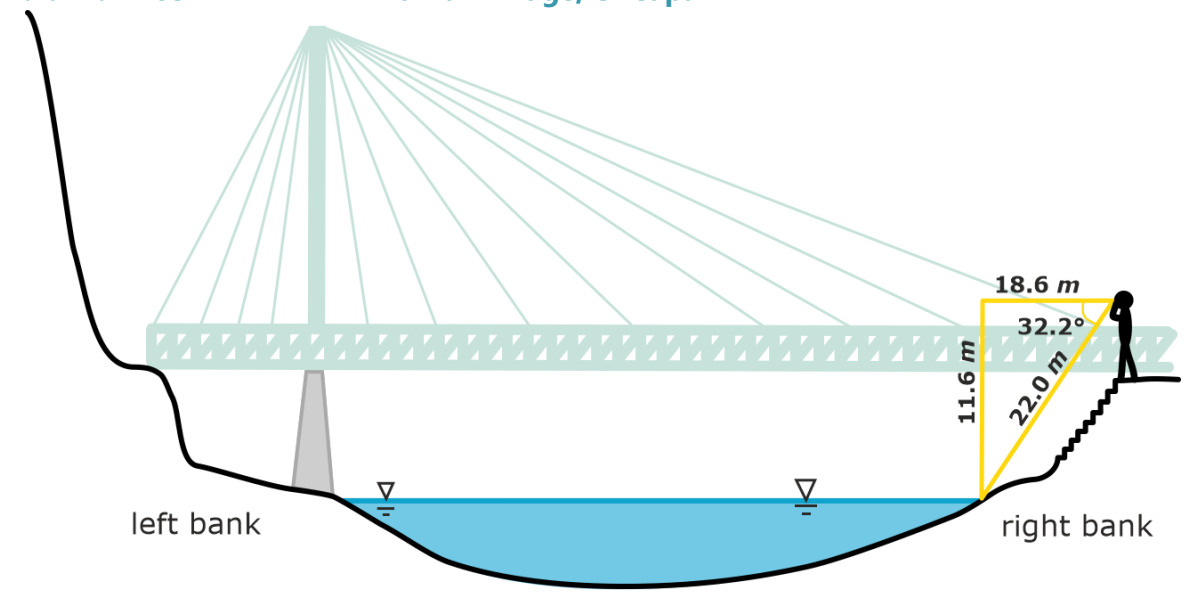

Sketch 10: Relative Water Level Karnali River at Karnali Bridge, Chisapani

D.1.ix. KU02 – Kauriala at Banghusra

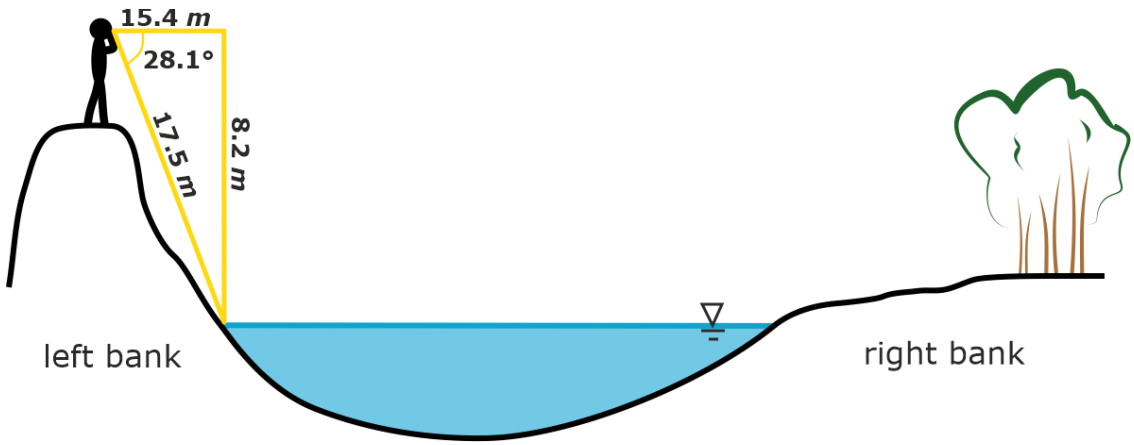

Sketch 11: Relative Water Level Kauriala River at Banghusra

D.1.x. KU04 – Kauriala at Marghua (upstream)

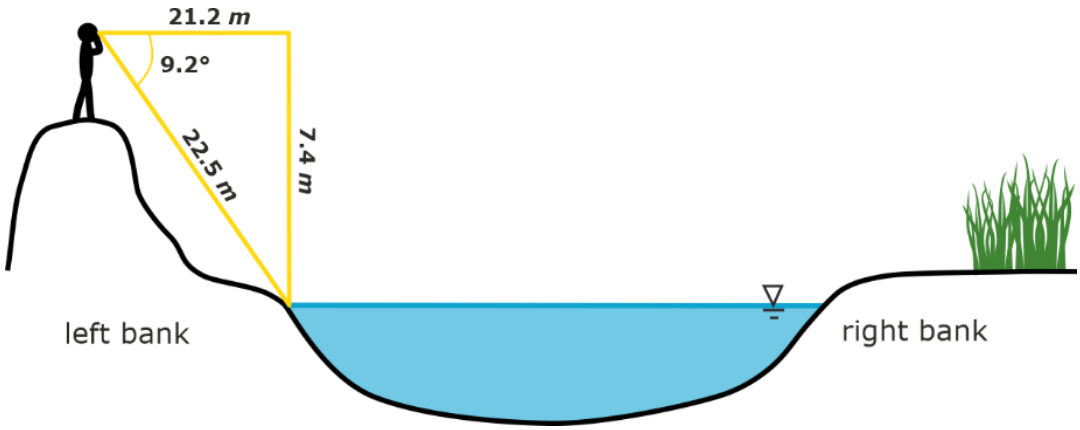

Sketch 12: Relative Water Level Kauriala River, at Marghua (upstream)

D.1.xi. KU06 – Kauriala at Daulatpur (steamer point)

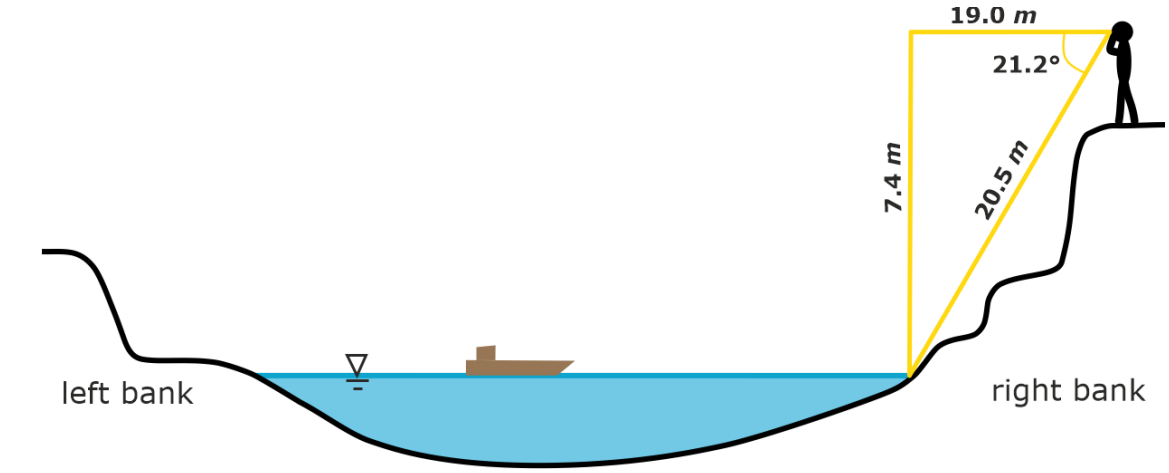

Sketch 13: Relative Water Level Kauriala River at Daulatpur

D.1.xii. KU07 – North of Kauriala Bridge

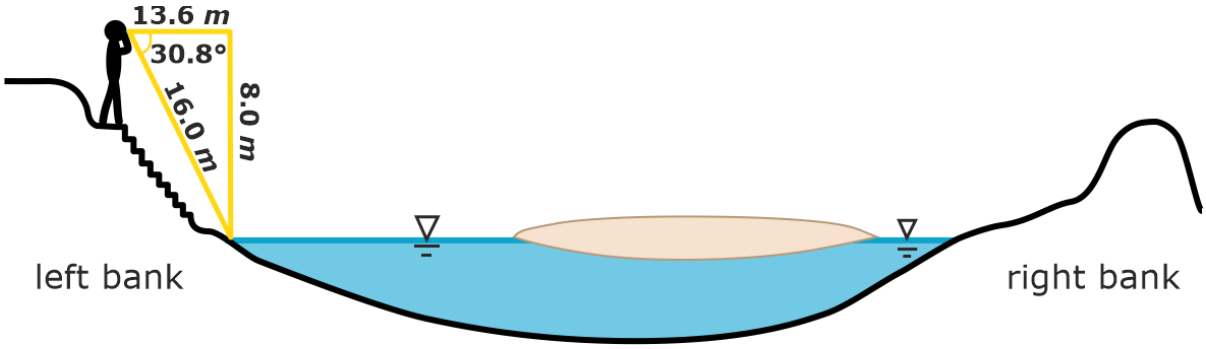

Sketch 14: Relative Water Level Kauriala River, North of Kauriala Bridge, From Top of Stairs (1/2)

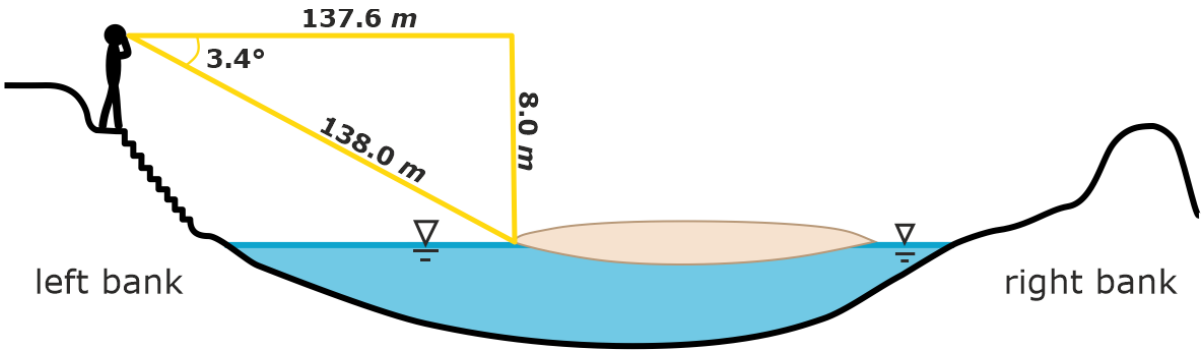

Sketch 15: Relative Water Level Kauriala River, North of Kauriala Bridge, From Top of Stairs (2/2)

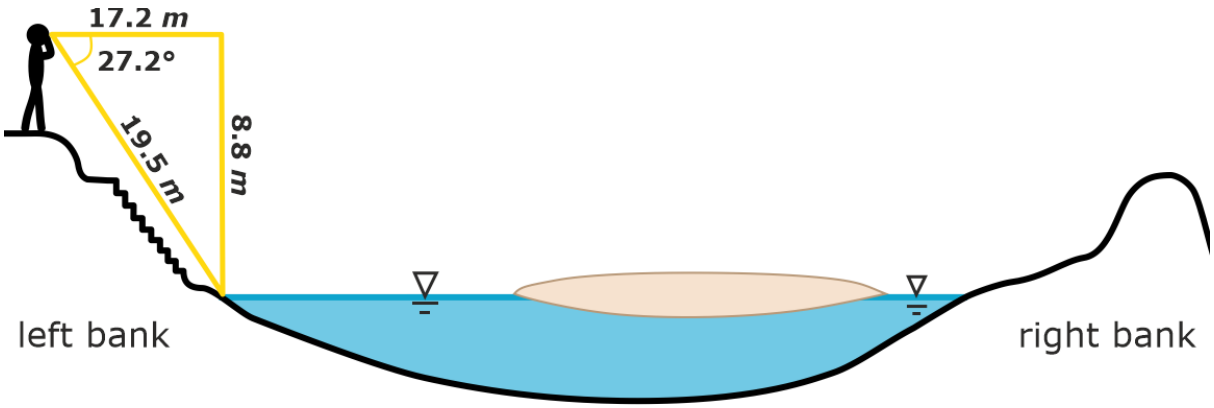

Sketch 16: Relative Water Level Kauriala River, North of Kauriala Bridge, From Top of Dike

D.1.xiii. KU08 – Kauriala Bridge: Sattighat

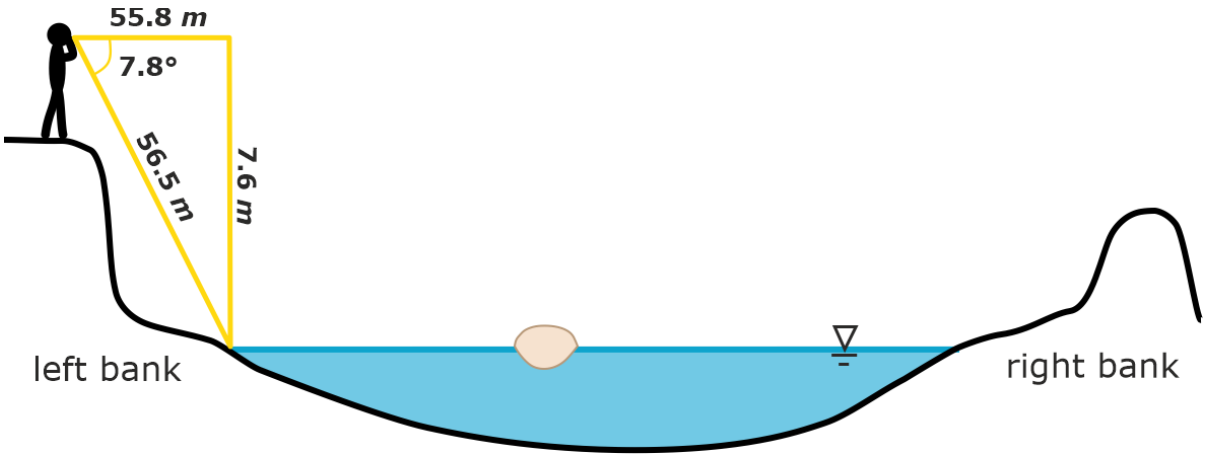

Sketch 17: Relative Water Level Kauriala River at Kauriala Bridge, at Benchmark BM1

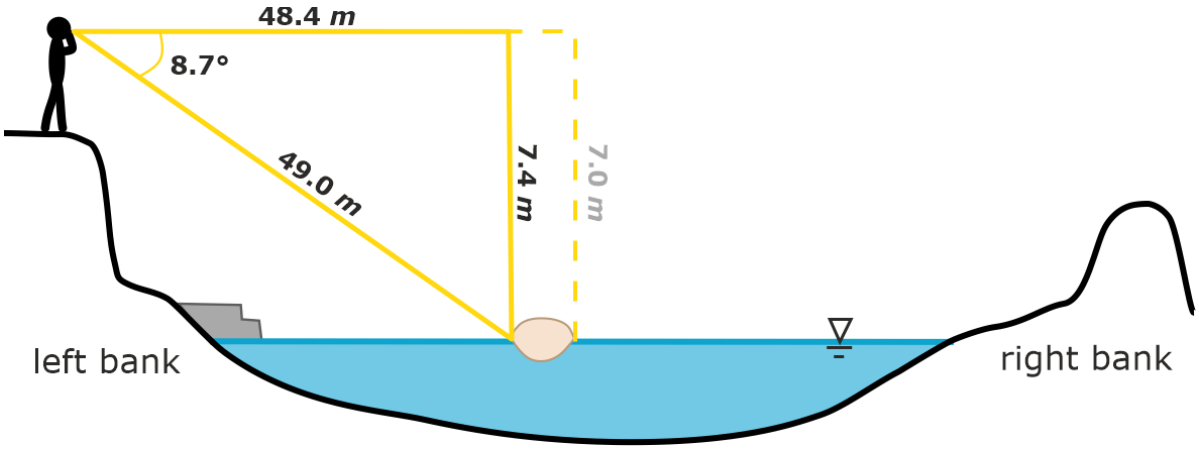

Sketch 18: Relative Water Level Kauriala River at Kauriala Bridge, at Benchmark BM2

D.2. Relative Water Level Observation Data Overview

Note that heights have been measured from eye height (1.53 m above the ground). The measured heights are listed in the column 'measured height', the corrected heights are listed in the column 'relative height'.

Campaign SN	nr.	from bank	to bank	measured height [m]	relative height [m]	diagonal [m]	distance [m]	river width [m]	angle [deg.]	notes
BI03	1	left	left	12.6	11.1	16.0	9.8	154.2	52.0	upstream
BI03	2	left	right	12.6	11.1	164.5	164.0	154.2	4.4	upstream
BI03	3	left	right	15.0	13.5	205.5	204.8	164.4	4.2	downstream
G01	1	left	left	15.0	13.5	38.5	35.2	19.6	23.2	left channel
G01	2	left	right	14.8	13.3	57.0	54.8	19.6	15.2	left channel
G01	3	left	left	15.0	13.5	69.0	67.2	164.2	12.6	right channel
G01	4	left	right	16.0	14.5	232.0	231.4	164.2	4.0	right channel
G03	1	left	right	2.8	1.3	28.0	27.8	27.8	5.8	river width measurement, accuracy ~10cm
G06	1	right	left	7.6	6.1	85.0	84.6	64.0	5.2	
G07	1	left	left	7.0	5.5	26.5	25.4		7.0	riverwidth not measured
G08	1	right	left	6.2	4.7	143.5	143.2	68.0	2.5	
K02	1	right	right	22.4	20.9	55.0	50.0	160.0	24.2	
K03	1	right	right	11.6	10.1	22.0	18.6	283.0	32.2	
KU02	1	left	left	8.2	6.7	17.5	15.4	182.6	28.1	
KU04	1	left	left	7.4	5.9	22.5	21.2	342.0	9.2	
KU06	1	right	right	7.4	5.9	20.5	19.0	310.0	21.2	
KU07	1	left	left	8.0	6.5	16.0	13.6	124.5	30.8	river width is width of left channel
KU07	2	left	right	8.0	6.5	138.0	137.6	124.0	3.4	*accuracy river width ~0,5m*
KU07	3	left	left	8.8	7.3	19.5	17.2	124.0	27.2	
KU08	1	left	left	7.6	6.1	56.5	55.8		7.8	BM1; river width not measureable
KU08	2	left	right	7.4	5.9	49.0	48.4		8.7	BM2; river width not measureable

E. Flow Velocity Data

E.1. Flow Velocities with Current Meter and Floaty at Daulatpur (KU06)

River bank / location	Measurement tool	Distance travelled by floaty [m]	Time to arrive [s]	Flow velocity	
7m from right bank	Floaty (wood)	36	24.98	1.44	*m/s*
15 m from right bank	Floaty (PET bottle)	36	20.09	1.79	*m/s*
23 m from right bank	Floaty (PET bottle)	36	17.3	2.08	*m/s*
1 m from right bank	Current meter	-	-	0,48	*m/s*
20 cm from right bank	Current meter	-	-	0,2	*m/s*
2 m from left bank	Current meter	-	-	0,95	*m/s*
3 m from left bank	Floaty	57.5	55	1.05	*m/s*
13 m from left bank	Floaty	57.5	40.99	1.40	*m/s*
20 m from left bank	Floaty	57.5	46.16	1.25	*m/s*
AVERAGE LEFT				1.23	*m/s*
AVERAGE RIGHT				1.77	*m/s*
AVERAGE TOTAL				1.50	*m/s*

F. Transects

F.1. BI03 – Lalmati, Japanese Camp

BI03 Lalmati 10/11/2022 13:15

width [cm]	150	2500	4000	(estimated) 6755	9550	11550	13550	15050	15500		
depth [cm]	depth unkonwn	450	600	450	depth unknown	190	65	40	10		
left bank										right bank	
10	0.4	0.85	1.2	1.2	1.1	0.5	0.16	0.08	0.1		
20	0.4	0.85	1.2	1.2	1.1	0.5	0.16	0.08			
30	0.4	0.85	1.2	1.2	1.1	0.5	0.16	0.08			
40		0.85	1.2	1.2	1.1	0.5	0.16	0.08			
50		0.85	1.2	1.2	1.1	0.5	0.16				
60		0.85	1.2	1.2	1.1	0.5	0.16				
70		0.85	1.2	1.2	1.1	0.5	0.16				
80		0.85	1.2	1.2	1.1	0.5					
90		0.85	1.2	1.2	1.1	0.5					
100		0.85	1.2	1.2	1.1	0.5					
110		0.85	1.2	1.2	1.1	0.5					
120		0.85	1.2	1.2	1.1	0.5					
130		0.85	1.2	1.2	1.1	0.5					
140		0.85	1.2	1.2	1.1	0.5					
150		0.85	1.2	1.2	1.1	0.5					
160		0.85	1.2	1.2	1.1	0.5					
170		0.85	1.2	1.2	1.1	0.5					
180		0.85	1.2	1.2	1.1	0.5					
190		0.85	1.2	1.2	1.1	0.5					
200		0.85	1.2	1.2	1.1						
210		0.85	1.2	1.2	1.1						
220		0.85	1.2	1.2	1.1						
230		0.85	1.2	1.2	1.1						
240		0.85	1.2	1.2	1.1						
250		0.85	1.2	1.2	1.1						
260		0.85	1.2	1.2	1.1						
270		0.85	1.2	1.2	1.1						
280		0.85	1.2	1.2	1.1						
290		0.85	1.2	1.2	1.1						
300		0.85	1.2	1.2	1.1						
310		0.85	1.2	1.2	1.1						
320		0.85	1.2	1.2	1.1						
330		0.85	1.2	1.2	1.1						
340		0.85	1.2	1.2	1.1						
350		0.85	1.2	1.2	1.1						
360		0.85	1.2	1.2	1.1						
370		0.85	1.2	1.2	1.1						
380		0.85	1.2	1.2	1.1						
390		0.85	1.2	1.2	1.1						
400		0.85	1.2	1.2	1.1						
410		0.85	1.2	1.2	1.1						
420		0.85	1.2	1.2	1.1						
430		0.85	1.2	1.2	1.1						
440		0.85	1.2	1.2	1.1						
450		0.85	1.2	1.2	1.1						
460			1.2		1.1						
470			1.2		1.1						
480			1.2		1.1						
490			1.2		1.1						
500			1.2		1.1						
510			1.2		1.1						
520			1.2		1.1						
530			1.2		1.1						
540			1.2		1.1						
550			1.2		1.1						
560			1.2		1.1						
570			1.2		1.1						
580			1.2		1.1						
590			1.2		1.1						
600			1.2		1.1						
610											
620											
											Total Q [m3/s]
Q= [m3/s]	0.18	89.8875	108	148.77	184.47	19	2.08	0.48	0.045		552.91

water temperature	18.6	°C
conducttivity	225	µS
HFL	4 (above current water level)	m
slope	131m away, 0.6m down	
Instruments used	Nikon Forestry Pro, current meter, CHIRP, Hawkeye	

F.2. BI03 – Geruwa Inlet Channels

G01L **Geruwa left inlet** **10/11/2022** **15:30**

width [cm]	200	1700	2700	3700	4700	4900		
depth [cm]	90	150	120	65	45			
left bank							right bank	
5	0.3	0.6	0.55	0.5	0.3			
10	0.3	0.6	0.55	0.5	0.3			
15	0.3	0.6	0.55	0.5	0.3			
20	0.3	0.6	0.55	0.5	0.3			
25	0.3	0.6	0.55	0.5	0.3			
30	0.3	0.6	0.55	0.5	0.3			
35	0.3	0.6	0.55	0.5	0.3			
40	0.3	0.6	0.55	0.5	0.3			
45	0.3	0.6	0.55	0.5	0.3			
50	0.3	0.6	0.55	0.5				
55	0.3	0.6	0.55	0.5				
60	0.3	0.6	0.55	0.5				
65	0.3	0.6	0.55	0.5				
70	0.3	0.6	0.55					
75	0.3	0.6	0.55					
80	0.3	0.6	0.55					
85	0.3	0.6	0.55					
90	0.3	0.6	0.55					
95		0.6	0.55					
100		0.6	0.55					
105		0.6	0.55					
110		0.6	0.55					
115		0.6	0.55					
120		0.6	0.55					
125		0.6						
130		0.6						
135		0.6						
140		0.6						
145		0.6						
150		0.6						
155								
160								
								Total Q [m3/s]
Q= [m3/s]	0.54	13.5	6.6	3.25	1.35			25.24

Location description	same sediments as #2B3, weather: sunny & hazy
Instruments used	Current meter, CHIRP, Nikon Forestry Pro, Hawkeye

G01R **Geruwa right inlet** **10/11/2022** **16:00**

width [cm]	250	450	650	*775*	*900*	*assumed*
depth [cm]	40	65	65	*40*		*assumed*
left bank					right bank	
5	0.25	0.5	0.46	0.25		
10	0.25	0.5	0.46	0.25		
15	0.25	0.5	0.46	0.25		
20	0.25	0.5	0.46	0.25		
25	0.25	0.5	0.46	0.25		
30	0.25	0.5	0.46	0.25		
35	0.25	0.5	0.46	0.25		
40	0.25	0.5	0.46	0.25		
45		0.5	0.46			
50		0.5	0.46			
55		0.5	0.46			
60		0.5	0.46			
65		0.5	0.46			
70						
75						
80						
85						
						Total Q [m3/s]
Q= [m3/s]	0.25	0.65	0.598	0.25		**1.748**

Location description	nearly rectangular cross section; river bed full of stones + boulders
Instruments used	Current meter, CHORP, Garmin GPS, EC-meter

F.3. BI03 – Geruwa at Bagh Tapu

G02 Bagh Tapu 11/11/2022 12:15 - 13:10

width [cm]	100	300	500	700	900	1100	1300	1500	1700	2000	2200	2400	2600	2900	3200	3500	3800	4100	4400	4700	5000	5300	5500	5700	5900	6100		
depth [cm]	65	80	85	90	80	65	70	65	65	80	80	70	80	80	85	95	95	100	100	70	65	50	too shallow	too shallow	too shallow	too shallow		
left bank																											right bank	
5	0	0.14	0.18	0.2	0.41	0.4	0.35	0.45	0.3	0.4	0.4	0.7	0.55	0.6	0.6	0.7	0.6	0.7	0.7	0.6	0.5	0.3	0	0	0	0		
10	0	0.14	0.18	0.2	0.41	0.4	0.35	0.45	0.3	0.4	0.4	0.7	0.55	0.6	0.6	0.7	0.6	0.7	0.7	0.6	0.5	0.3						
15	0	0.14	0.18	0.2	0.41	0.4	0.35	0.45	0.3	0.4	0.4	0.7	0.55	0.6	0.6	0.7	0.6	0.7	0.7	0.6	0.5	0.3						
20	0	0.14	0.18	0.2	0.41	0.4	0.35	0.45	0.3	0.4	0.4	0.7	0.55	0.6	0.6	0.7	0.6	0.7	0.7	0.6	0.5	0.3						
25	0	0.14	0.18	0.2	0.41	0.4	0.35	0.45	0.3	0.4	0.4	0.7	0.55	0.6	0.6	0.7	0.6	0.7	0.7	0.6	0.5	0.3						
30	0	0.14	0.18	0.2	0.41	0.4	0.35	0.45	0.3	0.4	0.4	0.7	0.55	0.6	0.6	0.7	0.6	0.7	0.7	0.6	0.5	0.3						
35	0	0.14	0.18	0.2	0.41	0.4	0.35	0.45	0.3	0.4	0.4	0.7	0.55	0.6	0.6	0.7	0.6	0.7	0.7	0.6	0.5	0.3						
40	0	0.14	0.18	0.2	0.41	0.4	0.35	0.45	0.3	0.4	0.4	0.7	0.55	0.6	0.6	0.7	0.6	0.7	0.7	0.6	0.5	0.3						
45	0	0.14	0.18	0.2	0.41	0.4	0.35	0.45	0.3	0.4	0.4	0.7	0.55	0.6	0.6	0.7	0.6	0.7	0.7	0.6	0.5	0.3						
50	0	0.14	0.18	0.2	0.41	0.4	0.35	0.45	0.3	0.4	0.4	0.7	0.55	0.6	0.6	0.7	0.6	0.7	0.7	0.6	0.5	0.3						
55	0	0.14	0.18	0.2	0.41	0.4	0.35	0.45	0.3	0.4	0.4	0.7	0.55	0.6	0.6	0.7	0.6	0.7	0.7	0.6	0.5	0.3						
60	0	0.14	0.18	0.2	0.41	0.4	0.35	0.45	0.3	0.4	0.4	0.7	0.55	0.6	0.6	0.7	0.6	0.7	0.7	0.6	0.5							
65	0	0.14	0.18	0.2	0.41	0.4	0.35	0.45	0.3	0.4	0.4	0.7	0.55	0.6	0.6	0.7	0.6	0.7	0.7	0.6	0.5							
70		0.14	0.18	0.2	0.41		0.35			0.4	0.4	0.7	0.55	0.6	0.6	0.7	0.6	0.7	0.7	0.6								
75		0.14	0.18	0.2	0.41					0.4	0.4		0.55	0.6	0.6	0.7	0.6	0.7	0.7									
80		0.14	0.18	0.2	0.41					0.4	0.4		0.55	0.6	0.6	0.7	0.6	0.7	0.7									
85			0.18	0.2											0.6	0.7	0.6	0.7	0.7									
90				0.2												0.7	0.6	0.7	0.7									
95																0.7	0.6	0.7	0.7									
100																		0.7	0.7									
105																												
110																												
																											Total Q [m3/s]	
Q = [m3/s]	0	0.224	0.306	0.36	0.656	0.52	0.49	0.585	0.39	0.96	0.64	0.98	0.88	1.44	1.53	1.995	1.71	2.1	2.1	1.26	0.975	0.45	0	0	0	0		20.551

LEFT BANK	latitude	28°33'51.864"	°N
	longitude	81°15'35.703"	°E
	altitude	149	m
RIGHT BANK	latitude	28°33'51.106"	°N
	longitude	81°15'33.473"	°E
	altitude	158	m

water temperature	19.4	°C
conductivity	239	µS

	Instruments used	Current meter, Nikon Forestry Pro, CHIRP, phone GPS, EC-meter, Measuring tape

F.4. BI03 – Geruwa at Gola

G04 Gola 14/11/2022 12:45

width [cm]	300	500	700	900	1050	1300	1550	1850	2100	2400	2700	2950	3200	3500	3700	3900	4100	4400		
depth [cm]	too shallow	too shallow	too shallow	25	30	40	45	58	60	70	70	70	65	65	60	25	10	too shallow		
left bank																			right bank	
5	0	0	0	0.15	0.2	0.15	0.25	0.25	0.33	0.35	0.4	0.45	0.4	0.35	0.25	0.2	0.1	0		
10				0.15	0.2	0.15	0.25	0.25	0.33	0.35	0.4	0.45	0.4	0.35	0.25	0.2	0.1			
15				0.15	0.2	0.15	0.25	0.25	0.33	0.35	0.4	0.45	0.4	0.35	0.25	0.2				
20				0.15	0.2	0.15	0.25	0.25	0.33	0.35	0.4	0.45	0.4	0.35	0.25	0.2				
25				0.15	0.2	0.15	0.25	0.25	0.33	0.35	0.4	0.45	0.4	0.35	0.25	0.2				
30					0.2	0.15	0.25	0.25	0.33	0.35	0.4	0.45	0.4	0.35	0.25					
35						0.15	0.25	0.25	0.33	0.35	0.4	0.45	0.4	0.35	0.25					
40						0.15	0.25	0.25	0.33	0.35	0.4	0.45	0.4	0.35	0.25					
45							0.25	0.25	0.33	0.35	0.4	0.45	0.4	0.35	0.25					
50								0.25	0.33	0.35	0.4	0.45	0.4	0.35	0.25					
55								0.25	0.33	0.35	0.4	0.45	0.4	0.35	0.25					
60								0.25	0.33	0.35	0.4	0.45	0.4	0.35	0.25					
65										0.35	0.4	0.45	0.4	0.35						
70										0.35	0.4	0.45								
75																				
80																				
85																				
																				Total Q [m3/s]
Q = [m3/s]	0	0	0	0.075	0.09	0.15	0.2813	0.435	0.495	0.735	0.84	0.7875	0.65	0.6825	0.3	0.1	0.02	0		**5.641**

	location description	gravel bed	
RIGHT BANK	**latitude**	28.5023	*°N*
	longitude	81.23005	*°E*

	altitude	138	*m*
	HFL	6.2m (above water level)	*M*
	Instruments used	Nikon Forestry Pro, Chirp, current meter, Phone GPS, Garmin GPS	

F.5. G05 – Geruwa at Lalpur

G06 Lalpur 15/11/2022

width [cm]	300	500	700	900	1100	1300	1500	1700	1900	2100	2300	2500	2700	2900	3100	3300	3500	3700	3900	4100	4300	4500	4700	4900	5100	5300	5500	5700	5900	6100	6300		
depth [cm]	20	30	30	40	50	50	50	50	50	45	40	45	40	40	40	40	30	30	25	10	too shallow	too shallow	too shallow	too shallow	too shallow	too shallow	too shallow	too shallow	too shallow	too shallow	too shallow		
left bank																																right bank	
5	0.2	0.4	0.5	0.55	0.6	0.55	0.5	0.55	0.55	0.6	0.65	0.55	0.65	0.65	0.65	0.65	0.5	0.35	0.25	0.07	0	0	0	0	0	0	0	0	0	0	0		
10	0.2	0.4	0.5	0.55	0.6	0.55	0.5	0.55	0.55	0.6	0.65	0.55	0.65	0.65	0.65	0.65	0.5	0.35	0.25	0.07													
15	0.2	0.4	0.5	0.55	0.6	0.55	0.5	0.55	0.55	0.6	0.65	0.55	0.65	0.65	0.65	0.65	0.5	0.35	0.25														
20	0.2	0.4	0.5	0.55	0.6	0.55	0.5	0.55	0.55	0.6	0.65	0.55	0.65	0.65	0.65	0.65	0.5	0.35	0.25														
25		0.4	0.5	0.55	0.6	0.55	0.5	0.55	0.55	0.6	0.65	0.55	0.65	0.65	0.65	0.65	0.5	0.35	0.25														
30		0.4	0.5	0.55	0.6	0.55	0.5	0.55	0.55	0.6	0.65	0.55	0.65	0.65	0.65	0.65	0.22	0.22															
35				0.55	0.6	0.55	0.5	0.55	0.55	0.6	0.65	0.55	0.65	0.65	0.65	0.65																	
40				0.55	0.6	0.55	0.5	0.55	0.55	0.6	0.65	0.55	0.65	0.65	0.65	0.65																	
45					0.6	0.55	0.5	0.55	0.55	0.6		0.55																					
50					0.6	0.55	0.5	0.55	0.55																								
55																																	
60																																	
65																																	
70																																	
75																																	
80																																	
85																																	
																																Total Q [m3/s]	
Q = [m3/s]	0.12	0.24	0.3	0.44	0.6	0.55	0.5	0.55	0.55	0.54	0.52	0.495	0.52	0.52	0.52	0.52	0.3	0.21	0.125	0.014	0	0	0	0	0	0	0	0	0	0	0		**8.134**

	water temperature	22.5	*°C*
	conducttivity	313	*µS*
	location description	gravel bed	
LEFT BANK	**latitude**	28.40673	*°N*
	longitude	81.19904	*°E*
	altitude	132	*m*
	Instruments used	Current meter, CHIRP, Garmin GPS, EC-meter	

G. Sediment sampling field observations

Sediment Field Data Collection Sheet

Project: Save the Tiger! Save the Grasslands! Save the Water!
WP4: Morphodynamics of Karnali River and Erosion of Vegetated Floodplains

Sample collector: Kshitiz Gautam/ Mo de Jong

Data Logger: Kshitiz Gautam/ Mo de Jong

Date	S.N.	Sample I.D.	Latitude (N)	Longitude (E)	Altitude (mAMSL)	Sediment weight (Kg)	Sample depth (cm)	Appearance	Color	Texture	Water Depth above sample (cm)	Location Description (floodplain/ bed)	Remarks
10-Nov-22	1	1B1	28.61963	81.27127	170	8	0-10	Dry	Grey	granular/ sand	0	floodplain flooded during high flow, mostly sand in the immediate bank but very course gravel as it extends away from the immediate bank	Left Bank @ first island of bifurcation
	2	1B2	28.6196	81.27085	160	7		wet	grey	sand	44	Bed sediment: 3 m towards the river from left bank	Left Bank @ first island of bifurcation
	3	1B3	28.61853	81.27	175	5.5		wet	grey	sand + pebbeles	76	Bed sediment: 3 m towards the river from right bank	Right Bank @ first island of Bifurcation
	4	1B4	28.61884	81.26992	181	7.5	0-18	dry	grey/ white	sand + pebbeles	0	5m on right bank of the river, higher floodplain with mixed sediments : sand and boulders upto 50 cm dia , lot of driftwood, grass and a few trees	Right Bank @ first island of Bifurcation
	5	1B5	28.61893	81.26962	169	7.5	0-18	dry	grey/ white	sand + pebbeles	0	30 m on the right bank	Right Bank @ first island of Bifurcation
	6	1B6	28.61853	81.26988	183	5.5	0-21	semi dry	white /grey /silver	very fine sand and silt		7m from right bank, looks like bank of microchannels	Right Bank @ first island of Bifurcation
	7	2B1				7		wet			9	right bank, bed sediment	

	8	2B2	28.606273	81.2704853	190	7	0-10		white			70 m from right bank, mix of san and stones. Stone layer found after 10 cm depth from surface	Right Bank @ Lalmati immediately before bifurcation
	9	2B3	28.604789	81.2725839	179	6	0-16	semi dry	grey	sand	0	higher floodplain here contains loam/clay and boulders/stones near the river bank, steep terrain	Left Bank @ Lalmati immediately before bifurcation
11-Nov-22	10	1G1	28.564196	81.2592981	158	7	0-10	dry	white/mix	mixed	0	Steep right bank, top layer mostly soil followed underneath by older deposited sediments	Right bank @ Gerua (Bagh Tapu)
	11	1G2	28.564339	81.2598944	154	7		wet			60	3m into the river from left bank	Left bank @ Gerua (Bagh Tapu)
	12	1G3	28.564339	81.2598944	155	7	0-21	semi dry	grey	sand	0	3m away from river, on further 2m (5m away from river) boulder nad gravel deposition	Left Bank @ Gerua (Bagh Tapu)
	13	1G4	28.564349	81.2601289	167	6	0-12	Semi Dry	grey	Sand	0	Gravels after 12 cm from surface, 25m away from river into the floodplain, gravel deposition	Left bank @ Gerua (Bagh Tapu)
14-Nov-22	14	2G1	28.50236	81.2316	149	7	0-10	dry	white	sand + silt	0	higher floodplain, near grassland, gravel after 10 cm depth, 100 m from the left bank (144 m from right bank, i.e. width of river 44 m)	Left bank@ Gola
	15	2G2	28.50177	81.23038	147	6	0-10	semi dry	grey	sand	0	50m from left bank on the higher floodplain, gravel after 10 cm, 100 m from right bank	Left bank @ Gola
	16	2G3	28.50179	81.23032	151	11	0-10	semi dry	mix	mostly gravel	0	25 m from left bank, floodplain mix of sand and gravel, finer gravels, 70m from right bank	Left bank @ Gola
	17	2G4	28.50221	81.2292	153	10		wet		sand and gravel mix	13	small bifurcation branch (small rapid) in the river on right side close to right bank, slightly d/s of the bend at Gola	Right bank @Gola
	18	2G5	28.50222	81.22927	151	6	0-18	semi dry	grey	sand	0	right bank near sand deposition	Right bank @ Gola
	19	2G6	28.50265	81.22918	156	10	0-5	Dry	mix	gravel and sand mix	0	right bank (steeper) higher step, floodplain wall (a dike?)	Right bank @ Gola
	20	2G7	28.50276	81.22844	152	6	0-10	dry	white	silt + sand	0	just below HFL, upper step of floodplain, flood deposition (after 10 cm from surface: land with vegetation)	right bank @ gola
	21	3G1	28.44999	81.20386	129	5	0-18	semi dry - wet	grey	sand	0	water seeping into the sediment dug hole, right bank, second branch from the right	right bank @ manau

	22	3G2	28.45098	81.20356	133	5.5	0-5	dry	white	fine sand and silt with big gravels	0	after 0-5 cm large gravel floodplain between first and second branch	
	23	3G3	28.45178	81.20345	137	6	0-20	dry	white	sand + silt+ clay	0	flood plain, top right bank of first branch	right bank @ manpur
	24	4G1	28.40672	81.19933	121	8	0-10	dry	mix	gravel and sand mix	0	floodplain top left bank	gravel bed river @ Lalpur
	25	4G2	28.40668	81.19925	120	6	0-18	dry	white / grey	sand	0	floodplain left bank	gravel bed river @ Lalpur
	26	5G1	28.3672	81.20236	113	6		wet	grey/ black	sand and silt	15	20 cm inside the river from left bank, banks mostly sand probably because of gravel extraction upstream of the gerua bridge	left bank @ kothiyaghat bridge
	27	5G2	28.36695	81.20224	119	6	0-15	dry	white /grey	sand and silt	0	20 m from the left bank	left bank @ kothiyaghat bridge
	28	5G3	28.36677	81.20192	120	6	0-18	wet	black /grey	sand + silt + clay	0	3 m from the left bank	left bank @ kothiyaghat bridge
16-Nov-22	29	1K1	28.473038	81.1136169	131	8		wet		sand	23	70 cm into river from right bank, sand bed, high flow velocity of about 0.2 m/s at 20 cm depth and 0.5 m from the bank and about 0.48 m/s at 1 m from bank	right bank @ Daulatpur
	30	1K2	28.473129	81.1137006	133	10		wet		sand	10	40 cm into river from right bank, sand bed, gravels or stones from damaged gabion walls	right bank @ Daulatpur
	31	1K3	28.473136	81.1137589	139	6	0-18	dry	white	sand	0	higher flood plain right bank	right bank @ Daulatpur
	32	1K4	28.471175	81.1162628	137	7		wet		sand	20-25	80 cm into river from left bank, velocity is about 0.95 m/s 2m inside the river from left bank	left bank @Daulatpur
	33	1K5	28.471195	81.1163028	130	6	0-10	wet		sand+very fine pebbles	0	20 cm inside the river from left bank	left bank @ Daulatpur
	34	2K1	28.484716	81.1377192	125	11	0-10	wet		gravel and pebble	10	in dynamic section with islands and channels, 20 cm inside river channel closer to left bank, gravel bed , significant amount of sand in floodplain	left bank @ Murgauwa
	35	2K2	28.484509	81.1378839	144	7	0-10	semidry - wet	grey	sand and silt	0	20 m from the river cahnnel, on the left bank active floodplain, after 10 cm of depth we hit gravel layer	left bank @ Murgauwa

Mixed bed on left bank @ Daulatpur i.e. more pebbles and stones than right bank possibly because of sediment mining on the right bank upstream which is not allowed on the left bank

	36	2K3	28.484186	81.1385931	125	6	0-21	semi dry	grey	sand + silt + clay	0	140 m from the left bank on the active floodplain	left bank @ Murgauwa
	37	3K1	28.50823	81.16694	144	8	5-12	wet		gravel + sand	5	1 m inside the channel from left bank, midchannel bars with sand and gravel, banks mostly sand	Left bank near shantibazar
	38	3K2	28.50823	81.16694	144	8	0-13	wet		sand	water after 5 cm deep	50 cm n the flood pain from the left river bank, midchannelbars, dynamic area, many channels, high flow velocities	Left bank near shantibazar
	39	3K3	28.508298	81.1670228	130	9	12-22	wet		sand + gravel + clay	12	left bank between two groynes/spurs, 1.5 m from spur bank, 3.5 m from dike, affect of backflow	Left bank near shantibazar
	40	4K1	28.573929	81.2336694	149	8	20-30	wet		gravel +sand	20	2.5 m inside the channel from right bank	Right bank of main flow channel @ sattighat
	41	4K2	28.573921	81.2337175	147	7	0-15	wet		sand +gravel	0	8 m towards the floodplain from the right channel bank, higher floodplain contains sand whereas normal floodplain has mostly gravel with sand	Right bank of main flow channel @ sattighat
	42	4K3	28.573921	81.2337175	147	6	0-12	semidry/wet		sand	0	8 m from channel (4m north of 4K2), right bank floodplain, mostly gravel with sand but gravel bed, hit gravel bed after 12 cm of digging	Right bank of main flow channel @ sattighat
17-Nov-22	43	5K1	28.434489	81.0810053	119	10	14-20	wet		gravel + silt + clay	14	3 m from right bank (towards left side in the channel) of midchannel bar (1-3 m from bank) active floodplain, finest silts removed by draining of sample, patches of gravel bars mostly sand and silt in the floodplain	
	44	5K2	28.433987	81.0809394	126	7	24-30	wet		sand	24	3 m right bank (left side) of the midchannel bar, hit gravels after 30 cm	
	45	5K3	28.434806	81.0806147	116	8	0-15	dry		sand+gravel	0	On mid channel bar, about 100 m from left channel active floodplain (high flow channels), gravel on top, mix on bottom	
	46	5K4	28.435479	81.0795206	122	6	0-20	dry	white	sand	0	on top (highest point) of mid channel bar, ponded water at 20 m from this point from seeping river water	

H. Sediment Particle Size Distribution Curves

H.1. BI02 – Bifurcation Main Channel (1B)

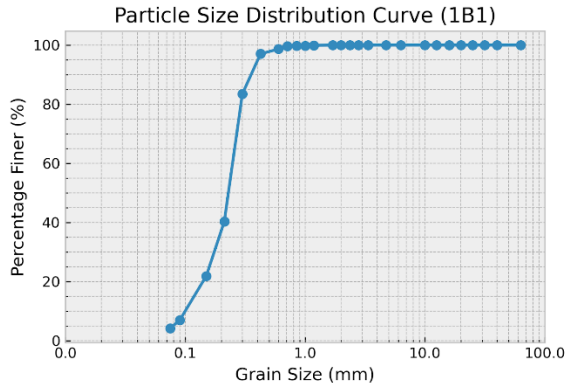

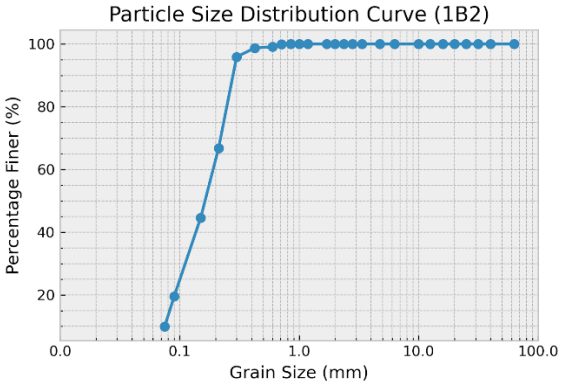

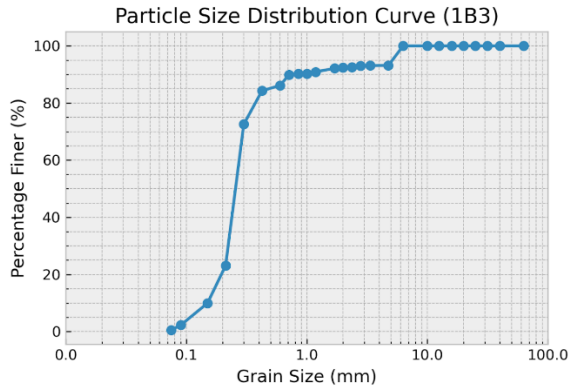

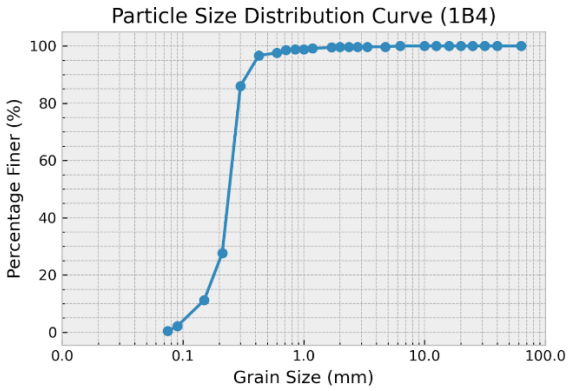

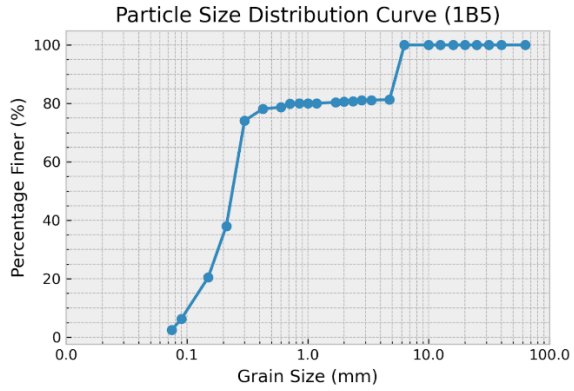

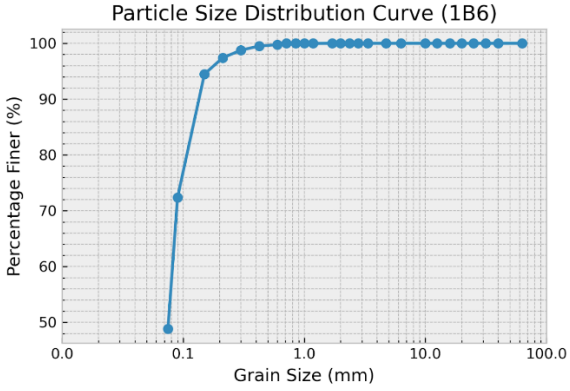

H.2. BI03 – Lalmati, Japanese Camp (2B)

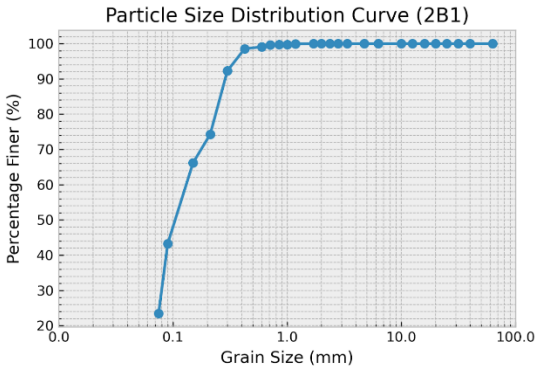

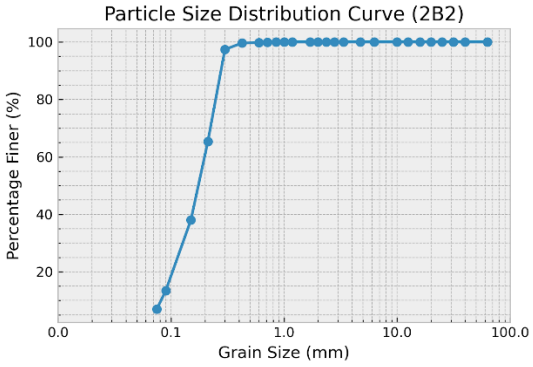

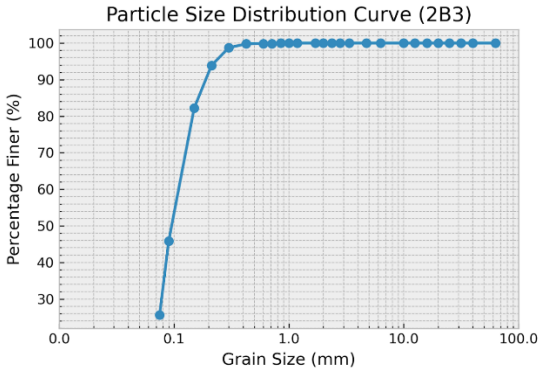

H.3. G02 – Geruw River at Bagh Tapu (1G)

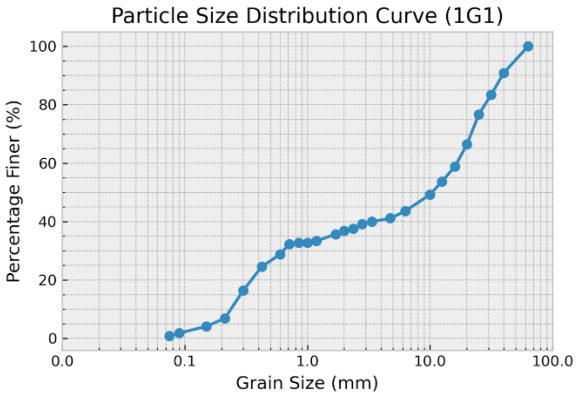

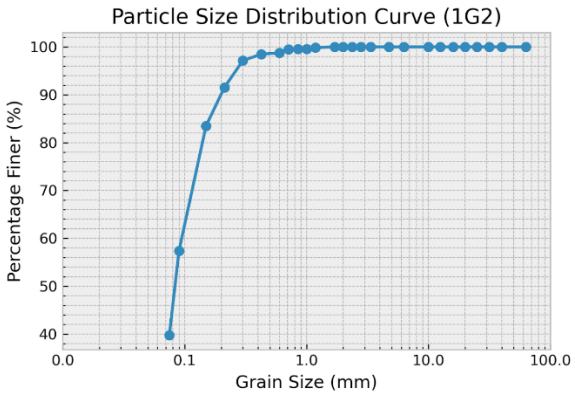

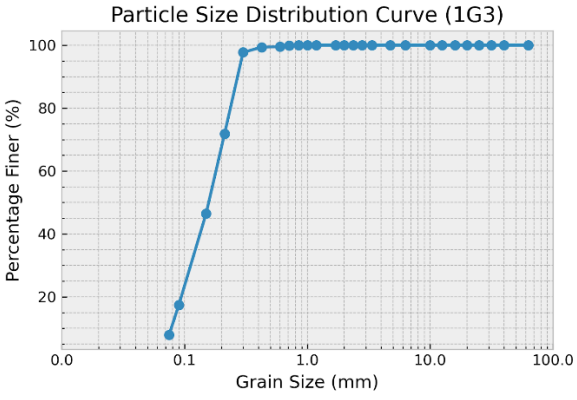

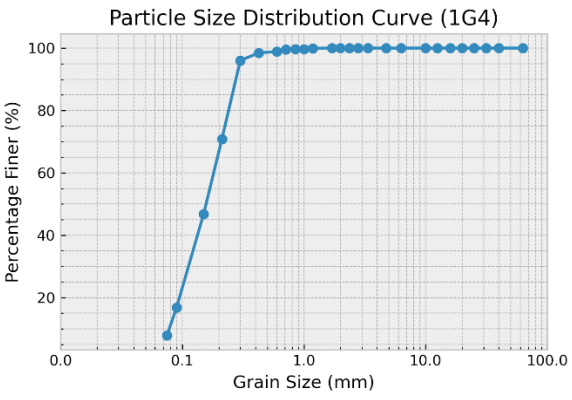

H.4. G04 – Geruwa River at Gola (2G)

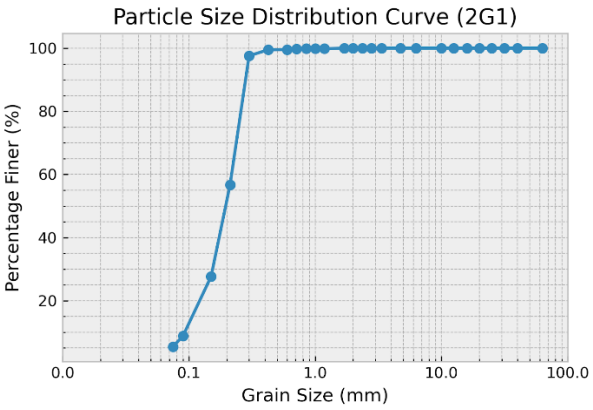

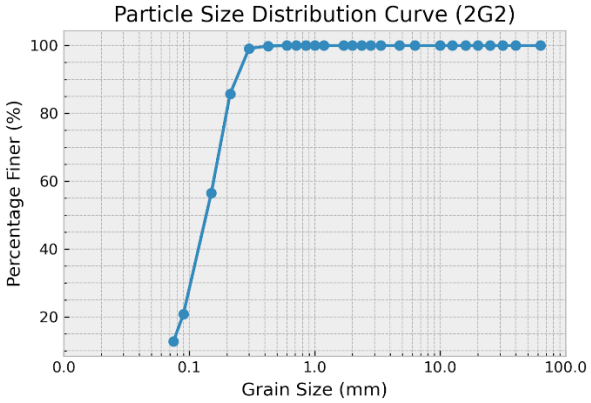

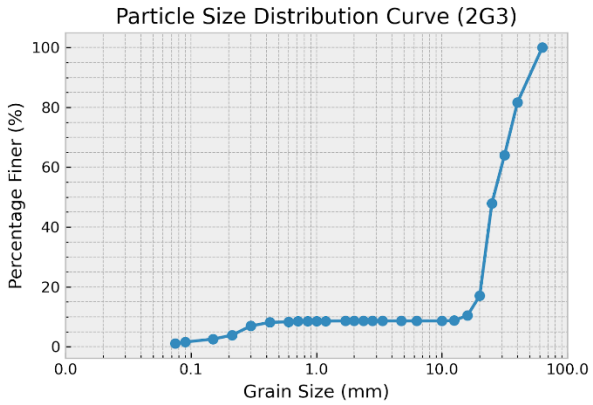

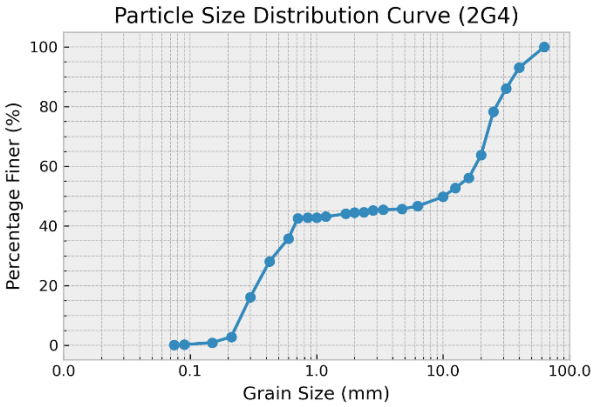

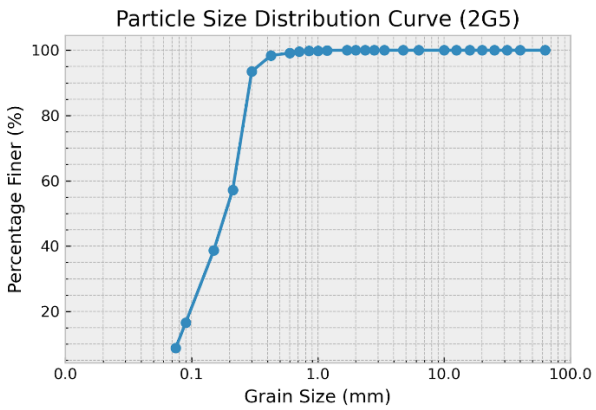

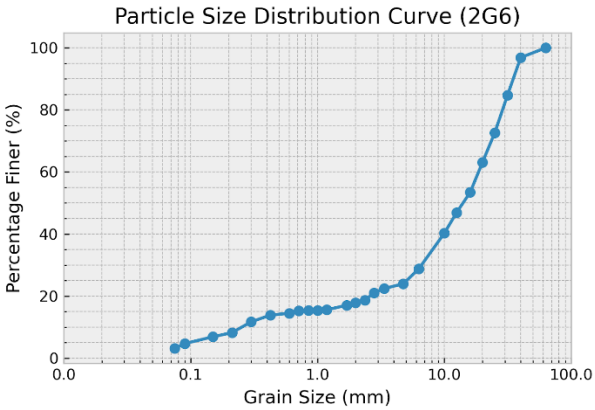

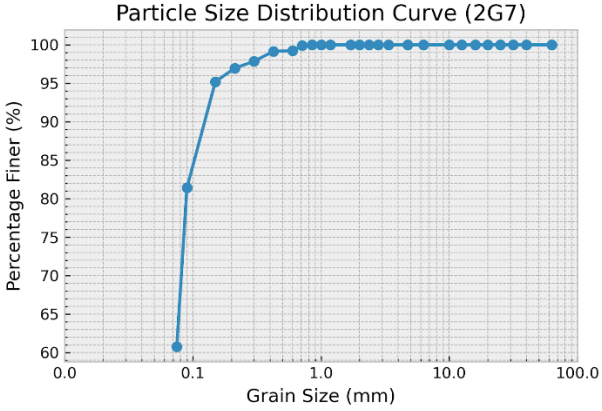

H.5. G05 – Geruwa River at Manpur (3G)

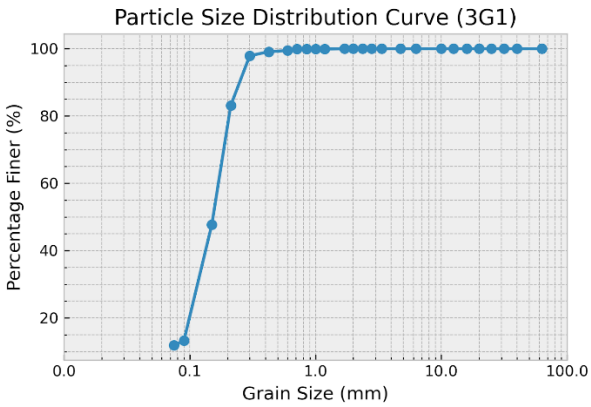

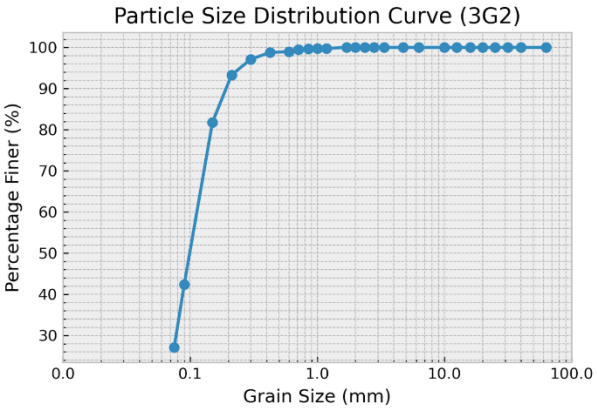

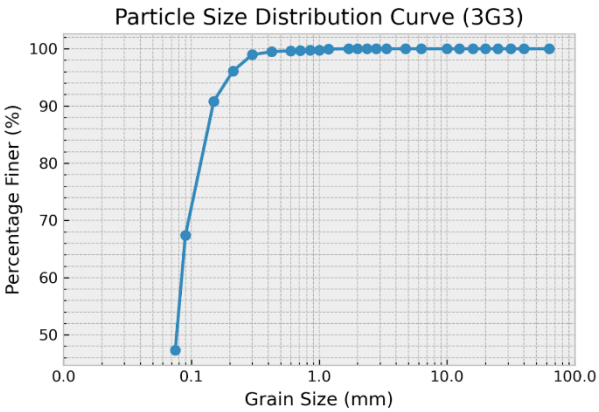

H.6. G06 – Geruwa River at Lalpur (4G)

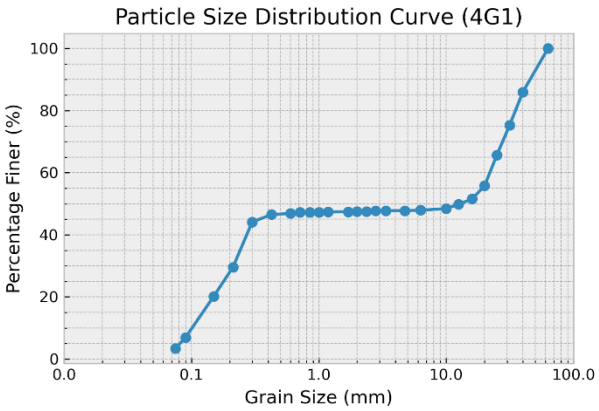

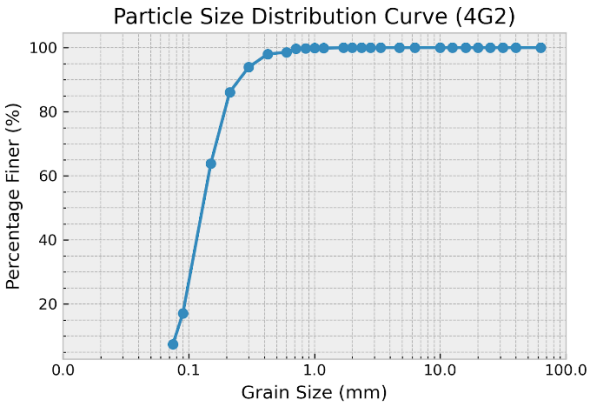

H.7. G07 – Geruwa Bridge: Khotiyaghat (5G)

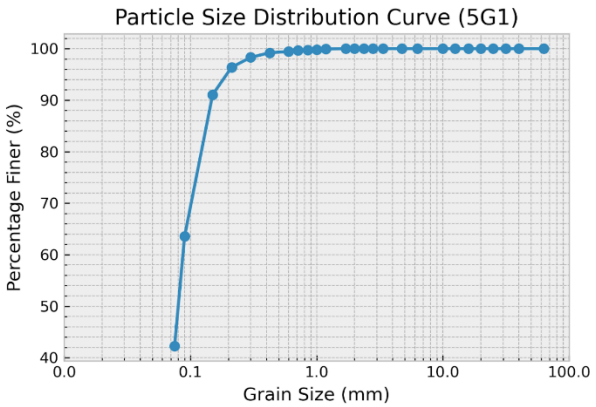

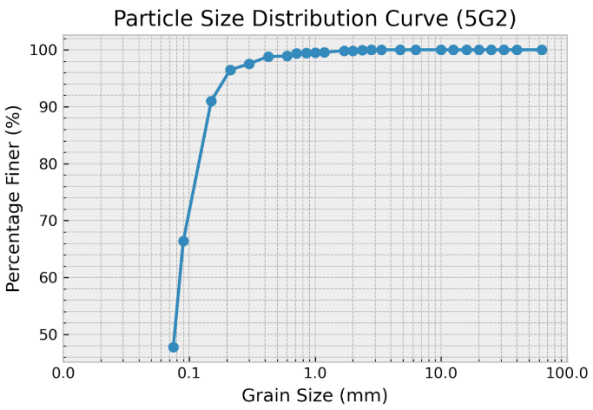

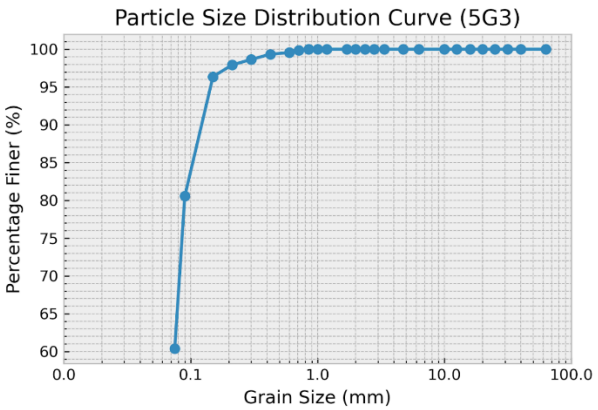

H.8. KU06 – Kauriala River at Daulatpur (1K)

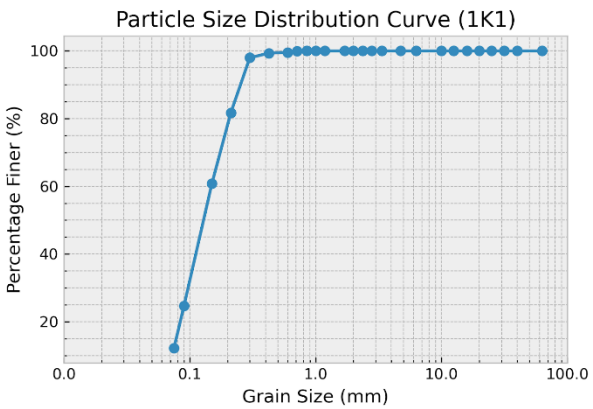

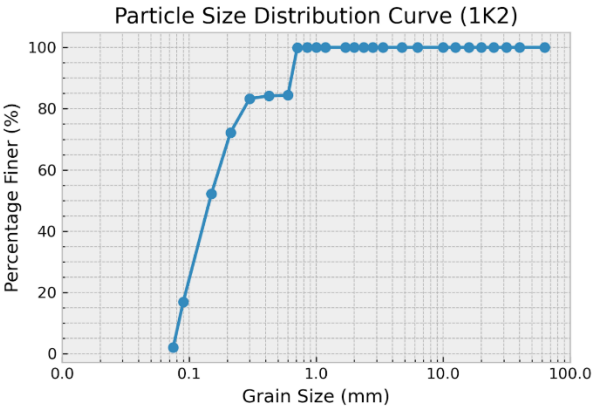

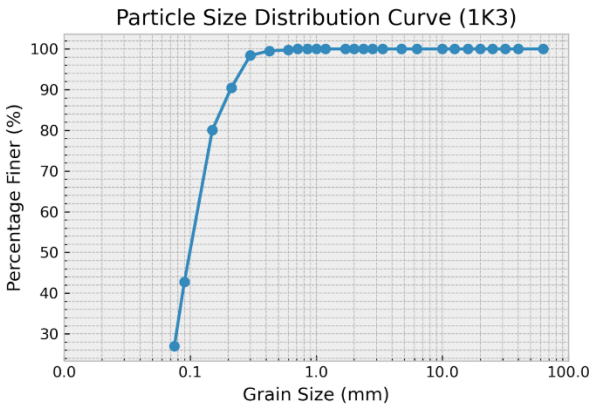

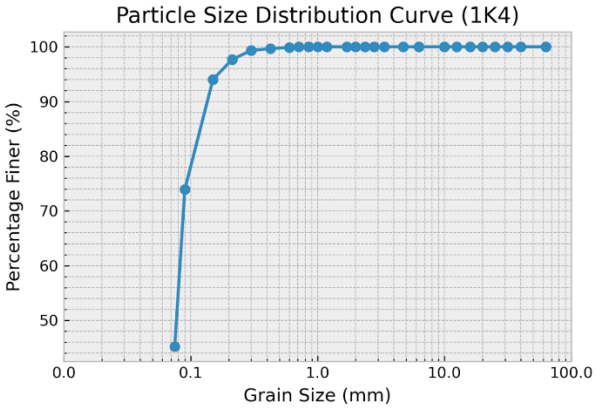

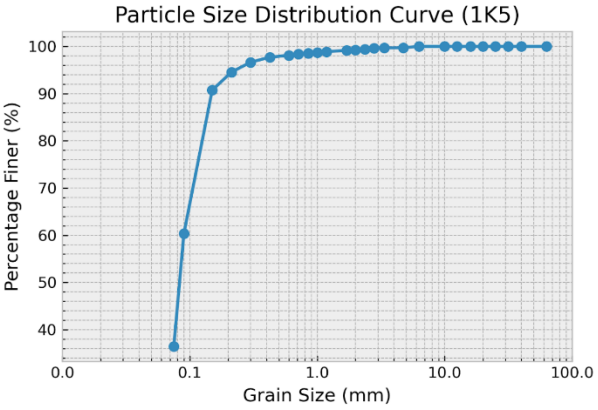

H.9. KU05 – Kauriala River at Marghua (downstream) (2K)

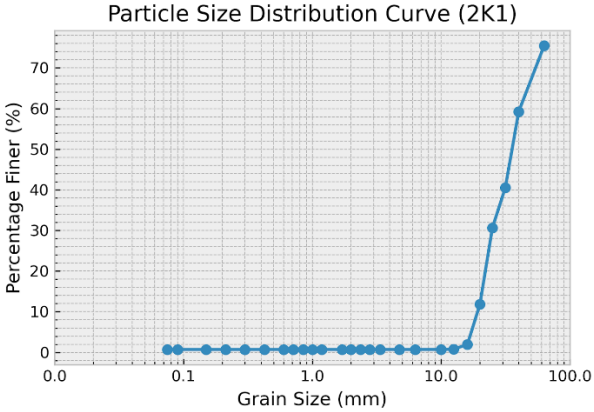

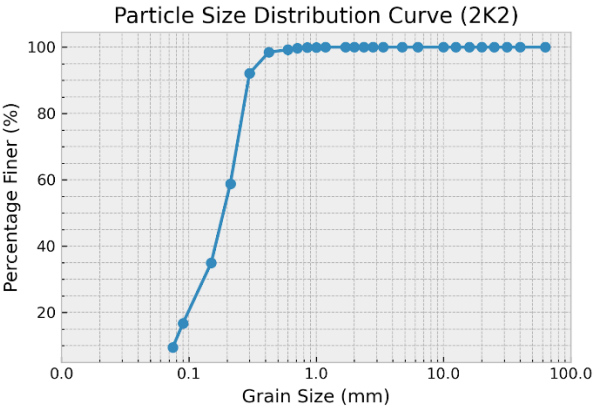

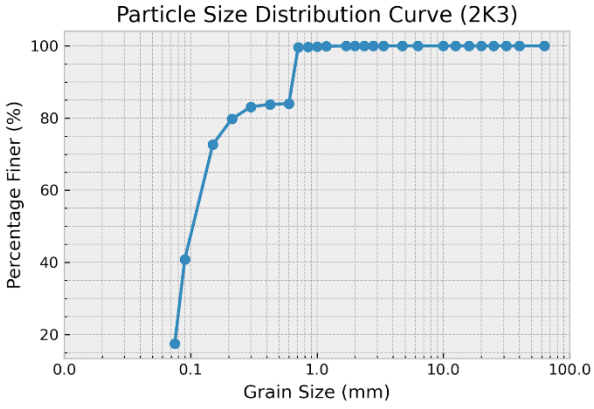

H.10. KU03 – Kauriala River at Shantibazar (3K)

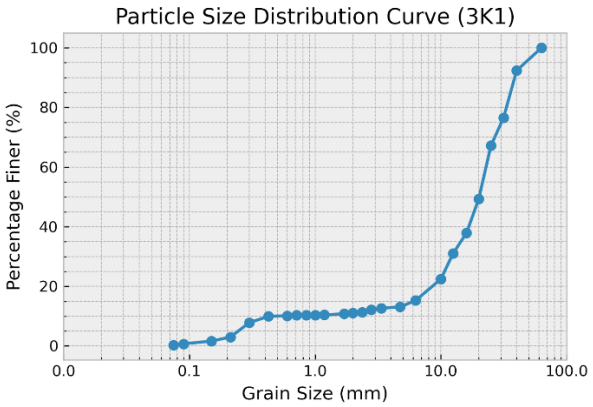

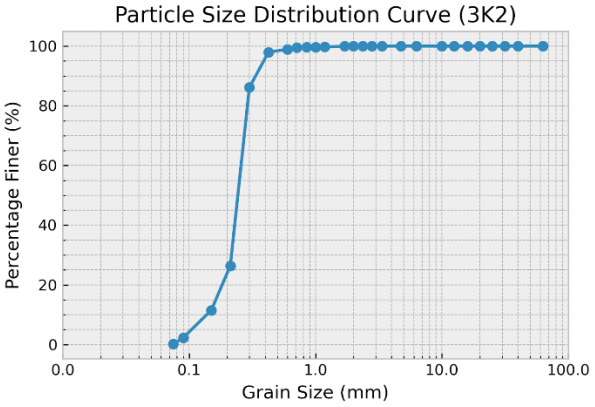

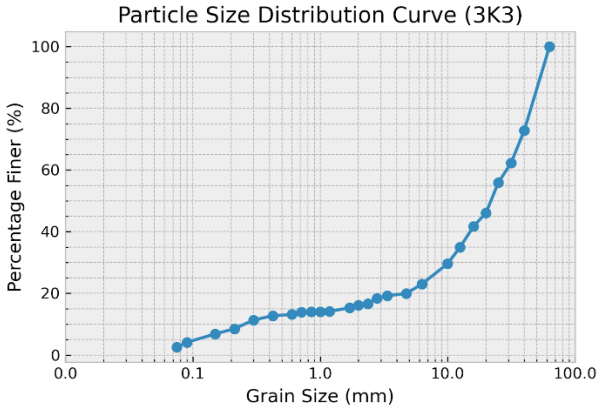

H.11. KU01 – Kauriala River at Patabhar (4K)

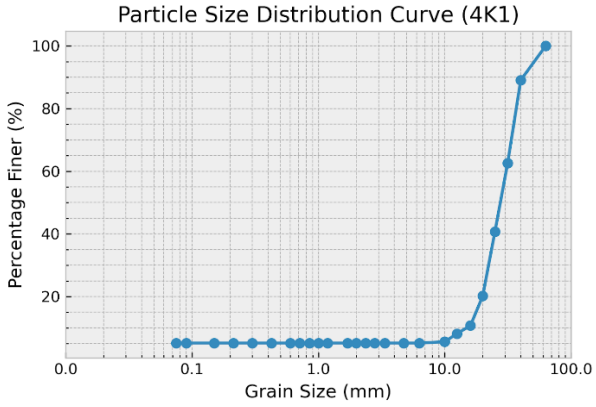

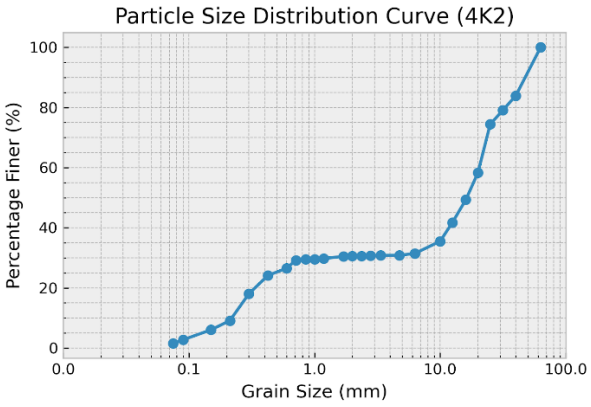

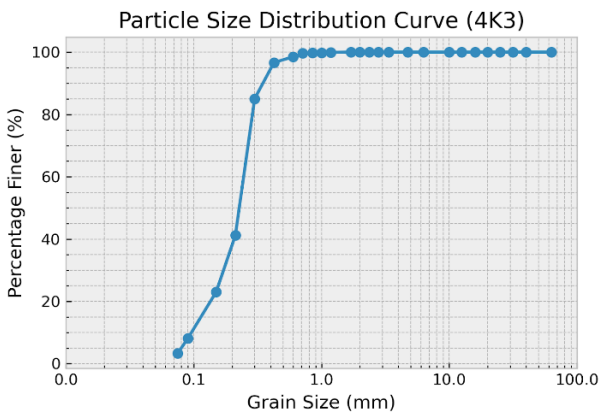

H.12. KU07 – Kauriala Bridge: Sattighat (5K)

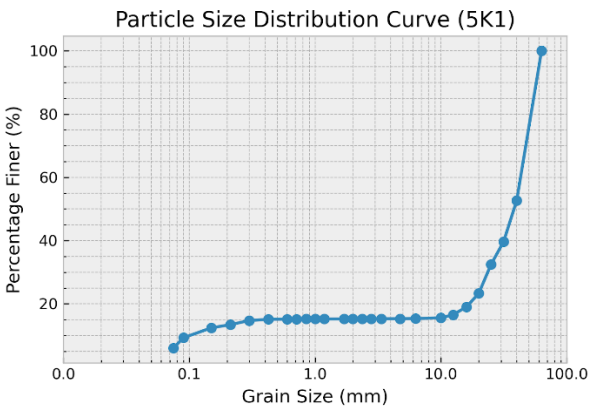

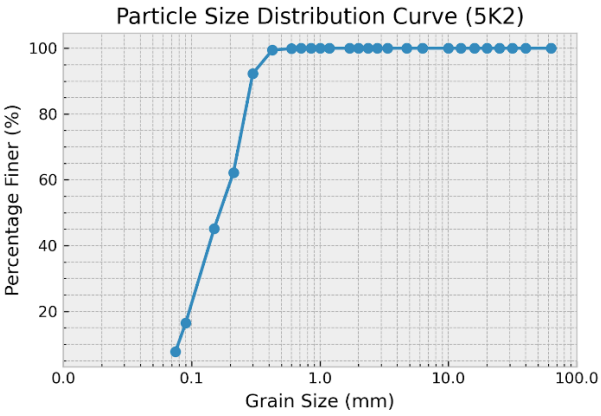

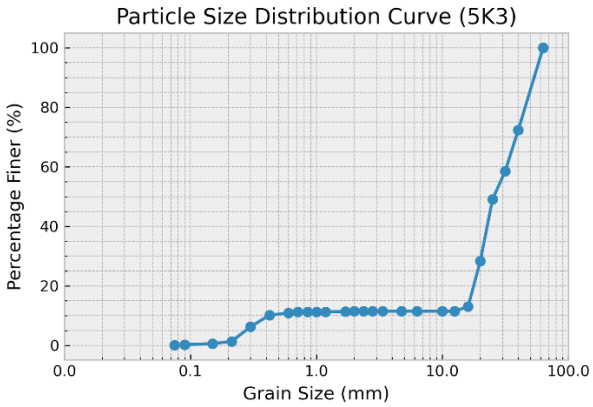

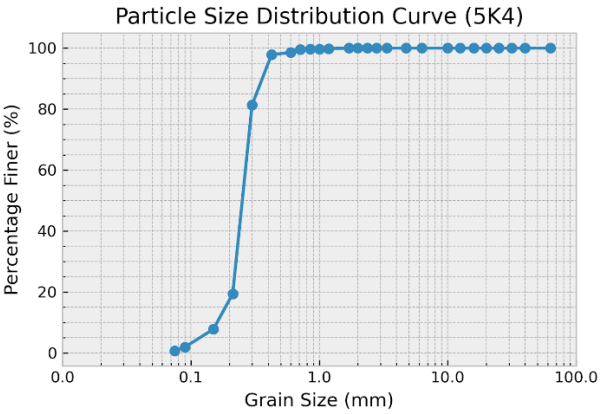

H.13. BH01 – Bheri Bridge at Ghatgaun (1BHE1)

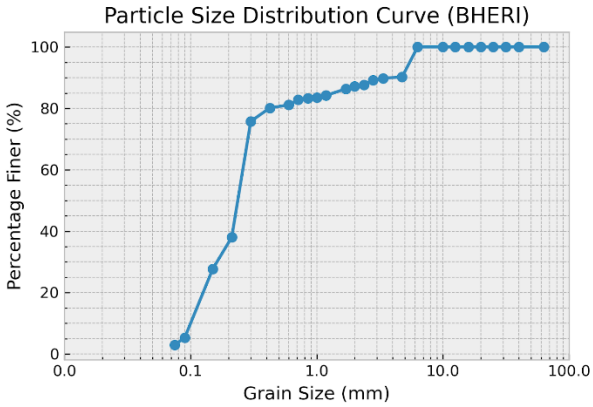

H.14. BA04 – Babai River at ICESat Overpass Downstream (1BAB1)